

# HOLOCENE TECTONO-SEDIMENTARY EVOLUTION OF THE HARYANA PLAINS, INDIA

## A THESIS

*Submitted in partial fulfilment of the  
requirements for the award of the degree  
of*  
DOCTOR OF PHILOSOPHY  
*in*  
EARTH SCIENCES

*by*

**VIVEKANAND ACHARYA**



DEPARTMENT OF EARTH SCIENCES  
INDIAN INSTITUTE OF TECHNOLOGY ROORKEE  
ROORKEE - 247 667 (INDIA)

APRIL, 2009

**©INDIAN INSTITUTE OF TECHNOLOGY ROORKEE, ROORKEE- 2009  
ALL RIGHTS RESERVED**



# INDIAN INSTITUTE OF TECHNOLOGY ROORKEE ROORKEE


## CANDIDATE'S DECLARATION

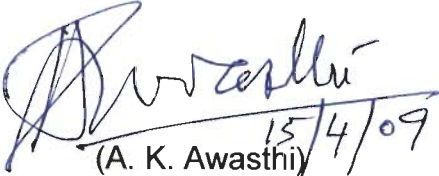
I hereby certify that the work which is being presented in this thesis entitled "HOLOCENE TECTONO-SEDIMENTARY EVOLUTION OF THE HARYANA PLAINS, INDIA" in partial fulfilment of the requirements for the award of the Degree of Doctor of Philosophy and submitted in the Department of Earth Sciences, Indian Institute of Technology Roorkee, Roorkee is an authentic record of my own work carried out during a period from July 2004 to April 2009 under the supervision of Dr. A. K. Awasthi, Professor and Dr. B. Parkash, former Emeritus Fellow, Department of Earth Sciences, Indian Institute of Technology Roorkee, Roorkee.

The matter presented in this thesis has not been submitted by me for the award of any other degree of this or any other University/Institute.

  
(VIVEKANAND ACHARYA)

This is to certify that the above statement made by the candidate is correct to the best of our knowledge.

  
(B. Parkash)  
Supervisor

  
(A. K. Awasthi)  
Supervisor

Date: 15<sup>th</sup> April, 08

---

The Ph.D. Viva-Voce Examination of **Mr. Vivekanand Acharya**, Research Scholar, has been held on \_\_\_\_\_.

Signature of Supervisors

Signature of External Examiner

## **ABSTRACT**

The Haryana Plains form a drainage divide between the Indus and Gangetic drainage systems. These plains may have been affected by neotectonic activity and climatic changes during the Holocene period, as observed in the adjoining Gangetic Plains. The Haryana Plains are known to be host to the Vedic Civilization (>3000 B.C.), which was intimately related to the Sarasvati, the Lost River. The hypothesis of the Yamuna River, flowing through the Haryana Plains, forming a major tributary of the Sarasvati, (flowing along the presently small, ephemeral Ghaggar River) has been suggested by a number of archaeologists, but geological evidence for the same is still to be worked.

Keeping the above points in view, Haryana region was mapped for its landforms and soil-geomorphic units, using remote sensed digital data. Other investigations involved field checking of these units, study of typical pedons from each unit for their morphological features, collection of soil samples for granulometric and micromorphological studies and dating of C-horizons of soils, construction of Digital elevation models and study of changes in modern/paleo-drainage to locate faults, and study of by Ground Penetration Radar studies for confirmation of faults and deciphering of subsurface facies to infer the absence/presence of the large Yamuna River in Haryana in the recent past. All data were integrated to work out drainage evolution in the Haryana and adjoining region.

Using Landsat MSS images, digital elevations models (DEMs), and digital terrain models (DTMs) for Haryana Plains, we recognized major landforms like floodplains of rivers, aeolian plain, old fluvial plains, piedmont



zone and terminal fans. Further depending upon the degree of development within various landforms, 25 soil-geomorphic units were identified.

Based ages obtained from the Optically Stimulated Luminescence Technique and the degree of soil development, 25 soil-geomorphic units were grouped into six members of a Morphostratigraphic Sequence (QIMS-I to VI) (Quaternary Indus Morphostratigraphic Sequence) (Frye and William, 1962. in Fairbridge, 1968, p. 915): QIMS-VI 9.86-5.38 Ka, QIMS-V- 5.38 -4.45 Ka, QIMS-IV- 4.45 - 3.60 Ka, QIMS-III - 3.60 -2.91 Ka, QIMS-II - < 2.91-1.52 Ka and QIMS-I - < 1.52 Ka.

Clay accumulation indices (C.A.I.) of Levine and Ciolkosz (1983) calculated from grain size data for soils of QIMS-II-VI members vary in ranges 227-484, 166-485, 186-714, 300- 855 and 885-1147, respectively. Broad systematic increase in C.A.I with age suggests increase of pedogenic clays with the increasing age of soils.

Micromorphological investigation shows that QIMS-II and III member soils show very weak to moderate pedality, whereas the soils of the older members such as QIMS-IV to VI show moderate to well developed peds in B-horizons. Also, thickness of argillans and ferriargillans increase from QIMS-II to QIMS-VI soils with loamy parent material.

Faults were identified following a new approach adopted by Singh et al. (2006) and Bhosle et al. (2009). Nine major faults are identified from study area: Ambala-I and II, Markanda, Patiala, Jind, Rohtak and Hissar Faults, running almost in NWW-SEE direction, sub-parallel to the Himalayan trend, are longitudinal in nature, whereas the faults bounding the study area i.e. Ghaggar and Yamuna Faults are transverse in nature. Throws of longitudinal

faults are 7-12m and are towards south except the Hissar fault, which has throw towards north. The Ghaggar fault and Yamuna Faults have a curvilinear trend with convexity towards southeast and southwest, respectively. The Himalayan Frontal Fault defines the boundary between the Siwalik ranges and Piedmont zone.

Radar lithofacies studies indicate that almost all the profiles from different parts of the Haryana plains show that the lower parts of radar profiles were deposited by a large river with a depth of >7m and upper parts were deposited by wind reworking or as terminal fan/ young piedmont sediments.

GPR traverses across 5 out of six faults inferred from remote sensing and GIS studies confirm the presence of these faults. Also, these faults are sets of a number of faults, and majority of faults show downthrown side in direction inferred from the DEMs, and the rest show downthrow in the opposite direction. The Patiala and Hissar Faults show effects of activity of faults contemporaneous with sedimentation by thickening of beds on downthrown blocks.

GPR studies of mainly terminal fans in the adjoining Ganga-Yamuna Interfluvium provide a model for terminal fan deposition. It consists of lower part comprising wide channels filled with vertical accretion deposit /lateral accretion sands, overlain by wide spread floodplain mudfacies and commonly further overlain at the top by many, narrow (rarely wide) shallow channels filled with vertical accretion deposits. The tops of terminal fan deposits exhibit moderate to weak soil development.

Reviews of previous studies on paleo-climatic studies in adjoining area of Rajasthan suggest initiation of drier climate at about 3000 B.C. This

change is considered to have caused lower discharge of rivers including that of the Sarasvati River and led to first wave of dispersal of the Harappan culture from the Sarasvati Valley to north into the Indus Valley.

Longitudinal faults (except Hissar fault) of the Haryana plains are considered to have formed by compression from a direction perpendicular to them. Most probably that they (except for Hissar fault) are imbricates of the Himalayan Frontal Fault and thus these are basically thrusts in nature. Their near normal character in the shallow subsurface as observed in GPR profiles is probably due to the fact these thrusts are curved in nature and these are seen apparently as normal faults near the surface.

Mukerji (1976) first introduced the name and described morphology of a terminal fan (Markanda Terminal fan) from the Haryana plains. It was considered to have formed in the plain area, away from the Himalayan Mountain front, due to the loss of discharge due to evapotranspiration under semiarid climate. Later many terminal fans related to faults have been recognized from dry subhumid to sub-humid semiarid Haryana Plains in the present study.

Comparison of our work with published studies suggest that the most of terminal fans formed by distributary stream system seem to be related to semiarid to dry subhumid climate and under wetter climate.

The Markanda, Old Yamuna, Karnal and Sonipat Terminal Fans were developed by splays from the different streams on the downthrown blocks of some faults and are thus are also 'splay terminal fans'. However, the Young Chautang Terminal Fans-I-IV were formed by involvement of the whole Chautang River.

Integrating our studies with archaeological information with two phases in drainage evolution history of the Haryana region can be deciphered. In first phase of 3000 B.C. to about 2200 B.C., the Yamuna was first flowing along the Chautang River course forming the Drishadvati River, it migrated northwestward slowly due to tilting of the Haryana plains towards NW. Then it shifted to its present position by 2100 B.C., though a minor flow through the Old Yamuna. The Sutlej River also started shifting by 1900 B.C. and soon became an independent entity, from a tributary of the Ghaggar (Sarasvati) River. These changes were caused by tilting of Haryana and Panjab blocks. In second phase, different longitudinal faults became active and some more terminal fans (Markanda Terminal Fan and Chautang Terminal Fans-I-IV) were deposited due to their activity.

Neotectonic activity since about 3000 B.C. have controlled geomorphology and drainage and sedimentation in the Haryana and adjoining plains.

## ACKNOWLEDGEMENT

Writing acknowledgement is not an easy task and this I realized after completion of my thesis because there are many wonderful people associated directly or indirectly with the work that made this dissertation possible. It is not possible to write names of all those but I thank all of them.

First and foremost I am greatly indebted to my Supervisor, former Professor & Emeritus Fellow Dr. B. Parkash for his contributions to all aspects of my work in this thesis. He is a great teacher, educator, and advisor, who provided a lot of ideas and inspiration for the thesis, and taught me the beauty and importance of Quaternary Geological Studies with his unparalleled perception and excitement.

Mere words are not enough to extend my gratitude to Professor A.K. Awasthi who I think is the most enthusiastic and generous research co-supervisor. He has suggested very logical solutions at time. I was always astonished by his approaches, ideas and his knowledge of the subject as I communicated more and more. Without the contribution and guidance of both of my supervisors this work would not have been possible.

I would also like to thank my committee members, Dr. R. Anbalagan, Dr. S.K. Tripathi and Dr. Pachauri, for their valuable time and many helpful comments about the work and thesis.

My thanks are due to Prof. R. P. Gupta, Head, Department of Earth Sciences, IITR for providing me all the possible research facilities especially GPR system as and when I felt the need. The services provided by the Institute Instrumentation Centre, IITR for carrying out analytical work is duly acknowledged.

My sincere thanks goes to all the faculty members of the Department of Earth Sciences, IITR for their help and moral boosting at various stages of the research endeavor. My special thanks are due to Dr. R. Krishnamurthi and Dr. A.K. Sen for providing me microscope for micro-morphological studies.

Heartfelt thanks are due to Dr. Sanjay Trignath, Dr. D.K. Deolia, Dr. G.P Singh, Dr. Rathore, Dr. V. Gadgill and Prof. P.K Mishra, Department of Geology, Govt. Autonomous Science College, Jabalpur, who introduced me to Quaternary Geology and always been a source of inspiration during the ups and downs during the research work.

Thanks are due to Dr. Jitendra Prasad of IIRS Dehradun for his time and help in soil classification.

I am indebted to the institute for awarding me Ministry of Human Resources and Development (MHRD) Institute fellowship to carry out all the research work.

Help and support extended by the technical and non-technical staff of the department especially Nairji, Rameshji, Kameshji, Subodhji Mishraji, Agarwalji, Sainiji, Shreepalji, Sarveshji, Devanand and Rakeshji, all those names has skipped from the list are nonetheless deserves big thanks.

Thanks are due to my entire present and past TL laboratory comrades, Dr. Satvinder Singh, Dr. Balaji Bhosle, Ranaboti Madam, Dr. Pitambar Pati, Mrs. Seema Singh, Rajendra Prasad Jakhamola, Qaiyum, Gaurav, Lalit, Lekhraj Sir, Kuldeep and Vijay for their support, help and the wonderful working environment provided during the whole work.

Not to mention I am very lucky to have great friends like Dr. Nihar, Dr. Tejpal, Dr. Nikunj, Dr. Manish Rana, Dr. Anshuman, Vinay Sir, Mohan Poddar Sir, Madhukar Waware Sir, V.L Krishnan Sir, Govardhan, Rajiv Sachadeva, Jay Singh Meena, Rituraj Dubey, Satya Prakash Singh, Krishna, Devendar, Abhishek, Srikanth, Tarun Sharma, Seshi Reddy, K.T. Rao, Murlidhar, Amrendra, Sanjay Gupta, Suhel and Priti Singh. They are the most wonderful humans with great sense of humor and sharp minds always looking forward to help and for me they are my instant moral boosters.

Of course, I would not be who I am without the love and support I have always received from my family. By their example, my mother and father showed me that I could do anything I wanted to. They lovingly accepted and tolerated all my interests, which they often could not understand, but were proud of never-the-less. They taught me that education was the most beautiful and important thing in the world, and for this I would like to thank them. My great appreciations are due to my lovely brothers Amar, Dharmanand and Parkash madam for their constant support and encouragement during the happy as well as sad moments during my work.

My present status in life, this Ph.D. included, is a result of the extraordinary will, efforts, patience and sacrifices of my parents. And finally I thank all mighty GOD because of whom we all are here.

**VIVEKANAND ACHARYA**

## CONTENTS

TITLE	PAGE NO.
CANDIDATE'S DECLARATION	i
ABSTRACT	iii
ACKNOWLEDGEMENT	ix
LIST OF FIGURES	xvii
LIST OF TABLES	xxiv
<b>CHAPTER-1</b>	<b>1-27</b>
1.1 INTRODUCTION	1
1.2 LOCATION, GEOLOGY AND GEOMORPHOLOGY OF THE STUDY AREA	2
1.2.1 Geology of the study area	2
1.2.2 Basement	4
1.2.3 Structural features	7
1.2.4 Geomorphic Units of the Study Area	8
1.2.4.1 Older Fans and Piedmont	8
1.2.4.2 Central Alluvial Plains	8
1.2.4.3. Aravalli Hills and Pediplains	9
1.2.4.4 Aeolian Plains	9
1.3 CLIMATIC CONDITIONS	9
1.4 SOIL MOISTURE REGIMES	11
1.5 LANDUSE	12
1.6 PREVIUOS WORK	12
1.6.1 Soils and Geomorphology	12
1.6.2 Sarasvati, The Lost River	20
1.7 RESEARCH OBJECTIVES	23
1.8 OUTLINE OF THESIS	24
<b>CHAPTER-2</b>	<b>27-109</b>
2.1 INTRODUCTION	27

<b>2.2 REMOTE SENSING AND GEOGRAPHIC INFORMATION SYSTEM (G.I.S) STUDIES</b>	27
2.2.1 Data Processing	28
2.2.2 Digital Elevation Models (DEMs) and Digital Terrain Models (DTMs)	28
<b>2.3 IDENTIFICATION OF GEOMORPHIC FEATURES AND SOIL-GEOMORPHIC UNITS</b>	30
<b>2.4 FIELD INVESTIGATIONS</b>	30
2.4.1 Colour	32
2.4.2 Oxidation Mottles and Fe-Mn /Carbonate concretions	35
2.4.3 Consistence	36
2.4.4 Texture	36
2.4.5 Structure	37
2.4.6 Soil Pores	37
2.4.7 Horizon Boundary	38
2.4.8 Roots	38
<b>2.5 MAJOR LANDFORMS IN THE STUDY AREA</b>	38
2.5.1 Fluvial Plains	39
2.5.1.1 <i>Floodplains</i>	39
<u>2.5.1.1.1 Ghaggar Floodplain</u>	39
<u>2.5.1.1.2 Yamuna Floodplain</u>	40
2.5.1.2 <i>Old Sutlej Plains –I and II</i>	43
2.5.1.3 <i>Old Yamuna Plains</i>	44
2.5.1.4 <i>Old and Young Katha Plains</i>	45
2.5.1.5 <i>Fluvial Plain</i>	45
2.5.1.6 <i>Fluvio-Aeolian Plain</i>	45



2.5.2 Piedmont	46
2.5.2.1 Oldest Piedmont (OdPt)	46
2.5.2.2 Old Piedmont-I (OdPt-I)	46
2.5.2.3 Old Piedmont-II (OdPt-II)	47
2.5.2.4 Young Piedmont (YgPt)	47
2.5.3. Aeolian Plain	47
2.5.4 Terminal Fans	48
2.5.5 Aravalli Hills and Pediments	55
2.5.6 Aravalli Piedmont (Sahibi Fan)	55
2.5.7 Paleochannels in the Study Area	55
<b>2.6 MORPHOSTRAITAGRAPHY OF THE STUDY AREA</b>	<b>59</b>
<b>2.7 SOIL MORPHOLOGY OF DIFFERENT MEMBERS OF MORPHO- STRAITIGRAPHIC SEQUENCE</b>	<b>60</b>
2.7.1 Member QIMS –VI	60
2.7.2 Member QIMS –V	73
2.7.3 Member QIMS –IV	74
2.7.4 Member QIMS –III	74
2.7.5 Member QGMS –II	75
<b>2.8 SALINITY ON THE BASIS OF THE TEST PERFORMED IN THE FIELD</b>	<b>77</b>
<b>2.9 LINEAMENTS</b>	<b>77</b>
<b>2.10. MAJOR STRUCTURAL FEATURES OF THE STUDY AREA</b>	<b>78</b>
2.10.1 Methodology Used to Identify Faults	78
<b>2.11 FAULTS</b>	<b>85</b>
2.11.1 Ambala Faults-I and II	86
2.11.2 Patiala Fault	86

2.11.3 Markanda Fault	86
2.11.4 Karnal Fault	89
2.11.5 Rohtak Fault	89
2.11.6 Jind Fault	90
2.11.7 Hissar Fault	97
2.11.8 Yamuna Faults	97
2.11.9 Sohana Fault	98
2.11.10 Ghaggar Fault	98
<b>2.12 TECTONIC BLOCKS</b>	<b>99</b>
2.12.1 Piedmont Block	99
2.12.2 Jind-Rohtak Block	99
2.12.3 Hissar Block	100
2.12.4 Punjab Block	100
2.12.5 Saharanpur Block	100
<b>2.13 RELATION BETWEEN OCCURRENCE OF EARTHQUAKES AND FAULTS</b>	<b>100</b>
<b>2.14 SUMMARY</b>	
<b>CHAPTER-3</b>	<b>111-125</b>
<b>3.1 INTRODUCTION</b>	<b>111</b>
<b>3.2 PRINCIPLE</b>	<b>111</b>
3.2.1 Physical Mechanism of Luminescence	113
3.2.2 The Luminescence Processes	115
3.2.2.1 <i>Thermally stimulated luminescence (TL)</i>	115
3.2.2.2 <i>Optically stimulated luminescence (OSL)</i>	115
3.2.3 Sample Collection and Preparation Techniques	116
3.2.4 Equivalent Dose/Palaeodose	118

3.2.6 Luminescence Measurements	119
3.2.7 Annual Radiation Dose	120
3.2.7.1 <i>Thick Alpha Source Counting</i>	121
<b>3.3 SUMMARY</b>	124
<b>CHAPTER-4</b>	<b>127-146</b>
<b>4.1 INTRODUCTION</b>	127
<b>4.2 PARTICLE SIZE DISTRIBUTION</b>	127
4.2.1 Methodology	127
<b>4.3 TEXTURAL AND AMOUNT OF PEDOGENIC CLAY VARIATION IN SOILS OF DIFFERENT SOIL GEOMORPHIC UNITS</b>	128
<b>4.4 CHEMICAL ANALYSIS</b>	130
4.4.1 Soil Reaction (pH)	131
4.4.2 pH Variation in Soils of Different Soil-geomorphic Units	132
4.4.3 Electrical Conductivity (EC)	133
<b>4.5 MICROMORPHOLOGY OF soils of THE STUDY AREA</b>	134
4.5.1 Methodology	134
<b>4.6 MICROMORPHOLOGICAL CHARACTERS OF SOIL</b>	141
4.6.1 Microstructures	141
4.6.2 Groundmass	142
4.6.3 Mineral Components	142
4.6.4 Pedality	143
4.6.5 Coatings	143
4.6.6 Voids	144
4.6.7 Coarse and Fine Ratio	144
4.6.8 Development of b-Fabrics	144

4.6.9 Concretion and Nodules	145
4.6.10 Infillings	145
<b>4.7 SUMMARY</b>	145
<b>CHAPTER-5</b>	<b>147-229</b>
<b>5.1 INTRODUCTION</b>	147
<b>5.2 BASIC TECHNIQUE/PRINCIPLES OF IN GPR INVESTIGATIONS</b>	148
<b>5.3 PROCEDURE/METHODOLOGY</b>	149
<b>5.4 DATA ACQUISITION PROCEDURE</b>	150
<b>5.5 GROUND PENETRATING RADAR STUDIES IN THE STUDY AREA</b>	151
5.5.1 Instrumentation	152
5.5.2 Interpretation and Processing GPR Data	153
<b>5.6 ARCHITECTURAL ELEMENTS, FACIES, MACROFORMS, AND RADAR FACIES</b>	155
5.6.1 ARCHITECTURAL ELEMENTS	155
5.6.2 MACROFORMS	158
5.6.2.1 <i>Braid bar</i>	158
5.6.2.2 <i>Channels</i>	159
5.6.3 Facies	159
5.6.3.1 <i>Trough cross-bedding</i>	160
5.6.3.3 <i>Horizontal bedding</i>	160
5.6.3.4 <i>Mud facies</i>	160
5.6.4 <i>Radar Sequences</i>	160
<b>5.7 HARYANA REGION- LITHOFACIES</b>	161
5.7.1 Piedmont Zone	161
5.7.1.1 <i>Young Piedmont</i>	161

5.7.1.2 <i>Old Piedmont-II</i>	162
5.7.2 Terminal Fans	167
5.7.2.1 <i>Markanda Terminal Fan</i>	167
5.7.2.2 <i>Young Chautang Terminal Fan-I</i>	174
5.7.2.3 <i>Old Yamuna Terminal Fan</i>	182
5.7.3 Plains	183
5.7.3.1 <i>Old Yamuna Plain-II</i>	183
5.7.3.2 <i>Fluvial Plain</i>	184
5.7.3.3 <i>Aeolian Plain</i>	185
<b>5.8. HARYANA REGION-FAULTS</b>	<b>185</b>
5.8.1 Ambala Faults I and II	186
5.8.2 Patiala Fault	187
5.8.3 Markanda Fault	187
5.8.4 Rohtak Fault	188
5.8.5 Hissar Fault	189
<b>5.9 GANGA-YAMUNA INTERFLUVE- SET-UP</b>	<b>189</b>
<b>5.10. GANGA-YAMUNA INTREFLUVE – GPR LITHOFACIES</b>	<b>191</b>
5.10.1 Paleochannels	191
5.10.2 Terminal Fans	197
5.10.2.1 <i>Iqbalpur Terminal fan</i>	199
5.10.2.2 <i>Khurja-Aligarh Terminal Fan</i>	200
5.10.2.3 <i>Karhal Bidhuna Terminal Fan</i>	208
5.10.2.4 <i>Kanpur Terminal Fan</i>	216
<b>5.11 GANGA-YAMUNA INTERFLUVE- FAULTS</b>	<b>216</b>
5.11.1 Ghaziabad Fault	216

5.11.2 Delhi Fault	223
5.11.3 Aligarh Fault	223
5.11.4 Sikandra Rao Fault	224
5.11.5 Kanpur-Ghatampur Fault	224
<b>5.12 SUMMARY</b>	<b>225</b>
5.12.1 Haryana Region	225
5.12.2 Ganga-Yamuna Interfluve	226
<b>CHAPTER-6</b>	<b>229-275</b>
<b>6.1 INTRODUCTION</b>	<b>229</b>
<b>6.2 METHODOLOGIES USED</b>	<b>230</b>
6.2.1 Remote Sensing and Geographic Information SYSTEM (G.I.S.) Studies	230
6.2.2 Digital Elevation Models (DEMs) and Digital Terrain Models (DTMs)	230
6.2.3 Luminescence Dating of Soils	231
<b>6.3 IDENTIFICATION OF GEOMORPHIC FEATURES and SOIL- GEOMORPHIC UNITS</b>	<b>232</b>
<b>6.4 FIELD INVESTIGATIONS</b>	<b>232</b>
<b>6.5 MAJOR LANDFORMS IN THE STUDY AREA</b>	<b>233</b>
6.5.1 Fluvial Plains	233
6.5.1.1 <i>Floodplains</i>	233
6.5.1.1.1 <i>Ghaggar Floodplain:</i>	233
6.5.1.1.2 <i>Yamuna Floodplain:</i>	234
6.5.1.2 <i>Old Sutlej Plains –I and II</i>	235
6.5.1.3 <i>Yamuna Plains</i>	236
6.5.1.4 <i>Old and Young Katha Plains</i>	237

6.5.1.5 <i>Fluvial Plain</i>	237
6.5.1.6 <i>Fluvio-Aeolian Plain</i>	237
6.5.2 Piedmont	238
6.5.2.1 <i>Oldest Piedmont</i>	238
6.5.2.2 <i>Old Piedmont-I</i>	239
6.5.2.3 <i>Old Piedmont-II</i>	239
6.5.2.4 <i>Young Piedmont</i>	239
6.5.3. Aeolian Plain	240
6.5.4 Terminal Fans	240
6.5.5 Aravalli Hills and Pediments	241
6.5.6 Aravalli Piedmont	241
6.5.7 Paleochannels in the study area	241
<b>6.6 MORPHOSTRAITAGRAPHY OF THE STUDY AREA</b>	<b>242</b>
<b>6.7 SOIL MORPHOLOGY OF DIFFERENT MEMBERS OF MORPHO- STRAITIGRAPHIC SEQUENCE</b>	<b>243</b>
6.7.1 Member QIMS –VI	243
6.7.2 Member QIMS –V	244
6.7.3 Member QIMS –IV	244
6.7.4 Member QIMS –III	245
6.7.5 Member QIMS –II	246
<b>6.8 GRAIN SIZE ANALYSIS AND MICRO-MORPHOLOGY OF SOILS-247</b>	
6.8.1 Grain Size Analysis, and pH and EC Studies	247
6.8.2 Micromorphology	249
<b>6.9 SOIL SALINITY IN THE STUDY AREA</b>	<b>250</b>
<b>6.10 LINEAMENTS</b>	<b>251</b>
<b>6.11. MAJOR STRUCTURAL FEATURES OF THE STUDY AREA</b>	<b>251</b>

6.11.1 Methodology Used to Identify Faults	251
6.11.2 Faults	252
6.11.2.1 Ambala Faults-I and II	253
6.11.2.2 Patiala Fault	253
6.11.2.3 Markanda Fault	254
6.11.2.4 Karnal Fault	254
6.11.2.5 Rohtak Fault	254
6.11.2.6 Jind Fault	255
6.11.2.7 Hissar Fault	255
6.11.2.8 Yamuna Faults	256
6.11.2.9 Sohana Fault	256
6.11.2.10 Ghaggar Fault	256
6.11.3 Tectonic blocks	256
6.11.3.1 Piedmont Block	256
6.11.3.2 Jind-Rohtak Block	257
6.11.3.3 Aravalli Block	257
6.11.3.4 Punjab Block	257
6.11.3.5 Saharanpur Block	257
<b>6.12 Distribution of Earthquakes</b>	258
<b>6.13 GPR STUDIES</b>	258
6.13.1 Haryana Region	258
6.13.2 Ganga-Yamuna Interfluve	259
<b>6.14 INTERPRETATION AND INTEGRATION OF DATA</b>	260
6.14.1 Role of climate in the Development of the Geomorphology and soils and Cultural Changes	260
6.14.2 Structure of the Area and Nature of Faults	261



6.14.3 Tectonics, Sedimentation and Terminal Fans	263
6.14.4 The Lost Sarasvati and Drishadvati Rivers Evolution of Drainage in the Haryana Region	267
<b>6.15 CONCLUSIONS</b>	277
<b>BIBLIOGRAPHY</b>	279-291
<b>LIST OF APPENDIX</b>	
APPENDIX-1	293-306
APPENDIX-2	307-309
APPENDIX-3	310-322

## LIST OF FIGURES

FIGURE NO.	TITLE	Page No.
Fig. 1.1.	Location map of the study area with major cities and the rivers.	3
Fig. 1.2	Map showing surface geological features together with basement depth and Bouguer gravity anomaly variations (modified after Geological Survey of India, 2000).	5
Fig. 1.3	Rainfall and temperature diagrams for typical areas After C.G.W.B (2004).	10
Fig. 1.4.	Soil-moisture regime map for the study area After C.G.W.B (2004).	13
Fig 1.5	Distribution of preharappan inhabitation in Haryana and adjoining areas (after Joshi et al., 1982.). High concentration of these habitations in Jind-Rohtak and Hissar triangle present.	22
Fig. 2.1	Systematic flow-chart of the work carried out.	30
Fig. 2.2	Study area showing sample point locations, important cities and major rivers.	31
Fig. 2.3.	Boundaries soil-geomorphic units superimposed on a mosaic of Landsat MSS FCC images (WRS-1, Path- 158, Row 39 and WRS-1, Path 158, Row 40, 25 Jan & 23 Feb 2003). Abbreviations for soil-geomorphic units explained in Table 2.2.	33
Fig. 2.4	Major landforms in the study area i.e. Piedmont zone, fluvial plains, terminal fans, aeolian plain, fluvio-aeolian plain, Aravalli Hills and Pediments.	41
Fig. 2.5	Areas around terminal fans/fans, for which DEMs were prepared, are shaded. Abbreviations ending with TFn indicate terminal fans.	50
Fig. 2.6	Digital Elevation Model for areas around (a) Karnal Terminal fan (b) Markanda Terminal fan and (c) Sonipat Terminal fan.	51
Fig. 2.7	Digital Elevation Model generated for areas around (a) Katha Terminal fan (b) Young Chautang Terminal fan-IV and (c) Sahibi fan.	53
Fig. 2.8	Wetlands in the study area (After Agricultural Ground Water Cell, Haryana, (2008).	56
Fig. 2.9	Google Earth image showing Paleochannels in the study area with soil- geomorphic unit boundaries superimposed. Paleochannels are	

widely distributed in the southern part of the study area and their source lies to the north/northeast, suggesting flow of the Yamuna in this region in the past. 57

- Fig. 2.10 Distribution of soils of different members of the Morphostratigraphic Sequence of the study area. 61
- Fig. 2.12 Field photographs of QIMS-VI soils pedon A) VS-1 B) VA C) VS36 and D) Morni Hills from Oldest piedmont (OdPt). 63
- Fig. 2.13 Field Photographs of QIMS-V soils pedon A) VC-39(OdPt-II) B) V-47(ArHPm) C) V-44 (KrTFn) D) G (OdPt-I) and e) abandoned channel near Balsamand Village in Aeolian plain (APn). 65
- Fig. 2.14 Field Photographs of QIMS-IV soils pedon A) V-12 (OdYPn-III) B) V-61(OdYPn-II) C) V-36 (Fl-Al-Pn) D) VB-1 (OdYPn-I). 67
- Fig. 2.15 Field Photographs of QIMS-III soils pedon A) V-43 (OdYTFn) B) V-58 (StTFn) C) V-73 (YgKaPn) D) V-38 (OdKaPn). 69
- Fig. 2.16 Field Photographs of QIMS-II soils pedon A) V-53 (YgCgTFn- III) B) V-3 (YgChTFn- I) C) V-71 (YgCTFn- II) D) G-5 (OdSjPn-II). 71
- Fig. 2.17 DTM (Digital Terrain Model) showing lineaments directions flow of the Drishtavati River (D-I & D-II) present in the southern part of the study area changing directions with the time. The vertical exaggeration is 600 with sun angle N30<sup>o</sup>W. 79
- Fig. 2.18 Major faults in the study area superimposed over soil-geomorphic units. and major streams in the area also shown. 81
- Fig. 2.19 (a) Locations DEM areas (shaded) around faults and terminal fans. Lines along which profile are drawn across faults are drawn, also shown (Fig. 2.20a). Lines of major profiles AB and CD in Fig. 2.20b also marked. (b) Area of DEM (Fig. 2.24c, d) around the Yamuna Fault. 82
- Fig. 2.20 (a) Profiles drawn across the Faults, Ambala fault I & II (AF-I and AF-II), Rohtak fault (RkF), Patiala fault (PtF), Jind fault (JdF), Markanda fault (MaF), Hissar fault (HrF), Karnal fault (KrF) and Sohana fault (SaF). 83
- Fig. 2.20 (b) Full Profile Section drawn across the Faults a) (A-B profile) showing Ambala fault I & II (AF-I and AF-II), Patiala fault (PtF), Markanda fault (MaF), Karnal fault (KrF), Rohtak fault (RkF) and Hissar fault (HrF), b) C-D profile showing Markanda fault (MaF), Karnal fault (KrF), Jind (JdF)Rohtak fault (RkF) and Hissar fault (HrF) 84
- Fig. 2.22. Several paleochannels on the upthrown block abruptly ending against the Jind Fault. ETM+ WRS-2, Path 147, Row 039 (2000-10-15)

- Fig. 2.23 Digital Elevation Models generated by SURFER-8 around (a) Patiala Fault (b) Ambala Faults I & II and (c) Hissar Fault. 91
- Fig. 2.24 Digital Elevation Model (DEM) generated for areas (a) Rohtak Fault (b) Markanda Fault (c & d) Yamuna Faults. 93
- Fig. 2.25 Digital Elevation Model for areas around (a) the Sohana Fault (b) Jind Fault (c) Karnal Fault. 95
- Fig. 2.26 Digital Terrain Model of the study area showing tectonic blocks, major terminal fans, and faults. 101
- Fig. 2.27 Epicenter of the earthquakes occurred in the study area along with the major faults (Source-<http://asc-india.org/seismi/seis-cdh.htm>). 103
- Fig. 3.1 Schematic representation of the Luminescence Dating Principle (based on Vancreaynest 1998). 112
- Fig. 3.2 Schematic diagram showing lattice defects in crystals (after Aitken, 1998). 114
- Fig. 3.3 Energy-level diagram of TL and OSL processes (based on Aitken, 1998): (a) ionization due to exposure to nuclear radiation with trapping of electrons and holes at crystal defects; (b) storage during antiquity; (c) the electron is evicted from its trap by heating or shining light and recombines with a luminescence center under emission of TL/OSL signal. 114
- Fig. 3.4 (a) IRSL shine down curve (b) growth curves and (c) Equivalent dose plateaus for some typical samples of the study area. 117
- Fig. 3.5 Schematic instrumental setup for OSL measurements (after Aitken, 1985, 1998). 120
- Fig. 3.6. Bar diagrams for 55 IRSL ages from different soil-geomorphic units with ages arranged in a descending order. Tectonically stable periods are marked by the flat or gently sloping portions of the curve joining the tops of bars. Sharp breaks in the curve are used to define different members of the Morphostratigraphic Sequence. 125
- Fig. 4.1 Sand, silt and clay distribution with depth in QIMS-II & III soils. 129
- Fig. 4.2. Sand, silt and clay distribution with depth in the QIMS-IV-VI soils. 130
- Fig. 4.3 Variation of Total clay and Pedogenic clay in different members of QIMS. 130

- Fig. 4.4 Combined texture triangle (Schoenberger et al., 1998) and triangular plots of soils of QIMS-II. 131
- Fig. 4.5 Triangular plots of soil texture of typical pedons of QIMS-III and IV. 132
- Fig. 4.6 Triangular plots of soil texture of typical pedons of QIMS-V and VI 133
- Fig. 4.7 QIMS-II (a) moderately developed peds and partially decomposed root nodule replaced by the clay (Cy), Pedon V-53. (b) Voids filled with clay and fine silt material (green arrow) and features related to animal activity, Pedon V-3. (c) Vughs coated with thin typic calcretans and coating of void-walls with iron rich material (blue arrow). Pedon V-71. (d) Very weakly developed peds and channels coated with calcretans, Pedon V-G5. 135
- Fig. 4.8 QIMS-III (a) Channel and the roots are filled with typic-micritic calcite materials (CN) and Fe/Mn hypo-coating, granostriated b-fabric, Pedon V-43. (Please Fe-Mn coating and granostriated fabric by different coloured arrow and mentioned with brackets aster each feature) (b) Granostriated b-fabric with weakly developed ped, channel filled with calcite material and chamber structure, Pedon V-58, (c) Weakly developed ped faces with voids coated with calcretans, Pedon V-73 (d) Thin ferriargillan quasi-coating along the channel, bow-like structure present towards left central part, suggesting animal activity, Pedon V-38. 135
- Fig. 4.9 QIMS-IV (a) Moderately developed sub-angular blocky structure, channels coated with at places with calcium carbonate and ferriargillan, Pedon V-12, (b) Channels upper part filled with ferriargillan material and lower part filled with CaCO<sub>3</sub> material, voids coated with typic micritic calcretans, Pedon No. V61 (c) Porous micro-aggregates composed of humified excrement features and ferriargillan coating Pedon V-36, and (d) Root channels filled CaCO<sub>3</sub> and later replaced Fe/Mn materials Pedon VB-1. 137
- Fig. 4.10 QIMS-V (a) Thin pellicular alteration of biotite, and weakly developed reticulate b-fabric, Pedon G, (b) Moderately to well developed peds separated with chambers coated with calcretans, Pedon V-25, (c) Well impregnated Fe/Mn nodule (ND) with sharp boundaries, Pedon V-44, and (d) strongly developed rounded ped structure, serrate to smooth ped-void surface poro striated and stipple-speckled b-fabrics in groundmass, Pedon V-47. 137
- Fig. 4.11 QIMS-VI (a) Well developed peds with multi-nucleated well impregnated Fe/Mn nodule (ND), Pedon VS-1, (b) Moderately to strongly developed prismatic structure (P), partially accommodating ped faces Pedon VA, (c) Deformed reticulated b-fabric with minute Fe/Mn nodules, and pellicular alteration of biotite released Goethite, Pedon No. V-36 (d) Very well developed peds with well accommodated ped faces, Pedon VC-3. 139

Fig. 5.1 Schematic diagram of working principle of GPR system (After Neal, 2004).	149
Fig. 5.2 Location of the GPR profile sites in the study area.	152
Fig. 5.3 Systematic Diagram of GPR system hardware.	153
Fig. 5.4 (a) Annotated GPR profile T-1 across the Ambala Fault, showing sequences/subsequences, lithofacies and faults. (b) Outline diagram showing different features of the GPR profile T-1.	163
Fig. 5.5 Annotated GPR profile T-10 is from the Old Yamuna Terminal Fan near Narwana city, showing sequences/subsequences and lithofacies.	163
Fig. 5.6 (a) Annotated GPR profile T-2 across the Ambala Fault-II, showing sequences/subsequences, lithofacies and faults. (b) Outline diagram showing different features of the GPR profile T-2.	165
Fig. 5.7 (a) Annotated GPR profile T-3 across the Patiala fault, showing sequences/subsequences, lithofacies and faults. (b) Outline diagram showing different features of the GPR profile T-3.	169
Fig. 5.8 Annotated GPR profile T-11 is from Fluvial plain near Hansi city, showing sequences/subsequence and lithofacies	169
Fig. 5.9 (a) Annotated GPR profile T-4C across the Markanda fault, showing sequences/subsequences, lithofacies and faults. (b) Outline diagram showing different features of the GPR profile T-4C.	171
Fig. 5.10 Annotated GPR profile T-4A is from the middle part of Markanda Terminal Fan, showing sequences/subsequences and lithofacies.	171
Fig. 5.11 Annotated GPR profile T-4B is from the distal part of Markanda Terminal Fan, showing sequences/subsequences and lithofacies.	175
Fig. 5.12 a) Annotated GPR profile T-5 across the Rohtak fault, showing sequences/subsequences, lithofacies and faults. (b) Outline diagram showing different features of the GPR profile T-5.	175
Fig. 5.13 (a) Annotated GPR profile T-6 across the Hissar fault, showing sequences/subsequences, lithofacies and faults. (b) Outline diagram showing different features of the GPR profile T-6.	177
Fig. 5.14 Annotated GPR profile T-7 is from the distal part of Young Chautang Terminal Fan-I, showing sequences/subsequences and lithofacies	177
Fig. 5.15 Annotated GPR profile T-8 is from the middle part of Young Chautang Terminal Fan-I, showing sequences/subsequences and lithofacies.	179

- Fig. 5.16 Annotated GPR profile T-9 is from the proximal part of Young Chautang Terminal Fan-I, showing sequences/subsequences and lithofacies. 179
- Fig. 5.17 Structural map of the Ganga, Yamuna & Doab region showing important fault locations and their associated Terminal Fans, Piedmont Plain, Flood Plains, Paleochannels and Old and Young River Plains of Ganga and Yamuna Rivers. After Bhosle et al.(2008). 191
- Fig. 5.18 (a) Shows soil geomorphic units, faults and GPR location superimposed on IRS 1D False colour Composite of Wifs data of March, 2000. Abbreviations for different faults and soil-geomorphic units given in Fig. 18c. 193
- Fig 5.18 b) Show the Landsat MSS image (band combination 1-4-2) of the Iqbalpur Terminal Fan showing GPR points location and the Jhaberera Fault c) Ganga Yamuna interfluve marked with soil geomorphic units faults and GPR locations.  
Abbreviation used for Faults- HFFt- Himalayan Frontal fault, SFt Solani Fault MuFt- Muffaranagar Fault, GFt- Ghaziabad Fault, DFt Delhi Fault, KAF- Aligarh Fault, SRFt- Sikandra Rao Fault, AMFt- Aliganj-Mianpuri Fault, KBFt- Kannauj-Bidhuna Fault, Kanpur-Ghatampur Fault. Abbreviation used for the soil geomorphic units- PdP- Piedmont plain, RP- Roorkee Plain, GSP- Ganga-Solani Plain, OGYF, Old Ganga Yamuna Plain, EMF- East Mujaffarnagar fan, YHP- Young Hindon Plain, MHP- Meerut Hapur Plain, Bf- Baghpat fan, YPa- Yamuna Paleochannel, SJP, Sikandra Rao-Jewar Plain, KAF- Khurja Aligarh fan, IRF- Iglas-Raya fan, OGP-I&II- Old Ganga Plain-I & II, EP-I & II- Etawah Plain -I & II, KBF- Karhal-Bidhuna fan, KF- Kanpur fan, SRF- Sirathu fan. 195
- Fig. 5.19. DEM of the Iqbalpur Terminal fan and the Jhaberera fault region. 197
- Fig. 5.20 (a) Annotated GPR profile D-5 across the Gaziabad Fault, showing sequences/subsequences, lithofacies and faults. (b) Outline diagram showing different features of the GPR profile D-5. 201
- Fig. 5.21 Annotated GPR profile D-4 from Deoband area over a Ganga River paleochannel, showing sequences/subsequence and lithofacies 201
- Fig. 5.22 (a) Annotated GPR profile D-7 across the Aligarh Fault, showing sequences/subsequences, lithofacies and faults. (b) Outline diagram showing different features of the GPR profile D-7. 205
- Fig. 5.23 Annotated GPR profile D-11 from the Karhal-Bidhuna Terminal Fan, showing sequences/subsequence and lithofacies 205
- Fig. 5.24 (a) Annotated GPR profile D-6 across the Delhi Fault, showing sequences/subsequences, lithofacies and faults. (b) Outline diagram showing different features of the GPR profile D-6. 209

- Fig. 5.25 Annotated GPR profile D-9 from the Akarabad area on the Aligarh-Khurja Terminal Fan, showing sequences/subsequence and lithofacies. 209
- Fig. 5.26 (a) Annotated GPR profile D-13 across the Kanpur-Ghatampur Fault, showing sequences/subsequences, lithofacies and faults. (b) Outline diagram showing different features of the GPR profile D-13. 211
- Fig. 5.27 Annotated GPR profile D-15 is from the central part of Aligarh-Khurja Terminal Fan, showing sequences/subsequence and lithofacies. 211
- Fig. 5.28 (a) Annotated GPR profile D-8 across the SikandraRao Fault, showing sequences/subsequences, lithofacies and faults. (b) Outline diagram showing different features of the GPR profile D-8. 213
- Fig. 5.29 Annotated GPR profile D-16 is from the Karhal-Bidhuna Terminal Fan, near Mainpuri Town, showing sequences/subsequence and lithofacies 213
- Fig. 5.30 Annotated GPR profiles (a) D-1 from the proximal area (Iqbalpur village), (b) D-2 from central part (Jhaberera Village) and (c) D-3 from (Zabardastpur Village) distal part of Iqbalpur Terminal fan, respectively, showing sequences/subsequence and lithofacies. 217
- Fig. 5.31 Annotated GPR profile D-17 over the Ganga Paleochannel near Barla village, showing sequences/subsequence and lithofacies. 219
- Fig. 5.32 Annotated GPR profile D-12 from the Karhal-Bidhuna Terminal Fan, showing sequences/subsequence and lithofacies. 219
- Fig. 5.33 Annotated GPR profile D-10 near Nidhauri village on Aligarh-Khurja Terminal Fan, showing sequences/subsequence and lithofacies 221
- Fig. 5.34 Annotated GPR profile D-14 from the Aligarh-Khurja Terminal Fan, showing sequences/subsequence and lithofacies. 221
- Fig. 6.1 Displacement pattern in the in case where the northern boundary is fixed. Compression is from SW. (after Das et al., 2009). 263
- Fig. 6.2 Diagrammatic sketch showing different longitudinal faults in the Haryana plain as imbricates of the HFT (Himalayan Frontal Thrust). 265
- Fig. 6.3 The Proto-historic sites lie in straight lines (marked in red), which on northward extension meet the modern Yamuna River, suggesting that the Proto-Yamuna River flowed through these regions in those times(modified after Valdiya (2002)). 267
- Fig. 6.4 Schematic diagrams showing shifting of the Rivers Yamuna and Sutlej since about 3000 B.C. 269



## LIST OF TABLE

TABLE NO.	TITLE	Page No.
Table 1.1	Litho-stratigraphy of study area (Modified after Kochhar 1984 and Pareek 1984).	2
Table 2.1	Information of Terminal fan and their DTMs in the study area	49
Table 2.2	Ages of Members of Morphostratigraphic Sequence and various soil-geomorphic units included in each member.	59
Table 2.3	Important field characteristics of soils of the study area.	107
Table 2.4	Strike, exposed length, throw of faults, time of last activity of various faults observed in the study area. Characteristic features of DEMs of regions around these faults also given.	90
Table 3.1	Radioactivity values, depth of IRSL samples, equivalent dose and absolute ages of dated samples from different morphostratigraphic members (QIMS-VI - I).	122
Table 5.1	Showing annotation used in description of GPR profiles.	161

---

## 1.1 INTRODUCTION

Major parts of the Haryana state lie in the western part of the Indo-Gangetic plains of India (Himalayan Foreland Basin) between the Aravalli Hills in the south (northernmost extensions) and the Siwalik Hills of the Sub-Himalayas in the north (Fig. 1.1). This basin has been a scene of tectonic activities since about the Mid Miocene (Parkash et al., 1980). Also, parts of the Thar Desert just southwest of this area witnessed significant climatic fluctuations in the middle and late Holocene period (Singh, 1971; Singh et al., 1974) and this adjoining area appears to have been and extensively referred to in the *Vedas* (Oldest scriptures of the Hindus) affected by these climatic vicissitudes. The region was drained by the mighty rivers-Sarasvati and Drishadvati (now extinct or represented by smaller streams). This also points to the significant changes in the courses/discharges of the rivers of the area in the late Holocene. Archeological records show that the area has been inhabited by human settlements at least from the time of Pre-Harappan period (>5000 B.P). Presently with overpopulation, the region is over exploited leading thereby to environmental degradation.

The climatic changes as well as instability caused by tectonic activities are expected to be reflected in the form of typical landforms and soils of the area. The present study attempts a detailed mapping and descriptions of the landforms and related soils and aims at the reconstruction of controlling factors i.e. climatic changes and the tectonic activity in the area during the Holocene period and their effects on drainage pattern changes in the area. For achieving these objectives, as first step, soil geomorphic units of the area

have been mapped using remote sensing and GIS techniques. This was followed by extensive field studies of these units for soil-morphological description of typical profiles and collection of soil samples. Laboratory studies were done for micromorphological and granulometric investigations of selected profiles, along with the Optical Stimulated Luminescence dating of soils from typical profiles. In addition, Ground Penetrating Radar studies were also carried out for confirmation of faults inferred from geographic information approach and analysis of sedimentary facies up to a depth of 15 m. Further attempts have been made for finding clues regarding the presence/absence of a large river (Yamuna River) in the recent past.

## **1.2 LOCATION, GEOLOGY AND GEOMORPHOLOGY OF THE STUDY AREA**

Haryana is a landlocked state in the northern India. It is located between 27° 39' to 30° 55' N and 74° 27.9' to 77° 36' E (Fig. 1.1). The altitude varies from 200 to 312 m (a.m.s.l.) in the plains (Indogangetic plains), though it may reach up to 2000 m in the Siwalik hill ranges in the northeastern region. Plains are marked by flat topography, except for a steeper slope toward SW in the northeastern alluvial piedmont (locally called as '*Bhabbar*') located south of the Siwalik Hills. Undulating, low height Aravalli hills are present and are exposed in the southern part.

### **1.2.1 Geology of the study area**

Along the southeastern margin of the area in Aravalli Hills, Delhi Supergroup including Alwar and Ajabgarh Groups, consisting of quartzites, marble interactions, phyllites and slates are exposed (Table. 1.1). These rocks are intruded by more than one phase of acidic and basic intrusives,

which mainly comprise dykes and sills of amphibolites, rhyolite, granite plutons, and pegmatite, quartz and aplite veins. The rocks of Delhi Supergroup are supposed to be deposited in linear trenches, which were slowly sinking in the NNE direction (Singh, 1982; 1988).

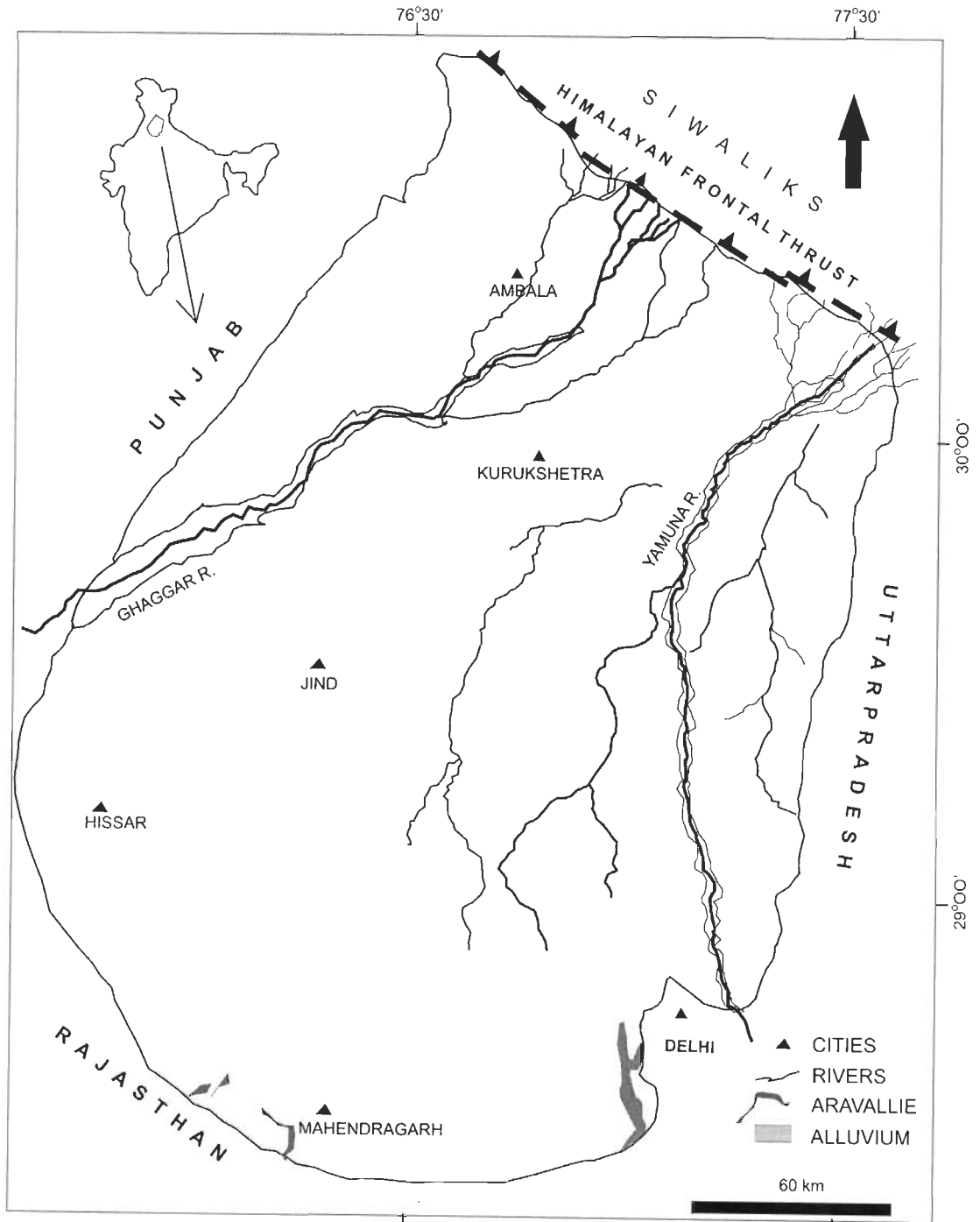


Fig. 1.1. Location map of the study area with major cities and the rivers.

Along northern boundary of the study area, the Siwalik Supergroup rocks are exposed and essentially comprise a sequence of sandstone, conglomerate and clay alteration, representing Upper and Middle Siwalik. Between the Siwalik Ranges and Aravalli Hills lie the vast flat plains in the area with little significant topographic relief.

Table 1.1. Litho-stratigraphy of study area (Modified after Kochhar 1984 and Pareek 1984).

Age	Formation
Holocene	Aeolian Sediments Younger Alluvium of Ghaggar and Yamuna river basin. Ambala Older Alluvium of Central plains
Upper to Middle Pleistocene	..... <b>Disconformity</b> ..... Older Fans and Piedmont ..... <b>Fault</b> .....
Middle Pleistocene to Middle Miocene	Siwaliks ..... <b>Unconformity</b> .....
Lower Cambrian to upper Proterozoic	Sandstone-claystone of Marwar Supergroup of Rajasthan Basin. ..... <b>Unconformity</b> .....
Lower part of Upper Proterozoic-Middle Proterozoic	Delhi Supergroup

### 1.2.2 Basement

Basement Structure has a very strong influence on the evolution of the Indo-Gangetic basin (Agarwal, 1977; Singh, 1987, 1992, 1996; Bajpai, 1989; Singh et al., 1989, 1996, 1997, 1999b; Mohindra et al., 1992; Parkash et al., 2000). The present study area lies in the western part of the Indo-Gangetic basin bounded in the south and southeast by the rocks of the Delhi supergroup, the exposures of which form

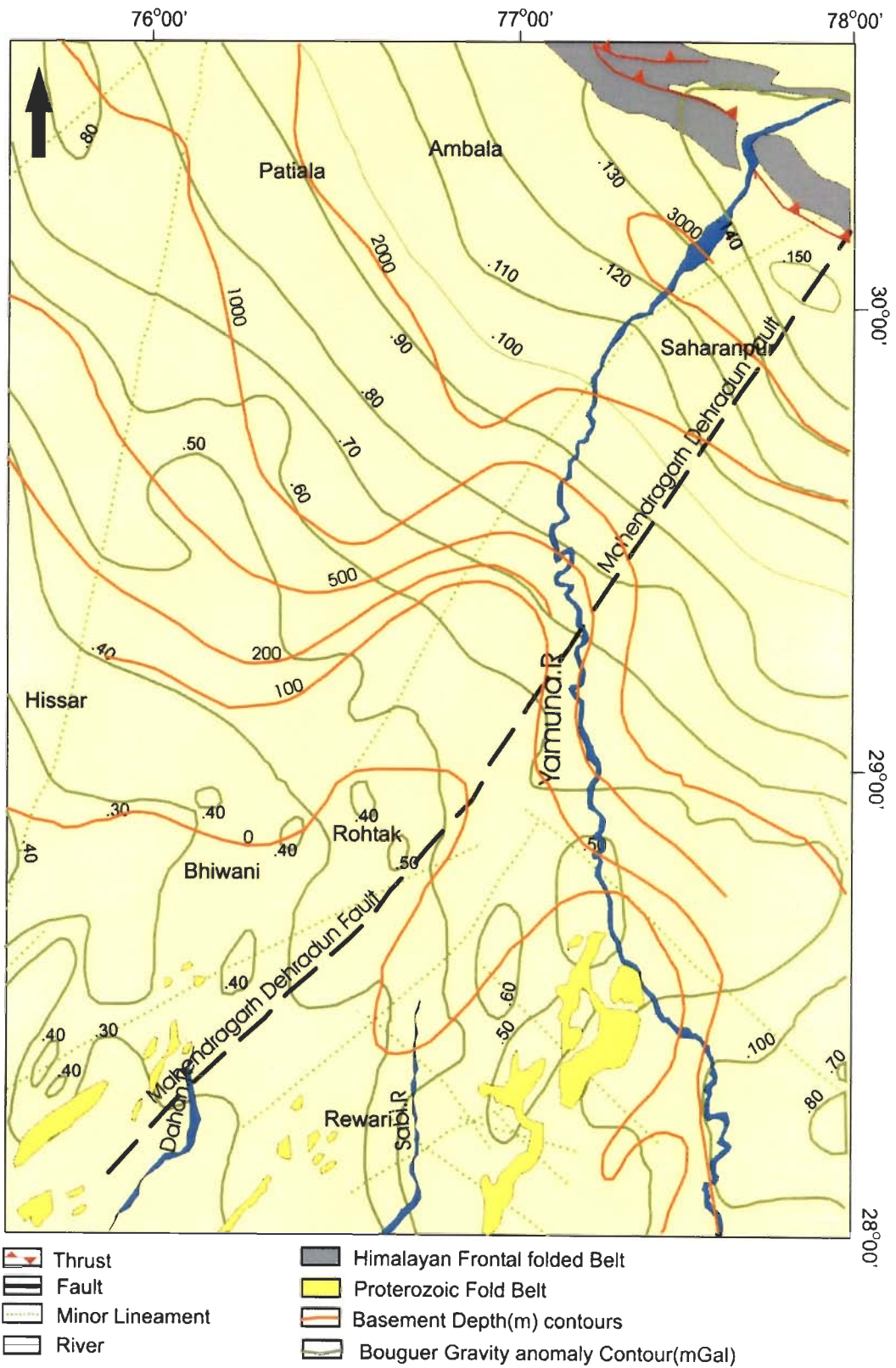


Fig. 1.2 Map showing surface geological features together with basement depth and Bouguer gravity anomaly variations (modified after Narula et al., (2000)).

northeast-southwest trending Aravalli ridges and in the north by the Himalayan orogen. In the southeastern margin the rocks of the Delhi and Aravalli tectonic trend extend towards the Himalayan orogen up to Muzarfarnagar, north of which, there is a basement low (>6000 km<sup>2</sup>) (Eremenko and Negi, 1989). This ridge was considered to have acted as drainage divide between the Indus River and Gangetic River drainages till about the Pleistocene, based on the aeromagnetic surveys (Sastri et al., 1971; Rao, 1973; Khan et al.; 1996). Basement map by Geological Survey of India (2000) shows that the basement below the Haryana plains is a broad surface which gently slopes towards southeast. A subsurface ridge striking NE-SW is present below the Yamuna River (Fig. 1.2).

### **1.2.3 Structural features**

Contact of the Gangetic Plains with Siwalik Ranges was observed to be a thrust, named as Himalayan Frontal Fault (HFT) by Nakata (1982). Singhai et al. (1991) mapped this thrust in the present area. Garlapuri (1981) postulated a fault called Yamuna fault on the western side of the Yamuna Floodplain and the Aravalli ridge is bounded in the east by this fault. Later Singhai (1991) extended this fault from the point where the Yamuna enters the plains to Delhi and Kumar et al. (1991) extended it to Allahabad and found it be curved in nature with convexity to the SW. From soil-geomorphological mapping, Singhai et al. (1991) also postulated Ghaggar Fault, as Panjab and Haryana blocks had acted independently during the Late Holocene period, and a fault at the base of the old Piedmont Zone, north of which it was uplifted and was incised highly by streams coming out of the Siwalik Ranges.

#### 1.2.4 Geomorphic Units of the Study Area

Geomorphically the area is subdivided into the following four geomorphic units from South to North (<http://wikipedia.org/wiki/Haryana>):

1. Older Fans and piedmont bordering the Siwaliks in the North.
2. Central Alluvial Plains.
3. Pediplains and structural cum denudational hills of the Delhi Supergroup in the south.
4. Aeolian Plains.

##### 1.2.4.1 Older Fans and Piedmont

The older fans occur individually, as well as composite Piedmont, abutting against the southern slopes of the Siwalik Ranges. The fans have a gentle slope of  $3^{\circ}$  to  $5^{\circ}$  towards south. The piedmont is fairly well incised by the present day drainage of the Ghaggar and the Yamuna Rivers. Sediments of this region consist of the pebble-boulder sequence derived from the Siwaliks. Major soils are Udic Ustocherpts.

##### 1.2.4.2 Central Alluvial Plains

It is a featureless alluvial plain with minor rolls in the topography. The altitude varies from 200 m in the south to 312 m in the north, with gentle slope towards south. Several paleochannels have been identified in these plains by Bakhiwal and Grover (1988); Chopra et al. (1988). These are mainly of fluvial regions. However, at places in southern and western regions, fluvial sediments are reworked into dunes locally. Dominant soils are Typic Ustorepts in well drained areas and Natric Ustochrepts and Fluventic Ustochrepts in moderately to poorly drained areas. In southern and western



areas, where these have been reworked by wind, we get Typic Torripsamments.

#### *1.2.4.3. Aravalli Hills and Pediplains*

In southern parts, mainly Aravalli Hills (structural-cum-denudational hills) consisting of Delhi Supergroup of rocks (mainly red quartzites) are exposed. Pediplains have developed skirting Delhi Supergroup both along the northern as well as the eastern side of the hills. The pediplains on the eastern side form a narrow strip before imperceptibly merging with fluvial sediments of the Yamuna River (Thussu, 1995).

#### *1.2.4.4 Aeolian Plains*

Sand flats consisting of loose sands are the major features of the area, and are overlain by the Typic Torripsamments. At places low height dunes are observed.

### **1.3 CLIMATIC CONDITIONS**

The hot and arid desert known as Thar dessert occupies in the south west of the Haryana where as the Himalaya forms the northern boundary of the state. The climate of Haryana over most of the year is of a pronounced continental character. It is very hot in summer and markedly cold in winter. The hottest months are May and June and the coldest being December and January (<http://wikipedia.org/wiki/Haryana>). Most of the area of study fall falls under arid to semiarid climatic zone with an average rainfall of 455 mm. Around 70-80% of rainfall is received during the months from July to September and the remaining 20-30% rainfall is received during December to February. Rainfall varies aerielly also, with the Siwalik Hills region in the

northeast being the wettest and the Aravalli Hills region in the southwest, being the driest. Haryana region has no other perennial river except the Rivers Yamuna flowing in the east and Ghaggar in the west. The only river which flows through Haryana is the Ghaggar River, which passes through northern fringes of the state. Overall climate of the area can be broadly referred to as subtropical and semiarid with average annual rainfalls of 993.8

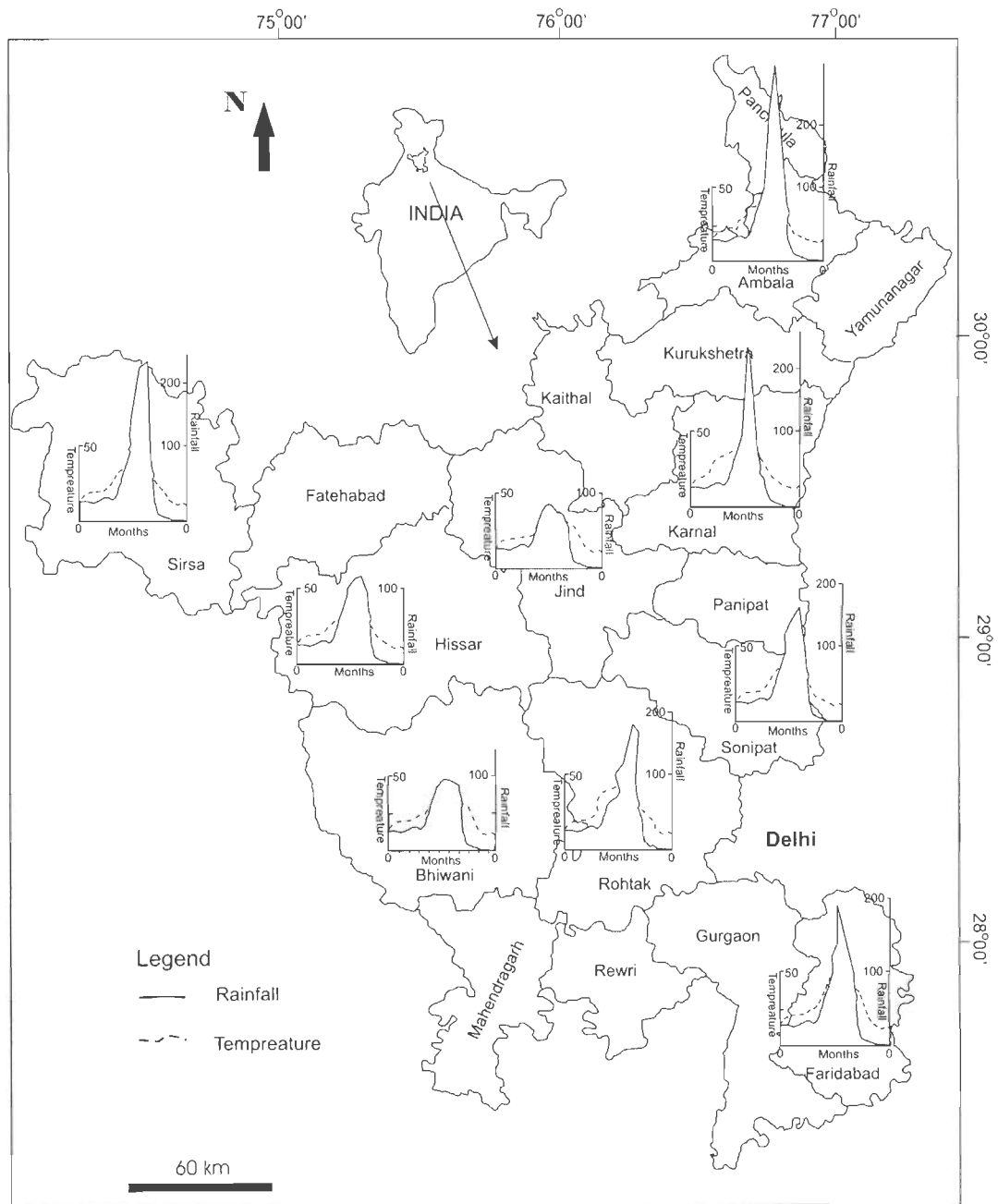


Fig. 1.3 Rainfall and temperature diagrams for typical areas After C.G.W.B (2004).

mm in the northeast and 290.3 mm in the southwest, respectively. A considerable variation exists between the normal, mean, maximum (June) and minimum (January) temperatures for the study area. The mean monthly temperature is as high as 40°C during the hottest months i.e. May and June in the plains and 30°C in the hilly areas, while the mean monthly temperature is as low as 1° to 3° C in the plains and +/- 2° C in the hilly areas in the coldest months (Fig. 1.3). The temperature variation follows an upward trend from February until it reaches maximum (about 40°C) in the month of June. During the intense summer months, high velocity dust storms have also been experienced. With the onset of monsoon, although temperatures tend to drop, fairly high temperature prevails till October, beyond which the monthly minimum is reached in the month of January.

In general, summers are extremely hot and winters cool (<http://www.webindia123.com/Hariyana/land/land.htm>). The presence of the mountains in the northeastern region greatly modifies the temperature. Temperature increases and the rainfall decreases as the southward distance from the Himalaya, increases.

#### **1.4 SOIL MOISTURE REGIMES**

Temperature and rainfall being the two basic components of climate, other parameters like relative humidity, potential evapo-transpiration (PET) follow nearly similar trends in the area. It is seen that PET – demand records steep rise with rising temperature and decrease in the relative humidity from the month of February to May. The increased relative humidity during monsoon months results in the low evaporative demands, whereas prevailing temperature conditions are responsible for low PET during winter months.

As mentioned earlier, there is climatic trend of decreasing rainfall and increasing temperature from the Himalaya in the northeast toward southwest. Likewise, Soil-moisture regimes also exhibit a systematic variation from the NE to SW i.e. from Perudic, Typic Udic, Typic Ustic, Aridic Ustic to Typical Ardic (Fig. 1.4).

## **1.5 LANDUSE**

Major parts of the plains are under cultivation, except for minor areas, which are barren, due to mainly salinity and/or alkalinity of soils. Currently efforts are being made to treat and reclaim such areas for the cultivation and other uses. The Siwalik Ranges and parts of the Piedmont zone are forested. Mainly the crops of Haryana are Kharif and Rabi crops. The main Kharif crops are sugarcane, groundnut, paddy and maize. Minor Kharif crops include chillies, bajra, jowar, pulses and vegetables. The main Rabi crops are gram, wheat, barley and oil seeds. Minor Rabi crops are massur, barseen, methi, onion and winter vegetables. Extensive network of canals and tube-well system have put Haryana into one of the front line states of India in terms of agricultural production.

## **1.6 PREVIOUS WORK**

### **1.6.1 Soils and Geomorphology**

Geomorphological and soil characters of this area have been of interest to both the soil scientists and geoscientists. Most of the studies deal with small area for soil characters such as granulometry, clay mineralogy,

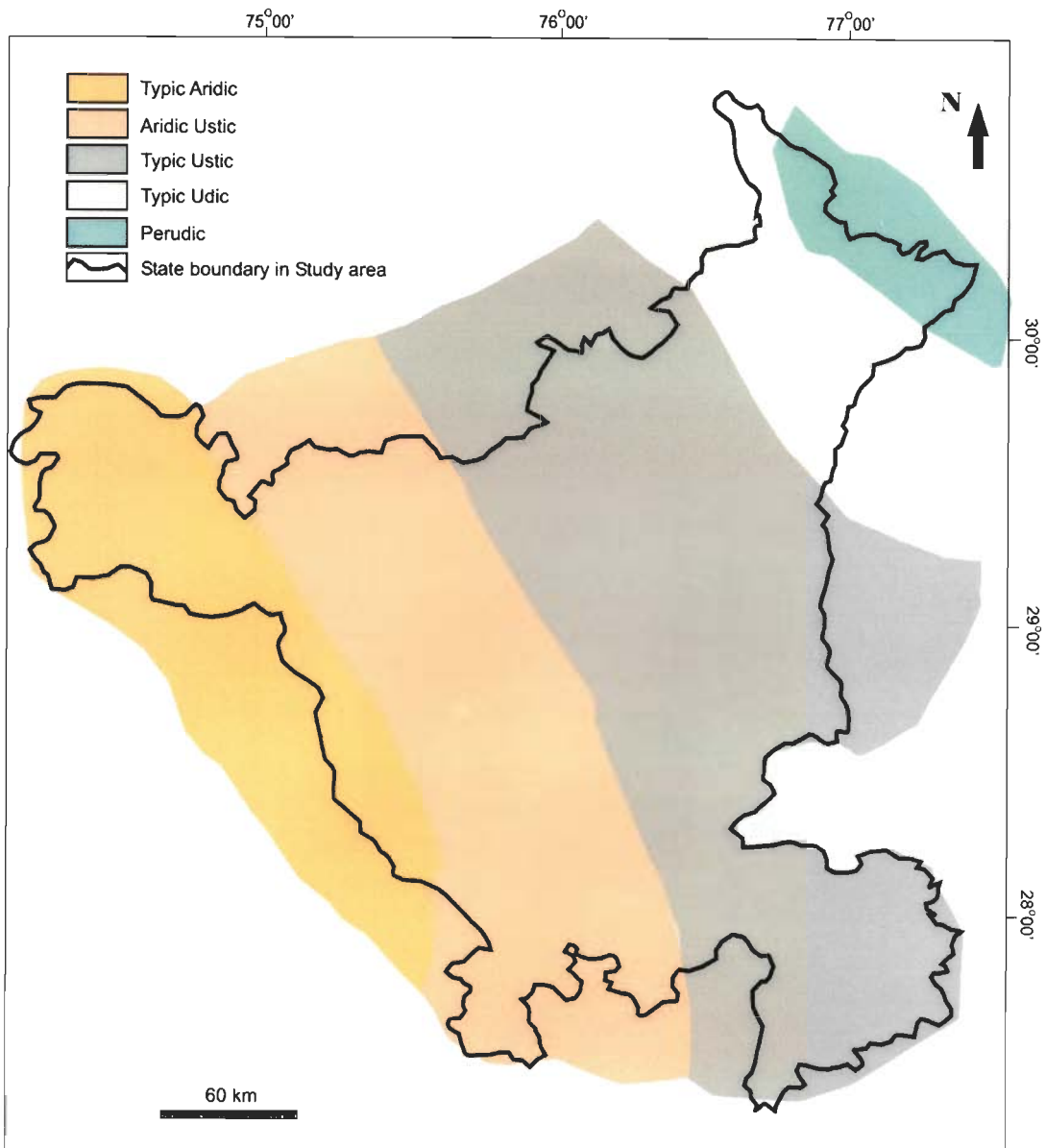


Fig.1.4. Soil-moisture regime map for the study area After C.G.W.B (2004).

micromorphology and soil taxonomy and only a few workers have provided regional picture of the area.

A major report by Dhankar et al. (1983), related to the geomorphology, soil and land-use of Haryana state has been prepared but relates mainly to the agricultural point of view. Some studies of soil and geomorphological interrelationship for limited fluvial area were conducted by a number of

workers (Bhandari et al., 1976; Khanna et al., 1977, Ahuja et al. 1978; Sangwan, 1978; Garalapuri et al., 1978, Manchanda and Khanna, 1979; Goyal, 1981).

Some of the pioneer workers like Ahuja and Khanna (1983) subdivided the Ghaggar river basin into i) relict channel courses, ii) levees and bars, iii) undifferentiated plain, and iv) old basin. The Yamuna alluvial plain has been classified into four Plains (i) Recent floodplain, (ii) Young meander plain, (iii) Old meander plain, and (iv) Old alluvial plain.

Roy et al. (1967) brought out the role of the fluvial and aeolian processes in the development of various soil groups in the western Rajasthan and Shankarnarayan and Hirekerur (1972) worked on similar lines in the northern Indian plains, including Haryana. Gupta et al. (1976) clearly brings out that the alternate layers of the aeolian and fluvial origin strata in the Ghaggar-Hakra river basins in Rajasthan, indicating that these processes have been acting in this region for a fairly long time in the adjoining Rajasthan state, probably including the adjoining Haryana.

Soil salinity has drawn the attention of scientists since the late eighteen century, when Medlicott (1878), Voelcher (1897), Center (1880), Leather (1897), Desigmon (1927) and Sen (1958) tried to find answer to the salinity of Indian soils taking scanty rainfall as the major factor for soil salinity, followed by temperature as a minor factor. Later in the seventies some workers (Govindrajan et al., 1970; Bhargava et al., 1972; Kaushik and Shukla, 1977) tried to explain the cause of the salinity on the basis of the poor drainage and high water table. Manchanda (1979) found a strong relationship between the landform units and salinity-alkalinity.

Manchanda et al. (1983) pointed out that thin-section analysis of the soil in these areas is very important because mere increase in the clay content and the shining ped faces as observed in the field are not sufficient for the recognition of an argillic horizon. In the studies made in the Haryana and Northwestern parts of the Indo-Gangetic plains, Bhargava et al. (1985) reported the clay illuviation in the sodic soils.

Mineralogical studies have been made by many workers giving the essential and accessory mineral assemblages in the soils of the Haryana State (Ahuja et al., 1978; Sidhu et al., 1976). Manchanda (1979, 1984) investigated the coarse fraction mineralogy of the alluvial soils of Haryana state and revealed that the essential minerals in the soil of these areas are quartz, muscovite and albite, whereas the minor constituents are tourmaline, hornblende biotite, chlorite etc. Other accessory minerals in the soils of Haryana State are zircon, garnet, rutile and apatite. In many cases secondary calcites are also reported in this area.

Distribution of the clay minerals in the region of the Punjab and Haryana was given in the report by Sehgal and Coninck (1971) and Sehgal (1974). They found that in addition to the dominant mineral illite some kaolinite and inter-grade minerals such as chloritised vermiculites in place of the chlorite are present in the soils. Sidhu and Gilkes (1977) contended that the true chlorite is of wider occurrence in the northwestern India. Shehgal and Coninck (1971) found the contents of various clay minerals as illite (2-13%), kaolinite (10-26%), chlorite (10-40%), smectite (2-13%) in the clay fractions of soils of Haryana. In addition Kapoor et al. (1982) found that apart from illite (24-34%) and chlorite (10-20%) appreciable amounts of smectite (10-40%)

and mixed layers of mineral like illite-chlorite and illite-smectite (15-30%) are present in clay fraction of the soils from the Hissar, Tohana, Suniarheri and Bhauri soil series of Haryana and Punjab.

Calcium carbonate accumulation in the soils of Haryana State was a point of interest since it was reported first by Sen (1958) in the soils around Karnal. In this area alkalinity of the soil was found to be very high, which was explained due to the excessive presence of the calcium carbonates in the form of nodules. This report was further confirmed by the Roy Choudhary (1963), who reported the presence of calcium carbonate nodules from B and C horizons. Further Sehgal and Stoops (1972) inferred that carbonate accumulation of the pedogenic calcite in the soils of the arid and semiarid plain regions of erstwhile Punjab including Haryana.

Total elemental analysis of Haryana soils has been carried out by Ahuja (1978), Manchanda (1979) and Goyal (1981) and they computed molar ratios like  $\text{SiO}_2 / \text{Al}_2\text{O}_3$ ,  $\text{Al}_2\text{O}_3 / \text{Fe}_2\text{O}_3$  etc. for working out weathering intensity of the soils in the area. Bhumla et al. (1964) have reported total traces elements and available micronutrients from the alluvial soils of Panjab and Haryana. They find that the copper and zinc contents increase with the increasing contents of clay + silt in the soils, whereas the manganese contents increase with the depth.

Limited studies of the micromorphology of the soils of Haryana have been given by the Kooistra (1982) and Manchanda and Hilwig (1983). Kooistra (1982) has investigated two soil profiles for micro-morphologically i.e. Zarifa Viran Series (Central Soil Salinity Research Institute Farm, Gudah, Karnal) and Ladwa series profile (Haryana Agriculture University Farm,



Hissar) as a part of study of micro-morphology of seventy benchmark soils of India. He reported common infillings of the voids, composed of clay (e.g. argillians) in the soils of Zarifa Viran Series.

Courty and Fedoroff (1985) described in detail micromorphology of four recent soils and eleven buried soils under the archeological sites of the Proto-Historic period (5000 BP) to the 1500 AD in the plain areas of the districts of the Hissar, Sirsa and Hansi. Major micro-morphological features of both buried and recent soils are attributed to the biological activity and translocation clay and silt and carbonates. A proportion of mica flakes in sand becoming smaller is taken as the evidences of lack of alluvial sedimentation and greater aeolian activity since the proto-historic time. As soils are comparatively young, influence of parent material on the pedogenesis is found to be significant. They also proposed a model of formation of dense kankar in these soils.

Surfacial sediments of the Indo-Gangetic Plain have been divided into the Older Alluvium and the Younger Alluvium locally called as *Bhangar* and *Khaddar*, respectively (Wadia, 1966, p.394). The *Bhangar* occurs in the elevated areas and contains calcite concentration (called *kankar*) and earlier assigned the Pleistocene age, though now this has found to of Early Holocene age in most of places (Singh et al., 2006; Bhalse et al., 2008). The *Khaddar* occurs at the lower terrains adjacent to the river channels. Manchanda (1981) has assigned the plains around Rohtak as *Khaddar*. However, no such detailed distinctions have been made on the regional scale for the soils of Haryana.

Ostracoda from the lacustrine marl deposits from Haryana have been described by the Bhatia and his students. They dated calcrete from Bhiwani area, using carbon radiometric methods and gave ages of 5363± to 3640 yrs BP. They attributed the presence of lacustrine deposits to a humid phase in the area (Bhatia and Khosla, (1977) and Singh, (1981)).

Haryana and its adjoining area of Punjab have witnessed changes in the river courses, discharges since the proto-historic time. The paleo-drainage i.e. paleo-channels of the area has been described up by many workers (Oldham, 1874, 1893; Cunningham, 1877; Riapson, 1914; Keith, 1922; Dey, 1927; Stein, 1942; Singh, 1952; Krishnan, 1952; Indras, 1967; Vashisitha, 1962; Wadia, 1966; Sarma, 1974; Kar and Ghosh, 1984). One of the interesting papers on this has been of Pal et al. (1980), who attributed the change in the course and discharges of the river under the consideration due to the tectonics. Kar and Ghosh (1984) found that the climatic change was the major cause and to a small extent tectonics is also a factor. Also, shifting of the River Yamuna alternately to the Indus and Ganga river systems has been assigned as a major factor in the observed changes.

Role of tectonism has been invoked by the Manchanda (1981) to explain the distribution of the salinity in the Punjab and Haryana regions. He suggested the presence of two faults, one fault being roughly along topographic depression on the western side of the Aravalli hills and is thought to extend in Punjab across the Ghaggar River and the other one trending roughly along Jind -Karnal towns. Movement along these faulting resulted in the ponding in this area was thus the major contributor of salinity in this region.

### 1.6.2 Sarasvati, The Lost River

The Sarasvati, 'the Lost River' has been of great interest to scholars of Archaeology, Ancient History and Geology. Based on seminar and other proceedings (Radhakrishna and Merh, 1999) and the review of status of research on Vedic Sarasvati River by the Valdiya (2002) the following can be summarized here. The Sarasvati River ranked as one among large mighty rivers of the NW India like Shatadaru (modern Sutlej), Vipasa (modern Beas), as amply eulogized in hymns of the Rigveda, the oldest oral tradition of human race. The Sarasvati River followed the course of the presently a seasonal, small Ghaggar River in the study area. Further west, it flowed along the courses of the Hakara and Nala streams in Pakistan to meet the Bay of Cambay.

The Sutlej River formed a tributary of the Sarasvati, as first propounded by R. D. Oldham (1886) and Pandya (1967) and later conclusively showed by Pal et al. (1980) by mapping of paleochannels of the Sutlej, using satellite images. They showed that earlier the Sutlej flowed southward to meet the Sarasvati near Patiala and later it migrated in distinct steps to join the Beas River.

Many workers have suggested that the Yamuna flowed through Haryana and joined the Ghaggar River (Oldham, 1886; Oldham, 1893; Raike, 1968) thus giving the Sarasvati a huge discharge. In fact Raike (1968) had suggested that the Yamuna changed its courses alternately to become parts of the Ganga and Indus drainage systems, but geological evidences for flow of the Yamuna through Haryana plains are lacking.

A large river called Drishadvati flowed along the presently seasonal small stream of Chautang (Bhargava, 1964, Wilhemy, 1969) and the region between the Sarasvati and Drishadvati was called Brahmavarta during the Mahabharata times (900 B.C.). This was a major distributary of the Sarasvati (Sarma, 1974). In fact Wilhemy (1969) thought that the Yamuna flowed through the present course of the Chautang to join the Sarasvati. However, Kar and Ghosh (1984) disagree with this suggestion, as the course of the Chautang River is considered to be too small to accommodate the large Yamuna River.

Development of the Vedic Civilization is inextricably related with the Sarasvati River. The Vedic Civilization flourished around the Sarasvati River during the period 6000 B.C. to 3000 B.C. in form of village dwelling and hermitages and 99 archaeological sites of this age have been discovered by Mughal (1982) along the Hakra stream. At about 3000 B.C., the Aryans fanned out to different parts of the Indus plains and Indus Valley Culture/Harappan Culture with a strong component urbanized life in well planned cities developed (Radhakrishna and Merh, 1999). Later this culture withered around 2000 B.C. and these people moved eastward in the Gangetic Plains. Two major events of 3000 B.C. and 2000 B.C. have been considered to be related to onset aridity or tectonic activity. At least first event caused significant decrease in discharge of the Sarasvati River.

Haryana plains have been traditionally considered to be an area through the Sarasvati River flowed. Numerous Pre-Harappan (Vedic Civilization) sites in the triangle area between Rohtak-Jind-Hissar cities (Fig. 1.5) and Harappan sites in other areas have been discovered. It was here that Lord Krishna

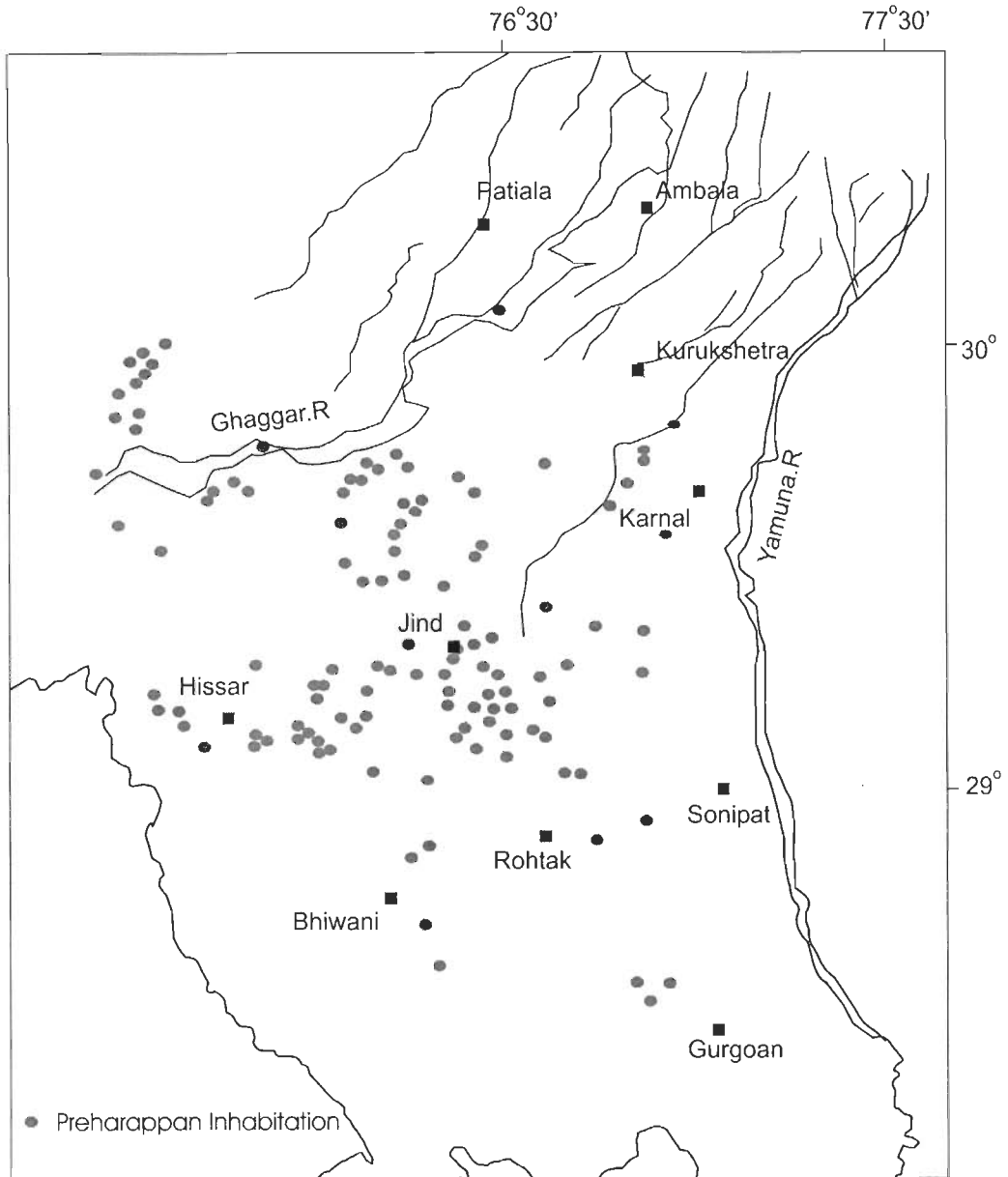


Fig 1.5 Distribution of pre-harappan inhabitation in Haryana and adjoining areas (after Joshi et al., 1984.). High concentration of these habitations in Jind-Rohtak and Hissar triangle present.

preached the Bhagvad-Gita to Arjun at the start of the battle of Mahabharata (900 B.C.) and numerous Mahabharata sites are known from this area. References in the Mahabharata Epic suggest that the Sarasvati River had lost its vigor by that time and it lost its water in the aridic region around Sirsa (Haryana).

## 1.7 RESEARCH OBJECTIVES

From the above reviews, it is obvious most of the work on soils has been carried out from point of view of agriculture and in small areas. Major regional study of geomorphology and soils undertaken Singhai et al. (1991) was carried out using 1:1 million scale satellite images and no dating of soils was undertaken. Thus there is a need to investigate geomorphology and soils of the area, using digital processing of remote sensing data and geographical Information system techniques and dating of geomorphic surfaces to work out landscape and pedological evolution of the area and work out roles of neotectonics and climatic changes in their evolution. Also, GPR studies need to undertaken to know the presence/absence the Yamuna and Drishadvati Rivers in the present area.

A review of previous work in the area indicates that there are a number of gaps in our knowledge about the evolution of the area. Therefore a brief outline of the objectives of these investigations has been highlighted.

1. To prepare a soil-geomorphic map of the study area.
2. To date soils from typical soil profile of various soil-geomorphic units and prepare a morphostratigraphic sequence of the area, to work out accurately landscape and pedological evolution of the area.
3. To study grain-size distribution and micro-morphology of typical soil profiles to decipher pedogenic processes acting in the relatively area.
4. To prepare and study digital elevation models of typical areas and infer and locate faults in the area.
5. To use Ground Penetrating Radar technique to confirm the inferred faults and to know their subsurface nature. These studies helped to determine

litho-facies up to 15 m and also the presence/absence of large Rivers (Yamuna and Drishadvati) in the study area.

6. Finally integrate all the observations to work out Holocene Tectono-Sedimentary evolution and establish the geomorphic and pedological relationship in the area.

## **1.8 OUTLINE OF THESIS**

Keeping the objectives in mind work was carried out and all the observations and interpretations are presented in the six chapter.

**Chapter 1** entitled **INTRODUCTION** provides a general background of the climatic and the soil moisture conditions, drainage, and geology of the area, including basement structure. An overview of the literature on the geomorphology and soils of Haryana and the lost River Sarasvati is included.

**Chapter 2** entitled **GEOMORPHOLOGY AND THE SOILS OF THE STUDY AREA** discusses at length the general geomorphology and soils of the study area. Also, the methodology related to Remote Sensing the GIS and their applications in the present studies are discussed in details. Different type of landforms and their characteristics, morphologies of soil of different soil-geomorphic units and different faults inferred from changes in drainage patterns and digital elevation models are described.

**Chapter 3** entitled **LUMINESCENCE DATING OF THE SOILS** deals with the optically stimulated dating technique adopted in the present study. Principles and the advantages of the OSL dating techniques and also the significance of OSL dates of the soils are discussed in this chapter of this thesis.

**Chapter 4** entitled **PHYSICO-CHEMICAL STUDIES AND THE MICROMORPHOLOGICAL DESCRIPTION OF THE SOILS**, discusses pH, EC and the particle size distribution in the typical pedons and also their variation in the different soil-geomorphic units. In the other part of the chapter we have discussed the methodologies for field sampling, preparation and the study of the thin-sections and also studied the detailed properties of the soil in terms of microstructures.

**Chapter 5** entitled **GROUND PENETRATING RADAR (GPR) STUDIES** is dedicated to the GPR studies in the study area-Haryana as well as adjoining area- Ganga-Yamuna Interfluve. In this chapter the theoretical framework, processing and the interpretation of the GPR profiles are given. Also, a model of sedimentation on terminal fans is derived. In addition, the presence of large river channels in Haryana and one paleo-channel below terminal fans deposits in the Ganga-Yamuna Interfluve are detected.

**Chapter 6** entitled **SUMMARY, SYNTHESIS AND CONCLUSIONS** summarizes all the field and laboratory work carried out. Also the characteristics of each soil-geomorphic unit in terms of morphology, micro-morphology and physical and chemical properties of the soils are described. Synthesis of the data is provided in terms of the role of the pedogenic processes, tectonics and the climatic changes in shaping the present day landscape and the surfacial soils. Also, this chapter lists the most important contributions made in the thesis.



# GEOMORPHOLOGY AND SOILS OF THE STUDY AREA

## CHAPTER 2

---

### 2.1 INTRODUCTION

In view of the extreme flatness and little variation in landforms and landscape over long distances in the Indo-Gangetic plains (Geddes, 1960), it is indeed a challenging area for studies such as identification and mapping of landforms, soil-geomorphic units and structural features like faults, lineaments etc. For these studies Remote Sensing and Geographic Information System (G.I.S) techniques have been of immense help. These studies combined with dating of soil C-horizons and soil morphological investigations have been used to construct a morphostratigraphic sequence of the area and locate and map active faults in the study area.

### 2.2 REMOTE SENSING AND GEOGRAPHIC INFORMATION SYSTEM (G.I.S) STUDIES

Kristaf and Zachary (1971) first used the multi-spectral remote sensing and computer processing techniques to map soils and soil surface conditions over small areas with a reasonable degree of accuracy. Since then this technique has been used extensively for mapping of soils. Singh et al., (2006) and Bhosle et al., (2008) used remote sensing and G.I.S. techniques to map the soils in the Upper Gangetic Plain. As regional studies in the study area, a part of the Indus plains, are limited (Singhai et al., 1991), our study is an attempt in this direction. As LANDSAT satellites data are freely accessible ([www.glcf.umiacs.umd.edu/](http://www.glcf.umiacs.umd.edu/)), the same have been used in the present investigations.

### 2.2.1 Data Processing

For the present studies mainly the Multi Spectral Scanning (MSS) images of spatial resolution of 82 m were used. Details of the images and their sensor characteristic are

Image-MSS	path/row	Date
a) WRS-P/R-1	158/039	23 Feb 03.
b) WRS-P/R-1	158/040	31 Jan 03.

The False Color Composite (FCC) was generated by coding bands 4, 3 and 2 as red, green and blue for MSS images, respectively. LANDSAT data are already geo-referenced in UTM co-ordinates and was converted into polyconic and geographic projections, as required.

### 2.2.2 Digital Elevation Models (DEMs) and Digital Terrain Models (DTMs)

Though SRTM (Shuttle Radar Topographic mission) images provide digital elevation data of 90 m resolution, but it is not useful for the present study due to its low vertical resolution  $\pm 6$  m. So Digital Elevation Model (DEM) was prepared by manually digitizing the point heights from the Survey of India topographic sheets, which have resolution of  $\pm 2$  m (*Pers. commun.* with Mr. R.P. Jhalina, Survey of India). First the topographic sheets were geo-referenced with the same co-ordinates as that of the MSS image. A total of 6579 points were taken from 105 number of 1:50,000 scale topographic sheets by using Arc View 3.2a, G.I.S. software and a DEM was prepared by using Linear rubber stretching interpolation method in ERDAS IMAGINE-8.5 software. 2-D topographic profiles (cross-sections) are generated from these DEMs were useful to find out the amount of throw of normal faults and the regional as well as the local slope across the faults. Then the MSS image was

draped upon the prepared DEM and a DTM was prepared for regional overview of the area. Lower and higher vertical exaggeration of 600 and 1200, respectively, were used to prepare DTMs to identify lineaments, and faults and land forms, respectively. These DEMs can be generated for any desired viewpoint and view angles.

However, DEMs of small areas around the possible faults and related terminal fans were prepared using krigging interpolation method of SURFER-8 program (Golden Software, Inc., 2003) (Figs. 2.6, 2.7, 2.24, 2.25 and 2.26). The details of the DEMs are given in the Tables 2.1 and 2.4. For DEM construction by SURFER-8 software, x-axis and y-axis of lengths of 6" for representing  $1/2^\circ$  are taken and the Z-axis is taken as default value. Normally Z-axis value of 1" or 0.75" is taken representing a height difference of 25 to 30 m to produce a near realistic DEM, which translates into a vertical exaggeration about 400 to 600 times (Tables 2.1, 2.4). Also, best possible viewing position and sun setting were used in construction of DEMs. DEMs thus obtained, show some artifact features like 'cliffs' in our case, which are indicative of faults (Bhosle et al., 2008).

Visualization of DEM to observe lineaments from a single azimuthal illumination source may introduce biases (Onorati et al., 1992, Smith and Clark., 2005). We changed the angle of the single source from  $0^\circ$  to  $180^\circ$  and  $0^\circ$  to  $-180^\circ$  and found that the orientation and the location of fault zones and lineaments are invariable with change of source. The most effective results were found by placing the light source in-between  $60^\circ$  to  $120^\circ$  from the strike of the faults on the upthrown blocks.

## 2.3 IDENTIFICATION OF GEOMORPHIC FEATURES AND SOIL-GEOMORPHIC UNITS

Using the elements of the image interpretation as described by Gupta (1991) like tone, texture, pattern, size, shape, site/association, twenty five soil-geomorphic units were identified and mapped (Fig. 2.3). Also, a number of landforms like river floodplains, piedmont, paleochannels, terminal fans, old river plains, aeolian plain and structural features like lineaments and faults were identified and mapped.

## 2.4 FIELD INVESTIGATIONS

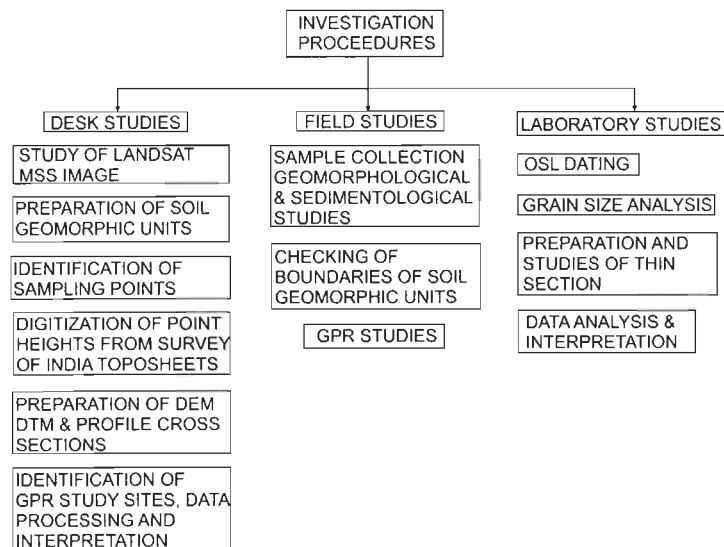


Fig. 2.1 Systematic flow-chart of the work carried out.

For the determination of different morphological properties of soils of various soil-geomorphic units mapped by remote sensing, to confirm various geomorphological and structural features and to identify the possible locations for Ground Penetrating Radar (GPR) studies, detailed field work was carried out between the months of October to March, when the climate is best to work in the field. Also, boundaries of the soil-geomorphic units and properties like salt efflorescence and water-logging conditions of the identified soil-geomorphic units identified from Landsat images were cross checked in the

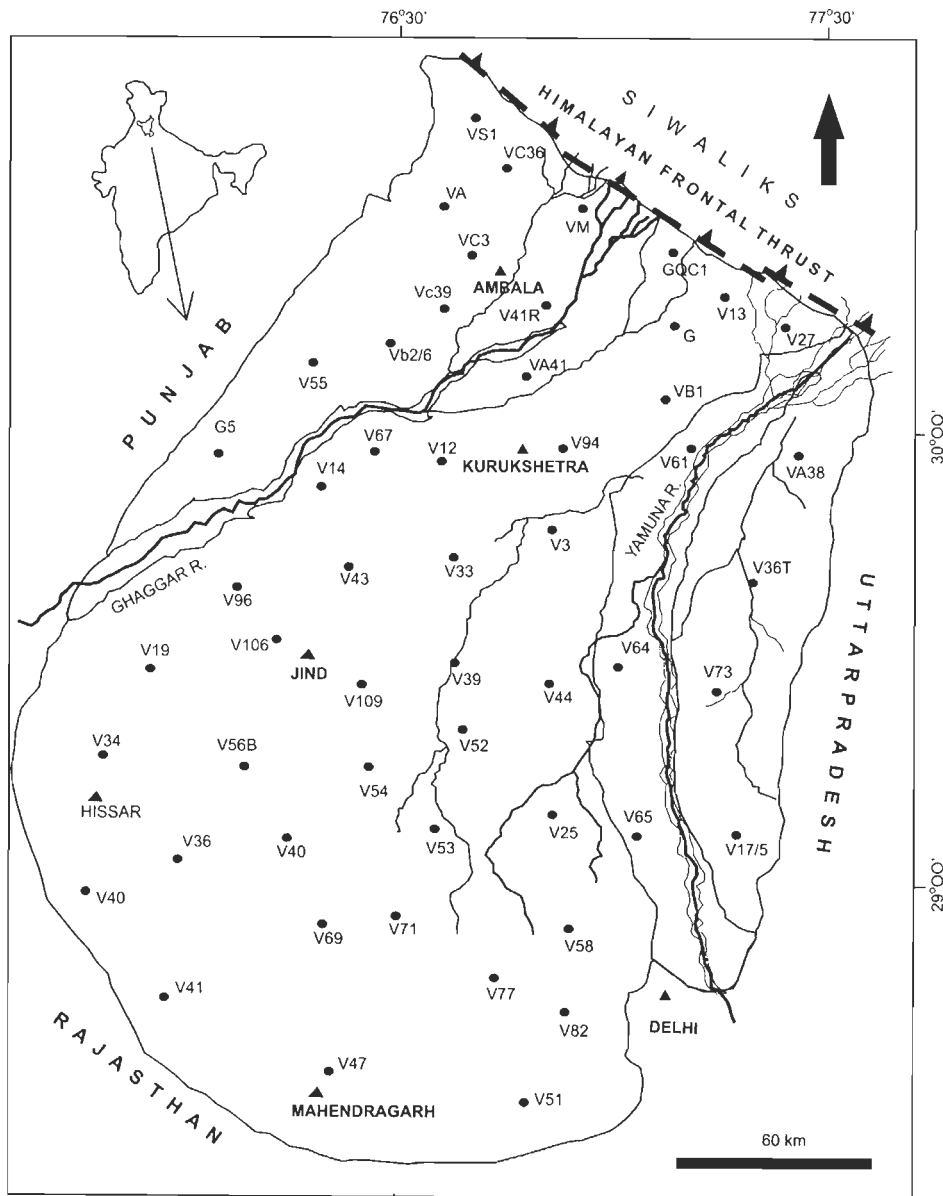


Fig. 2.2 Study area showing sample point locations, important cities and major rivers.

field. In most of the cases, brick kilns, if available were chosen, where excavations with a depth of about 1-2 m were available, for soil morphological studies. In case of necessity, these were deepened by trenching too. In other places excavations were made manually using a shovel. Excavations were made in such a way that it had at least one smooth vertical wall reaching the C-horizon of the pedon, facing in a direction so that sufficient sunlight falls on the surface to allow the examination of the soil characteristics and a proper

photograph with complete coverage of the pedon, can be taken. Then, a close view of the section is taken to recognize the different horizons and sub-horizons and prominent lines were drawn along their boundaries. Individual sub-horizons were named as A, Ap, AB, BA, B, B12, B21, BC, CB, C1 and C2 (as required) their thicknesses are measured according to the approach of the Soil Survey Staff (1995). Also, description of each sub-horizon is recorded with special attention to the morphological characteristic of the soil like horizon boundary, color, consistence, texture, structures, carbonate content, pores size and roots. The descriptions noted for different pedons of the study area are given in Appendix 1.

The field work was planned in such a way that the whole area was properly covered (Fig. 2.2). Fifty-six pedons in the different soil-geomorphic units were studied in detail for their soil morphology. Loose samples were collected from each horizon and sub-horizons for grain size analysis, undisturbed samples were collected in tin boxes for soil-micromorphological studies. Samples from C-horizons of each pedons were collected in one end closed iron pipes for Optical Stimulated Luminescence (OSL) dating (Chapter-3).

#### **2.4.1 Colour**

Munsell Colour system (MacBeth Division of Kollmorgen Instruments Corp., 1975) was used to describe the colour. The system has three components: (i) Hue - the specific colour, (ii) Value - lightness and darkness, and (iii) Chroma - colour intensity.

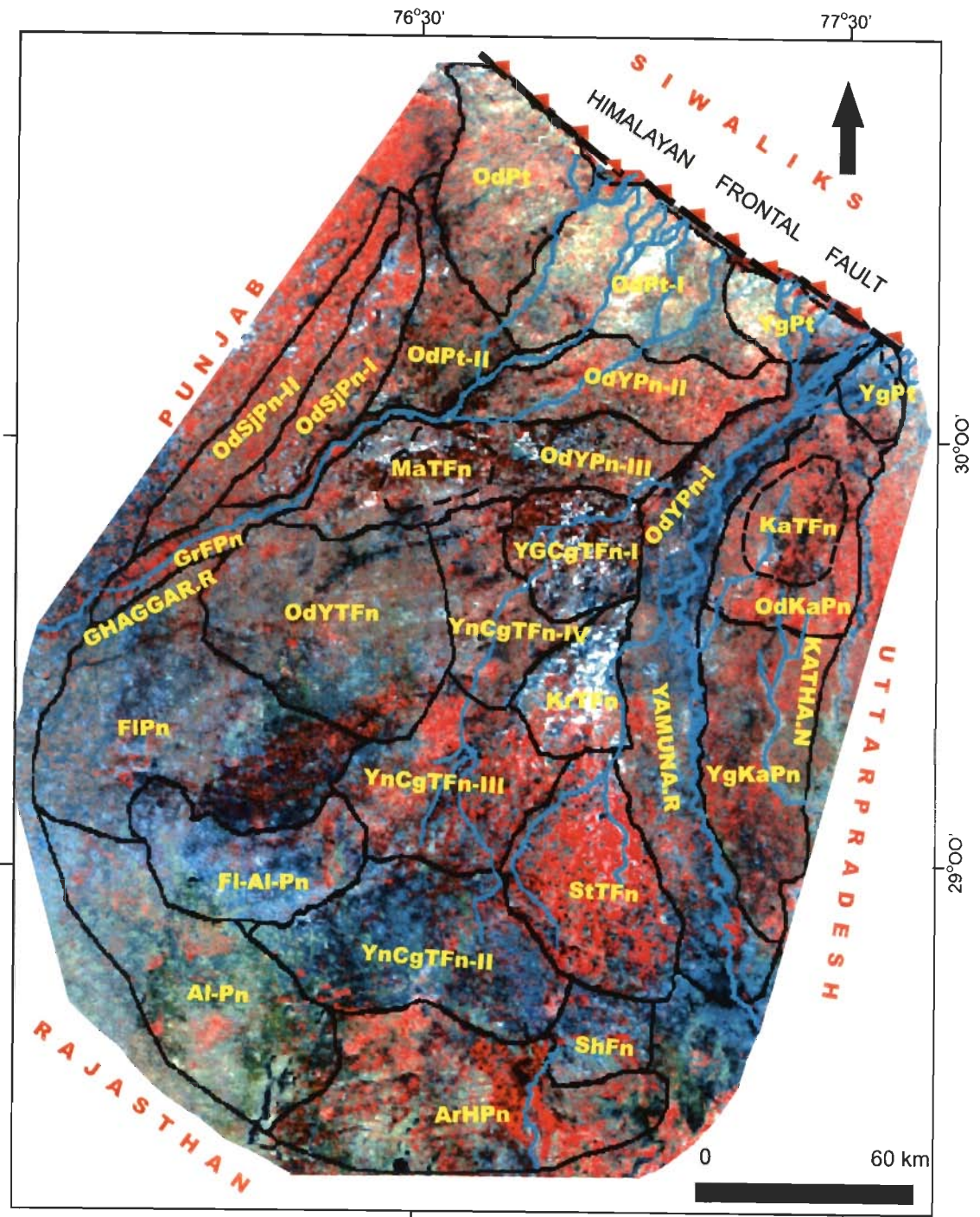


Fig. 2.3. Boundaries of soil-geomorphic units superimposed on a mosaic of Landsat MSS FCC images (WRS-1, Path- 158, Row 39 and WRS-1, Path 158, Row 40, 25 Jan & 23 Feb 2003). Abbreviations for soil-geomorphic units explained in Table 2.2.

A sample of soil obtained is used to make a visual match with the chip of colour in Munsell Colour Chart and the corresponding Munsell notation against it is assigned to the horizon or sub-horizon. For example, a brown soil may be noted as; hue value/chroma (10YR5/3).

#### **2.4.2 Oxidation Mottles and Fe-Mn /Carbonate concretions**

Mottling (refers to the repetitive colour change which is independent of the compositional properties of the soil) in soil varies from very few to high amount as well, very small size to big notable size and very soft to hard, depending upon the environmental/climatic conditions and its composition. These are mainly confined to the B and C horizons and constitute less than 5% of the soil mass, but in the piedmont zone, mottling are observed to constitute 15-20% of the soil mass. The presence of the mottles/Fe-Mn concretions indicates a degree of restricted drainage conditions. Such reducing and oxidizing conditions have been attributed to the seasonally fluctuating water table or intermittent presence of perched water table (Simonson and Boersma, 1972). In the field, different aspects of mottling observed are (i) Quantity: few - <2% of observed surface, common- 2-20% of the observed surface, many- > 20% of the observed surface, (ii) Colour, (iii) Size: Fine - <2 mm, medium - 2-5 mm, coarse - 5-20 mm, very coarse -20-76 mm, (iv) Contrast: faint, distinct and prominent, and (v) Shape: Streaks, bands and tongues.

Cold 2.87N (about 1:10 dilution of the concentrated hydrochloric acid (HCl)) was used to check the presence of the carbonates in the soil in the field. The amount and the expression of the effervescences are result of the size distribution, mineralogy as well as the amount of carbonate content. On



the basis of the effervescence produced four classes were recognized: (i) Few bubbles - weakly acidic, (ii) Bubbles readily seen - moderately acidic, (iii) Bubbles form low foam - acidic, and (iv) Bubbles come out violently with thick foam - highly acidic.

### **2.4.3 Consistence**

Soil consistency is a term used to describe the resistance offered by the soil towards the mechanical stress and the manipulations at the various moisture contents. Soil consistency is dependent on the moisture content in it and the composition of the soil and hence influenced by the soil water state and cementation (kind and degree). As this property of the soil depends upon the moisture content, a rough estimate of the moisture content is noted in the field. The wet consistence (natural wetness or the artificial wetness) is useful in determining the textural classes in the field and is composed of two quantities, stickiness and plasticity. The stickiness is measured by pressing the soil between forefinger and thumb, increasing the pressure slowly and noting the adherence of the soil to fingers. On this basis the classes recognized are sticky, non sticky and moderately sticky.

Plasticity is measured by rolling the wet soil between the forefingers and the thumb and an attempt was made to form a rod like thin roll of soil. Several classes are recognized: non-plastic (no rod form), slightly plastic (a weak rod forms and easily deformed and broken), and plastic (rod forms, which resists moderate deformation and breakage).

### **2.4.4 Texture**

Textural class can be determined fairly well in the field by feeling soil and estimating sand, silt and clay contents by the consistence and stickiness,

as described above. The textural classification of soil is further refined in the laboratory by determining the percentage of each constituent (sand, silt and clay) and plot the percentage on a triangular graph (Schoenberger et al., 1998).

#### **2.4.5 Structure**

Soil structures refer to how constituent particles are arranged and interlaced together to give large structure. Structure in the soils may be developed due to the animal activity, drying and wetting of the soils, growing plants roots, expansions and contractions, and addition of the lime or even due to the movement of the water through the soil. Soil structures are described as: (i) Shape - platy, prismatic, columnar, blocky and granular, (ii) Size - very fine, fine, medium, coarse, very coarse, and (iii) Grade (Distinctness of individual units) - weak, moderate and strong.

#### **2.4.6 Soil Pores**

Soil pores are widely observed in the field and are termed as matrix, non-matrix and intra-structural pore spaces. Identification and classification was done by visual examination of the section in the field and was jotted down based on the size in mm as: (i) very fine - <1 mm, (ii) fine - 1-2 mm, (iii) medium - 2-5 mm, (iv) coarse - 5-10 mm, (v) very coarse -  $\geq 10$  mm.

Abundance of soil pores was recorded as the few, common and many (<1%, 1-5%,  $\geq 5\%$  per unit area, respectively). Further the various characters such as shape, size and abundance are confirmed later during micro-morphological studies.

#### **2.4.7 Horizon Boundary**

Horizon boundary is a type of contact made by the horizons within the pedons with respect to each other. The width of the transition zone which is present between the overlying and underlying horizons and the topography of the contact zone are recorded. The distinct classes denoting transition between horizons are: (i) abrupt <2 cm wide, (ii) clear 2 -5 cm wide, (iii) graded 5 -12 cm wide and (iv) diffused >12 cm wide.

Topography of the boundary classes are smooth (straight line), wavy (packets are wider than the depth), irregular (packets are deeper than the width), diffused and broken (boundaries are not clear and discontinuous). Though all types of boundaries are recognized, but in most cases the observed horizontal boundaries are abrupt and irregular type.

#### **2.4.8 Roots**

Amount and size of the roots in the soil are recorded according to the Schoeneberger et al. (1998). Quantity of roots is described in the terms of numbers of size per unit area the quantity classes are: (i) few <1% of the area, (ii) common 1-<5% of the area, and (iii) many >5% of the area. Similarly they are classified on the basis of the size: (i) very fine <1 mm, (ii) fine 1-2 mm, (iii) medium 2-5 mm, and (iv) coarse >5 mm.

### **2.5 MAJOR LANDFORMS IN THE STUDY AREA**

Using the satellite images, topographic maps, DEMs, DTMs and detailed field work, major landforms like floodplains of rivers, aeolian plains, piedmont zone and terminal fans are identified (Fig. 2.4).

## 2.5.1 Fluvial Plains

Depending upon IRSL (Infra red Stimulated Luminescence) ages, eleven plains have been identified: Yamuna and Ghaggar floodplains, Old Yamuna Plain-I, Old Yamuna Plain-II, Old Yamuna Plain-III, Fluvial Plain, Fluvial-Aeolian Plain, Old Sutlej Plains-I & II, Old Katha Plains & Young Katha Plains II.

### 2.5.1.1 Floodplains

Two major rivers i.e. the Ghaggar and Yamuna have on the average 7 km and 9 km wide floodplains, respectively. Other small inland streams on the interfluvium are ephemeral in nature, have small discharges and narrow floodplains (<1.5 km). They flow in westerly direction, following the regional slopes. Since the floodplains are occasionally inundated during rainy season, their soils are marked by A/C horizons mainly.

2.5.1.1.1 Ghaggar Floodplain: The River Ghaggar originates from the Siwalik ranges i.e. Morni Hills and flows to the southwesterly direction. The average annual flow of the Ghaggar is  $2.159 \times 10^6 \text{ m}^3$  (Duggal, 1977). The floodplain of this river is narrow in the northeast and gradually widens up to 13 km in the Kurukshetra and the Hissar district and loses itself in the Thar Desert of Rajasthan.

Manchanda (1981) divided the Ghaggar plains into three zones i.e. upper, middle and lower. The upper zone mainly lies in the Union Territory of Chandigarh, Ambala and Kurukshetra districts. Due to steep slope the deposition is less and there is no problem of salinity, alkalinity or drainage in this zone.

The middle zone mainly lies in parts of Kurukshetra and Narwana Districts. Here the river has meandering nature and a number of levees, bars and abandoned channels are observed. This gently sloped floodplain is poorly drained, creating condition for development of the oxidation mottles. The dominant soils types are Ustochrepts, Ustipsamments, and Haplaquepts.

The lower reaches of the southern floodplain show salinity and alkalinity in general. Development of CaCO<sub>3</sub> concretions are reported in this floodplain by Ahuja (1981). In these reaches, a narrow active floodplain with a width of 0.3-0.7 km and older one with a width of 8-13 km are identified in the MSS image. Soil types are Ustochrepts, Ustipsamments.

2.5.1.1.2 Yamuna Floodplain: The River Yamuna crosses the Doon valley and breaks through the Siwalik Range along the Paonta Fault (Rao et.al., 1974). After the river enters the plains area from the Siwalik Ranges, it has a braided character up to a distance of 35 km and later it meanders through a wide floodplain. The width of floodplain is about 8 km in Bilaspur district and widens up to 13 km in Karnal and Sonapat districts, further narrows down to 6 km in Gurgaon district. Floodplain of the River Yamuna has an entrenched character and the entrenchment increase downstream of the present area. The landscape aspects are related to the channels remnants of the former river courses and related features like levees, basins, channel bars and the abandoned channels.

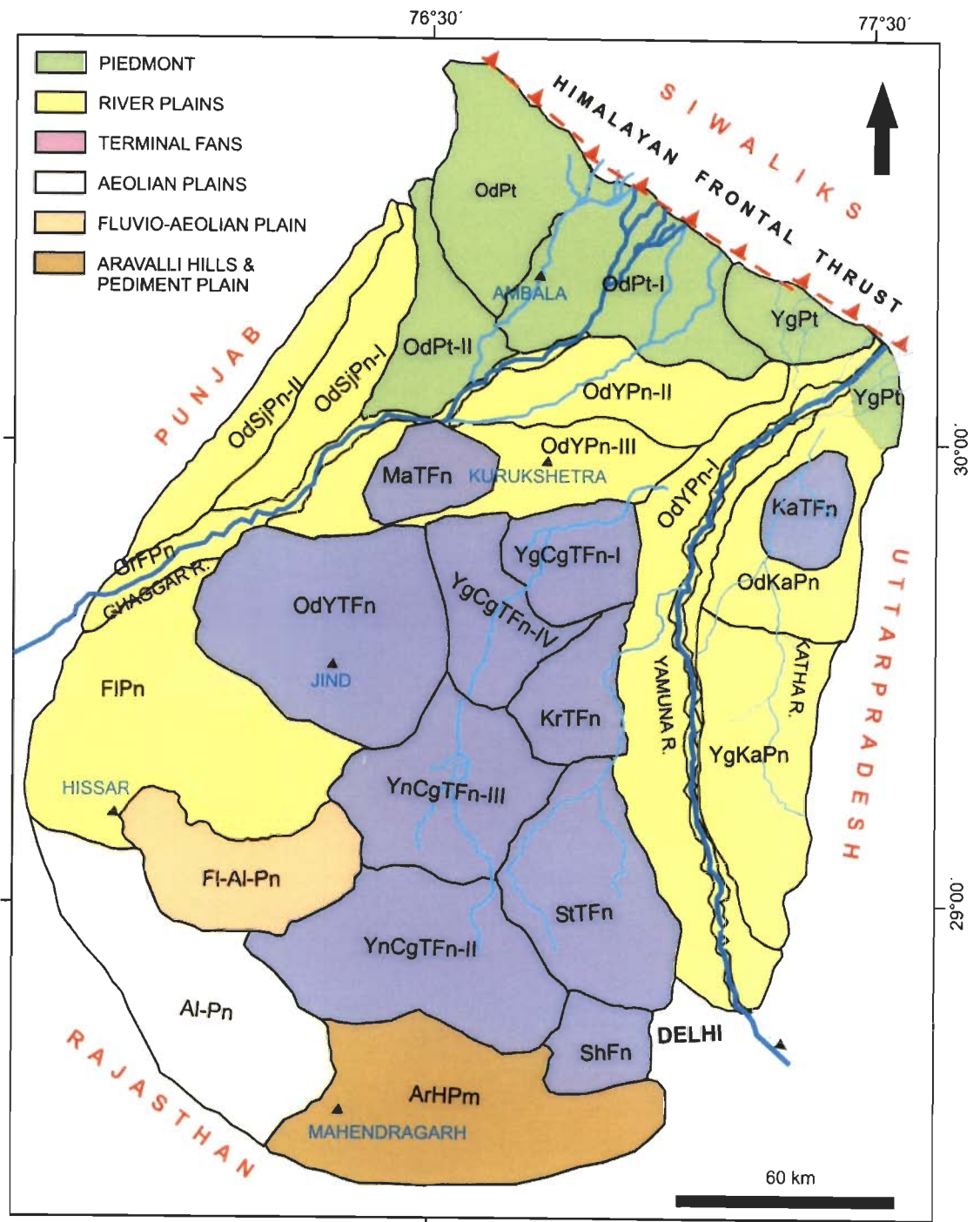


Fig. 2.4 Major landforms in the study area i.e. Piedmont zone, fluvial plains, terminal fans, aeolian plain, fluvio-aeolian plain, Aravalli Hills and Pediments.

### 2.5.1.2 Old Sutlej Plains –I and II

These plains lay between the Ghaggar floodplain and active course of the Sutlej River. These plains resulted due to northwestward shifting of the Sutlej River from its earlier course, which joined the Ghaggar River (Fig. 2.4). This is evidenced by the presence of a number of paleo-channels, starting from Ropar, where the Sutlej enters the plains from the Siwalik Ranges. These plains basically consist of coarse sand along the paleo-channels and silt and clay in the intervening areas. As seen in the old (1937) topographic maps, sands of the paleo-channels were heaped into elongated mounds, which have been removed in the last three decades. This plain is marked by abundance of impure calcareous irregular concretions i.e. '*kankar*'. Soil development is moderate in southern part and it decreases northward to very weakly developed soil. The diagnostic horizons observed in this area are, cambic, salic, calcic and argillic and nitric (Sehgal et al., 1972, Sehgal, 1974; Sidhu et. al., 1976; Anand et. al., 1977). Major soils are Ustochrepts, Ustipsamments, Haplaquepts and NatrustalFs. Based on IRSL ages, the Sutlej Plains in the study area have been divided into the Old Sutlej Plain-I (3.9 Ka) and Old Sutlej Plain-II (2.7 Ka), respectively.

Not only the part of the Sutlej Plains studied here, but whole of the region between the Ghaggar and Sutlej Rivers is marked by paleochannels of the Sutlej, which have been mapped using Landsat images (Pal et al., 1980; Singhai et al., 1991). These paleochannels have been interpreted to indicate that prior to 1700 B.C. the Sutlej River was an important tributary of the Ghaggar (Sarasvati River), instead of the Indus River.

### 2.5.1.3 Old Yamuna Plains

Three Yamuna Plains viz. Old Yamuna Plain –I, Old Yamuna Plain-II, and Old Yamuna Plain-III are identified in the present study.

The elongated Old Yamuna Plain-II, running at the base of the Piedmont zone in approximately E-W direction continue from the present Yamuna River course to the Ghaggar River course. This plain is traversed by numerous small streams coming out of the Piedmont zone. This plain is characterized by two soil profiles at places, the older profile being well-developed and with an age of 4.0 Ka age and the younger profile is of 2.8 Ka age. The soils of this plain are moderately developed and are classified as Typic Ustochrepts, Typic calciorthids and Typic Torripsamments.

The Old Yamuna Plain-III lies just south of the Old Yamuna Plain-II (Figs. 2.4, 2.18). Moderately to weakly developed soils in this unit are developed on the sandy parent materials and shows salt efflorescence. Due to low lying condition, the area appears as wet in the satellite image by darker tone. In some parts of the area, abandoned channels can be made out. Calcrete concretions are fairly common. The soils are mostly sandy loam and classified as Typic Ustochrepts, Aquic Comborhthids, Typic calciorthids and Typic Torripsamments.

The Old Yamuna Plain-I is an elongated plain along the Yamuna River strikes NE to SE directions. This unit continues well beyond the study area up to Mathura (Uttar Pradesh State) and is confined within the 13-15 m cliff of Yamuna Faults (Fig. 2.25 c, d). The sandy character of the plain is well reflected by lighter tone in the MSS image. Numerous small streams are now active in this plain and deposition is mainly confined in their floodplains. Soils



in this plain are moderately developed and classified as Typic Ustochrepts, Typic calciorthids and Typic Torripsamments.

#### *2.5.1.4 Old and Young Katha Plains*

The plain Old Katha Plain (OdkaPn) and Young Katha Plain (YgKaPn) lies in Uttar Pradesh and is formed by the tributary of the Yamuna River flowing in this area (Ganga-Yamuna interfluve) known as Katha River. The OdkaPn soils are weakly developed, and show little salt efflorescence. Due to low lying condition, the area appears as wet in the satellite image by darker tone. The soils are mostly sandy loam and classified as Typic Ustochrepts, Aquic Camborthids.

Young Katha Plain is marked by the presence of number of abundant paleochannels and show weakly developed soil on the sandy parent materials and is classified as Typic Ustochrepts

#### *2.5.1.5 Fluvial Plain*

Soils in this plain are weakly developed due to an arid climate. Morphologically this plain is marked by the major landforms like bars, old levees, relict channel courses, and salt affected plains and basin plains. Typical soils in unit are Typic Camborthids and Typic Ustochrepts.

#### *2.5.1.6 Fluvio-Aeolian Plain*

Fluvio-Aeolian Plain is situated in the west-central part of the study area. Soils occur dominantly on the fluvial plains modified by aeolian activity by the westerly winds from the adjacent Thar Desert. The moisture regime is ustic to aridic with annual rainfall not exceeding 350-400 mm. This area is marked by large numbers of paleochannels (Fig. 2.8) filled with the sandy materials, indicating a strong fluvial activity in the past. Dominant soils of this

area are sandy and calcareous, occurring on gently sloping plains, with sand at places are being reworked into dunes. Soils in this unit are classified as Typic Torripsamments.

### **2.5.2 Piedmont**

The piedmont zone is marked by steep slopes (average slope =0.6%), elongated in the east-west direction and lies south of the Siwalik Ranges with a length of about 40 km and maximum width of 54 km (Fig. 2.4). This zone is marked by parallel and sub-parallel drainage system. Most of the large streams join the bounding rivers at acute angles. This zone is marked by coarse sediments i.e. sand and gravels deposited by the streams coming out the Siwalik Ranges. On the basis of the degree of soil developments and IRSL ages, four soil-geomorphic units are identified within this zone: Oldest Piedmont, Old Piedmont-I, Old Piedmont –II and Young Piedmont.

#### *2.5.2.1 Oldest Piedmont (OdPt)*

The Oldest Piedmont is in the west of the Ghaggar River, extending from the foot of the Siwaliks to the south and has a maximum width of about 40 km. It has the thickest (~1.7 m) soil cover, which are eroded at places. This unit is well drained with parallel to sub-parallel drainage towards west and southwest. The streams in this unit are incised in nature and have narrow floodplains. Soils in this unit are sandy to loamy in nature and classified as Udic Ustochrepts. The OSL age of this unit varies from 7.6 to 9.8 Ka and is the oldest soil-geomorphic unit in this area.

#### *2.5.2.2 Old Piedmont-I (OdPt-I)*

Old Piedmont–I covers the maximum area in the piedmont zone. Well distributed drainage system of the area is marked by southwest flowing

streams like the Sarasvati, Chautang and Markanda streams. These streams are characterized by their incised courses. Soils are mainly developed on gravelly and sandy sediments and are well-developed. Sediments eroded from this piedmont are being spread over the Old Yamuna Plain-II. Smaller streams have removed the soil cover at places. Soils here are classified as coarse loamy to fine loamy Udic Ustochrepts.

#### *2.5.2.3 Old Piedmont-II (OdPt-II)*

This unit lies south of the Oldest Piedmont and was deposited by streams flowing from the Oldest Piedmont, as suggested by some paleochannels (Fig. 2.4). As compared to the Old Piedmont-I, the moisture content of this unit is more as suggested by a darker tone in the MSS image. Soils in this unit are moderately developed and mainly Ustorthents.

#### *2.5.2.4 Young Piedmont (YgPt)*

Young Piedmont forms a small portion in the northeastern part of the study area bordering the Siwalik Ranges. This is formed by the streams descending from the Siwalik ranges and turn eastwards to meet the River Yamuna. Alluvial fans formed by the small streams overlap each other in this unit (Fig. 2.4). Soils in this area are very weakly developed and are well drained. In some areas mottling is reported. Soils from this area are classified as Ustifluent and typic Ustochrepts. Young Piedmont is also observed east of the Yamuna River.

### **2.5.3. Aeolian Plain**

The Aeolian Plain is the southernmost soil-geomorphic unit of the study area with an age of 4.4-4.7 Ka. This unit is influenced by hot winds and dust storms are frequent from the neighboring Thar Dessert. On the whole it is a

flat aeolian plain dotted with isolated low height (<2 m) dunes at places. Aeolian processes are the major factor controlling landforms of the area.

The dominant soils are loose sand on dunes and are classified as Typic Torripsamments. The inter-dunal soils are moderate to poorly drained, calcareous and coarse-loamy. They are classified as Typic Camborthids. They are generally alkaline in nature. Calcrete precipitation is present in the pore spaces of the sediments.

#### **2.5.4 Terminal Fans**

Nine terminal fans have been recognized and mapped from the study area Table (2.1). DTM of the whole area prepared by ERDAS IMAGINE brings out Old Yamuna, Chautang-II, III & IV terminal fans. Further Karnal, Sonipat, Young Chautang-I, Katha, and Markanda TFn were identified from DEMs generated by SURFER-8 software. The Young Chautang terminal Fans II-IV and Yamuna terminal fan were identified from their plan form and OSL ages.

Out of nine terminal fans identified in the study area, the Sonipat and Karnal terminal fans in the eastern-central region are uplifted from the regional topographic level (Fig. 2.6a & c). All the terminal fans have are semicircular planform and convex upward in nature and their distal boundaries are gradational. The Young Chautang Terminal Fan-I shows dichotomic drainage for numerous paleochannels over its surface. All the terminal fans were formed due to activity of some faults in the present, as also earlier observed by Singh et al., (2006) and Bhosle et al., (2008). Geometric aspects like length, slope, related fault and the area of the fans are

Table 2.1 Information of Terminal fan and their DTMs in the study area

Terminal fans	Age (Ka)	Associated Fault	Area (km <sup>2</sup> )	Length (km)	Slope %	Vertical exaggeration & Fig no.	Light position angles V/H
Karnal	4.7	Karnal	244	30	0.01	248, 2.6a	45/135
Markanda	3.3	Markanda	294	17	0.09	312, 2.6b	45/135
Sonipat	3.2-3.4	Rohtak	1121	56	0.08	223, 2.6c	54/153
Old Yamuna	2.9-3.2	Karnal	1785	62	0.06	--	--
Katha	2.7	Patiala	284	23	0.07	306, 2.7a	49/152
Young Chautang-IV	2.3-2.4	Karnal	178	29	0.06	2.7b	--
Young Chautang-III	2.1-2.4	Karnal	1241	71	0.04	238	49/152
Young Chautang-II	1.9-2.3	Rohtak	1541	47	0.07	--	--
Young Chautang-I	1.5	Markanda	193	23	0.08	2.7b	--
DTM (Digital Terrain Model) INFORMATION							
DTM with lower vertical exaggeration	Lineament direction (D-I) is N76° in upper portion whereas in lower portion D-II lineament strikes N89° (Fig. 2.18),				600	N30°	
DTM with higher vertical exaggeration	DTM of whole area showing faults structural blocks, and terminal fans (Fig. 2.27).				1200	N40°	

given in Table (2.1). The largest fan identified is the Old Yamuna terminal fan.

Most of the Terminal fans in the study area are formed by the rivers, which used to flow in the recent past. The Sonipat Terminal Fan is supposed

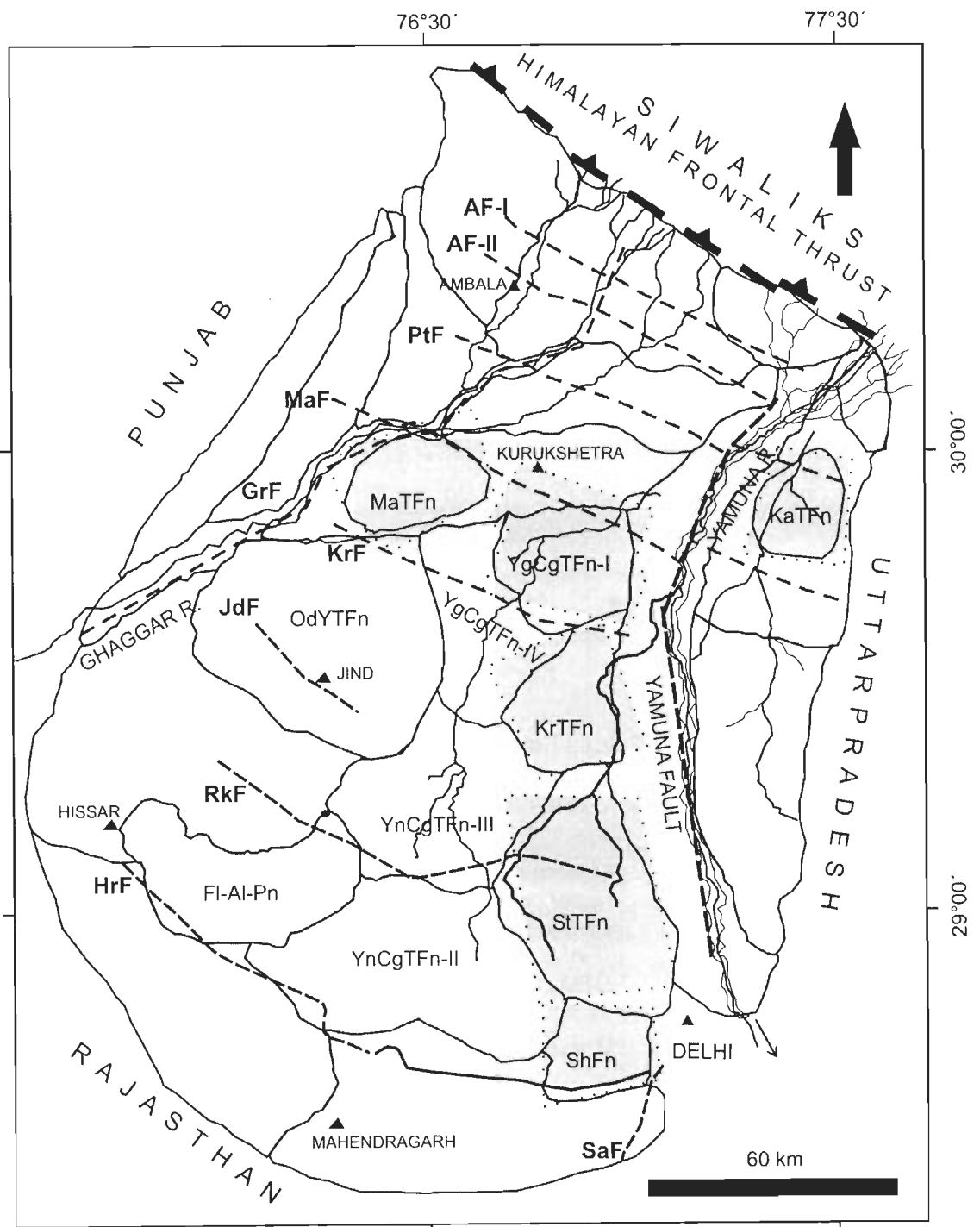


Fig. 2.5 Areas around terminal fans/fan, for which DEMs were prepared, are shaded. Abbreviations ending with TFn indicate terminal fans.

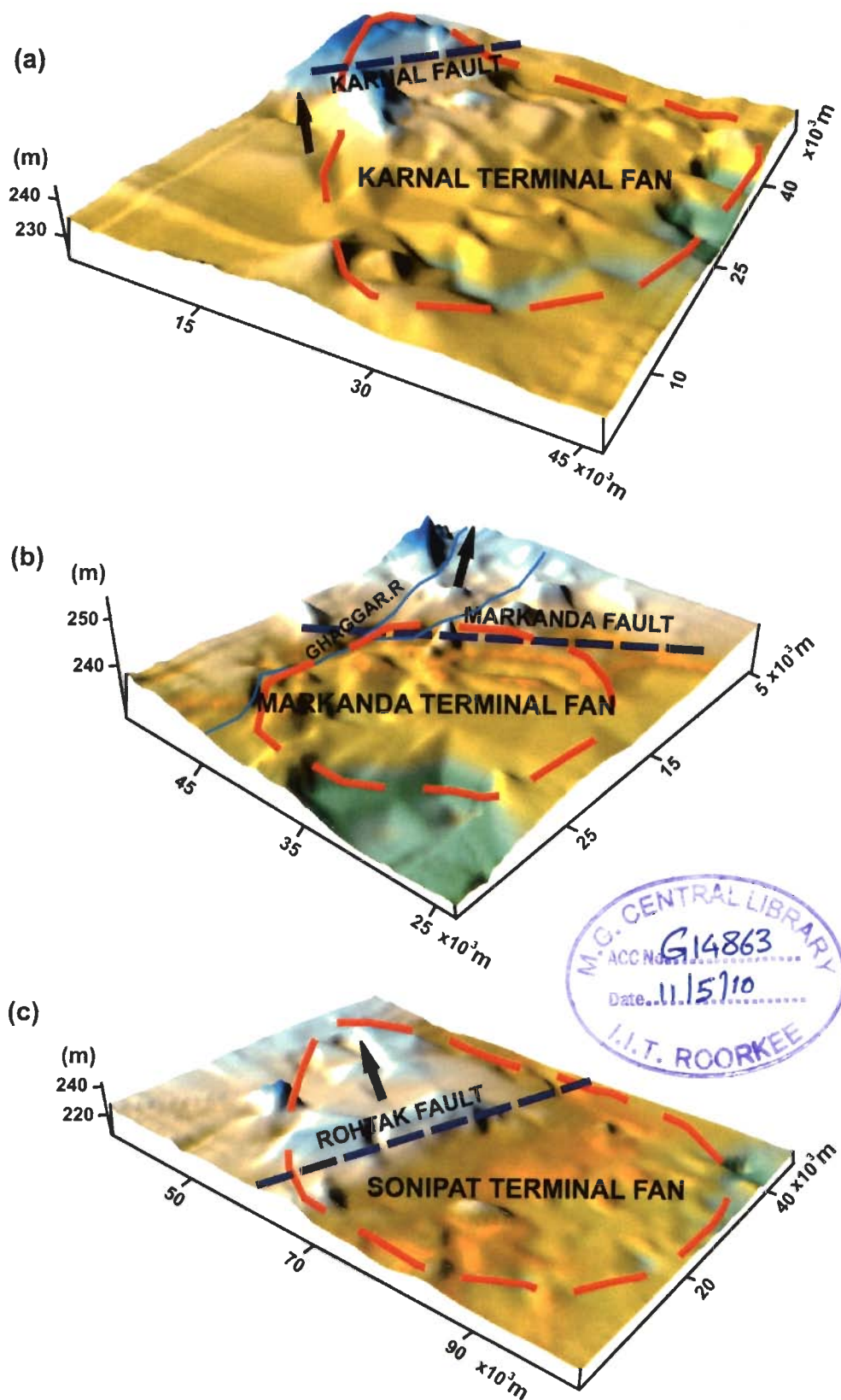


Fig. 2.6 Digital Elevation Model for areas around (a) Karnal Terminal fan (b) Markanda Terminal fan and (c) Sonipat Terminal fan.



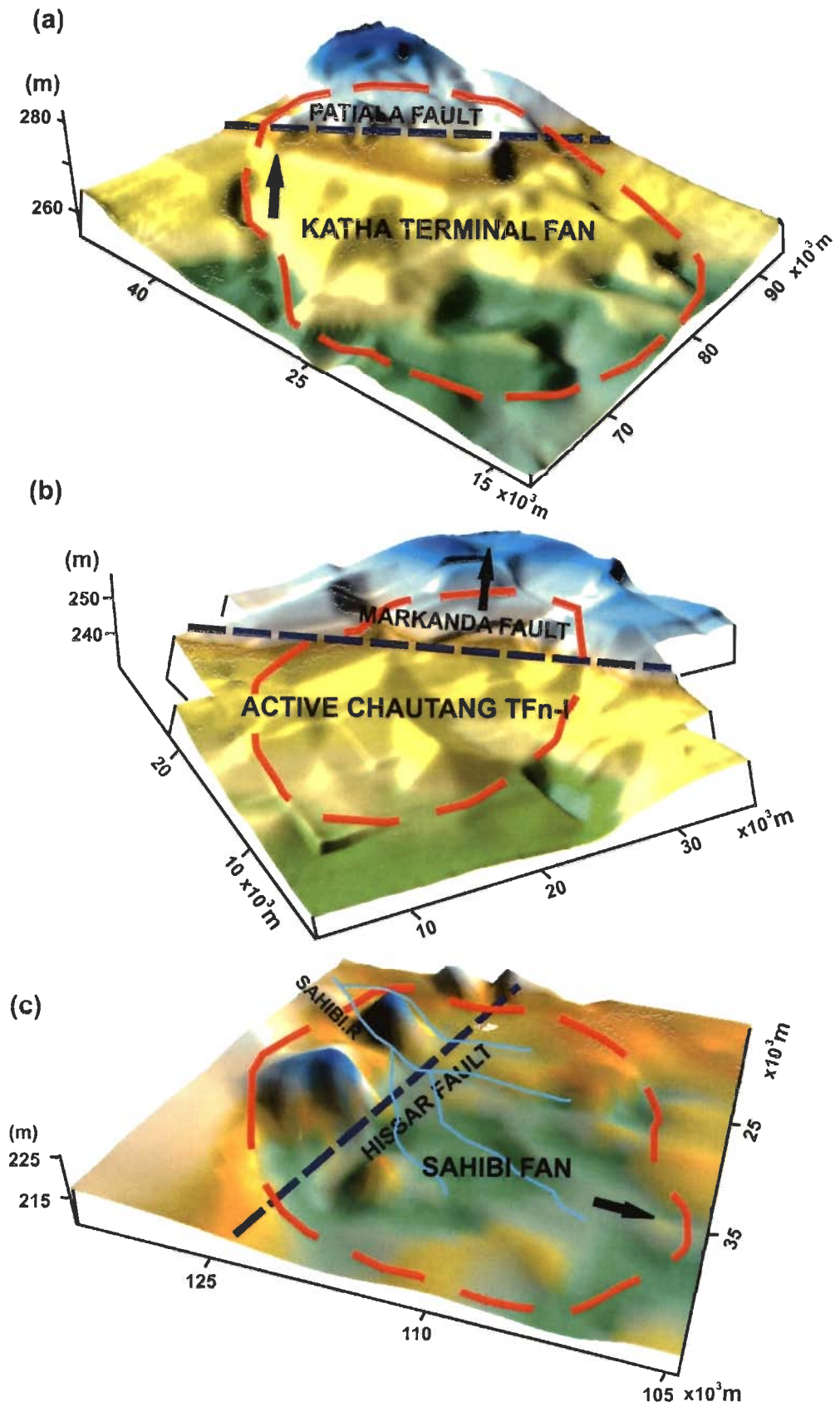


Fig. 2.7 Digital Elevation Model generated for areas around (a) Katha Terminal fan (b) Young Chautang Terminal fan-IV and (c) Sahibi fan.



to have been formed by the Burhi Yamuna River, which shows no existence in the present time. Similarly the Old Yamuna Terminal Fan was formed by the old Yamuna River, which used to flow in this area.

### **2.5.5 Aravalli Hills and Pediments**

This unit consists of low altitudes (<775 m) runs in the form of ridges trending northeast-southwest in the southwestern part near the Yamuna River and occurs in the southern most part of the study area. At places, the Aravalli Hills have been eroded to form undulating hillocks, forming pediments, especially along the marginal regions of these hills (Fig. 2.3). It is covered by sandy to fine loamy (loess) brought in from the Thar Desert in the west. The subsoil water is brackish. Calcium carbonate nodules are found at a depth of 1-2 m depending upon the thickness of the sand cover. Soils, in general, are classified as Typic Camborthids, Typic Torripsamments, Typic Torrifluents and Typic Haplaquepts.

### **2.5.6 Aravalli Piedmont (Sahibi Fan)**

The Aravalli Piedmont mainly lies northeast of the Aravalli Hill and Pediments Plain (Fig. 2.3). It has been constructed by monsoonal streams like the Dohan Nadi, Kali Nadi and Sahibi Nadi, draining the Aravalli Hills. Major part of the unit is occupied by a fan formed by the Sahibi River. Almost all the sediments brought by these streams are reworked by the aeolian activity during the dry months. Major soils in the area are Typic Camborthids and Typic Torripsamments. Its age is 2.7 Ka.

### **2.5.7 Paleochannels in the Study Area**

The MSS images available for the period January to March were not very useful in locating paleochannels. However, images taken from Google Earth probably of post-monsoon months, bring out numerous paleochannels with distributary pattern in southern half of the study area (Fig. 2.9). Distributary paleochannels are observed to be flowing from approximately NE direction, suggesting that some remnant channels of the Yamuna River may

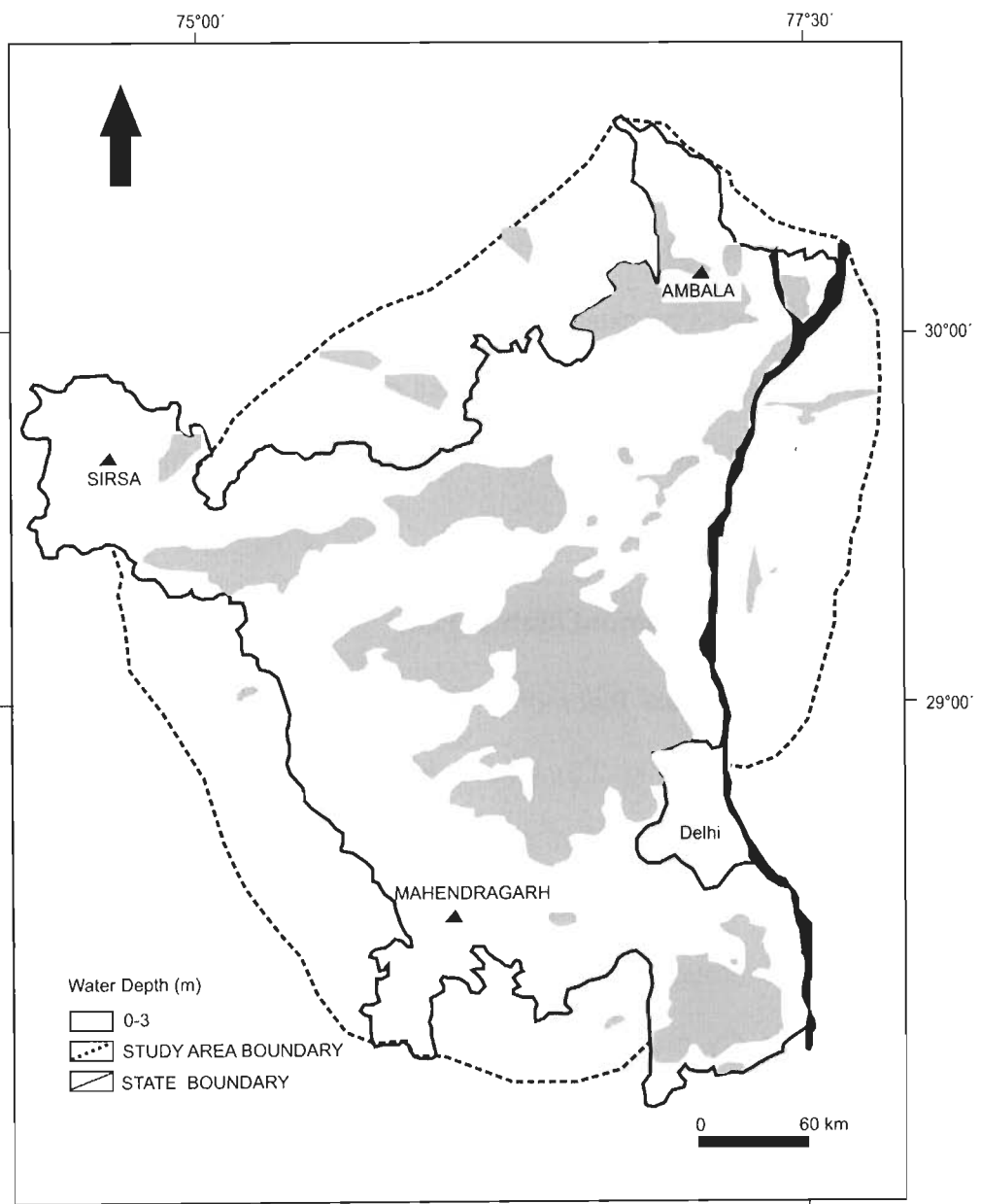


Fig. 2.8 Wetlands in the study area (After Agricultural Ground Water Cell, Haryana, (2008)).

have been responsible for their formation. Well-defined paleochannels are observed in the Young Chautang Terminal Fans-I, III & IV and Old Yamuna Terminal Fan. However, the Young Chautang terminal Fans- I & II may have been formed by contributions from the Chautang and some distributary of the Yamuna rivers.

In MSS image, salt afflorescence pattern also brings out the presence of paleochannels flowig from the NE and N in the Karnal and Young Chautang Terminal Fans, respectively. Most of the time in rainy season these

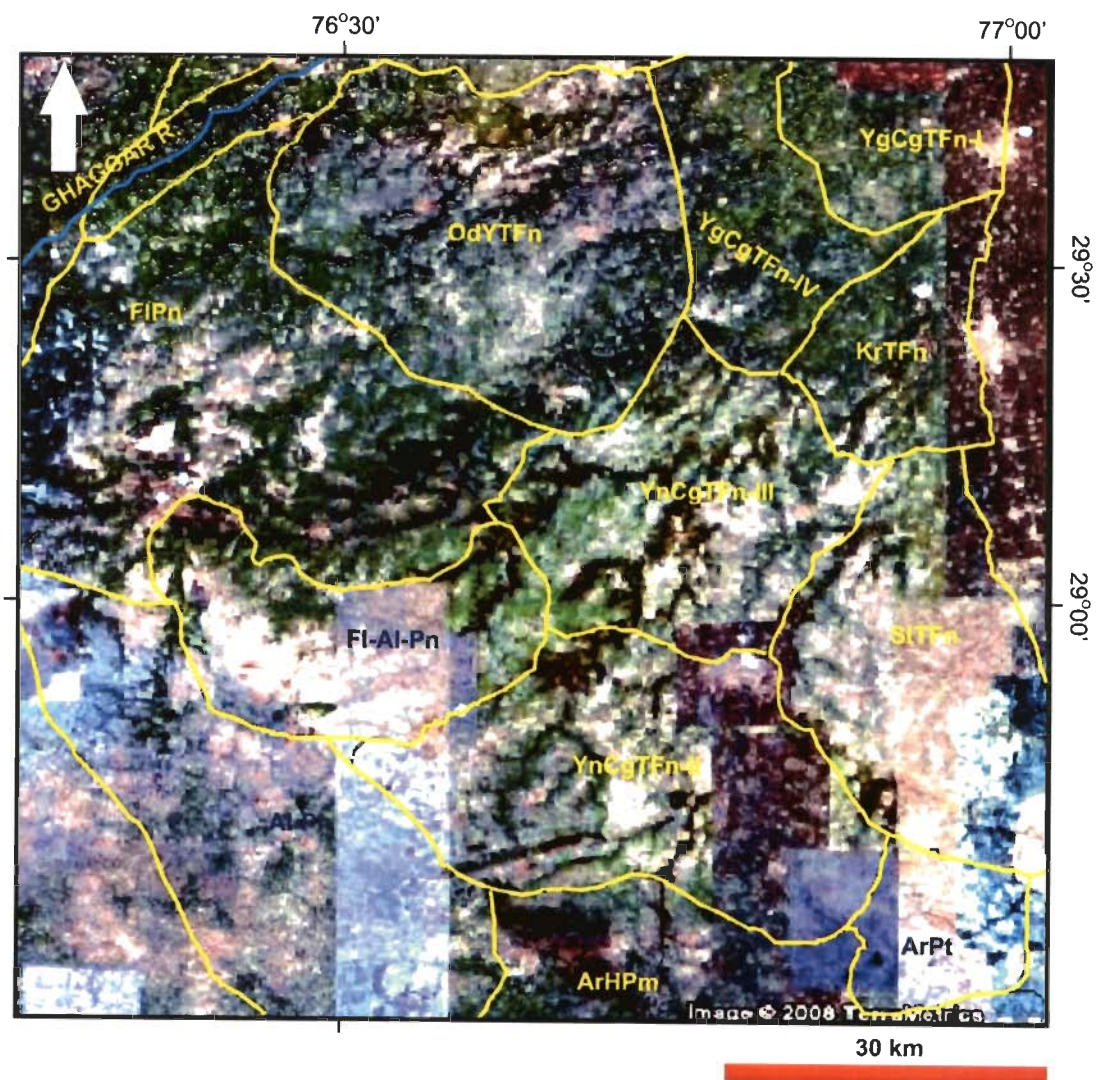


Fig. 2.9 Google Earth image showing Paleochannels in the study area with soil- geomorphic unit boundaries superimposed. Paleochannels are widely distributed in the southern part of the study area and their source lies to the north/northeast, suggesting flow of the Yamuna in this region in the past.

paleochannels are filled with the rain water causing marshy condition in the central portion of the study area, increase of the salinity and degradation of land condition (Fig. 2.8). This area is particularly treated by the CGWB regularly to minimise the salinity condition and let the land remain in cultivation condition.

## 2.6 MORPHOSTRATIGRAPHY OF THE STUDY AREA

Using remote sensing and detailed fieldworks, Singhai (1989) identified thirteen soil-geomorphic units in the study area and classified these soil-geomorphic units into three members as Q1 (1000 B.P), Q2 (3500 B.P) and Q3 (5000 B.P) of post-incisive soil-chronosequence. In the present study, MSS images along with DEMs and DTMs (Sec.2.2.2) were used to identify twenty-five soil-geomorphic units. Also, optical luminescence dating was carried out for C-horizons of soils in different soil-geomorphic units to provide absolute ages.

Table 2.2 Ages of Members of Morphostratigraphic Sequence and various soil-geomorphic units included in each member.

QIMS	AGE(Ka)	SOIL GEOMORPHIC UNITS
QIMS-VI	9.86-5.38	Oldest Piedmont (OdPt)
QIMS-V	5.38-4.45	Old Piedmonts I & II (OdPt-II, OdPt-I), Aeolian Plain (Al-Pn), Aravalli hills and Pediment (ArHPm), Fluvial Plain (Fl-Pn), Karnal Terminal Fan (KrTFn)
QIMS-IV	4.45-3.60	Old Yamuna Plains-I, II & III (OdYPn-I, OdYPn-II, OdYPn-III), Fluvial-Aeolian Plain (Fl-Al-Pn), Old Sutlej Plain-I (OdSjPn-I).
QIMS-III	3.60-2.91	Old Yamuna Terminal Fan (OdYTFn), Sonipat Terminal Fan (StTFn), Young and Old Katha Plains (YgKaPn, OdKaPn).
QIMS-II	2.91-1.52	Young Chautang Terminal Fans -I-IV (YgCgTFn- I,II,III & IV), Aravalli Piedmont (ArPt), Young Piedmont (YgPt), Old Sutlej Plain-II (OdSjPn-II).
QIMS-I	<1.5	Active Floodplain of different rivers.

Based on the OSL ages, six members (QIMS-I to VI) (Quaternary Indus Morphostratigraphic Sequence) of a Morphostratigraphic Sequence are identified (Frye and William, 1962. in Fairbridge, 1968, p. 915): QIMS-VI 9.86-5.38 Ka, QIMS-V- 5.38 -4.45 Ka, QIMS-IV- 4.45 - 3.60 Ka, QIMS-III - 3.60 - 2.91 Ka, QIMS-II - < 2.91-1.52 Ka and QIMS-I - < 1.52 Ka.

## **2.7 SOIL MORPHOLOGY OF DIFFERENT MEMBERS OF MORPHO-STRAITIGRAPHIC SEQUENCE**

### **2.7.1 Member QIMS –VI**

This is the oldest member of the study area and includes only one soil-geomorphic unit, i.e. the Oldest Piedmont. This unit is present in the extreme northwestern portion and covering approximately an area of 630 km<sup>2</sup>. In north, it is separated by the Himalayan Frontal Thrust from the Siwalik Hills and is elongated and parallel to Ghaggar River, which flows along the eastern boundary of the unit (Figs. 2.3, 2.4 and 2.10). It is well drained by the seasonal streams originating in the Siwalik Ranges and the Ghaggar River and its tributaries like the Chola Nadi, Siswa Nadi and Buoki Nadi, but shows low drainage density. Soils in this member are moderate to well develop with sub-angular blocky and prismatic structures. The matrix colour varies from 10YR3/2 (very dark grayish brown) to 10YR 6/4(light yellowish brown). The thickness of B-horizon varies from 80-65 cm and that of the solum varies from 95-135 cm. The detailed description of soil properties is given in Table 2.3. The pores size gradually decreases from upper to lower part of profiles from fine to very fine. Roots are medium in the upper A and B horizons and become finer with depth and absent in the C horizon. Thick clay cutans are observed in B-horizons. Hard, dark brown (7.5YR3/3) Fe-Mn nodules are well

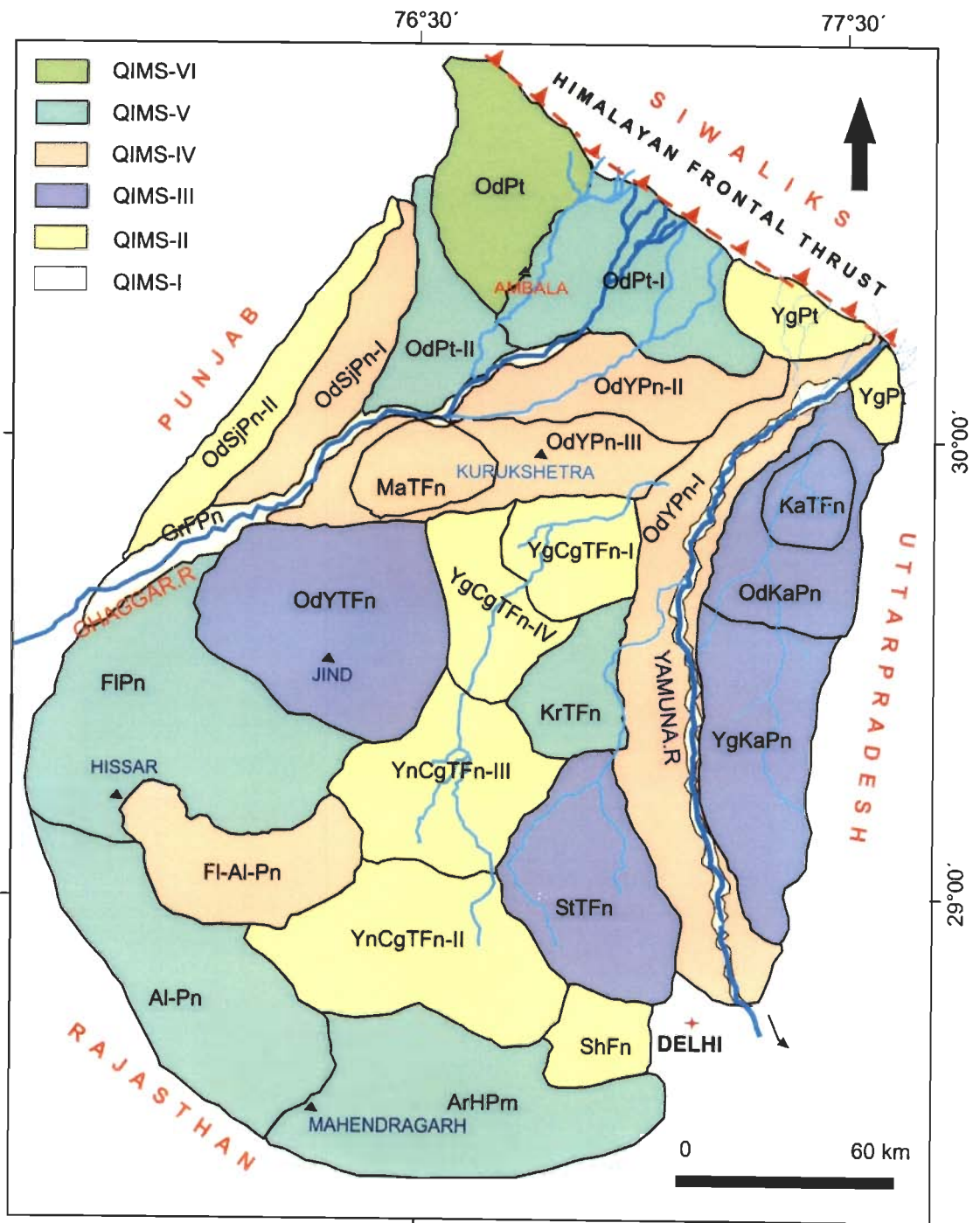
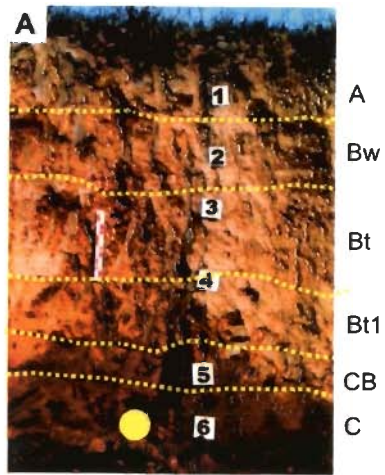
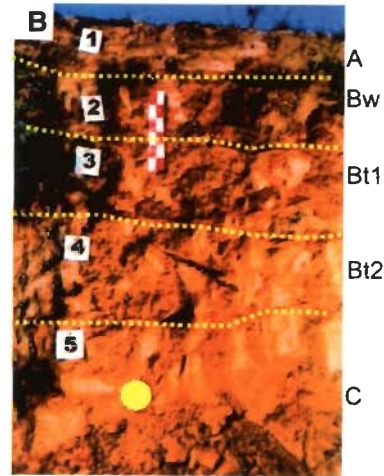


Fig. 2.10 Distribution of soils of different members of the Morphostratigraphic Sequence of the study area.

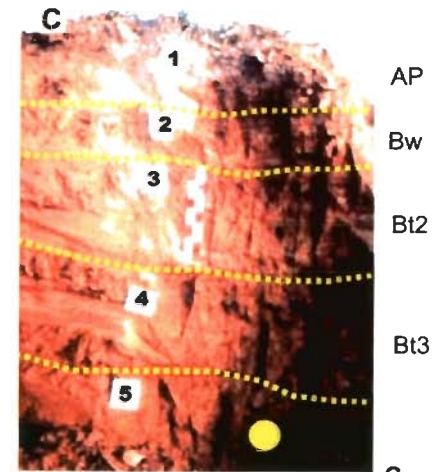




VS-1



VA



VC36

● Sample for dating



Fig. 2.12 Field photographs of QIMS-VI soils pedon A) VS-1 B) VA C) VS36 and D) Morni Hills from Oldest piedmont (OdPt).

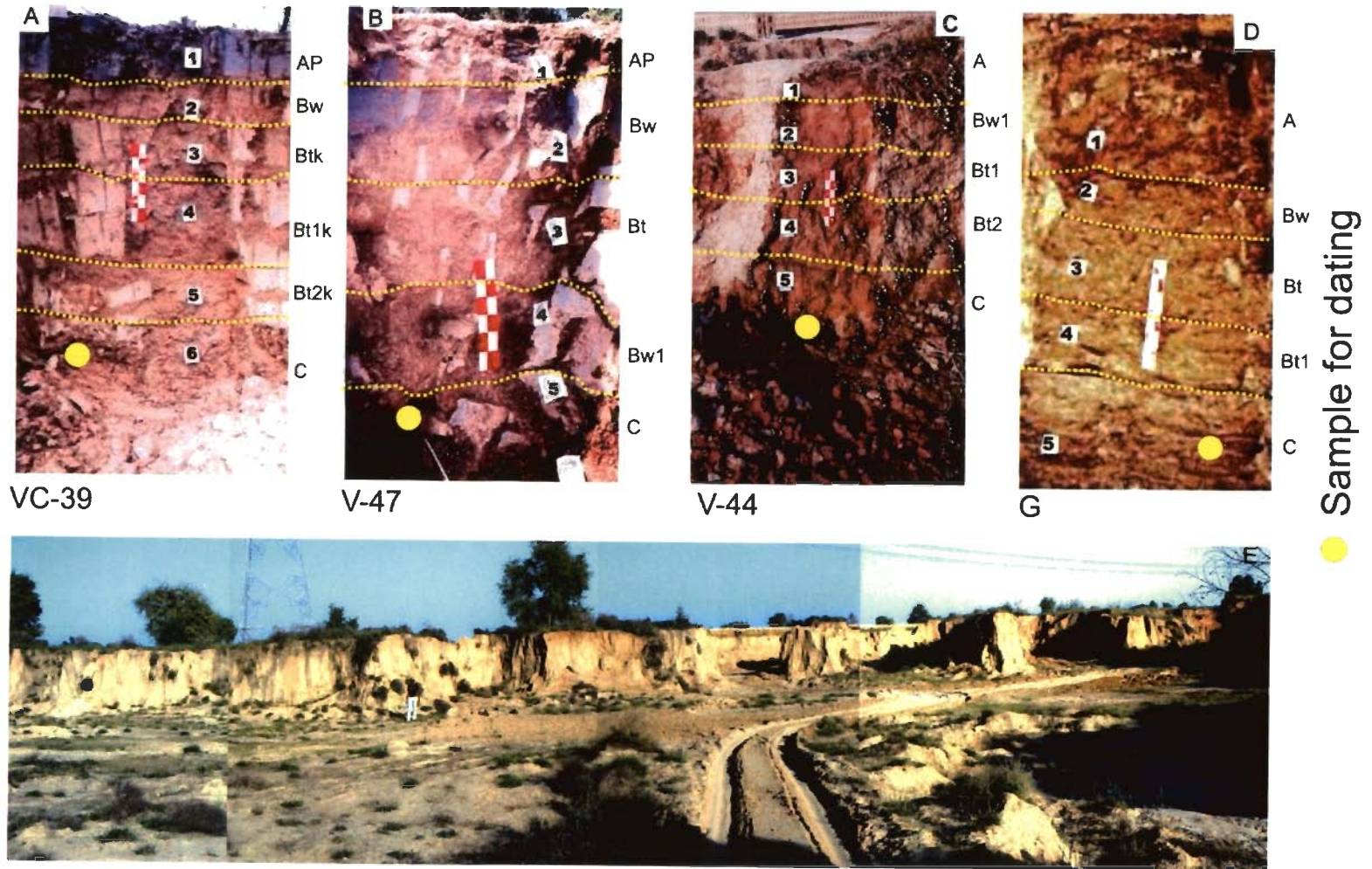


Fig. 2.13 Field Photographs of QIMS-V soils pedon A) VC-39(OdPt-II) B) V-47(ArHPm) C) V-44 (KrTFn) D) G (OdPt-I) and e) abandoned channel near Balsamand Village in Aeolian plain(APn)



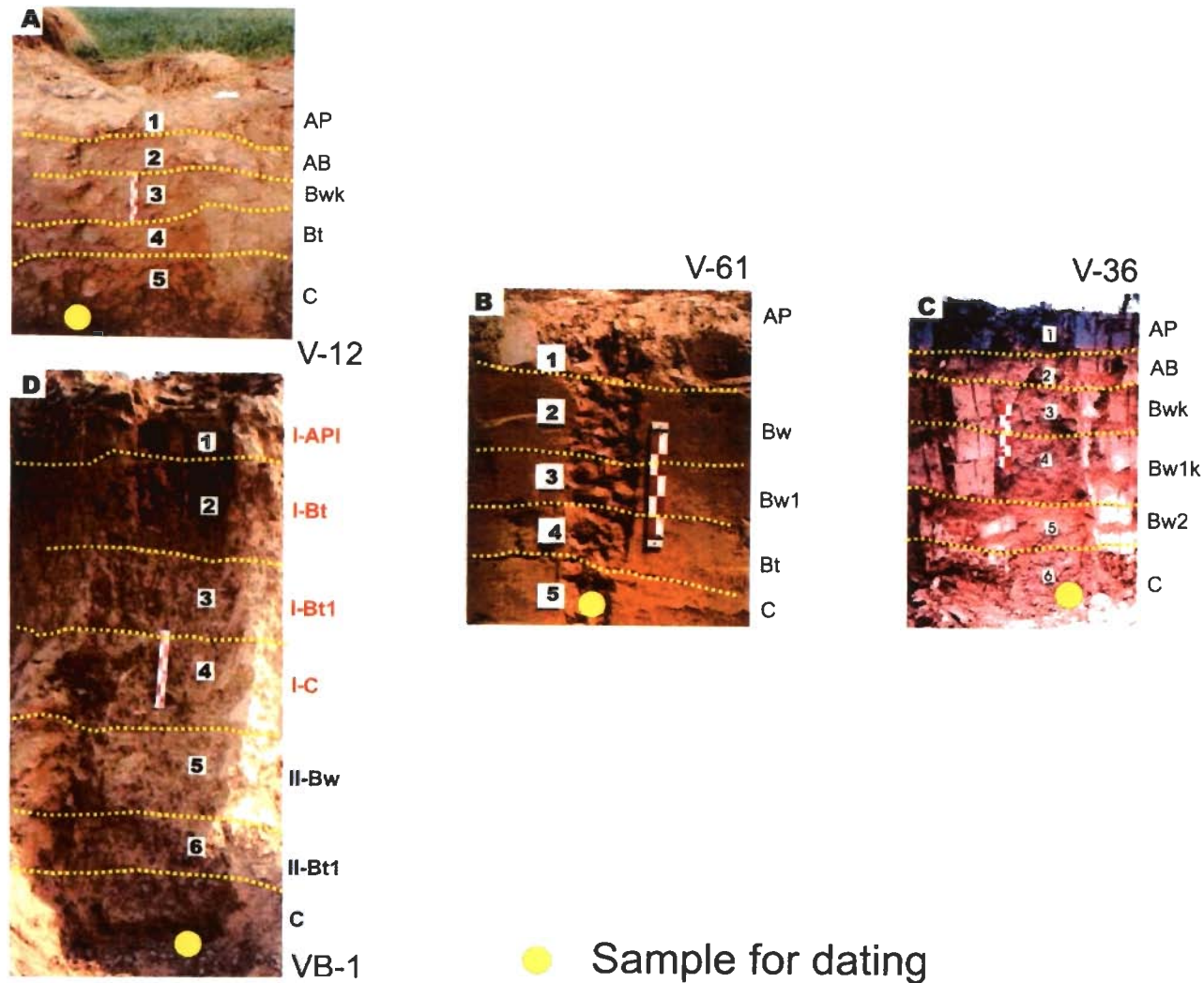


Fig. 2.14 Field Photographs of QIMS-IV soils pedon A) V-12 (OdYPn-III) B) V-61(OdYPn-II) C) V-36 (Fl-Al-Pn) D) VB-1 (OdYPn-I)

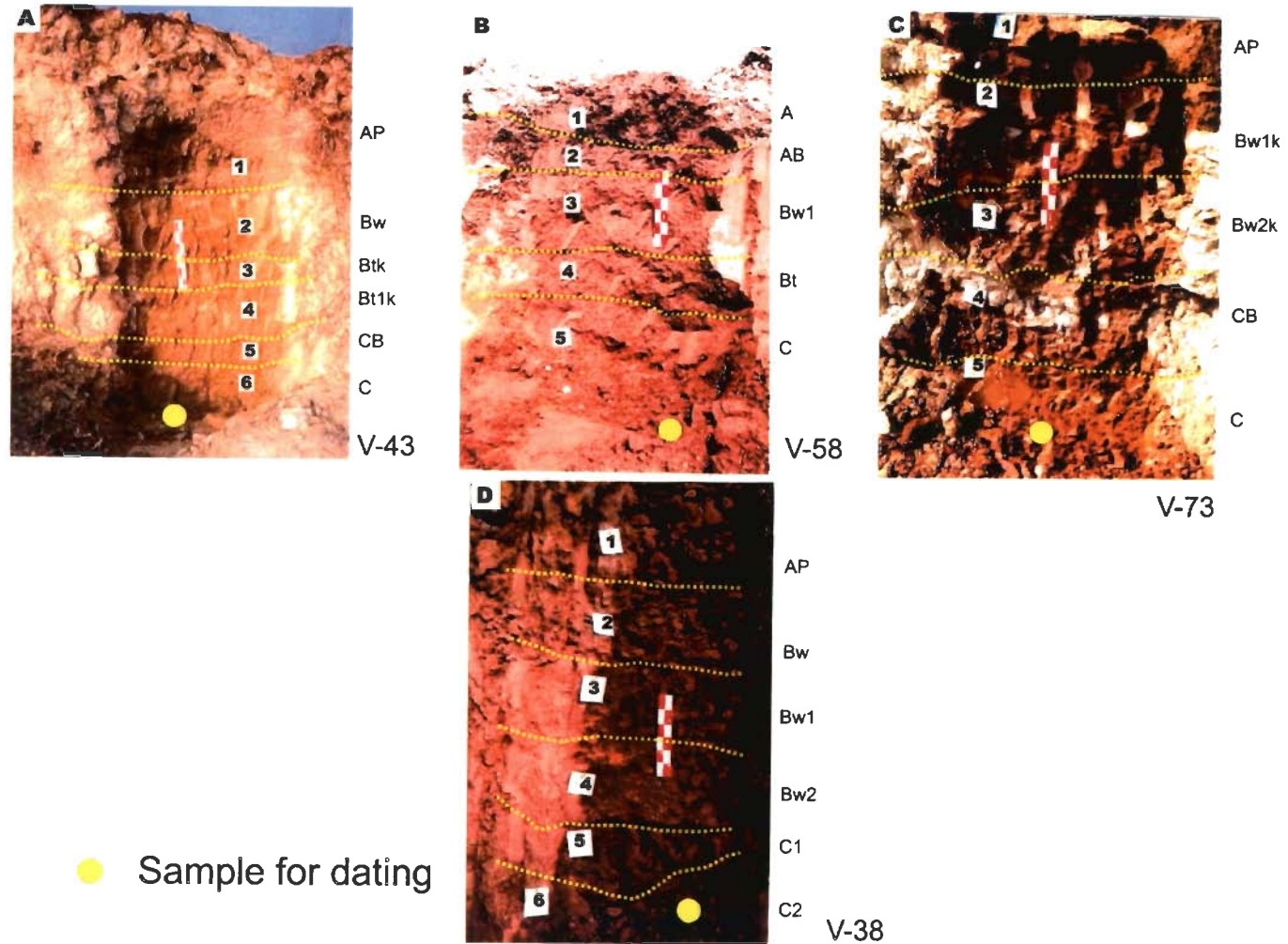


Fig. 2.15 Field Photographs of QIMS-III soils pedon A) V-43 (OdYTfn) B) V-58 (StTFn) C) V-73 (YgKaPn) D) V-38 (OdKaPn)

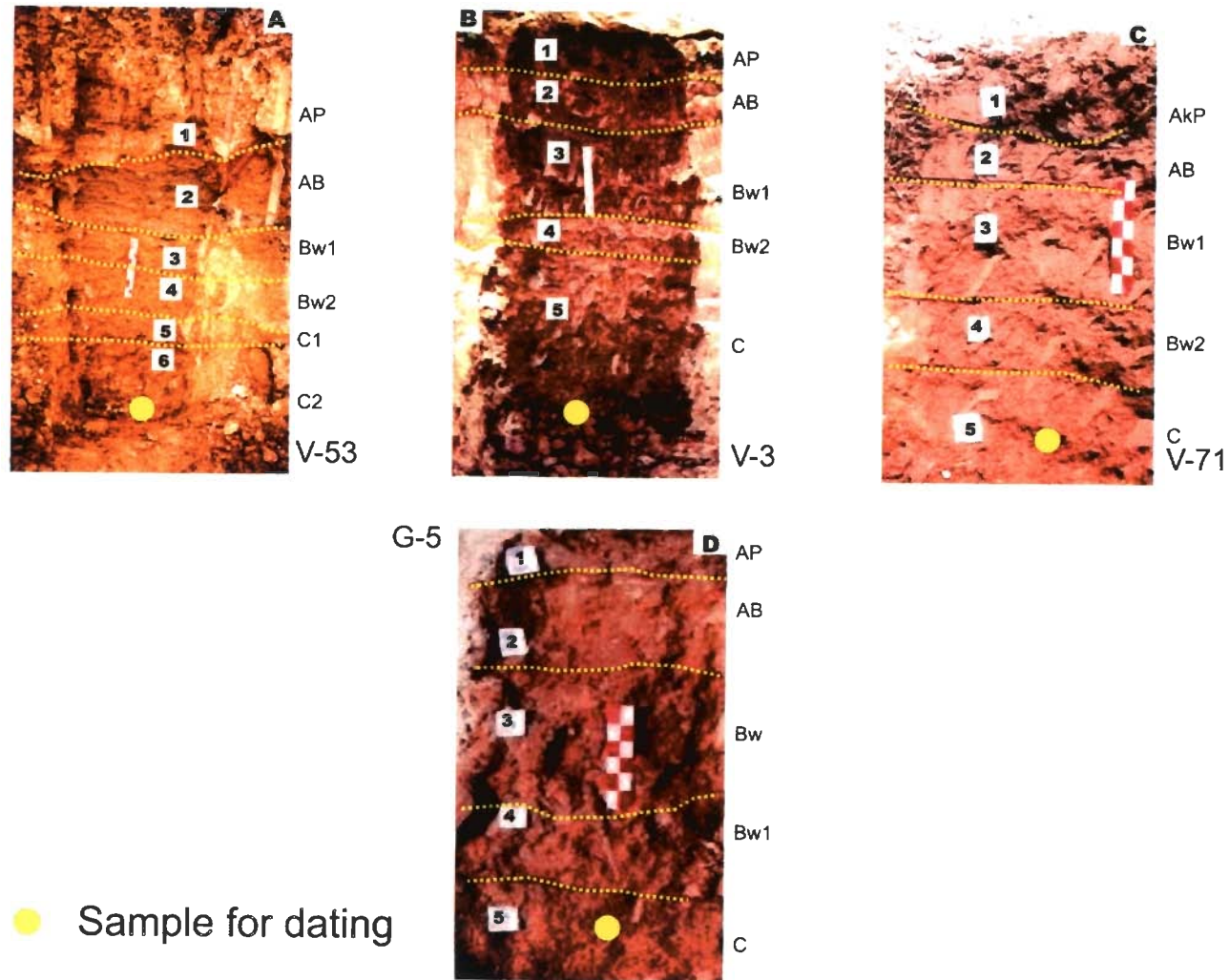


Fig 2.16 Field Photographs of QIMS-II soils pedon A) V-53 (YgCgTFn- III) B) V-3 (YgChTFn- I) C) V-71 (YgCTFn- II) D) G-5 (OdSjPn-II)

distributed in the B-horizons. pH varies between 6.2-7.4, indicating slight acidic to mildly alkaline nature of the soils. Absence of effervescence on being treated with hydrochloric acid indicates the soils in this unit are free of carbonates. Texture of the soil varies from sandy loam to loamy sand class (Fig. 2.12).

### **2.7.2 Member QIMS –V**

This member covers the major part of study area and includes six soil geomorphic units i.e. Old Piedmont-I, Old Piedmont-II, Aeolian Plain, Aravalli Hills and Pediment, Karnal Terminal Fan and Fluvial Plain are distributed in the northern, southern and central parts (Fig. 2.10).

The soils in this area are moderate to strongly developed having sub-angular blocky structures. Thickness of B-horizon varies from 34 to 96 cm and that of the solum varies from 65-119 cm. Common medium and distinct mottles and Fe-Mn nodules (7.5YR3/3) are well distributed, in the B- and C-horizons of OdPt-I, OdPt-II, and ArHPn. Medium thick clay cutans are well distributed in the B-horizons. Due to low lying nature, soils in the OdPt-II show gleying affects. The colour of the soils varies from light yellowish brown (10YR6/2) to dark brown (10 YR4/3m). Variation of pH from 5.89-7.5, indicates medium acidic to mildly alkaline nature of soils. Texturally, the soils in this member vary from sandy loam to loamy sand. In Karnal Terminal Fan and Aeolian Plain, the soils show sandy texture where as in Old Piedmonts-I and II show loamy sand, respectively (Fig. 2.13). Fine to very fine roots are observed in the A- and B-horizons, but the C-horizon shows absence of roots. The soils of this member are free of carbonates except the Aeolian Plain, which shows moderate effervescence.

### **2.7.3 Member QIMS –IV**

This member consists of six soil geomorphic units i.e. Old Sutlej Plain-I, Old Yamuna Plain-I, Old Yamuna Plain-II, Old Yamuna Plain-III, Markanda Terminal Fan and Fluvial-Aeolian Plain. Most soil geomorphic units in this member represent the old plains of the Yamuna and the Sutlej Rivers (Fig. 2.10). In most parts of these units, abandoned channels can be clearly visualized in the field, which are filled with the alternating sand and mud beds. The soils in this member area are moderately developed. The B-horizon thickness varies from 22 to 75 cm. The soils of this member show sub-angular blocky as well as prismatic structures along with the Fe-Mn and calcium carbonates nodules. Medium thick clay cutans are well distributed in the B-horizon and the BC horizons are marked by patchy thin clay cutans. The colour of the soil varies from dark grayish brown (10YR5/2) to dark brown (10YR4/3). The C-horizon is marked by absence of roots. Many medium and prominent mottles (10YR4/3) are well distributed in the B-horizons, but the BC and C-horizons are marked by the presence of dark brown (10YR4/1.5) Fe-Mn nodules. CaCO<sub>3</sub> nodules are seen in the C-horizons of the Fluvial-alluvial-Plain in the southern part of the area. Texturally the soils in this member fall in the sandy loam to sandy clay classes (Fig. 2.14). Variation of pH from 5.4-7.12 indicates the soils are strongly acidic to neutral in nature. Gleying is observed in the Old Yamuna Plains-I & II soils due to its low lying nature.

### **2.7.4 Member QIMS –III**

This member of the morphostratigraphic sequence includes five soil geomorphic units i.e. Old Yamuna Terminal Fan, Sonipat Terminal fan, Old



Katha Plain, Young Katha Plain and Katha Terminal Fan. These units are well distributed in the west-central and eastern part of the study area (Fig. 2.10).

Soils found in this member are moderate to weakly developed with sub-angular blocky structures. The B-horizon thickness varies from 26-61 cm and that of the solum varies from 53-96 cm. The matrix colour varies from pale yellowish brown (2.5YR7/4) to dark brown (10YR4/3) in colour. Many medium distinct mottles (10YR4/3) are well distributed in the B horizons of Old and Young Katha plains, but the same in the Sonipat and Karnal Terminal Fans are fine and faint. Fe-Mn concretions of light yellowish brown colour (10YR6/3) are reported from the units in the Old Katha Plain, Young Katha Plain and Katha Terminal Fan. Patchy, thin clay cutans are observed in the Old Katha Plain and in some pedons of the Young Katha Plain, but all other soil-geomorphic units don't show any significant clay illuviation features. The pH varies from 5.98-7.2 indicating medium acidic to neutral nature of soils. Texturally the soils in this member fall in the sandy to sandy loam classes (Fig. 2.15).

#### **2.7.5 Member QGMS –II**

This member includes six soil-geomorphic units i.e. Young Chautang Terminal Fans-I-IV, Sahibi Fan, Young Piedmont and Old Sutlej Plain-II (Fig. 2.4). Most of the units in this member were deposited in the form of terminal fans by the activity of Markanda, Karnal & Rohtak faults. However, the Young Piedmont in the northernmost region has been deposited by the activity of the Himalayan Frontal Thrust (HFT), by the various ephemeral rivulets rising from the Siwalik Ranges. The Old Sutlej Plain-II in the west was deposited by the Sutlej River.

Soils in this member are weakly developed and the B-horizon thickness varies from 13-47 cm and the Ap horizon is much thicker comparatively. The pH varies from 6.9-7.89, indicating that the soils in this unit vary from neutral to moderately alkaline nature (Fig. 2.16).

Patchy thin clay cutans are observed in some pedons of the Young Chautang Terminal Fan-II and other units on this member don't show any clay illuviation features. Fine faint mottles are observed in this member. The matrix colour varies from dark grey 2.5Y4/1 to dark grayish brown 2.5Y4/2. Roots are common and fine.

Soils in the Old Sutlej Plain-II consist sandy material occurring along the paleo-channels and silt and clay cover the intervening areas between the paleo-channels. This plain is marked by the abundance of calcareous material in the form of irregular concretions (called *kankar* locally) and in this area salt efflorescence is also common (Appendix-2). The soil matrix colour varies from brown (7.5YR4/4) to yellowish brown (2.5Y6/3). The animal activity is present in considerable amount and calcareous nodules predominant in the C-horizon (Fig. 2.16).

Soils in the Young Piedmont show a typical colour yellowish brown (2.5Y6/3) to dark yellowish brown (2.5Y3/3) and are dominated by the fine and very fine sand and their texture varies from sandy to sandy loam classes (Appendix-2). The matrix colour varies from dark olive brown (2.5Y3/3) to light olive brown (2.5Y5/4). Fe-Mn and calcium carbonate concretion are commonly observed in this unit.

## **2.8 SALINITY ON THE BASIS OF THE TEST PERFORMED IN THE FIELD**

Nearly 60% of the geographical area of Haryana state is underlain by saline ground water. The intra-basin transfer of surface water in the early sixties for irrigation has disturbed the hydrodynamic equilibrium resulting in water-logging and salinization on large parts of the state. The existing inland drainage basin conditions did not permit the disposal of effluent drainage resulting in the continuous increase in the salinity of groundwater (Singh et al., 2004). From the field data Appendix-2, it is seen that nearly 40% area is under the regime of moderately saline to highly saline (8.0-10.2). The Rohtak region can be easily demarcated on the imagery indicating the excessive white patch, which is the result of the high salt efflorescence, resulting high reflectivity. Similarly in the southern part of Haryana, the presence of the excessive canal irrigation has resulted in the water logging conditions on a wide scale, and thus causing increase in the salt content in soils (Fig. 2.8).

## **2.9 LINEAMENTS**

The DTM generated from DEM with vertical exaggeration 600 of by ERDAS IMAGINE 8.5 software brings out clearly two sets of lineaments D-I and D-II, striking in NE and ENE directions respectively. D-I stands for the Drishadvati River, which used to flow this area. The lineament D-II seems to younger than D-I, as the area showing this lineaments cuts across the D-II. Normally lineaments are interpreted as structural features. However, in the present case, both these lineaments are considered to have been created by the Drishadvati River, which shifted its position from D-I to D-II over a short period, as oldest soils in regions of both lineaments D-I and D-II have similar age (Fig. 2.17).



## **2.10. MAJOR STRUCTURAL FEATURES OF THE STUDY AREA**

### **2.10.1 Methodology Used to Identify Faults**

Faults were identified by the following suggestions made by Bhsole et al. (2008) with some modifications in the four steps given below.

- i) First the drainage is examined from topographic maps. Offset and convergent drainage and drastic change in width or direction of a river over a short distance, were taken to indicate possible faults. For example, tributaries of the Ghaggar River and some streams in Young Piedmont in the north eastern part of the study show offset drainage due to Ambala Fault-I. This fault causes convergence of the small streams like the Chola Nadi, Siswa Nadi and Buoki Nadi with the Ghaggar River. Offsetting and narrowing of floodplains of the Ghaggar and Yamuna is observed just downstream of the Markanda Fault.
- ii) As a second step, the DTM obtained by draping Landsat image over a DEM generated using ERDAS IMAGINE with a high vertical exaggeration was helpful in identifying and mapping Himalayan Frontal Thrust and Ghaggar, Yamuna, Markanda, Jind, Rohtak and Hissar Faults.
- iii) In the third step, surface profiles in a direction roughly at right angles to strike of probable faults already recognized through investigations made in accordance with the steps (i) and (ii) in the entire study area using the DEM already prepared by ERDAS software and inferred by breaks in soft in the profiles and lateral continuity of these breaks in slopes (Fig. 2.20a, b). In this process, we paid special attention to boundaries of soil-geomorphic units, which may lie along faults. Later we prepared DEM was prepared using SURFER 8 software with a very high vertical

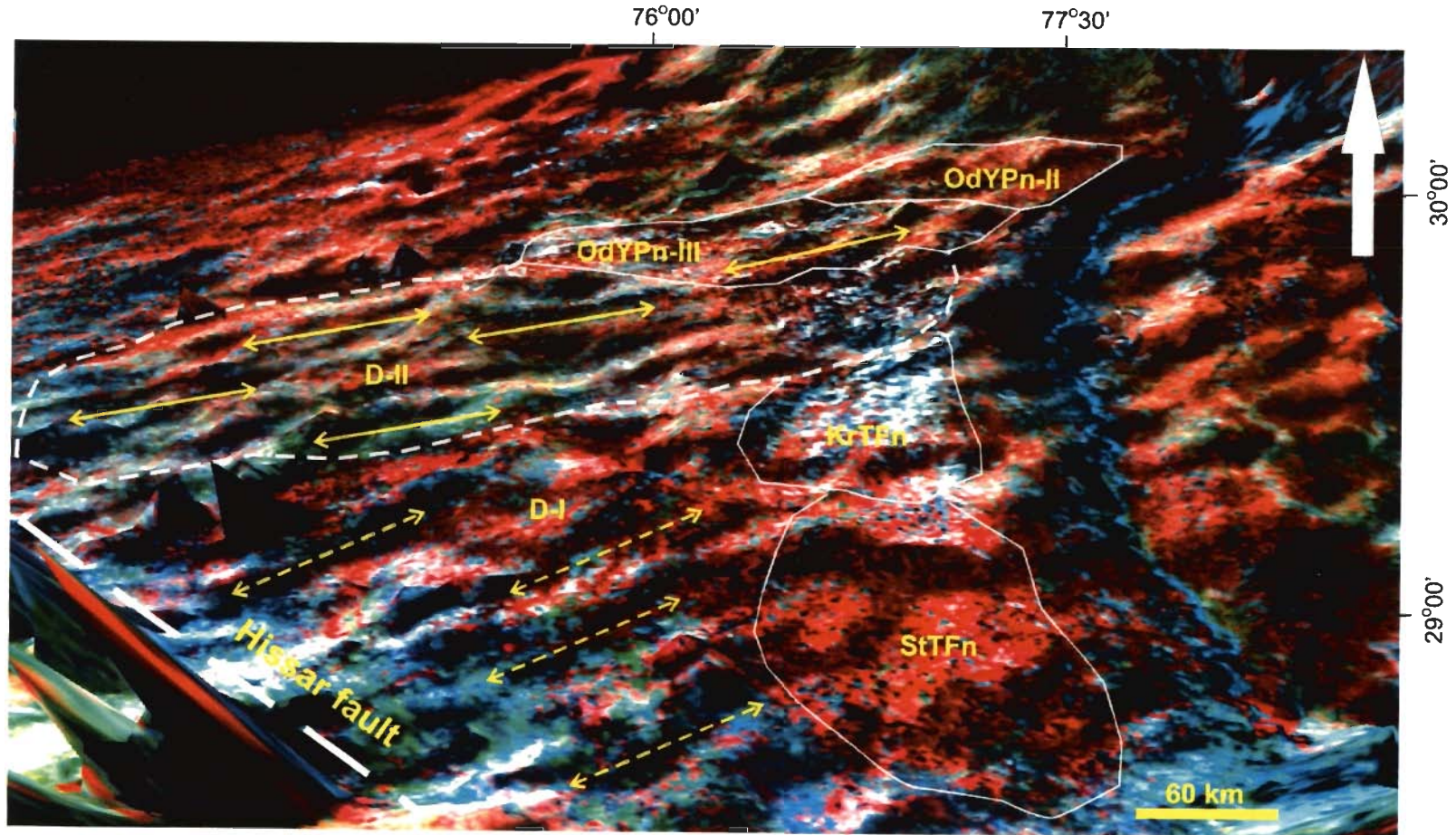


Fig. 2.17 DTM (Digital Terrain Model) showing lineaments directions flow of the Drishtavati River (D-I & D-II) present in the southern part of the study area changing directions with the time. The vertical exaggeration is 600 with sun angle N30°W.

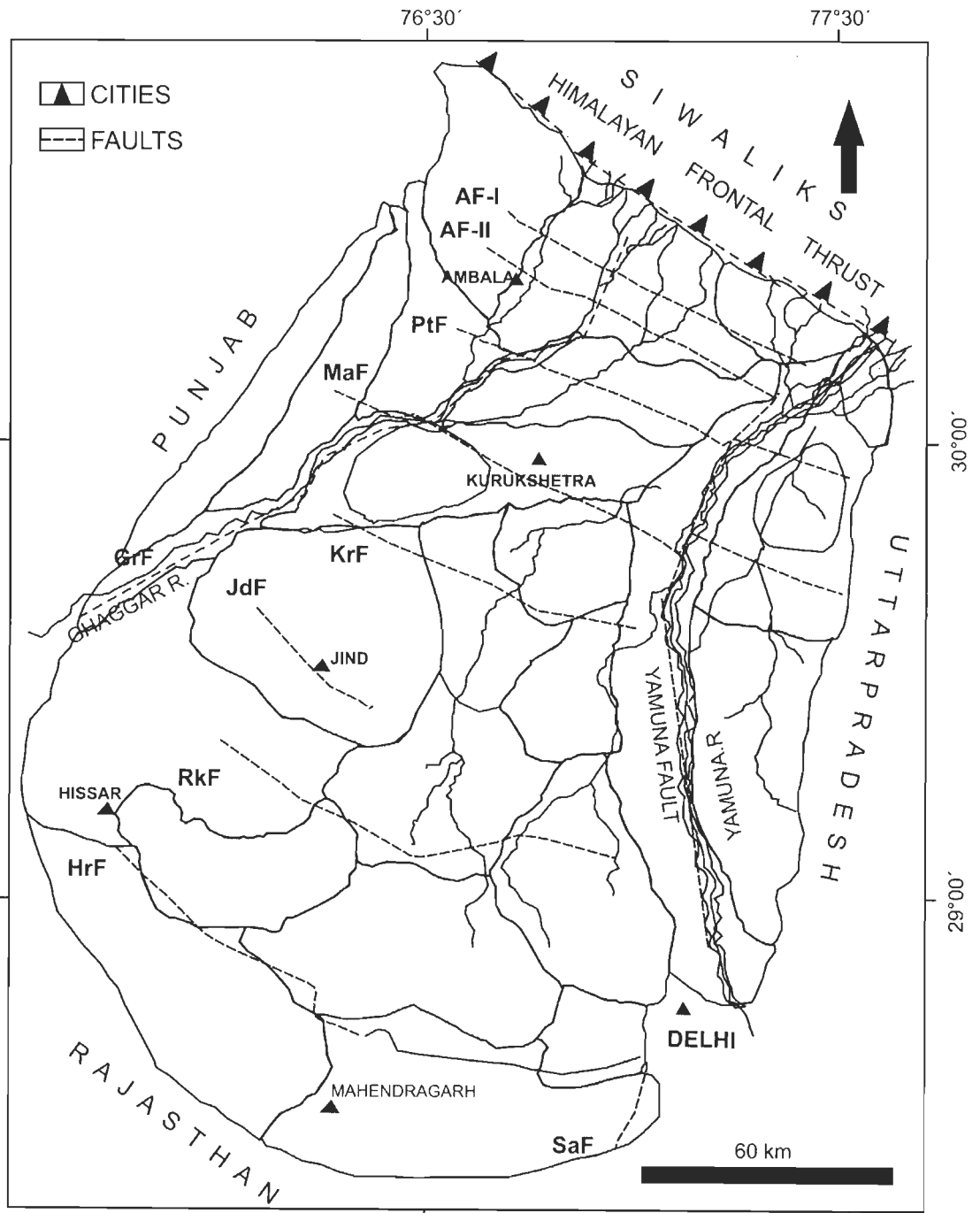


Fig. 2.18 Major faults in the study area superimposed over soil-geomorphic units. Major streams in the area also shown.

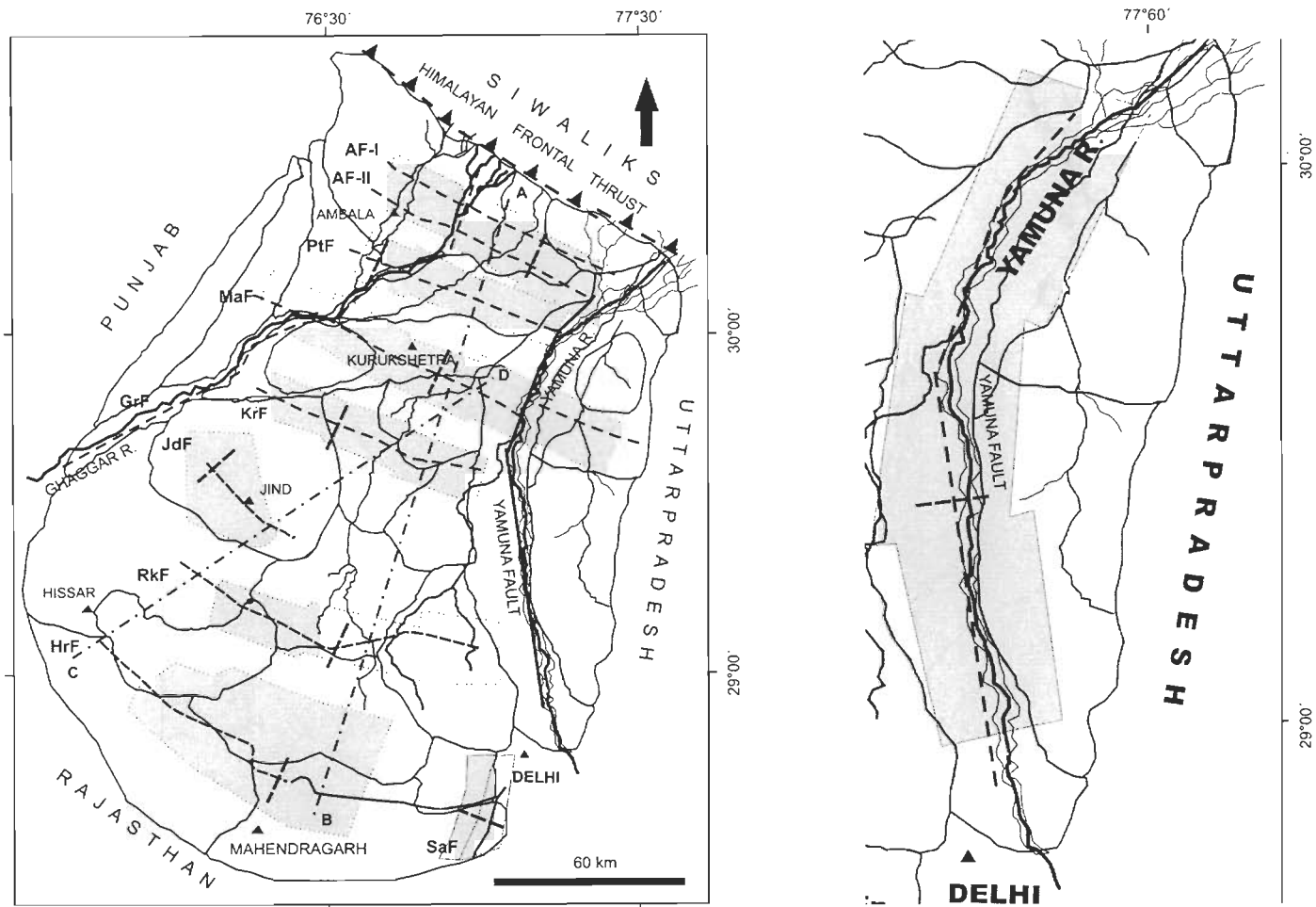


Fig. 2.19 (a) Locations DEM areas (shaded) around faults and terminal fans. Lines along which profile are drawn across faults are drawn, also shown (Fig. 2.20a). Lines of major profiles AB and CD in Fig. 2.20b also marked. (b) Area of DEM (Fig. 2.24c, d) around the Yamuna Fault.

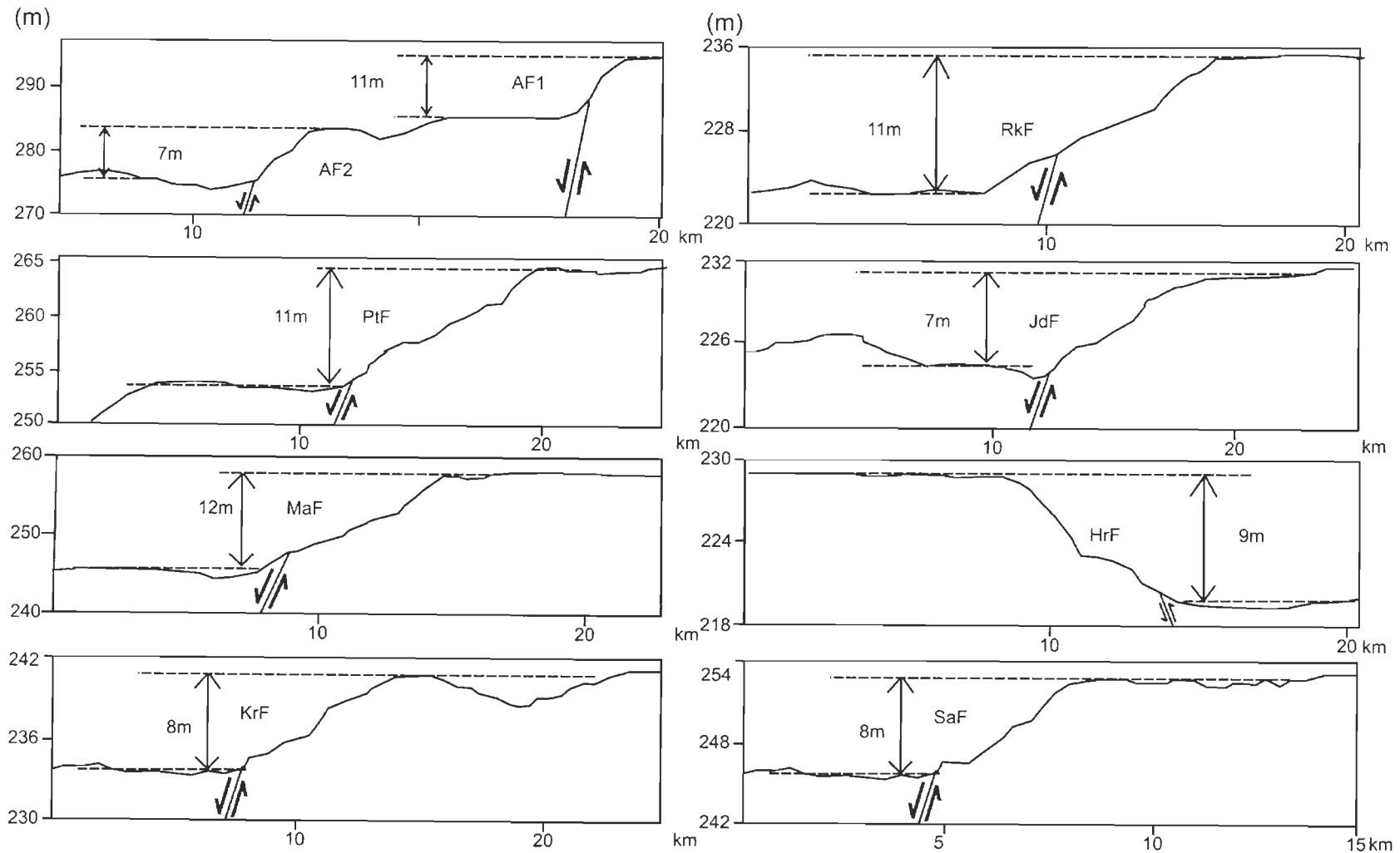


Fig. 2.20 (a) Profiles drawn across the Faults, Ambala fault I & II (AF-I and AF-II), Rohtak fault (RkF), Patiala fault (PtF), Jind fault (JdF), Markanda fault (MaF), Hissar fault (HrF), Karnal fault (KrF) and Sohana fault (SaF).

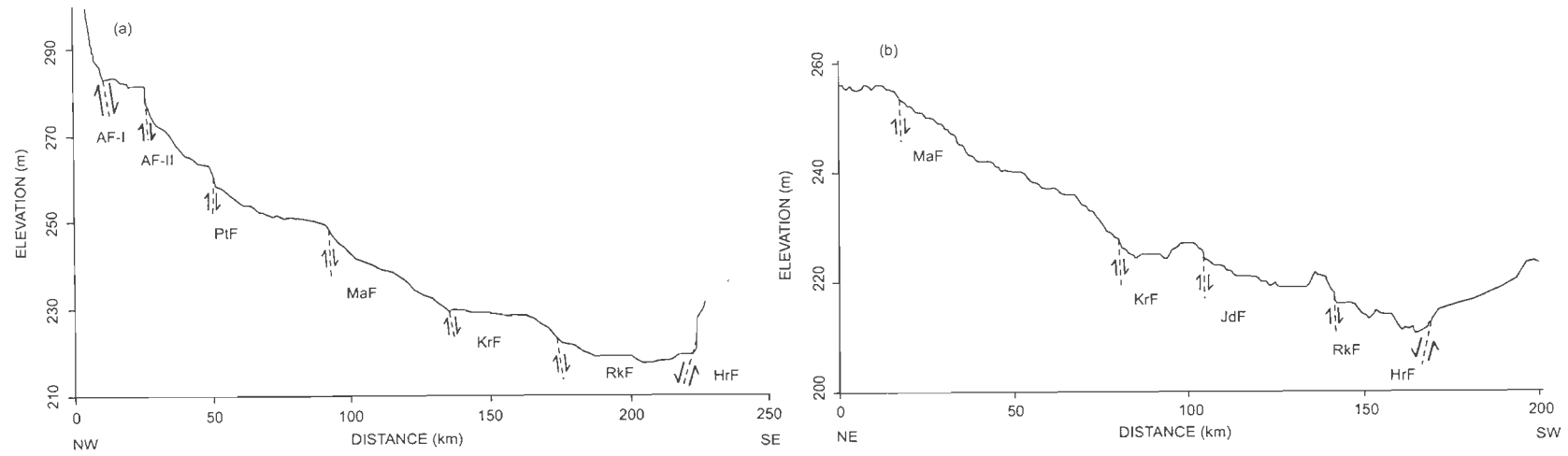


Fig. 2.20 (b) Full Profile Section drawn across the Faults a) (A-B profile) showing Ambala fault I & II (AF-I and AF-II), Patiala fault (PtF), Markanda fault (MaF), Karnal fault (KrF), Rohtak fault (RkF) and Hissar fault (HrF), b) C-D profile showing Markanda fault (MaF), Karnal fault (KrF), Jind (JdF)Rohtak fault (RkF) and Hissar fault (HrF).

exaggeration using krigging extrapolation technique in the region suspected to be faulted. Artifact 'cliffs' in such DEM were taken indicative of faults (Bhosle et al., in press). This way we identified additional faults like Ambala Faults I and II and Patiala Fault.

iv Terminal fans were identified from landsat images. These invariably associated with faults (Table 2.4) (Singh et al., 2006; Bholsse et al., 2008). As these develop on downthrown blocks of faults. Their presence and profiles across the inferred fault help to decipher the downthrown blocks.

v In the last step, GPR was used in the field to confirm and to know subsurface nature of the all the major faults identified above and this results are discussed in Chapter-5.

Based above techniques, eight faults and five tectonic blocks are identified.

## **2.11 FAULTS**

Parkash et al. (2001) classified the faults in the Indo-Gangetic Plain as longitudinal (parallel to the Himalayan trend) and transverse (at large angles to the Himalayan trend). In the study area, the Himalayan Ranges trend in the NW-SE direction. So Ambala-I and II, Markanda, Patiala, Jind, Rohtak and Hissar Faults run almost in NE-SW direction, sub-parallel to the Himalayan trend, are longitudinal in nature, whereas the faults bounding the study area i.e. Ghaggar and Yamuna Faults are transverse in nature (Fig. 2.18). The Ghaggar fault consists of a number of segments and as a whole it shows curvilinear trend with convexity towards southeast. Similarly the Yamuna faults follow a curvilinear pattern with convexity to the southwest and controls the course of the Yamuna River.



### **2.11.1 Ambala Faults-I and II**

The Ambala Fault -I and II are sub-parallel, strike in NW-SE direction, and are traceable for distances of 78 and 90 km, respectively. These faults have throws of 7-11 m (Figs. 2.20, 2.23b, 2.28). The Ambala-I Fault forms the southern boundary of the Young Piedmont in the northeast corner of the study area. This also causes offsetting of small tributaries of the Ghaggar and its tributaries like the Chola Nadi, Siswa Nadi and Buoki Nadi. The Ambala Fault - II forms boundary of the Old Piedmont-I with the Old Yamuna Plain-II for a distance of 30 km.

### **2.11.2 Patiala Fault**

The Patiala fault bounds the Old Piedmont-II on the southern side and is traceable for a distance of about 104 km with a throw of 11 m (Figs. 2.20, 2.23a). Also, this fault causes and offset of the Ghaggar River by ~1.5 km and convergence of the Ghaggar and its tributary. This fault is traceable on the eastern side of the Yamuna River, passes close to Saharanpur city and leads to formation of the Katha Terminal Fan (Fig 2.6).

### **2.11.3 Markanda Fault**

The Markanda Fault is traceable over 136 km in the study area, it passes through Kurukshetra cities and causes convergence of the Markanda and Ghaggar Rivers. Also, this fault has caused the formation of the Markanda and Young Chautang Terminal Fan-I. It continues across the Ghaggar and Yamuna Rivers, to the west and east respectively, as seen in



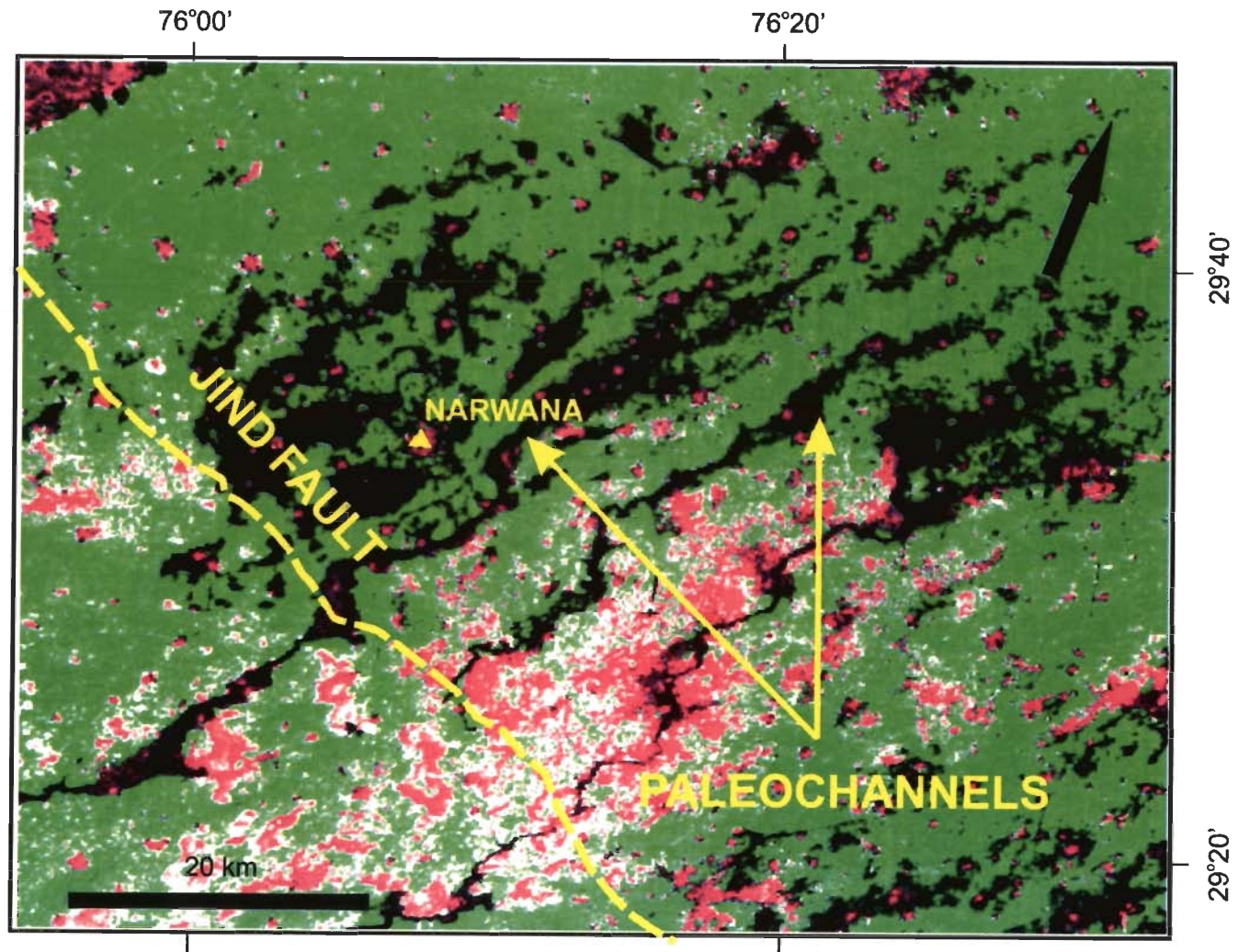


Fig. 2.22 Several paleochannels on the upthrown block abruptly ending against the Jind Fault. ETM+ WRS-2, Path 147, Row 039 (2000-10-15) image.

the DEM and DTM (Figs. 2.24b, 2.26). It continues east of the Yamuna River with a northerly offset of 3 km. The DEM shows that northern block is upthrown block with an average throw of around 12 m (Fig 2.20) Narrowing of the floodplains of the Ghaggar and Yamuna Rivers downstream of this fault are observed.

#### **2.11.4 Karnal Fault**

The Karnal Fault strikes along ESE-WNW direction and can be traced up for a distance of about 80 km up to the Kaithal city forming two important fans: Karnal Terminal Fan and the Old Yamuna Terminal Fan (Fig. 2.4). The throw of the fault is 7 m towards southwest. Also, it forms southern boundary of the Young Chautang Terminal Fan-I. Time of activity of eastern and western segments of this fault are 2.9-3.2 Ka and 4.7 Ka, respectively (Table 2.4, Fig. 2.25c).

#### **2.11.5 Rohtak Fault**

The Rohtak Fault strikes roughly NW-SE and is traced over a distance of 122 km and passes through the Rohtak city and extends up to Sonapat district. The DEM of the region around the fault shows that the northern block of this fault is an upthrown one with a throw of 11 m in the Rohtak area (Figs. 2.20, 2.24a). This fault approximately defines the boundary between the Young Chautang Terminal Fan-II and III. Soils of the northern block are much more saline and waterlogged as compared to those of the southern block. (Fig. 2.9)

Table 2.4 Strike, exposed length, throw of faults, time of last activity of various faults observed in the study area. Characteristic features of DEMs of regions around these faults also given

Name of the fault	Strike of the fault	Exposed Length (km)	Throw of the fault Amount (m) /Direction	Time of last activity (Ka)	Vertical Exaggeration of DEM and Fig. nos.	Light position angles V/H
Ambala (AF-I)	NW-SE	90	11/SSW	--	287 Fig. 2.23b	45/135
Ambala (AF-II)	NW-SE	78	7/SSW	--	287 Fig. 2.23b	45/135
Patiala fault (PtF)	NW-SE	104	11/SSW	3.3 (E)	234 Fig. 2.23a	44/136
Markanda (MaF)	WNW-ESE	136	12/SSW	3.3 (E), 1.5(W)	307 Figs. 2.26b	45/135
Karnal (KrF)	WNW-ESE	81	8/SSW	2.9-3.2 (E), 2.3-2.4(C), 4.7(W)	285 Fig. 2.25c	54/153
Jind (JdF)	NW-SE	35	7/SSW	2.1-2.4(E)	223 Fig. 2.25b	45/135
Rohtak (RkF)	NW-SE	122	11/SW	3.2-3.4 (E), 1.9-2.3(W)	301 Fig. 2.24a	49/152
Hissar (HrF)	NW-SE	157	9/S	–	218 Fig. 2.23c	54/153
Yamuna Faults (c)	NNE-SSW	65,	11/NNW	–	262 Fig. 2.24 c	54/153
Yamuna Faults (d)	N-S	111	9/E	–	244 Fig. 2.24 d	54/153
Sohana	S-N	70	8/E	–	296 Fig.2.25a	49/152
Ghaggar	NE-SW	130	–	–	–	–

### 2.11.6 Jind Fault

The Jind Fault is shortest of all the identified faults and is traceable over a distance of 35 km only in the western-central region of the study area

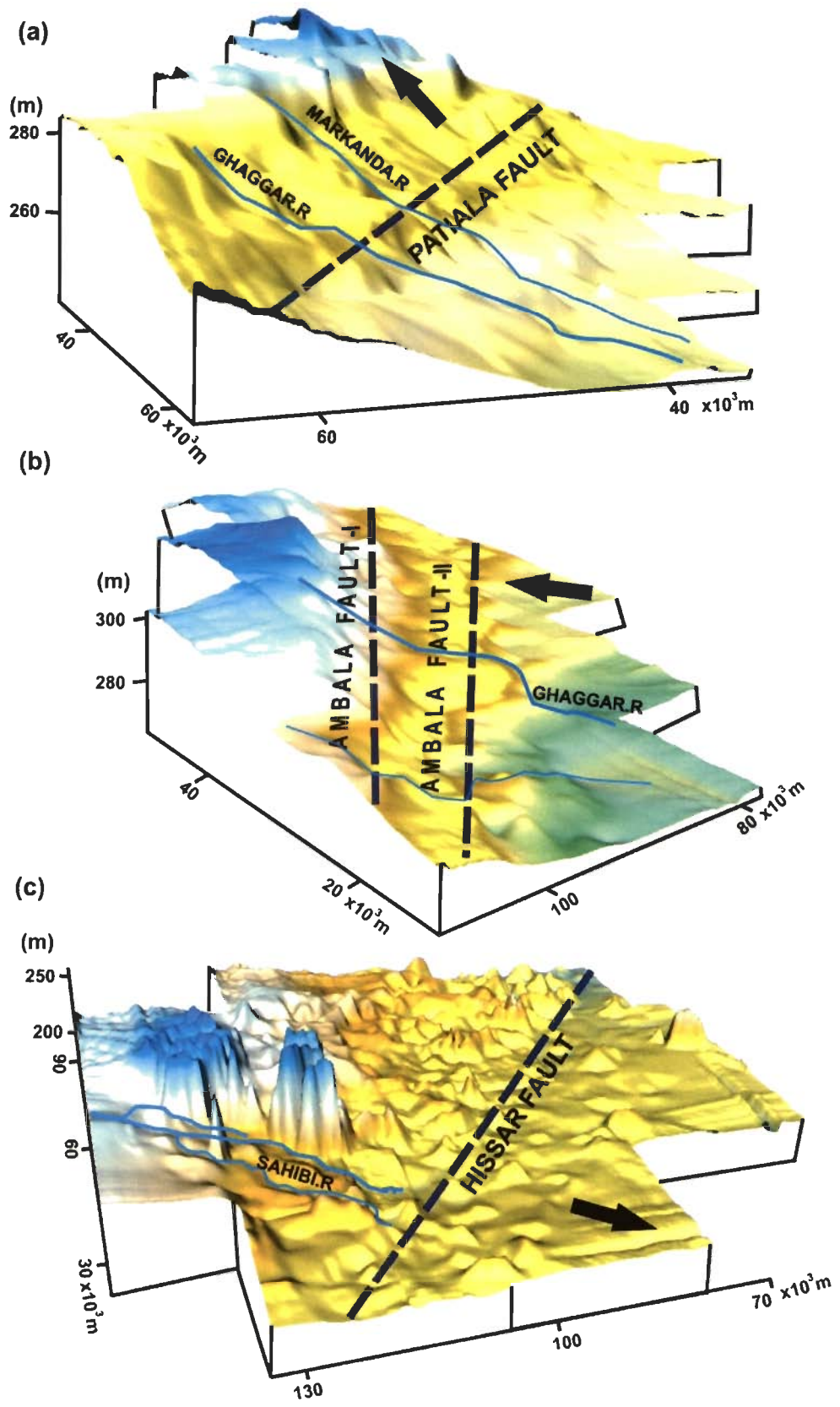


Fig. 2.23 Digital Elevation Models generated by SURFER-8 around (a) Patiala Fault (b) Ambala Faults I & II and (c) Hissar Fault.



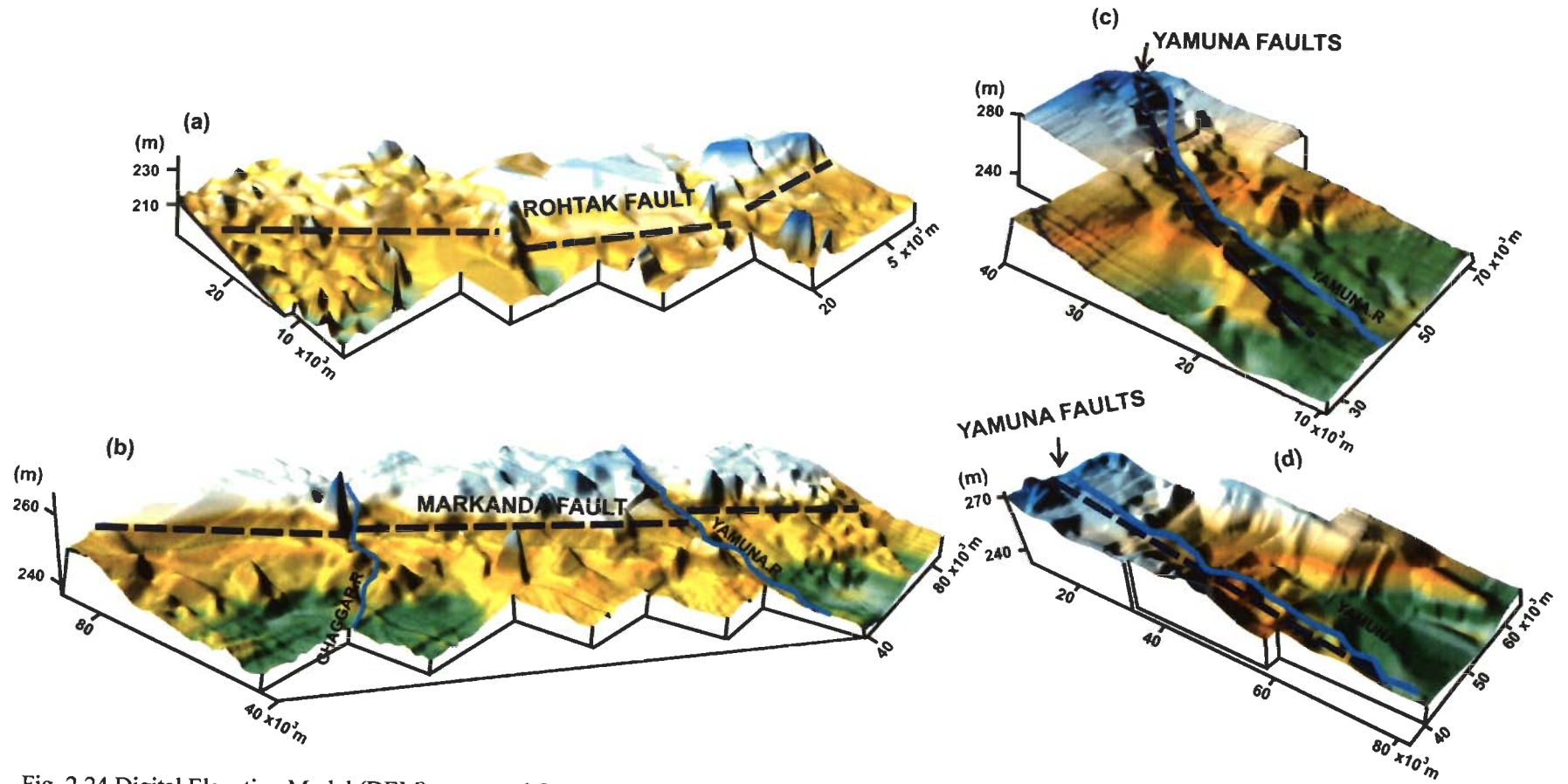


Fig. 2.24 Digital Elevation Model (DEM) generated for areas (a) Rohtak Fault (b) Markanda Fault (c & d) Yamuna Faults

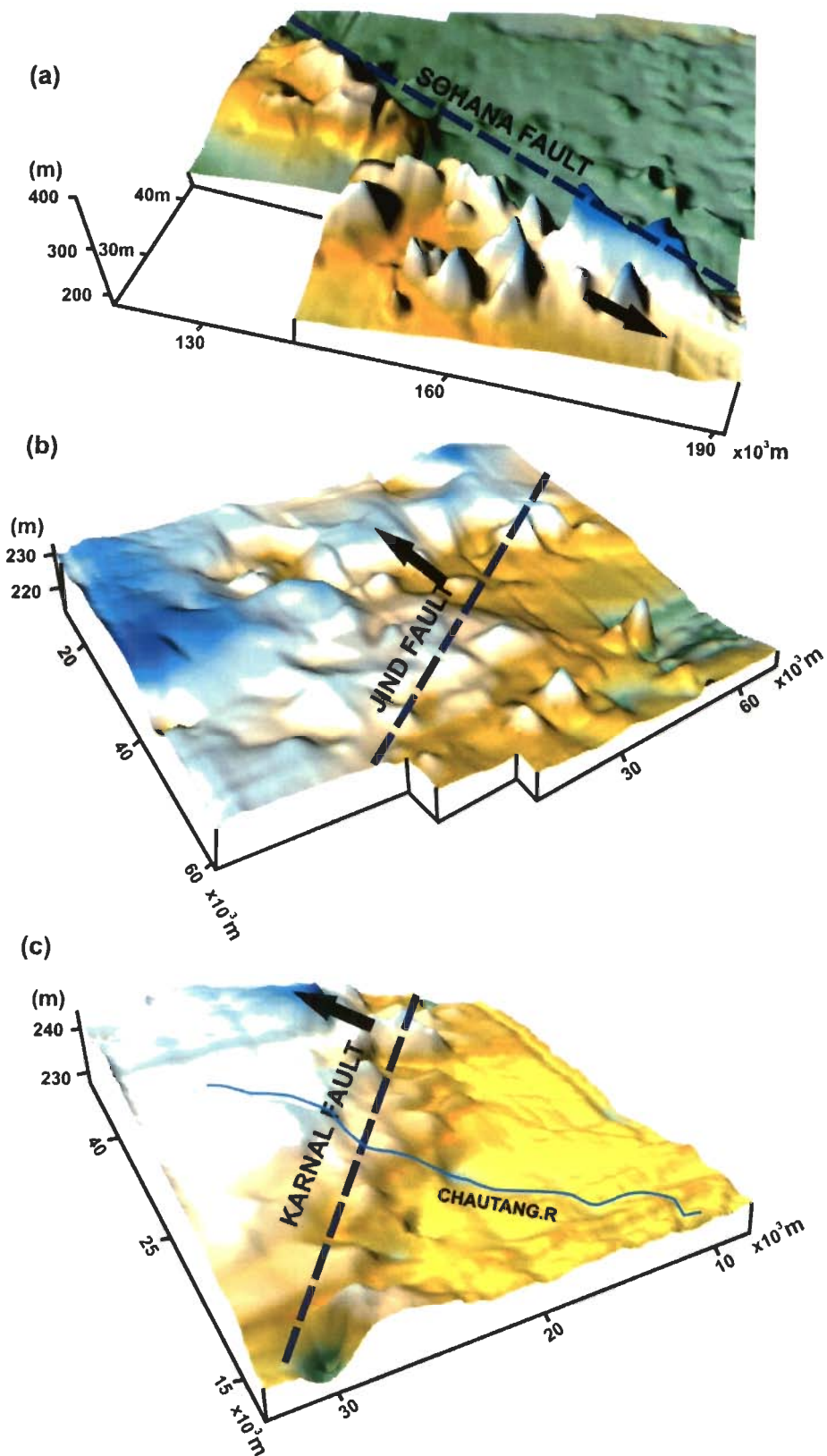


Fig. 2.25 Digital Elevation Model for areas around (a) Sohana Fault (b) Jind Fault (c) Karnal Fault.

and strikes in NW-SE direction. Over major part of its length, it has a throw of around 7 m (Fig. 2.25b). After an exceptionally wet rainy (ETM+ dated 2000-10-15 image) season in the year in this semiarid region, paleochannels north of this fault were filled with water, which end up against this fault and caused flooding of a large region around Narwana city (Fig. 2.22).

#### **2.11.7 Hissar Fault**

This Fault runs from region near Gurgaon up to Hissar strikes in a NW-SE direction for distance of about 157 km and is the longest fault in the study area. It is in the southernmost part of the study area and acts as a boundary between the Haryana plains and the Aravalli hills in the southwestern region near Gurgaon for a distance of 67 km, and displaces alluvial/aeolian sediments in northeastern region near Hissar (Fig. 2.23a) over a distance of 90 km. This is a major barrier to the Aeolian transport of sand from the Thar desert in the south. The DEM of region around the fault indicates that the western block is the upthrown block, and thus it is antithetic to the rest of the longitudinal faults, described above. The northern block is less saline comparatively to the southern block across this fault. In the southern portion of Haryana state, small streams originating in the Aravalli flow northward and the Sahibi River from this group forms a fan.

#### **2.11.8 Yamuna Faults**

The Yamuna fault system has a curvilinear shape with convexity towards the southwest. It strikes in almost NNE-SSW direction in the northern part, and strike changes to N-S direction in southern part of the study area.

The fault forms a continuous ridge on the western side of the Yamuna plains and western side is upthrown block, as shown by the DEM (Fig. 2.24 c& d)

#### **2.11.9 Sohana Fault**

The Sohana fault strikes in N-S direction and it starts from Gurgoan, Faridabad region and ends near Delhi (Fig 2.25a). It marks boundary of the Aravalli Formation with alluvium. As it joins the Yamuna faults in the north, it could be an extension of a segment of this fault system. Sohana water hot spring is located along this fault.

#### **2.11.10 Ghaggar Fault**

The Ghaggar Fault is curvilinear in nature, with convexity towards southeast. It starts in the Old Piedmont-I region, where it strikes almost N-S and further west it takes NE to SW direction and ends near Hanumangarh district in Rajasthan. The downthrow is towards NW. The Ghaggar River flows along this fault. This fault was first recognized by Manchanda (1981).

In summary, all the faults except the Hissar Fault in the piedmont and plain regions are of longitudinal nature and show a throw of 7-12 m towards SSW, as shown by DEMs and profile sections across the faults (Figs. 2.19). The Hissar Fault has a throw to the NNE and is antithetic to the other longitudinal faults. Also, two long NE-SW striking profiles A-B and C-D (Fig. 2.20 a, b) bring out the study area forms an asymmetrical basin. The shallow subsurface nature of the faults has been further checked by GPR studies (Chapter-5).

As discussed in a later Section (2.11), many of the faults identified in our study are presently active. The past activity of some of the faults has been



approximately dated by ages of soils on the terminal fans (TF) formed on downthrown blocks of these faults. Faults like the Markanda, Karnal and Rohtak Faults show two segments, which were active at different times to give rise to at least two terminal fans. Also, the eastern segment of the Markanda Fault was active at about 2.4 Ka and 1.5 Ka to develop the overlapping Young Chautang Terminal Fans-I and IV, respectively. Ages of the terminal fans indicate that most of the activity of various faults in the central region of the study area took place between 4.7 Ka and 1.5 Ka.

## **2.12 TECTONIC BLOCKS**

Five tectonic blocks are identified in the study area. These tectonic blocks are bounded by the transverse as well as longitudinal faults (Fig. 2.26).

### **2.12.1 Piedmont Block**

The Piedmont block is bound by the Himalayan Frontal Fault in the north, the Markanda Fault in the south. The block is marked by the presence of the different piedmont (oldest, old and the young), identified on the basis of upon ages and the degree of soil development.

### **2.12.2 Jind-Rohtak Block**

The Jind-Rohtak block is present in the central part of the study area between the Piedmont Block and the Aravalli block in north and south, respectively. The major portion of this block is covered by of the terminal fans with age from 3.5 to 1.5 Ka, formed due to activities of the Karnal Markanda and Jind faults. Most of the area in the south is marked by the presence of a number of paleochannels. The block is characterized by weakly to moderately developed soils.

### **2.12.3 Hissar Block**

This block is overlain by low elevation hills of the Aravalli Formations. The soil in this area is medium to well developed with an age of 5.3 - 4.4 Ka.

### **2.12.4 Punjab Block**

This Punjab Block lies on the northwestern side of the Ghaggar Fault (Manchanda 1981, Singhai et al, 1991). This block is marked by numerous paleochannels starting from Ropar, where the River Sutlej enters the plains from the Siwalik Ranges, suggesting that these were formed as a result of northward migration of the Sutlej River (Pal et al, 1980). This block is marked by some well developed soils in the southern portion and weakly-developed in the northern part.

### **2.12.5 Saharanpur Block**

This block lies on the eastern side of the river Yamuna in the Uttar Pradesh state and is separated by the Yamuna Fault from Haryana Plain. The soil in this area is moderately developed with an age of 3.5-4.4 ka. On this block the Katha Terminal Fan is observed, which developed due to activity of an extension of the Patiala Fault.

## **2.13 RELATION BETWEEN OCCURRENCE OF EARTHQUAKES AND FAULTS**

Major part of Haryana falls under seismic Zone-IV. Most earthquakes in this region are shallow, though a few earthquakes of intermediate depth have been recorded in Haryana (<http://asc-india.org/seismi/seis-cdh.htm>). Earthquake epicenters obtained from the above site were plotted on the map with faults. We find that the region between the Rohtak and Hissar faults is the most active. Rohtak Faults seems to be most active followed by Hissar

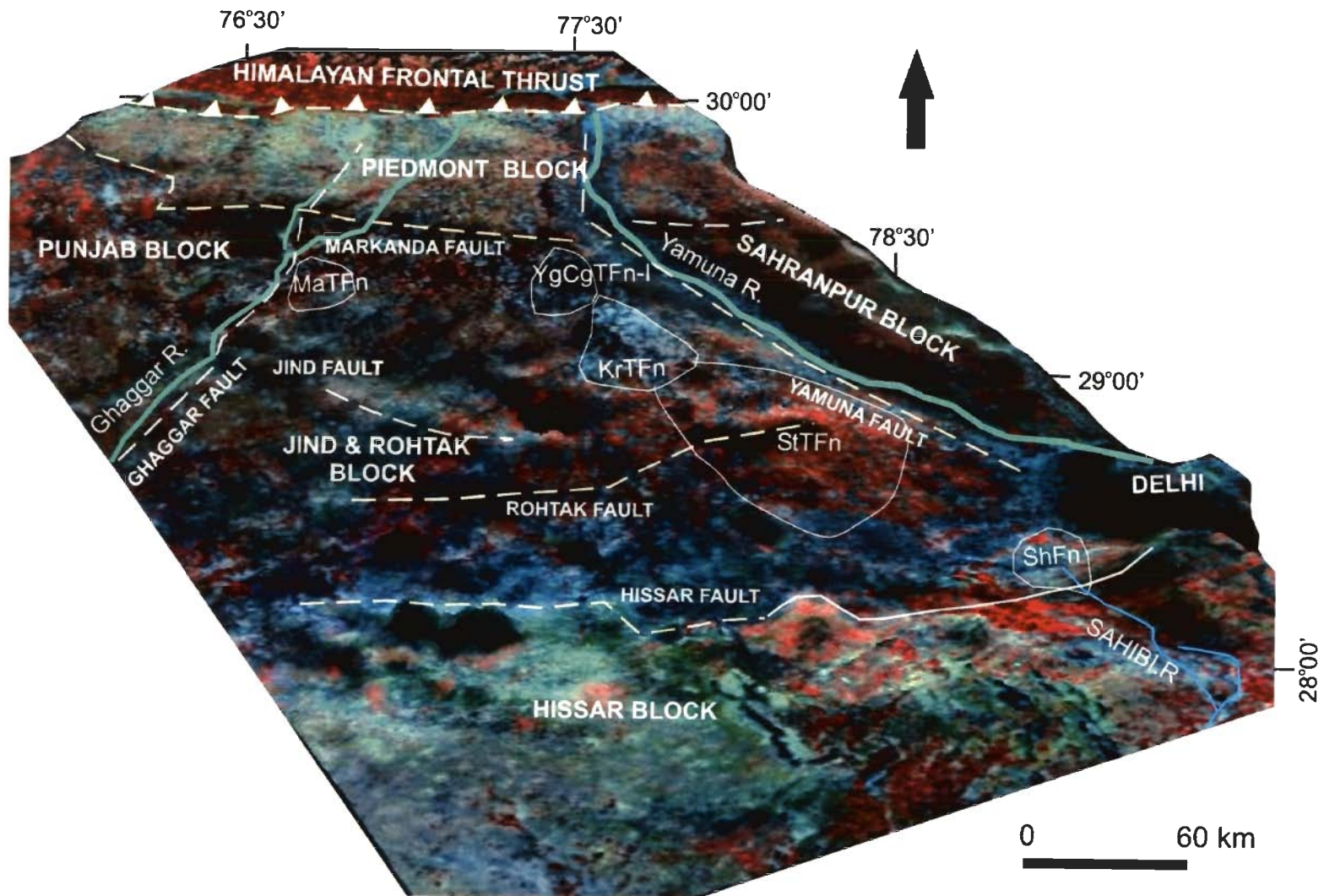


Fig. 2.26 Digital Terrain Model of the study area showing tectonic blocks, major terminal fans, and faults

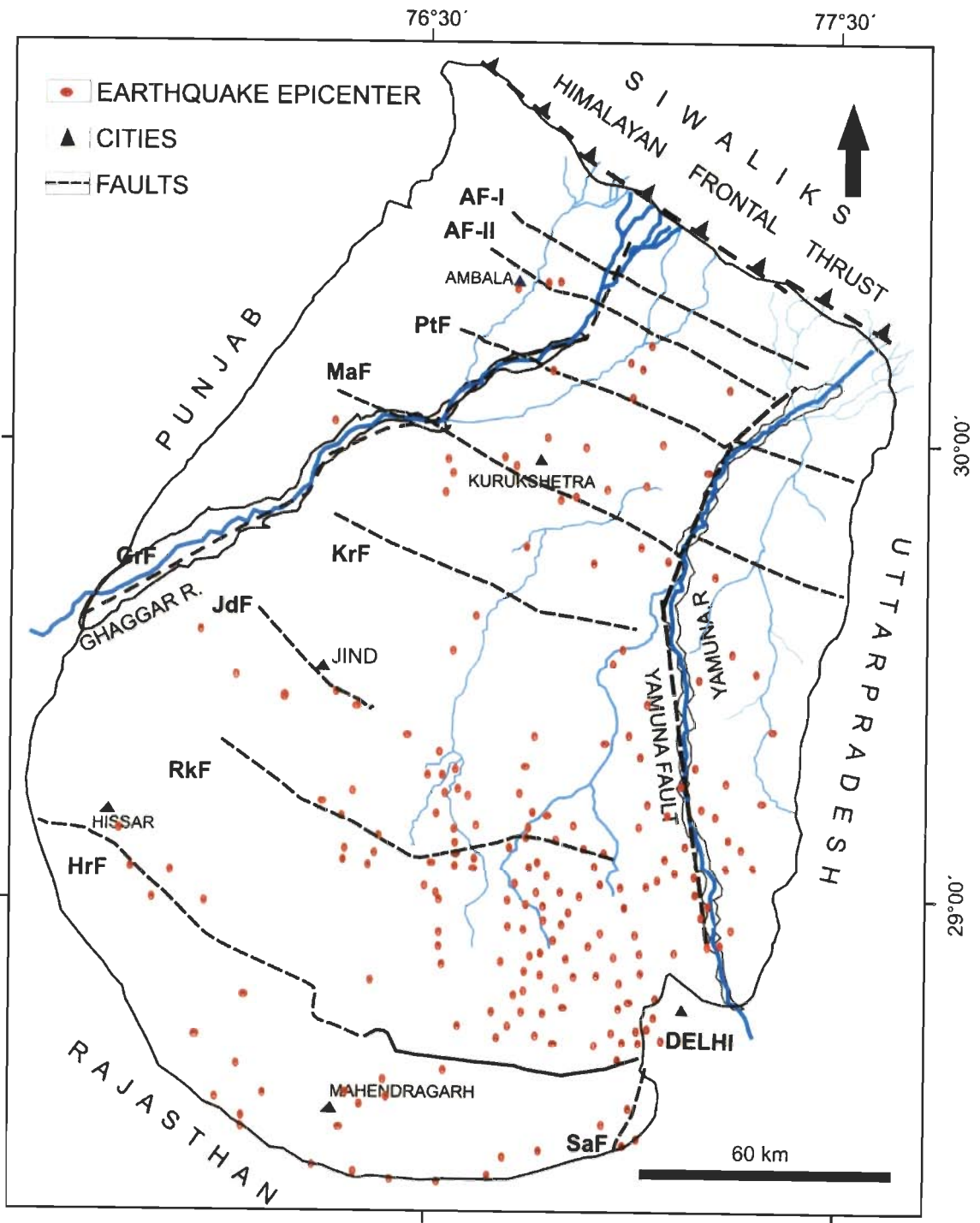


Fig. 2.27 Epicenter of the earthquakes (Source-<http://asc-india.org/seismi/seis-cdh.htm>) occurred in the study area along with the major faults.

fault. Also, the activity of the Jind fault and Ambala fault-II possibly created a few earthquakes. Local people of Jind town tell of frequent tremors, probably caused by the Jind fault (Fig. 2.25b).

## **2.14 SUMMARY**

Using the satellite images, topographic maps, DEMs, DTMs and detailed field work, major landforms like floodplains of rivers, aeolian plains, piedmont zone and terminal fans (Singh et al. 2006, Bhosle et al., 2008) are identified.

Twenty-five soil-geomorphic units were identified from the study area. Based on IRSL dates of C-horizons, these units are grouped in six members (QIMS-I to VI) (Quaternary Indus Morphostratigraphic Sequence) of a Morphostratigraphic Sequence QIMS-VI 9.86-5.38 Ka, QIMS-V 5.38-4.45 Ka, QIMS-IV 4.45 - 3.60 Ka, QIMS-III 3.60 -2.91 Ka, QIMS-II - < 2.91-1.52 Ka and QIMS-I - < 1.52 Ka. Studies of morphological characters of soils on all the soil-geomorphic units show that the soil characters like the thickness of B-horizons and degree of development increases from QIMS-I to VI soils.

Eight faults were identified in the study area (Fig. 2.18). The Patiala fault extends east and west across the Yamuna and Ghaggar Rivers, respectively. The Katha Terminal Fan was developed by the activity of the Patiala fault in the Saharanpur block. The Jind fault striking in the NW-SE direction in the middle part of the study area causes abrupt termination of the paleochannels on its upthrown block and is responsible of flooding in and around Narwana in the rainy season (Fig. 2.22).

Though five tectonic blocks, namely Piedmont block (north), Hissar block (south), Jind-Rohtak block (central), Punjab Block (west) and

Saharanpur block (east) are identified in the study area, detailed studies have been carried out in the former three blocks which lie in Haryana state.

The Piedmont block lies in the northern most part of the study area and bounded by the Markanda Fault and Himalayan frontal thrust, is mainly overlain by alluvial piedmont formed by rivers descending from the Siwalik Ranges. In this block slope is high 0.6% and it is traversed by two faults i.e. the Patiala and Ambala faults

The Jind-Rohtak block is bounded by the transverse Ghaggar and Yamuna faults in the west and east and the longitudinal Markanda and Hissar fault in north and south, respectively. The major portion of this block is covered by of the terminal fans, varying in OSL ages from 3.5 to 1.5 Ka, formed due to the activities of the Karnal, Jind, Rohtak and Markanda longitudinal faults.

The Hissar block lies in the southern most part of the study area and is separated by the Hissar fault from the Jind and Rohtak block. Hissar fault is antithetic in nature as compared to the other faults identified in the study area with downthrow to the north-west, other faults in Haryana have downthrows sides to north/northeast. This block is covered by the Aravalli Hills in the southeastern part of the study area.

The Punjab block lies north of the Ghaggar fault and is marked by numerous paleochannels starting from Ropar where the River Sutlej enters the plains from the Siwalik Ranges diverging in various directions, suggesting that these were formed as a result of northward migration of the Sutlej River. The Sutlej River was a tributary of the Ghaggar River and started shifting away from it due to northward tilting of the Panjab block at about 3.9 Ka.



	KrTFn	V-44	Coarse Loamy Hyperthermic Typic Haplustalf	100	90	Moderate to Strong	10YR6/ 3	loamy Sand	--	--
	FI-Pn	V19 V25 V56B	Coarse Loamy Hyperthermic Aridic Haplustalf	115 105 71	96 51 45	Moderate to Strong	10YR6/ 3	Silt loam	--	--
	OdSjPn-I	V-55	Fine loamy Mixed Hyperthermic Aridic Haplustepts	115	46	Moderate to weak	2.5Y6/3	silt loam	--	
4.45-3.60 Ka QIMS-IV	OdYPn-I	VA41 VB-1	Mixed loamy Mixed Hyperthermic Typic Haplustalf	122 106	56 71	Moderate to weak	10 YR 4/3, m	Silt loam	Bw1 & C	Bw2
	OdYPn-II	V-61 V-64 V-65	Coarse loamy Mixed Hyperthermic Typic Haplustalf	75, 140 53	40 58 34	Moderate to weak	10YR6/ 4,7/2,	sandy loam	--	Bw & C
	OdYPn-III	V-12 V-94 V-14	Fine loamy Mixed Hyperthermic Typic Haplustalf	98 72 57	65 43 21	Moderate	5Y4/3, 5Y6/4 2.5Y4/4	Sandy loam	Bkw &C	Bt &C
	FI-AI-Pn	V-36 V-40	Coarse Loamy Hyperthermic Aridic Haplustalf	105 48	75 18	Moderate	10YR6/ 3,6/4	Silt Loam	Bw1	Bt, C
	OdKaPn	V-38 V-36T	Fine loamy Mixed Hyperthermic Typic Haplustalf	96 68	75 26	weak	5Y4/1, 5Y6/5	Sandy- Loam	--	--
QIMS-III(3.60-2.91 Ka)	YgKaPn	V17/5 V-73	Fine loamy Mixed Hyperthermic Typic Haplustepts	80 70	52 40	weak	2.5Y4/3 ,5/6	Sandy- Loam	--	C
	OdYTFn	V-96 V-43 V109 V-106	Coarse Loamy Mixed Hyperthermic Typic Haplustepts	60 80 50 58	47 61 28 39	Moderate to weak	2.5Y4/4	sandy	C	--
	StTFn	V58 V-25	Fine loamy Mixed Hyperthermic	78 53	42 29	weak to v-weak	10YR6/ 2,6/3	Sandy- Silty	--	--



			Typic Haplustepts							
QIMS-II (2.91-1.52 Ka)	OdSjPn-II	G5	Fine loamy Hyperthermic Typic Haplustept	40	28	weak	2.5Y4/4	Sandy	--	--
	YgCgTF n- II	V-69 V-77 V-71	Coarse loamy Hyperthermic Typic Haplustept	73, 63, 55	47, 40, 35	Weak to v- weak	10YR6/ 3,	Sandy- Silty	--	Bt1
	YgCgTF n- IV	V-39 V-3,	Coarse loamy Hyperthermic Typic Haplustept	75, 68	24, 21	Very Weak	2.5Y6/6 6/3	Sandy	--	--
	YgCgTF n- III	V53 V-54 V-55	Coarse loamy Hyperthermic Typic Haplustept	90, 61, 58	40, 39, 24	Very Weak	2.5Y4/2	Sandy	--	Btk
	YgCgTF n- I	V-3	Coarse loamy Hyperthermic Typic Haplustept	42	23	weak	2.5Y6/6	Sandy- Silty	--	--
	ShFn	V-82	Fine loamy Hyperthermic Typic Haplustept	57	21	weak	2.5Y4/3	Sandy	--	--
	YgPt	V102 V-94	Coarse loamy Hyperthermic Typic Haplustept	42, 41	13, 24	weak	2.5Y3/3 3/5	Sandy	--	--
QIMS I (<1.52 Ka)			This QIMS mainly includes flood plains in the study area viz. Markanda flood plain, Ghaggar flood plain and Yamuna flood plain. There is no development recorded in the soil of these areas.							

---

### 3.1 INTRODUCTION

The reconstruction and dating of the past events and processes are important aspects of study especially in geology and archaeology. Isotopic methods and ancient remains in the sediments and soil are the important tools in this regard. Dating methods that seem to have made a real breakthrough in the chronometry of the last 100 Ka, is the discovery of Luminescence dating. Thermo-Luminescence (TL) and Optically Stimulated Luminescence (OSL) dating methods are the two important methods that are very useful especially in the study of the Quaternary Geology. Optical dating is being used increasingly in the Quaternary Sedimentology as a means of establishing the depositional chronology of sediments. It is unique because it uses the constituent mineral grains of the sediment itself (quartz, feldspars) instead of the associated material (as carbon in  $^{14}\text{C}$  dating method) that is often scarce or less reliable. Though initially the method was used mainly for dating aeolian sediments, later developments of the technique allow dating of fluvial sediments.

In the present area of study, records show that the data on dating of soil are very limited and pertain to scattered places, and therefore are not enough to establish a regional correlation and interpretation. In view of this, luminescence dating of soil samples has been undertaken and is discussed in details in the following sections.

### 3.2 PRINCIPLE

The luminescence dating method is based on the time-dependent accumulation of radiation energy stored in some non-conducting crystalline

materials as a result of natural radioactivity. In the laboratory, this stored energy can be released in the form of luminescence by stimulation, either via heating (thermo-luminescence) or illumination (optically stimulated luminescence).

As a result, the TL/ OSL signal acquired over a geological time i.e. since the last clock resetting event (e.g. signal zeroing by heating in the case

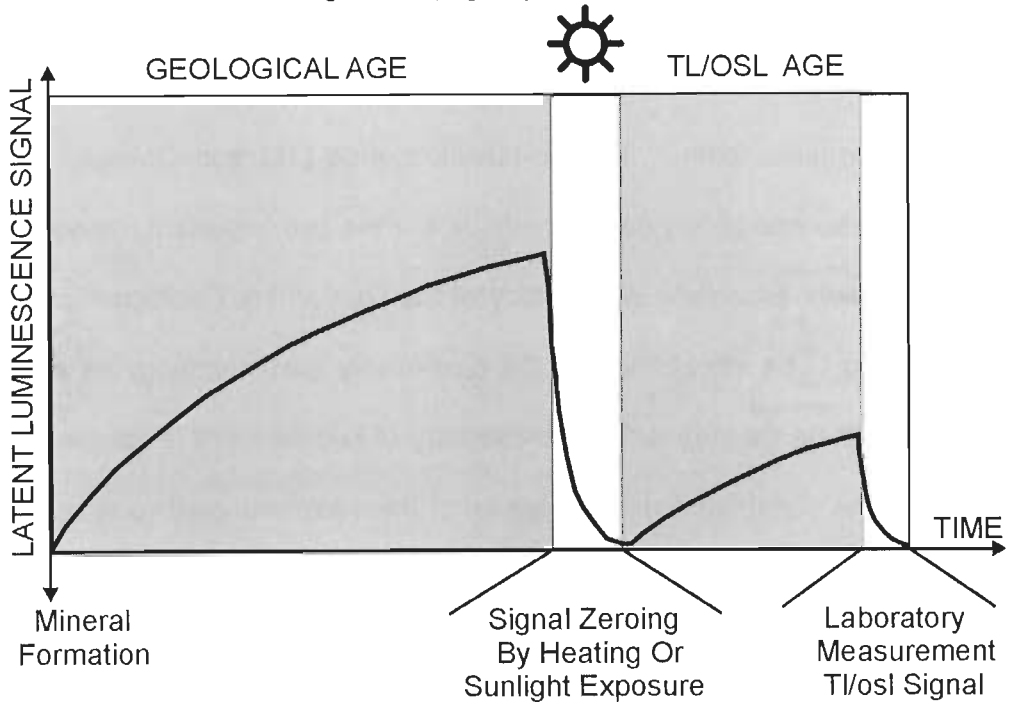


Fig. 3.1 Schematic representation of the Luminescence Dating Principle (based on Vancaeynest, (1998)).

of pottery or by exposure to sunlight in the case of windblown sediment) is removed and can be measured. This is schematically shown in Fig. 3.1. Division of the paleodose by the dose received per year or the annual radiation dose (assumed to be constant with time) gives the age of the sample (Eq. 3.1).

$$\text{TL/OSL (Age)} = \frac{\text{Paleodose (Gy)}}{\text{Annual Radiation Dose (Gy/unit of time)}} \quad (3.1)$$

### 3.2.1 Physical Mechanism of Luminescence

Although the mechanisms responsible for luminescence are much more complex, it is convenient to use a simplified model for explaining the behavior of luminescent crystals in the context of the dating method. In this model, an ideal insulating crystal is characterized by an occupied valence band and an empty conduction band, with an energetically forbidden zone in-between. Natural crystals, however, are not perfect and have structural defects (such as vacancies, dislocations and substitutional impurities), which lead to the localized energy levels within the forbidden zone. The first step in the luminescence process is the creation of electrons and holes due to the interaction of ionizing radiation within the mineral lattice (Fig. 3.2). These electrons and holes subsequently can get trapped at defects 'T' and 'L', respectively in the forbidden zone (Fig. 3.3b). The longer the mineral is exposed to ionizing radiation, the more charges are accumulating in the traps. The efficiency, by which the electrons are stored in the electron traps, is determined by the depth 'E' (Fig. 3.3 in stage 'a' and 'b') below the conduction band. In the context of dating, we are only concerned with those traps, which are deep enough so as to have insignificant leakage during the time span that is being dated. The trapped electrons can become free once again, if the crystal is heated to a certain temperature or is exposed to light of a specific wavelength (Fig. 3.3 in stage c). Luminescence finally occurs if the released electrons recombine with hole centers also called luminescence centers. When the luminescence is stimulated by applying heat or light, the resulting signal is known as thermo-luminescence (TL) or

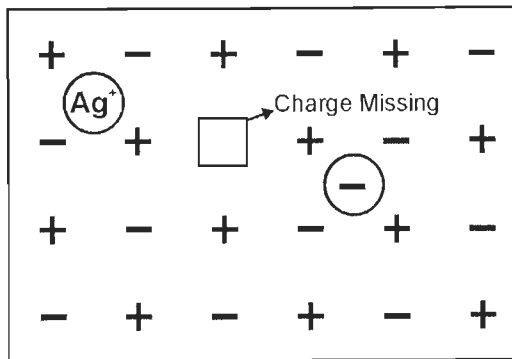


Fig. 3.2 Schematic diagram showing lattice defects in crystals (after Aitken, 1998).

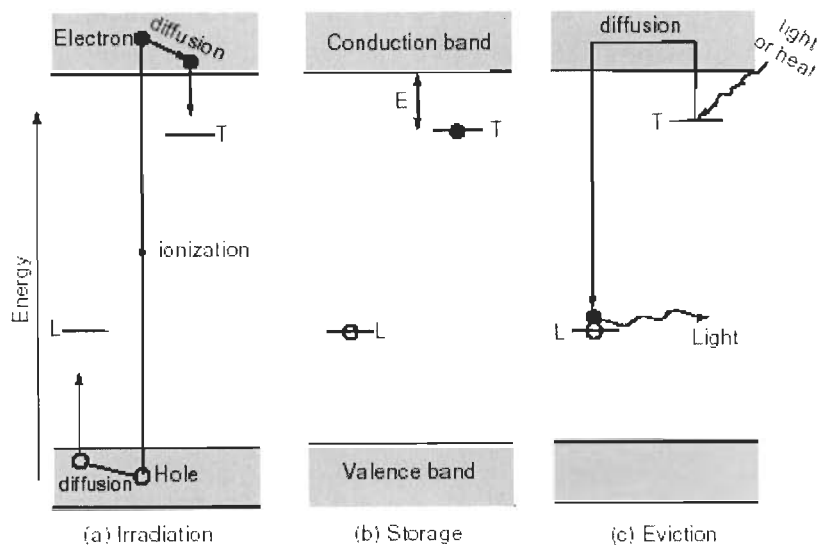


Fig. 3.3 Energy-level diagram of TL and OSL processes (based on Aitken, 1998): (a) ionization due to exposure to nuclear radiation with trapping of electrons and holes at crystal defects; (b) storage during antiquity; (c) the electron is evicted from its trap by heating or shining light and recombines with a luminescence center under emission of TL/OSL signal.

optically stimulated luminescence (OSL), respectively. The amount of luminescence emitted is proportional to the total absorbed radiation dose (ignoring the effects of signal saturation). This is the fundamental basis of TL and OSL dating.

### 3.2.2 The Luminescence Processes

#### 3.2.2.1 *Thermally stimulated luminescence (TL)*

In the early 1950s, this technique (thermo-luminescence (TL)) was used to measure nuclear radiation doses and they suggested using it for geological and archaeological age determination. If a sample is heated at a constant rate to some temperature (e.g. 500°C), there is emission of light. The luminescence emitted as a function of temperature is termed as glow curve. During heating, traps of increasing depth are emptied and thus the glow curve peaks reflect the thermal stability of the electron traps involved. Normally, glow peaks lower than 200°C are not useful for dating the Quaternary deposits, as electrons can be liberated from the shallow traps over a prolonged time even at environmental temperatures. Stable glow peaks suitable for dosimetry usually occur at greater than 300°C. In principle, TL-dating covers a wide age range of a few 100 Ka upto 1 Ma, the upper limit being controlled by long-term fading and/or saturation of the TL-signal.

#### 3.2.2.2 *Optically stimulated luminescence (OSL)*

Although thermo luminescence dating of sediments was well underway in the 1970s, problems associated with incomplete zeroing made the technique difficult to apply. Huntley et al. (1985) and Hütt et al. (1988) opened a new era of optical dating, showing that quartz and feldspar grains in the sediments exhibit luminescence signals, which are rapidly and completely zeroed by a few minutes of daylight exposure, thus avoiding the main problem of TL dating. If the OSL intensity of a sample is directly measured as the stimulation proceeds, a

decreasing intensity curve, the so-called shine-down curve, is obtained with increasing exposure time. The OSL shine-down curves of typical soil samples obtained by stimulating by Infra-red light are shown in Fig. 3.4. The OSL signal of quartz and feldspars is completely bleached away by stimulation for a few minutes with a light intensity of approximately  $6 \text{ mW cm}^{-2}$  (Aitken, 1998). Due to this characteristics, the OSL dating method enables the dating of very recent events (<100 Ka), whereas the upper limit should be the same as for TL.

### **3.2.3 Sample Collection and Preparation Techniques**

Soil samples were collected from the C-horizons of the soil profiles from all the soil-geomorphic units (Fig. 2.12, 2.13, 2.14, 2.15, 2.16). Care was taken to avoid exposure to light. In the absence of natural or artificial excavations up to the C-horizons at sampling site digging was carried out to C horizon of soil profile to take OSL samples. Sampling tubes of dimensions 5 cm (diameter) X 15 cm (length) made up of iron or steel were driven into the horizon to collect the luminescence sample. Tubes were driven in by a sledge hammer. However, a hard metal plate was used against the end being hammered to prevent shatter or collapse.

The sample tubes were then carefully pried or dug out from the hole by pushing a knife or chisel alongside the tube and levering it sideways. Samples were covered with a black opaque polyethylene bags after digging out from the horizon. Samples were marked with a water repellent pen. After taking the sample to the laboratory the sample was processed and discs were prepared for dating. All laboratory procedures were carried out under subdued red light.

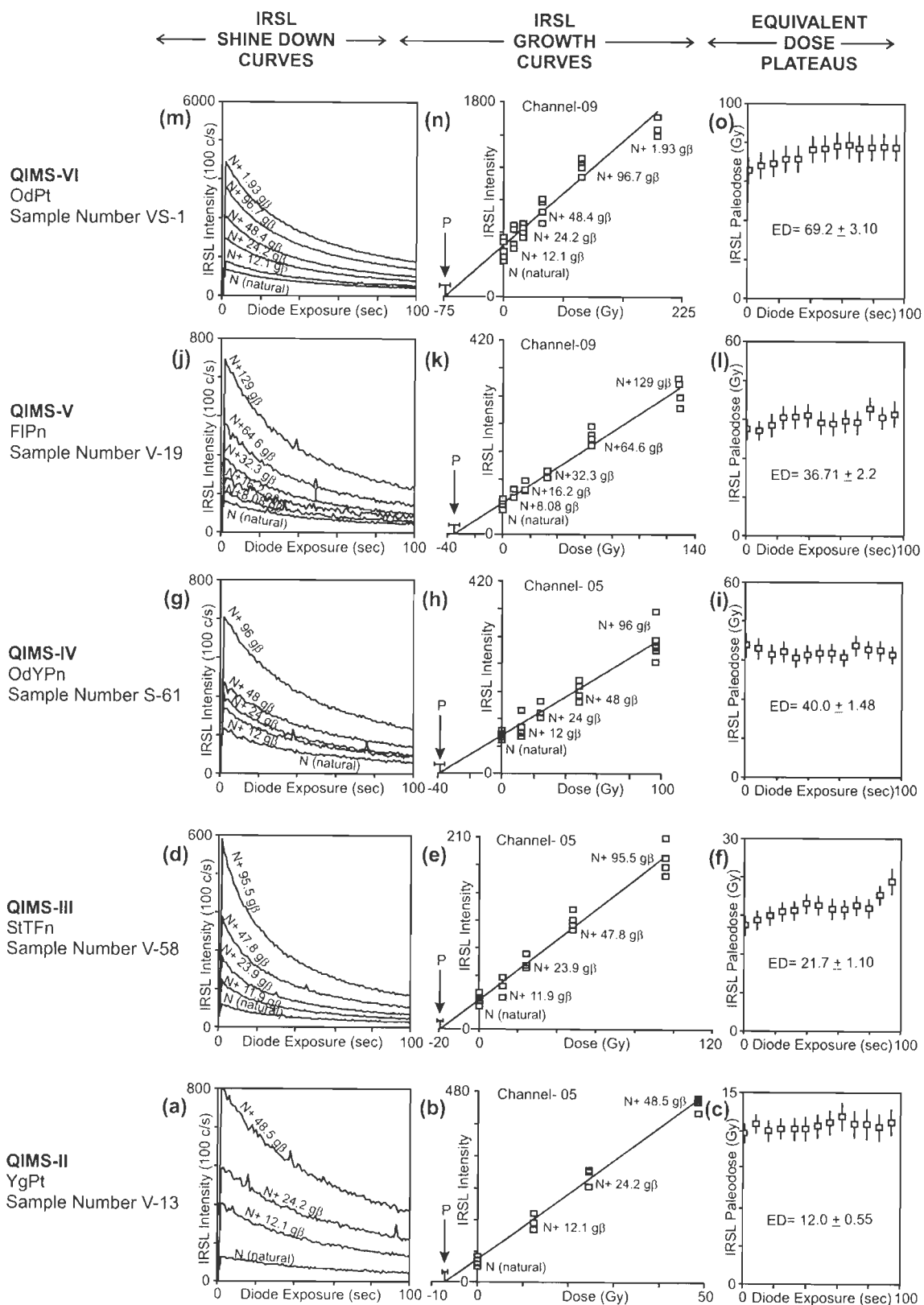


Fig. 3.4 (a) IRSL shine down curve (b) growth curves and (c) Equivalent dose plateaus for some typical samples of the study area.



One inch of the exposed sample from both ends of the metal cylinder was removed. Details of procedures of the dating were given by Aitken (1985) and Singhvi and Krbetschek (1996). In the present study, optically stimulated luminescence (infrared light source, IRSL) was used, as it uses charges, which are removed rapidly on exposure to sun (Godfrey-Smith et al, 1988, Hutt et al., 1988) and the sediments being dated are fluvial in nature that could have been exposed to the Sun light for short periods during transport.

Samples were pre-treated with 1N hydrochloric acid, hydrogen peroxide ( $H_2O_2$ , 6%-30%) and 0.01N sodium oxalate, in order to remove carbonates, organic matter and to disperse individual grains, respectively. The fine-grain fraction (4-11 $\mu$ m) was collected by Stoke's separation in acetone medium and it was deposited on 40 aluminum discs.

### **3.2.4 Equivalent Dose/Palaeodose**

Equivalent dose was measured in additive-dose methods. In this approach, a number of aliquots are prepared and divided in groups. From one group, the natural OSL signal is measured. The other groups are given known amount of increased radiation doses on the top of their natural dose, using a calibrated source in the laboratory. All the aliquots are subsequently preheated and measured. A plot of the measured luminescence intensity as a function of the added dose yields a dose-response or growth-curve. The unknown dose is obtained by extrapolation of this growth-curve to zero luminescence intensity (Fig. 3.3). As this technique involves extrapolation, the result depends strongly on the choice of the mathematical function (linear, exponential, polynomial, etc.) that is used for describing the growth of the signal with dose. This is especially problematic for cases where the

extrapolation is to be made over a large dose-span, where the growth is not linear and/or where there is a large scatter between the data points. This drawback is taken care of by the use of the regeneration method.

### 3.2.6 Luminescence Measurements

All luminescence measurements were performed on Daybreak Version-1150 Automated TL/OSL reader system. Irradiation was performed using beta source  $^{90}\text{Sr}/^{90}\text{Y}$  of strength 30 mCi with dose rate of 0.07 Gy/s. Luminescence from poly-mineralic grains (4-11  $\mu\text{m}$ ) was observed using Corning 7-59 blue transmitting filters and Schott BG-39 filter equipped to an EMI-9635QA PMT photomultiplier tube. The machine setup is shown through a schematic diagram (Fig. 3.5). For the IRSL technique, semi-automated system employing a source made by an array of 10 Infra Red (IR) diodes, emitting at  $880\pm 80$  nm was used. The luminescence output from individual discs was normalized using integrated luminescence obtained from the natural samples on short IR stimulations for 0.5 s. Prior to the measurements, the samples were preheated for 60s at  $220^{\circ}\text{C}$  to remove the unstable luminescence signal that is generated during the laboratory irradiation and bleaching procedures. In the analysis, the samples were measured for IRSL for 99 seconds. The growth curves (luminescence intensity v/s radiation dose) were fitted to linear regressions. Paleodose was calculated using the age plateaus. The dose rates were established by measuring the concentrations of Uranium and Thorium by thick source alpha counting system (Daybreak 583 alpha counters) and Potassium by means of Atomic Absorption Spectrometry (AAS). Once the values for paleodose, concentration of Uranium and Thorium and percentage of Potassium

were known, GRUN software was used to calculate the ages. Cosmic contributions to the samples are assumed to be  $150 \pm 30 \mu\text{Gy/ka}$  for all the samples.

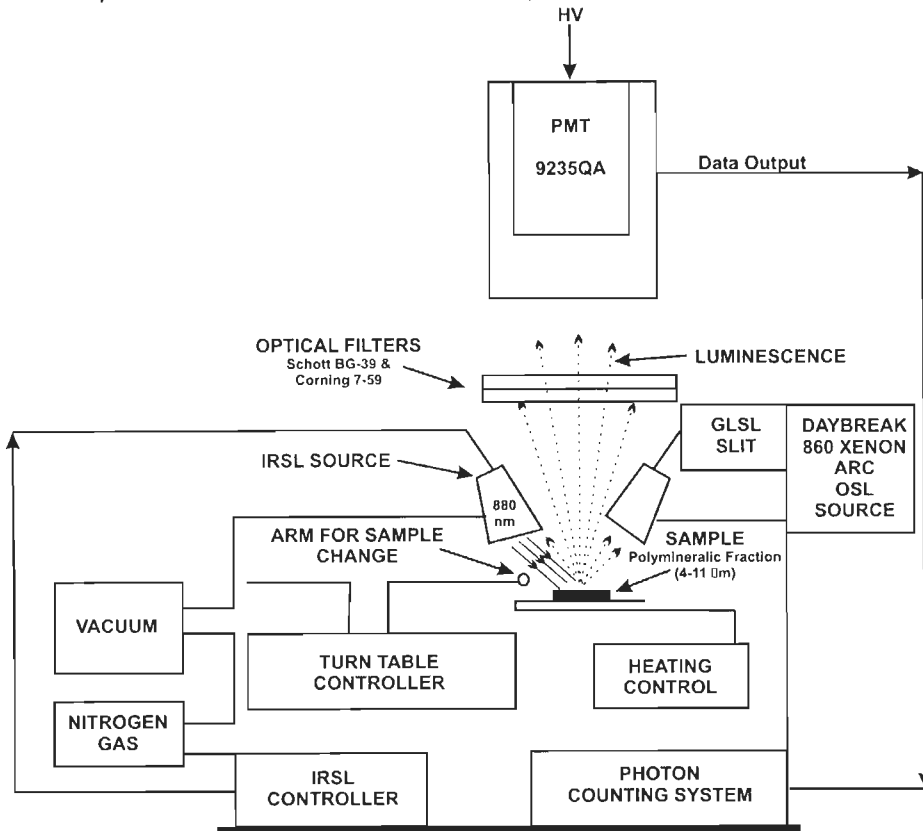


Fig. 3.5 Schematic instrumental setup for OSL measurements (after Aitken, 1985, 1998).

### 3.2.7 Annual Radiation Dose

The annual radiation dose in luminescence dating originates from the ionizing radiation ( $\alpha$ -,  $\beta$ - and  $\gamma$ -radiations) of naturally occurring, long-lived primordial radio-nuclides ( $^{235}\text{U}$ ,  $^{238}\text{U}$ ,  $^{232}\text{Th}$ ,  $^{40}\text{K}$  and  $^{87}\text{Rb}$ ) present in the sample and its immediate surroundings and from cosmic radiation (the contribution from  $^{87}\text{Rb}$  and cosmic radiation usually being less critical). When nuclei of  $^{40}\text{K}$  with a natural atomic abundance of 0.0117% undergo radioactive decay, beta particles and a gamma ray with energy of 1460.8 keV are emitted. It is generally assumed that the  $^{238}\text{U}$  to  $^{235}\text{U}$  ratio is constant in nature. Even though  $^{235}\text{U}$  accounts for

only 0.72% of the atoms in the natural uranium, it contributes to as much as ~ 4.4% in the combined uranium activity, because of the shorter half-life of  $^{235}\text{U}$  compared to  $^{238}\text{U}$ . During transformation of the Uranium concentration to the annual radiation dose, the constant  $^{238}\text{U}/^{235}\text{U}$  ratio is taken into account. The natural Th to U concentration ratio in the earth crust is about 4:1, and the limited variability of this ratio plays a role in the calibration of the ZnS alpha counting.

All these three types of radiation ( $\alpha$ ,  $\beta$  and  $\gamma$ ) discussed above are quite important for the luminescence dating methods, and the amount of luminescence induced in the sample depends both on the rate of emission and the energy carried by these radiations. The share of the  $\alpha$ - and  $\beta$ - radiation dose rate to the total annual radiation dose is mostly coming from the radio-nuclides present within the sample, whereas the share of the  $\gamma$ -radiation dose rate is mostly coming from the radio-nuclides present in the surrounding materials from where the samples have been collected. In the following sections various method for calculating the annual radiation dose are described.

#### *3.2.7.1 Thick Alpha Source Counting*

The principle of alpha counting is based on the property of some materials (scintillators) to emit light (photons or scintillations) when they interact with ionising radiation. The photons are measured using a photomultiplier tube, leading eventually to the registration of a number of pulses per unit of time (count-rate) that is proportional to the activity of the sample. In case of thick source alpha counting,

Table 3.1 Radioactivity values, depth of IRSL samples, equivalent dose and absolute ages of dated samples from different morphostratigraphic members (QIMS-VI - I).

Sample No.	DEPTH (cm)	<sup>238</sup> U (ppm)	<sup>232</sup> Th (ppm)	<sup>40</sup> K (%)	ED (Gy)	AGE (Ka)
<b>QIMS-VI (9.86-5.38 Ka)</b>						
Oldest Piedmont (OdPt)						
V-S1	210	9.65±3.34	5.43±0.76	2.75±0.06	69.2±3.1	9.86±2.24
VA	205	5.43±1.23	4.30±1.52	2.44±0.71	40.7±4.1	8.15±1.55
VC-3	215	12.40±4.31	5.21±1.99	2.37±0.68	59.0±2.6	7.71±1.84
VC-36	241	6.66±0.46	12.65±7.19	1.75±0.08	45.1±2.0	7.69±1.17
<b>QIMS-V (5.38-4.45 Ka)</b>						
Old Piedmont- I (OdPt-I)						
VM	106	20.32±5.12	11.21±3.45	2.98±0.97	64.5±2.1	5.38±1.03
V41R	182	04.56±1.52	2.60±0.91	2.65±0.88	23.6±0.6	5.07±1.08
GC1	167	13.65±3.88	4.56±1.33	2.45±0.83	51.7±1.7	5.17±1.07
G	146	16.54±4.31	8.97±2.54	2.98±0.96	50.1±3.1	4.88±0.98
Old Piedmont- II (OdPt-II)						
VC39	97	16.22±8.98	3.98±1.87	2.07±0.49	41.0±1.0	4.76±1.31
VB2/6	176	22.12±5.89	15.87±2.43	1.87±0.43	54.5±3.9	4.49±0.92
Fluvial Plain (FIPn)						
V-19	128	14.50±0.30	9.80± 3.40	1.70±0.43	36.7±2.23	4.50±0.73
V-34	135	25.40±7.67	21.50±7.50	1.25±0.30	66.6±2.6	4.91±1.17
V-56B	145	12.40±3.40	7.70±2.60	2.50±0.43	37.5±2.2	4.64±0.86
Aeolian Plain (AIPn)						
V-40	128	9.30±3.2	3.40±1.20	2.49±0.49	30.0±1.1	4.70±1.00
V-41	154	15.40±4.5	4.30±1.18	2.34±0.54	38.9±1.4	4.45±0.96
Aravalli hills and Pediments (ArHPm)						
V-47	197	16.50±5.7	6.51±2.10	2.43±0.54	46.1±2.0	4.97±1.23
V51	167	17.80±5.8	4.31±2.50	2.31±0.57	49.9±2.7	5.10±1.26
Karnal Terminal fan (KrTFn)						
V-44	156	14.30±4.30	11.20±4.38	2.13±0.53	42.2±2.8	4.77±1.03
<b>QIMS-IV (4.45-3.60 Ka)</b>						
Old Yamuna Plain-I (OdYPn-I)						
V-61	93	18.77±5.76	5.24±4.98	2.34±0.30	40.0±1.4	4.08±0.86
V-64	101	23.12±5.87	10.87±3.20	3.12±0.88	51.6±1.6	3.84±0.82
V-65	110	08.88±2.69	6.74±1.98	2.87±0.97	27.2±3.4	3.87±0.76
Old Yamuna Plain-II (OdYPn-II)						
VA-41	123	9.31±3.43	4.21±1.63	1.43±0.29	23.2±2.0	4.25±1.13
VB-1	158	7.60±2.87	4.11±1.68	1.74±0.23	21.1±1.4	4.17±0.97
Old Yamuna Plain-III (OdYPn-III)						
V-14	100	15.3±4.33	7.23±2.77	1.82±0.32	32.8±1.0	3.86±0.80
V-12	103	21.4±4.96	9.83±2.62	2.99±0.72	42.8±2.3	3.60±0.57
V-94	135	11.4±3.54	5.72±1.90	2.54±0.67	28.3±1.0	3.77±0.78
Fluvial Aeolian Plain (FI-AI-Pn)						
V-36	140	14.74±3.45	12.50±4.50	2.57±0.43	21.10±.72	3.87±0.66
V-40	154	10.50±3.20	13.70±4.13	2.43±0.59	34.90±.98	3.96±1.20

**Old Sutlej Plain (OdSjPn-I)**

V-55	160	15.68±5.72	4.87±1.63	1.44±0.29	31.04±2.3	3.90±1.13
------	-----	------------	-----------	-----------	-----------	-----------

**QIMS-III (3.60-2.91 Ka)****Old Katha Plain (OdKaPn)**

VA-38	145	9.12±3.21	3.40±1.45	1.22±0.21	17.3±1.8	3.36±0.86
-------	-----	-----------	-----------	-----------	----------	-----------

V-36T	172	20.12±5.33	9.23±2.10	1.99±0.76	37.1±3.1	3.46±0.71
-------	-----	------------	-----------	-----------	----------	-----------

**Young Katha Plain (YgKaPn)**

V-17/5	103	7.33±2.11	6.12±1.45	1.90±0.56	16.75±1.0	3.10±0.37
--------	-----	-----------	-----------	-----------	-----------	-----------

V-73	128	21.33±5.56	7.34±2.32	2.17±0.53	37.87±2.1	3.34±0.70
------	-----	------------	-----------	-----------	-----------	-----------

**Markanda Terminal fan (MaFTn)**

V-67	112	12.89±4.33	6.30±2.87	1.82±0.32	33.8±1.0	3.36±0.80
------	-----	------------	-----------	-----------	----------	-----------

**Old Yamuna Terminal fan (OdYTFn)**

V-96	133	13.48±4.11	2.89±1.19	1.97±0.58	22.8±1.33	2.91±0.67
------	-----	------------	-----------	-----------	-----------	-----------

V-43	105	5.70±2.50	3.66±1.12	1.54±0.34	13.61±.80	3.26±0.93
------	-----	-----------	-----------	-----------	-----------	-----------

V-109	50	8.60±4.34	7.60±3.57	1.42±0.25	17.3±.63	3.06±0.92
-------	----	-----------	-----------	-----------	----------	-----------

V-106	87	7.50±2.53	3.51±1.20	2.30±.55	16.5±.79	2.97±0.66
-------	----	-----------	-----------	----------	----------	-----------

**Sonipat Terminal fan (StTFn)**

V-58	126	9.86±3.20	4.50±1.20	2.50±0.48	21.7±1.1	3.22±0.66
------	-----	-----------	-----------	-----------	----------	-----------

V-25	240	18.90±5.60	3.46±1.23	1.46±0.43	31.7±1.8	3.46±0.87
------	-----	------------	-----------	-----------	----------	-----------

**QIMS-II (2.91-1.52 Ka)****Old Sutlej Plain (OdSjPn-II)**

G-5	230	22.67±5.65	4.31±1.32	1.38±0.25	29.10±0.7	2.75±0.70
-----	-----	------------	-----------	-----------	-----------	-----------

**Young Chautang Terminal Fan (YgCgTFn-I)**

V-3	330	16.50±5.42	8.28±2.30	2.41±.46	13.9±1.8	1.52±0.35
-----	-----	------------	-----------	----------	----------	-----------

**Young Chautang Terminal fan - II (YgCgTFn-II)**

V-69	120	10.50±0.85	5.88±2.39	1.85±0.52	12.9±0.8	1.97±0.47
------	-----	------------	-----------	-----------	----------	-----------

V-71	100	4.68±1.38	7.08±2.88	1.98±0.59	10.0±0.6	2.33±0.40
------	-----	-----------	-----------	-----------	----------	-----------

V-77	143	11.48±4.30	1.99±0.53	1.78±0.53	14.8±1.02	2.23±0.39
------	-----	------------	-----------	-----------	-----------	-----------

**Young Chautang Terminal fan - III (YgCgTFn-III)**

V-52	79	14.22±4.23	7.30±2.81	1.79±0.65	20.79±1.20	2.47±.50
------	----	------------	-----------	-----------	------------	----------

V-54	111	13.20±3.32	5.43±2.10	1.89±0.56	16.07±1.82	2.14±.42
------	-----	------------	-----------	-----------	------------	----------

V53	165	12.40±3.43	5.32±2.01	1.70±0.48	17.19±1.02	2.42±.54
-----	-----	------------	-----------	-----------	------------	----------

**Young Chautang Terminal fan – IV (YgCgTFn-IV)**

V-33	140	15.56±4.67	6.50±2.36	1.55±0.32	19.80±2.58	2.42±.33
------	-----	------------	-----------	-----------	------------	----------

V-39	165	14.42±4.33	5.93±2.18	1.80±0.45	19.9±1.44	2.30±.52
------	-----	------------	-----------	-----------	-----------	----------

**Sahibi Fan (ShFn)**

V-82	121	6.18±1.97	4.68±1.20	2.65±.67	14.8±1.02	2.71±0.57
------	-----	-----------	-----------	----------	-----------	-----------

**Young Piedmont (YgPt)**

V-13	102	8.54±2.13	4.53±1.37	2.58±.81	12.0±.55	1.84±0.37
------	-----	-----------	-----------	----------	----------	-----------

V-27	94	9.22±2.07	4.48±1.23	2.52±.37	13.5±0.9	2.14±0.33
------	----	-----------	-----------	----------	----------	-----------

**QIMS-I (<1.52 Ka)**

Flood plains of Markanda, Ghagghar and Yamuna

alpha particles emitted by the U and Th decay series are measured, making use of zinc sulphide as scintillator. The underlying theory of thick source alpha counting has been discussed by Aitken (1985). Commercially available ZnS screens for scientific purposes were used as scintillation screens. Alpha counting was carried out for all the samples. The measurements were carried out on about 1 gm of dried (air or oven at 100°C) and pulverized (< 63 µm, using an agate mortar) material that was spread out on the ZnS screens. As the most energetic alpha particles have only a range of about 50 µm, this means that the sample is presented as an infinitely thick source. All the measurements were made using Daybreak 583 alpha counters. The results are summarized in Table 5.1.

### **3.3 SUMMARY**

A total of 53 soil samples well distributed over the study area from different soil-geomorphic units were taken for dating and all the analytical results are presented in Table 3.1. All the samples show very good paleodose plateaus, which suggest that the samples passes the test of the validity of TL/OSL dating method in case of our mainly fluvial sediment samples. These paleodose plateaus were used for the calculation of ages.

Using breaks in the frequency curve of ages (Fig. 3.6) different soil-geomorphic units were classified into five Morphostratigraphic Sequence members QIMS-I to VI, with ages of ≤1.52 Ka, 1.5-2.9 Ka, 2.9-3.6 Ka 3.6-4.4 and 4.4-5.3 Ka, respectively. Active floodplains of different rivers in the study area were not dated and were taken as <1.5 Ka and included in QIMS-I. Though four members (QIMS-II –V) have ages in a small range (5.3-1.5 Ka), small ranges of ages in individual soil-geomorphic units and ages of members in the same stratigraphic order, as

expected from geomorphic considerations and the degree of soil development give us confidence to reconstruct evolutionary history of the region.

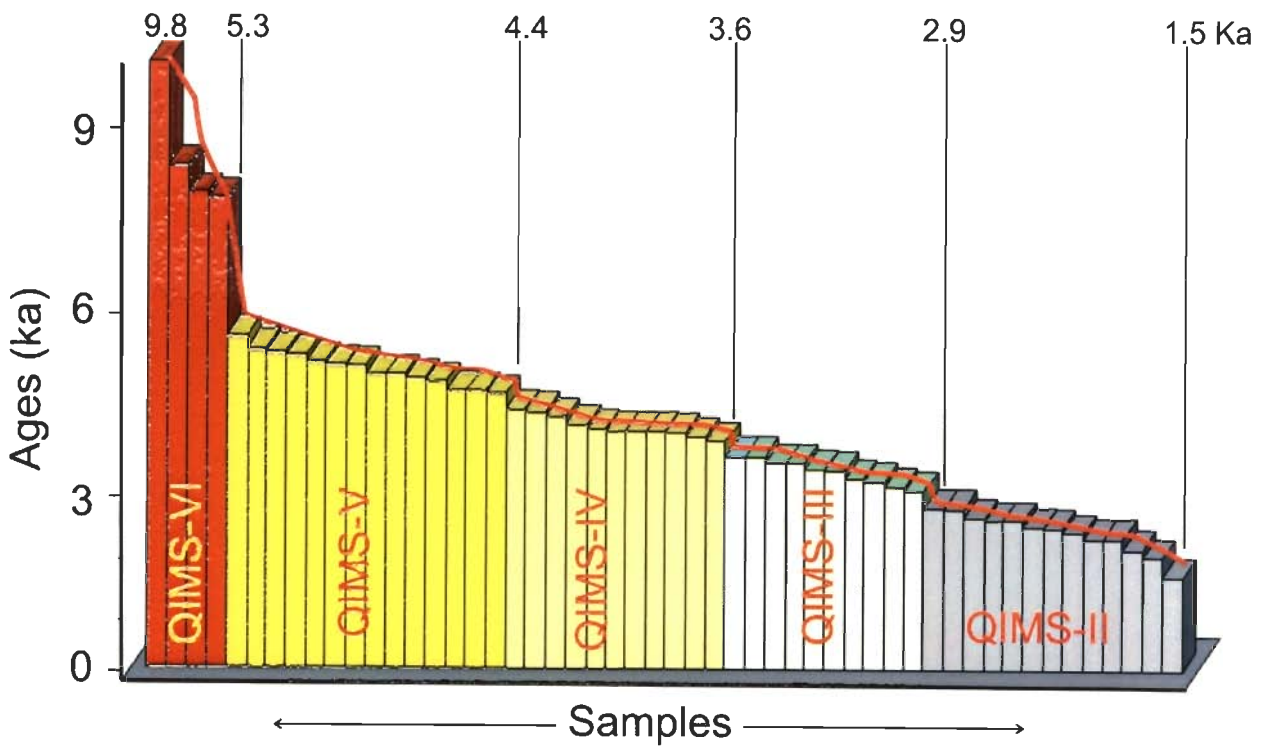


Fig. 3.6. Bar diagrams for 53 IRSL ages from different soil-geomorphic units with ages arranged in a descending order. Tectonically stable periods are marked by the flat or gently sloping portions of the curve joining the top of bars. Sharp breaks in the curve are used to define different members of the Morphostratigraphic Sequence.



# GRAIN SIZE ANALYSIS AND MICROMORPHOLOGY STUDIES

## CHAPTER-4

---

### 4.1 INTRODUCTION

Laboratory analyses of soil samples were used to study particle size distributions during deposition and to find out the effect of post-depositional pedogenic processes on grain size distribution. Other soil properties like pH, salinity and alkalinity were studied to characterize the soils. Micromorphological studies of soil profiles from various Morphostratigraphic Sequence Members have been carried out to decipher pedogenic processes acting in the study area and the degree of soil development.

### 4.2 PARTICLE SIZE DISTRIBUTION

A total number of 96 soil samples from typical profiles of different soil-geomorphic units (Fig.2.10) were investigated for the particle size distribution and to determine the soil texture and the amount of clay present in the soils (Catt, 1986, 1990). Soil textures have been used to work out the nomenclature of soil horizons and classification of soil profiles (Appendix-2).

#### 4.2.1 Methodology

Loose samples, collected during field work, were air-dried and disaggregated. The lumps and clods were thoroughly broken by a wooden pastel. Then the samples were thoroughly mixed and were split into quarters. The opposite quarters were taken for further analyses (Conning and Quartering method).

Generally soil particles are bound by carbonates, organic materials and iron oxides. So at first these materials were removed from the soils to get the

grains separated from each others. The removal of the binding materials was carried out by the methods described by Galehouse (1971). The carbonates were removed by the treatment of the samples with 1N HCl. Organic matters were removed by treating the samples with 6-30% concentration of H<sub>2</sub>O<sub>2</sub> gradually. Iron oxides were removed by putting an aluminum foil and 15 gm of oxalic acid in the soil-water mixture and by boiling it gently. Soluble salts were removed by repeated washing with distilled water. After removing all the binding materials, Sodium hexametaphosphate [Na (PO<sub>3</sub>)<sub>6</sub>] was used as dispersing agent for complete dispersion. Then different size fractions were separated by sieving and pipetting methods.

Sand fraction was separated from the dispersed sample by wet sieving with 230-mesh (>62.5 µm) sieve. Silt and clay fractions were separated by pipette method (Galehouse 1971). Sand, silt and clay percentages (Appendix-II) were calculated according to the size classification used by U. S. D. A. (1966) (i.e. sand = 2 to 0.05 mm, Silt = 0.05 to 0.002 mm and clay = < 0.002 mm size fraction).

#### **4.3 TEXTURAL AND AMOUNT OF PEDOGENIC CLAY VARIATION IN SOILS OF DIFFERENT SOIL GEOMORPHIC UNITS**

Textural classes were determined from the particle size data according to Schoeneberger et al. (1998) by plotting sand, silt and clay percentages in a combined texture triangular diagram (Fig. 4.4a, 4.5a & b, 4.6a & b). The results of the particle size studies are given in Appendix-2.

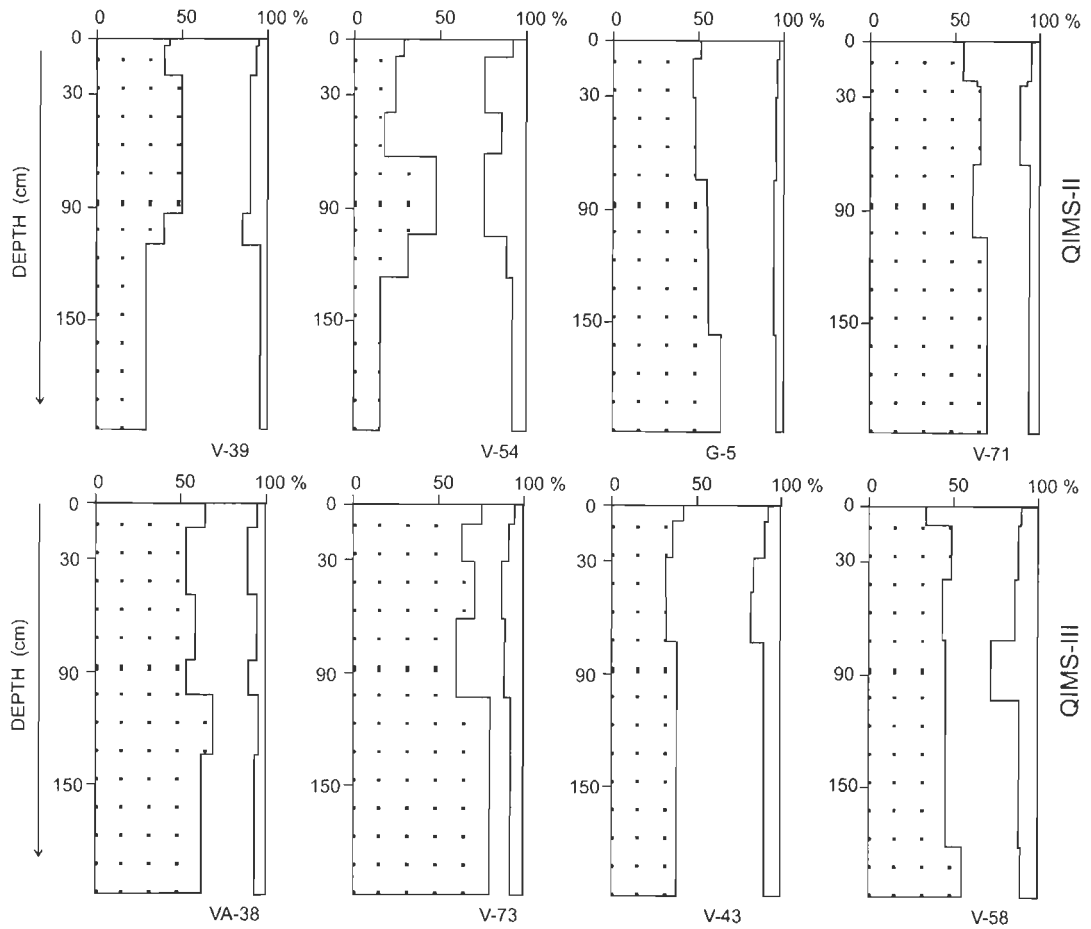


Fig. 4.1 Sand, silt and clay distribution with depth in QIMS-II & III soils.

Particle size distribution shows that the texture of most of the soils of the study area varies in a wide range between sandy loam to silty loam and become heavier especially in B-horizon with increasing soil development. However, the QIMS-III and IV soils have a larger range of textural variation from loamy sand to silty loam class (Figs. 4.5a, b).

The QIMS-I soils include the active floodplains of the rivers Yamuna, Sutlej and Markanda and show very weakly development soils and were not studied in detail. The QIMS-II soils do not show any significant change in sand, silt and clay percentage with depth, which suggests fluvial processes of deposition varied only in a small range (Fig. 4.4b). Plots of the total clay

content with pedogenic clay content are shown in the Fig. 4.3 and the degree of illuvial translocation has been assessed by calculating clay accumulation

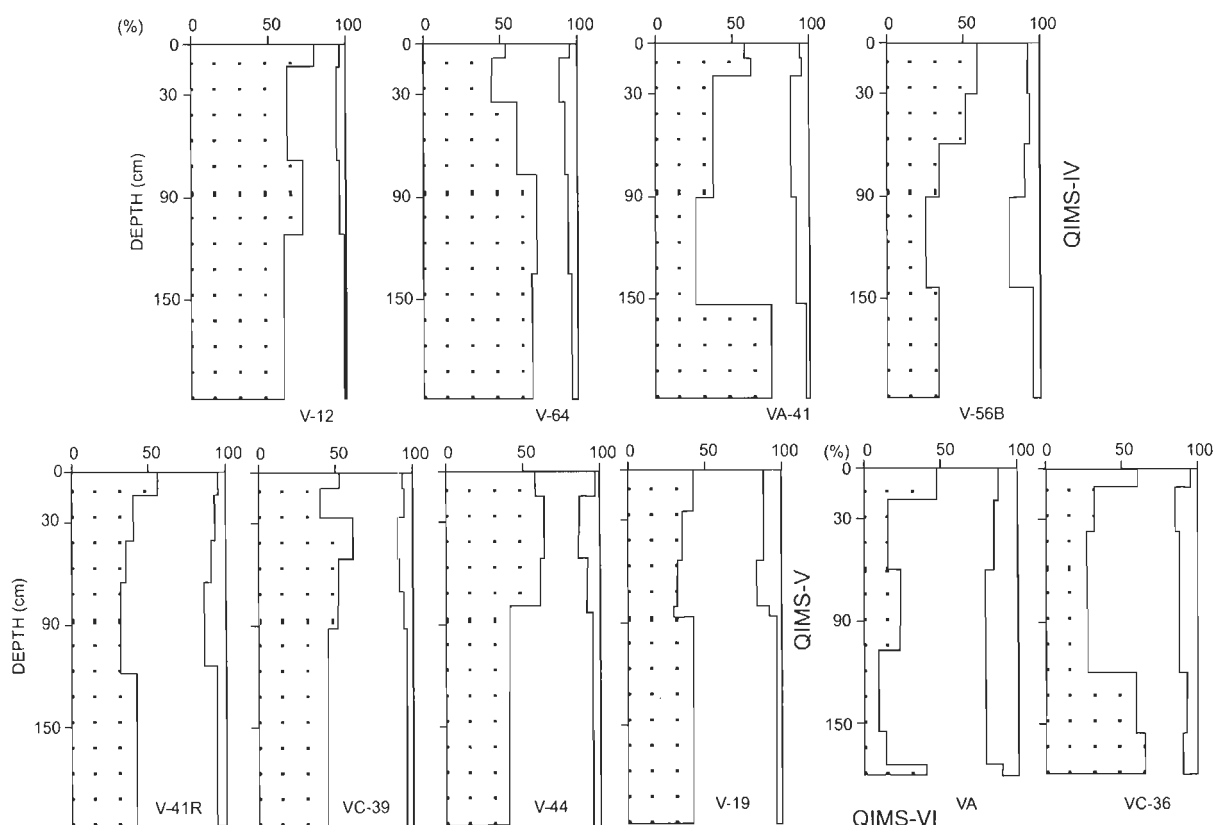


Fig. 4.2. Sand, silt and clay distribution with depth in the QIMS-IV-VI soils.

index (C.A.I) of Levine and Ciolkosz (1983). The clay accumulation index (C.A.I) for QIMS-II, QIMS-III, QIMS-IV, QIMS-V and QIMS- VI vary from 227-484, 166-485, 186-714, 300- 855 and 885-1147, respectively, indicating QIMS –II-V soils have similar degree of development, but it is significantly higher in QIMS-VI soil, as expected (Fig. 4.3).

#### 4.4 CHEMICAL ANALYSIS

A total of 96 samples from 18 profiles were analyzed in the laboratory for pH and EC and data are given Appendix-2. Classification of various soils in terms of acidity and alkalinity was carried out according to U.S.D.A. (1966).

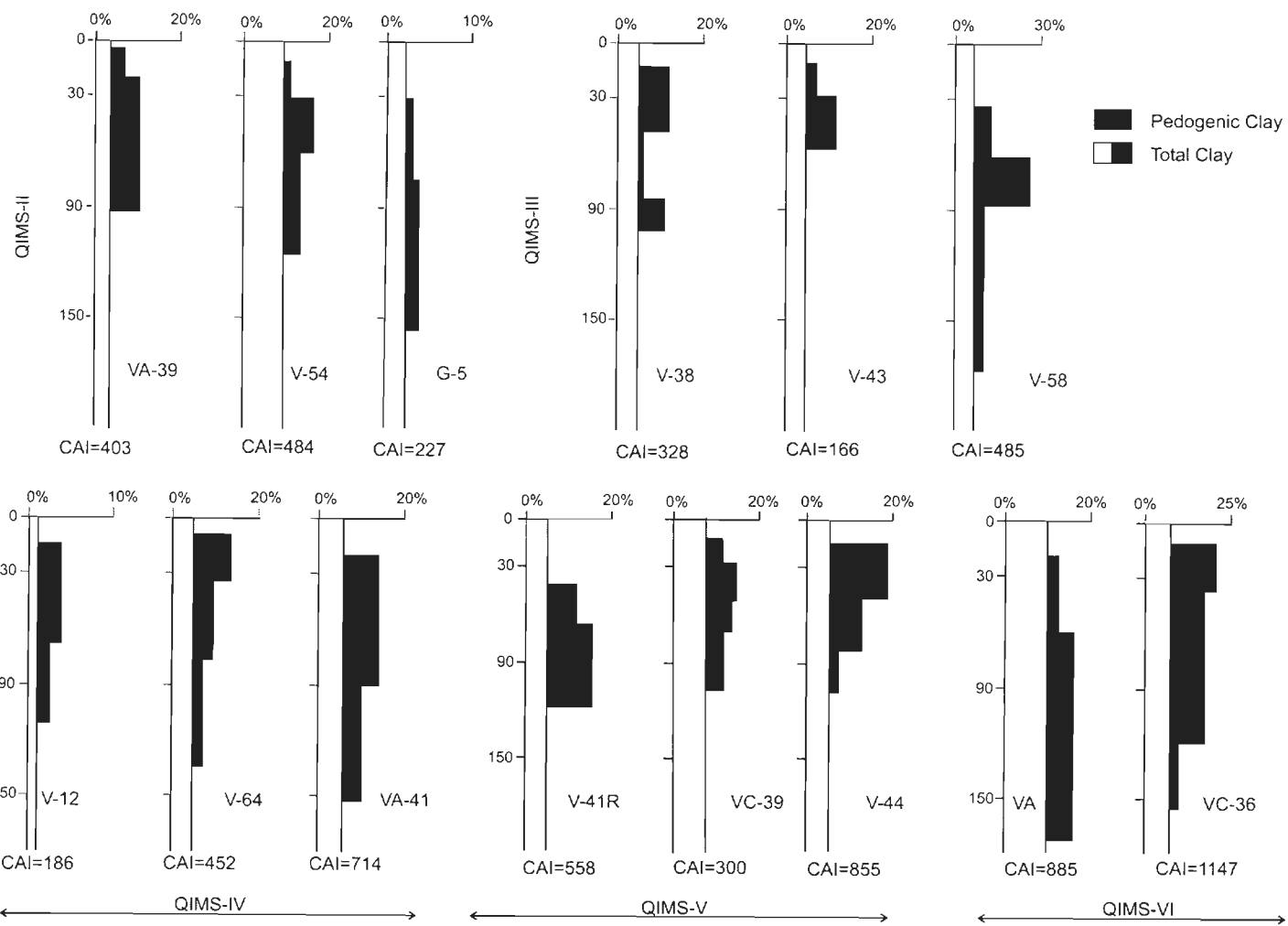


Fig 4.3 Variation of Total clay and Pedogenic clay in different members of QIMS

#### 4.4.1 Soil Reaction (pH)

The numerical designation of soil chemical reaction is expressed as pH (U.S.D.A., 1966). To determine pH, a mixture of soil and distilled water in the ratio of 1:2 was prepared and was shaken intermittently for one hour (U.S.S.L.S., 1968) pH reading for the mixture was taken by Lutron PH-201 digital pH meter.

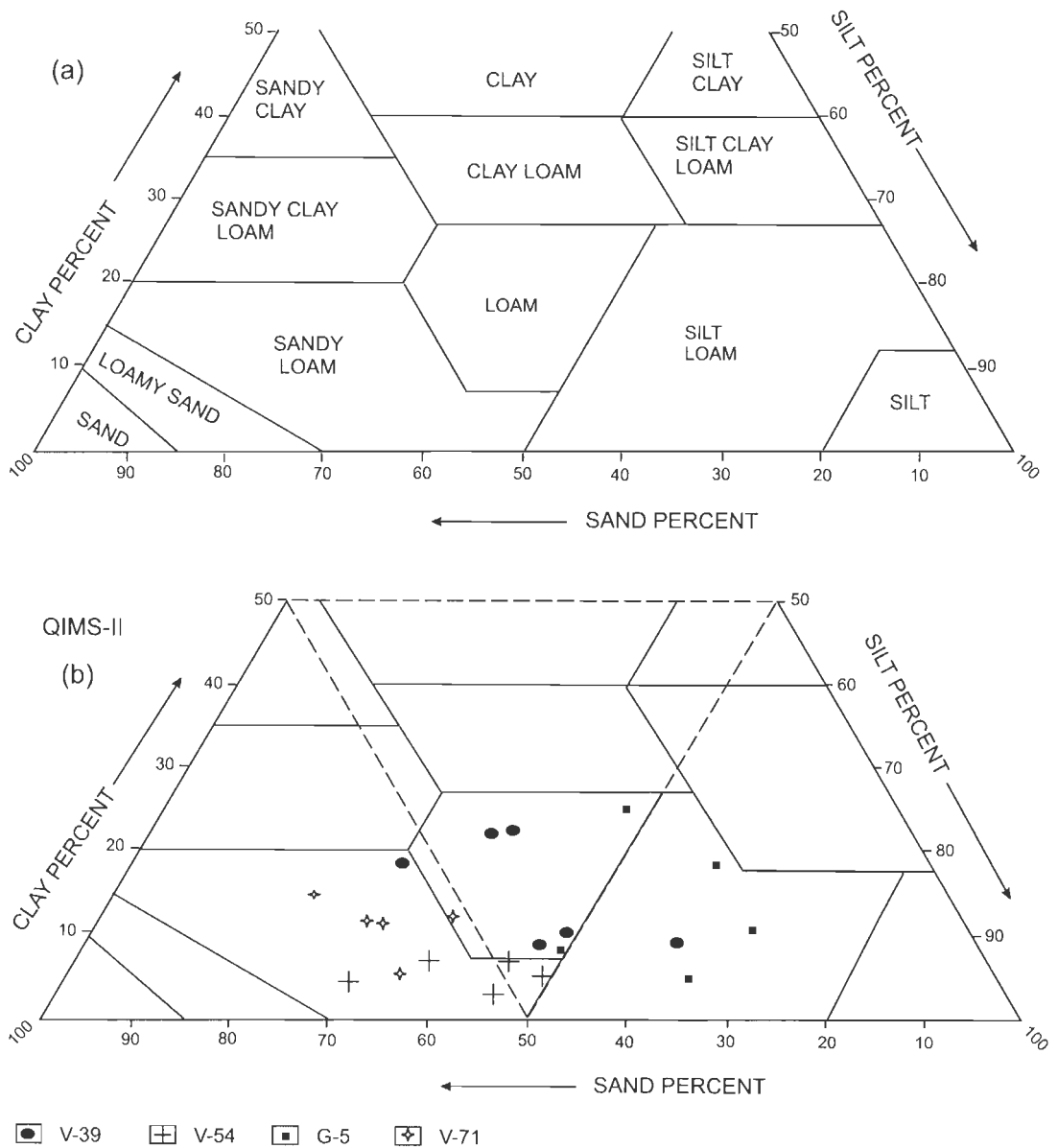


Fig. 4.4 Combined texture triangle (Schoenberger et al., 1998) and triangular plots of soils of QIMS-II.

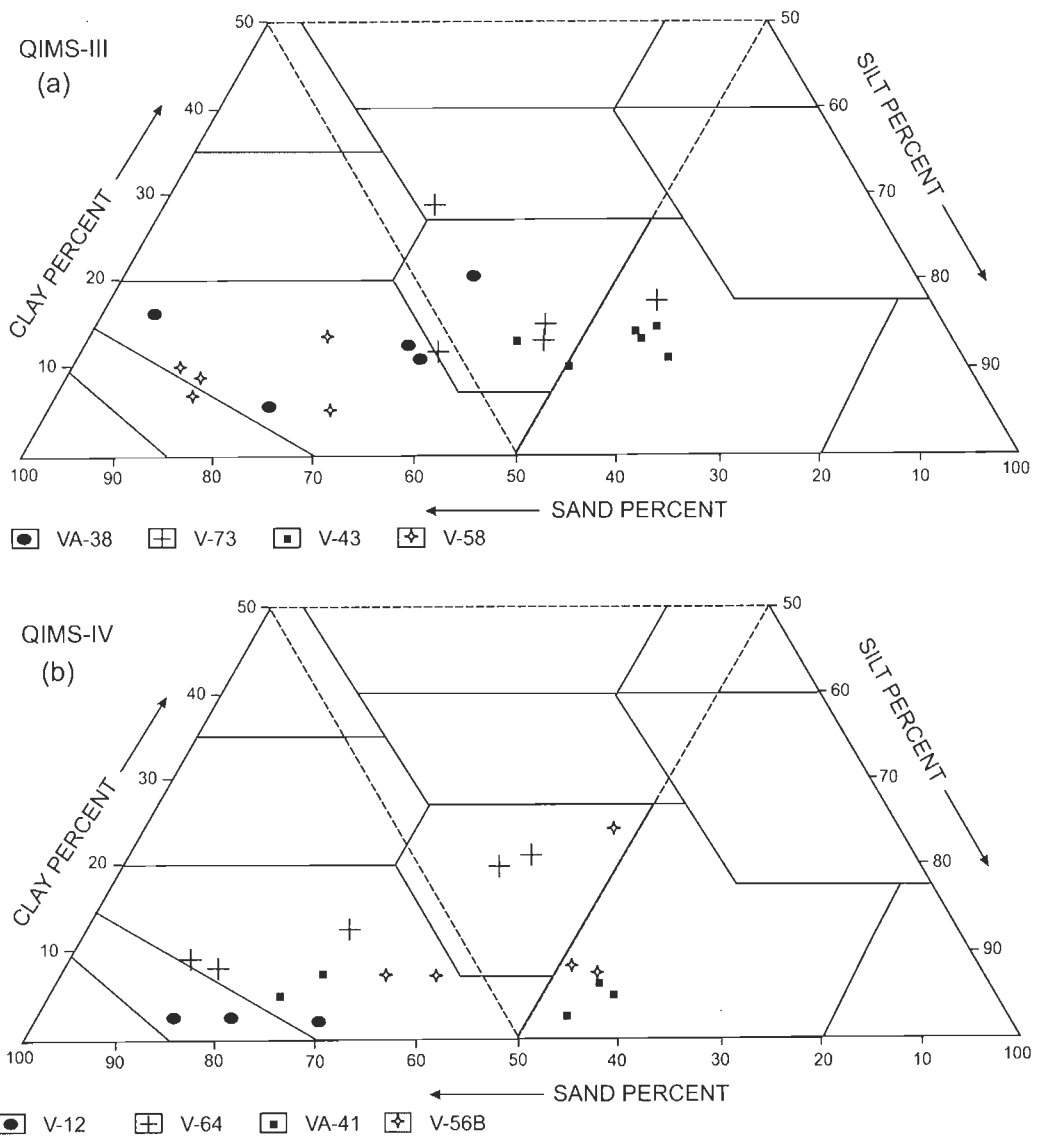


Fig. 4.5 Triangular plots of soil texture of typical pedons of QIMS-III and IV.

#### 4.4.2 pH Variation in Soils of Different Soil-geomorphic Units

In individual pedons, there is no definite order of increase or decrease of the pH value with depth. All the members of the morphostartigraphic units show neutral to moderately alkaline nature except the Old Katha Plain (QIMS-III), which is slightly acidic in nature. Similarly soils of the Old Yamuna Plains I-III and the Old Piedmonts show neutral to slightly acidic in nature.

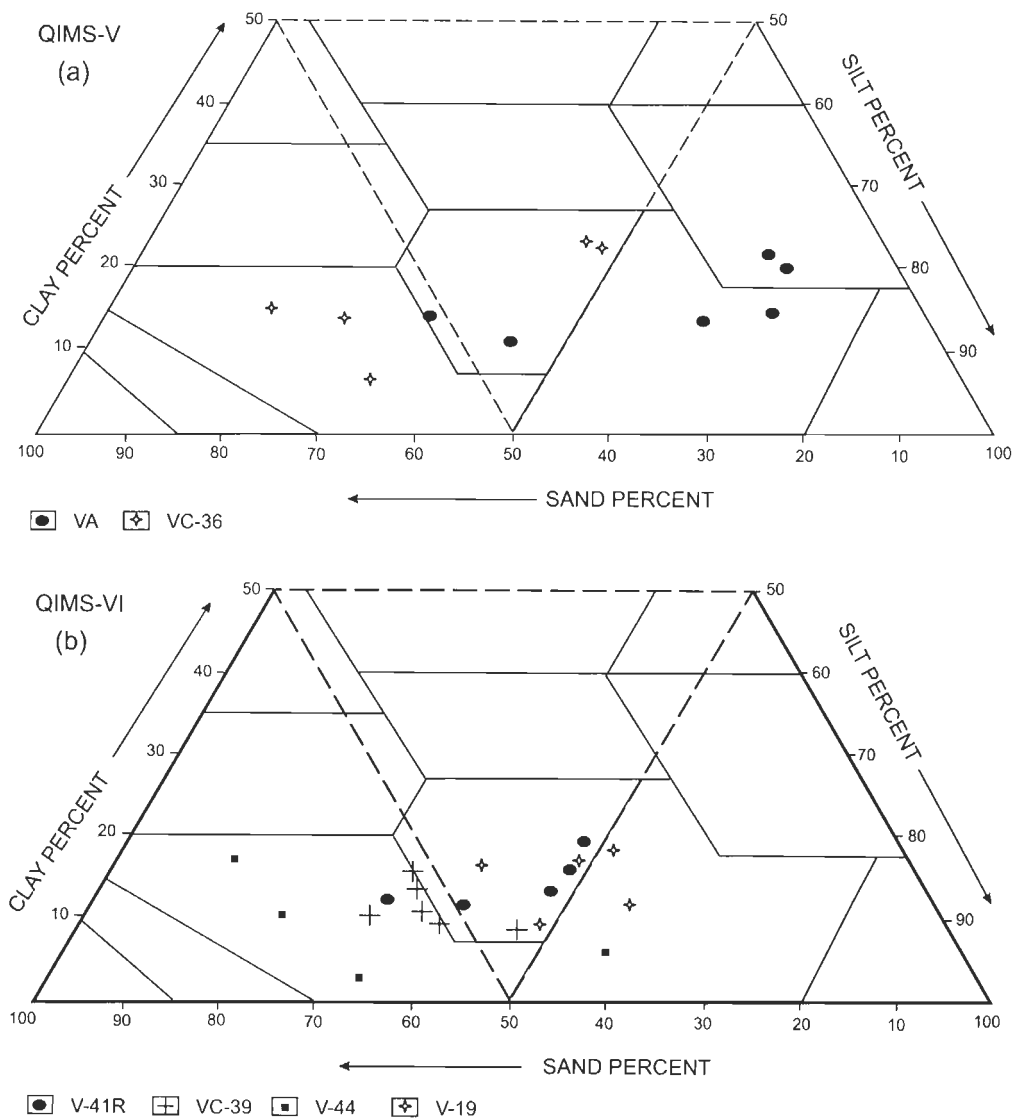


Fig. 4.6 Triangular plots of soil texture of typical pedons of QIMS-V and VI

#### 4.4.3 Electrical Conductivity (EC)

The EC is related with contents of the dissolved salts more soluble than gypsum in the soil, but it may includes a small contribution (up to 2 dS/m) from dissolved gypsum (U.S.D.A., 1966). The EC ( $EC_e = EC$  of 1:2 soil: water extracts, U.S.S.L.S., 1968) of a saturation extract is the standard measure of salinity. Soil: water (1:2) extracts were prepared by filtering the above suspension and electrical conductivity was determined by digital conductivity meter (R-314, Raina Instrument, Delhi). Appropriate temperature correction for



25°C is made for electrical conductivity (EC) data on soil extracts to the standard temperature as described by U.S.S.L.S. (1968, Table 15). Results of the EC values of individual pedons are given in Appendix-2. These data show that soils of most of the Morphostratigraphic Sequence members are non-saline in nature, except that soils of the Karnal Terminal Fan, Old Piedmont-II, Old Sutlej Plain-I, Chautang Terminal Fans-I and II are mildly to moderately saline, as indicated by their EC values,

#### **4.5 MICROMORPHOLOGY OF SOILS OF THE STUDY AREA**

Micro-morphology studies include the arrangements of the skeletal grains, groundmass, voids, microstructures and different pedo-features in the soil thin sections. It is a useful technique in understanding the processes involved in pedogenesis, degree of soil development and also to refine field observations about soil morphology. A total of 54 typical thin-sections have been studied from 20 soil profiles of different Morphostratigraphic Sequence members of the study area and have been described in Appendix-3.

##### **4.5.1 Methodology**

In-situ soil samples were collected during field work in metal boxes (7.5×5×5.5 cm) from the major horizons of pedons from different soil-geomorphic units. Thin-sections of the soil samples were prepared following the method proposed by Miedema et al. (1974) and Jongerious and Heintzberger (1975). The collected samples were first saturated with acetone and placed in vacuum desiccators for a couple of hours. Then the samples were impregnated with the mixture of crystic resin, thinner, catalyst and hardener in the following proportions: i) crystic resin (Synolite 544) 750 ml, ii) thinner (Isopropyl Alcohol)

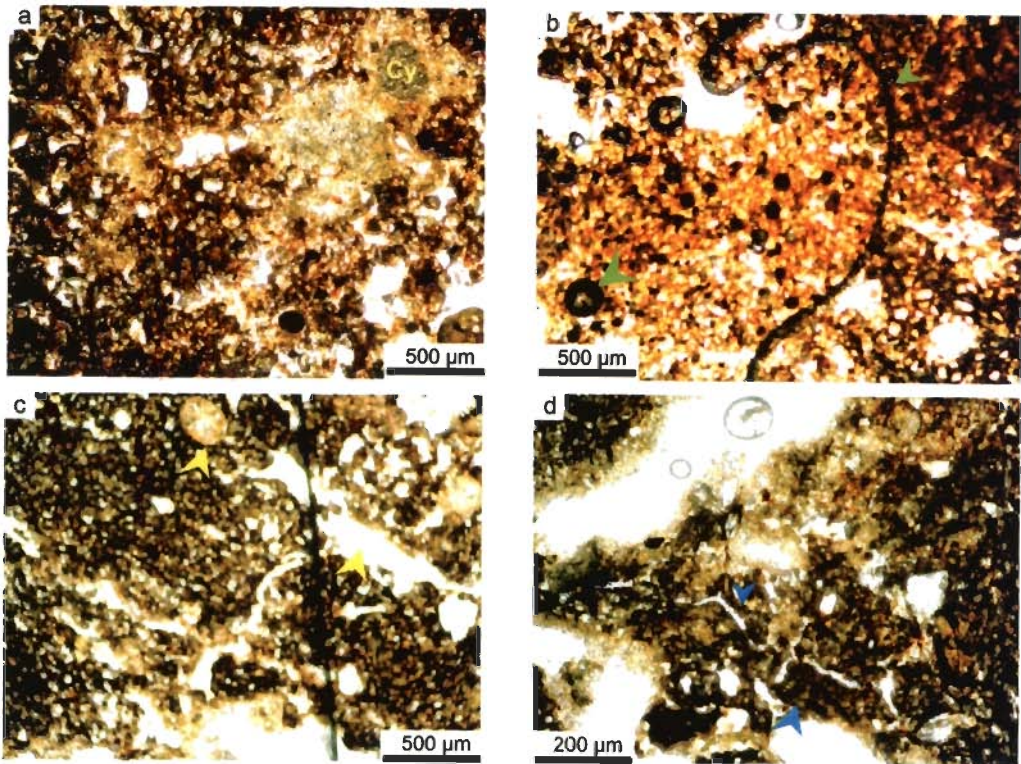


Fig. 4.7 QIMS-II (a) moderately developed peds and partially decomposed root nodule replaced by the clay (Cy), Pedon V-53. (b) Voids filled with clay and fine silt material (green arrow) and features related to animal activity, Pedon V-3. (c) Vughs coated with thin typical calcretans and coating of void-walls with iron rich material (blue arrow). Pedon V-71. (d) Very weakly developed peds and channels coated with calcretans, Pedon V-G5.

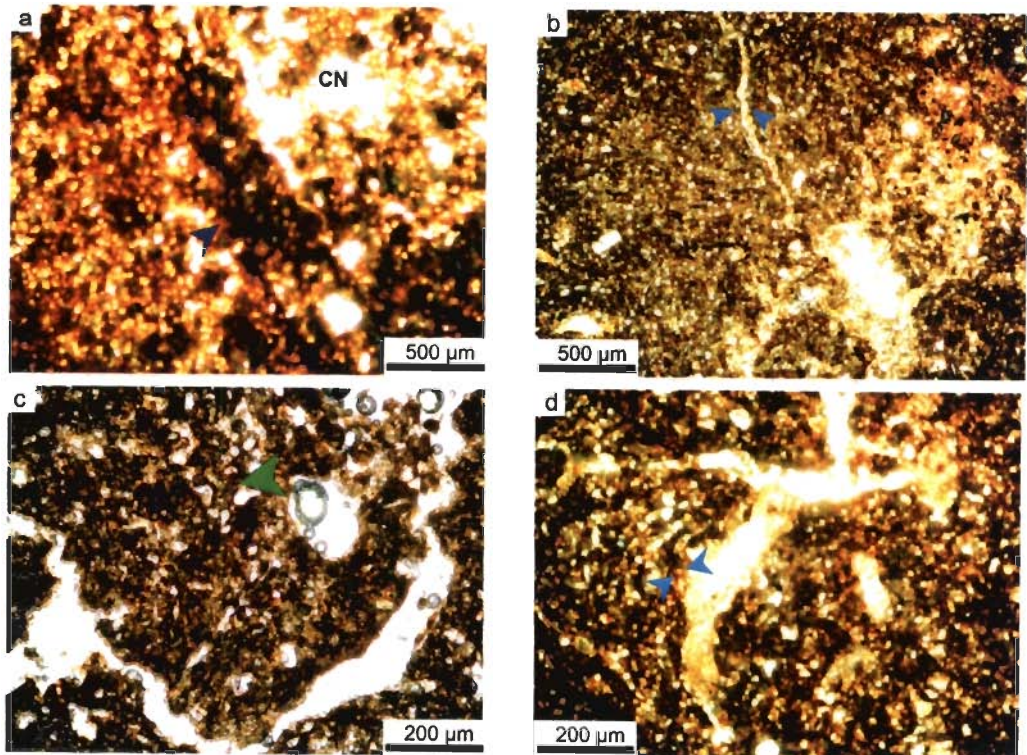


Fig. 4.8 QIMS-III (a) Channel and the roots are filled with typical-micritic calcite materials (CN) and Fe/Mn hypo-coating, granostriated b-fabric, Pedon V-43. (Please Fe-Mn coating and granostriated fabric by different coloured arrow and mentioned with brackets aster each feature) (b) Granostriated b-fabric with weakly developed ped, channel filled with calcite material and chamber structure, Pedon V-58. (c) Weakly developed ped faces with voids coated with calcretans, Pedon V-73 (d) Thin ferriargillan quasi-coating along the channel, bow-like structure present towards left central part, suggesting animal activity, Pedon V-38.



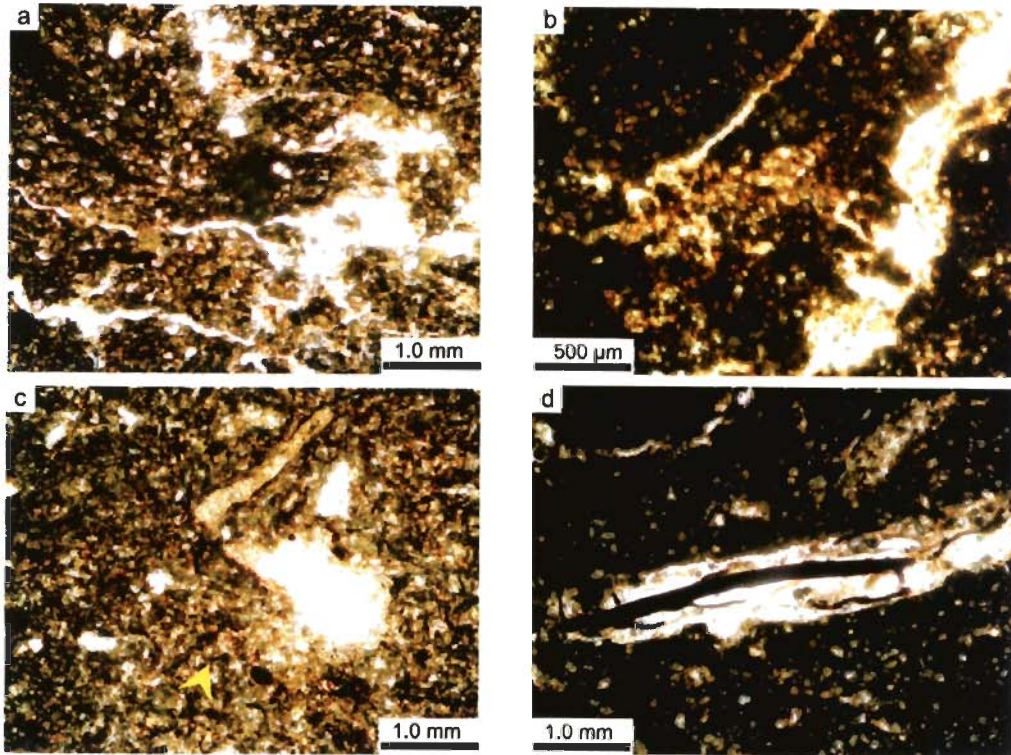


Fig. 4.9 QIMS-IV (a) Moderately developed sub-angular blocky structure, channels coated with at places with calcium carbonate and ferriargillan, Pedon V-12, (b) Channels upper part filled with ferriargillan material and lower part filled with CaCO<sub>3</sub> material, voids coated with typical micritic calcetans, Pedon No.V61 (c) Porous micro-aggregates composed of humified excrement features and ferriargillan coating Pedon .V-36, and (d) Root channels filled CaCO<sub>3</sub> and later replaced Fe/Mn materials Pedon .VB-1.

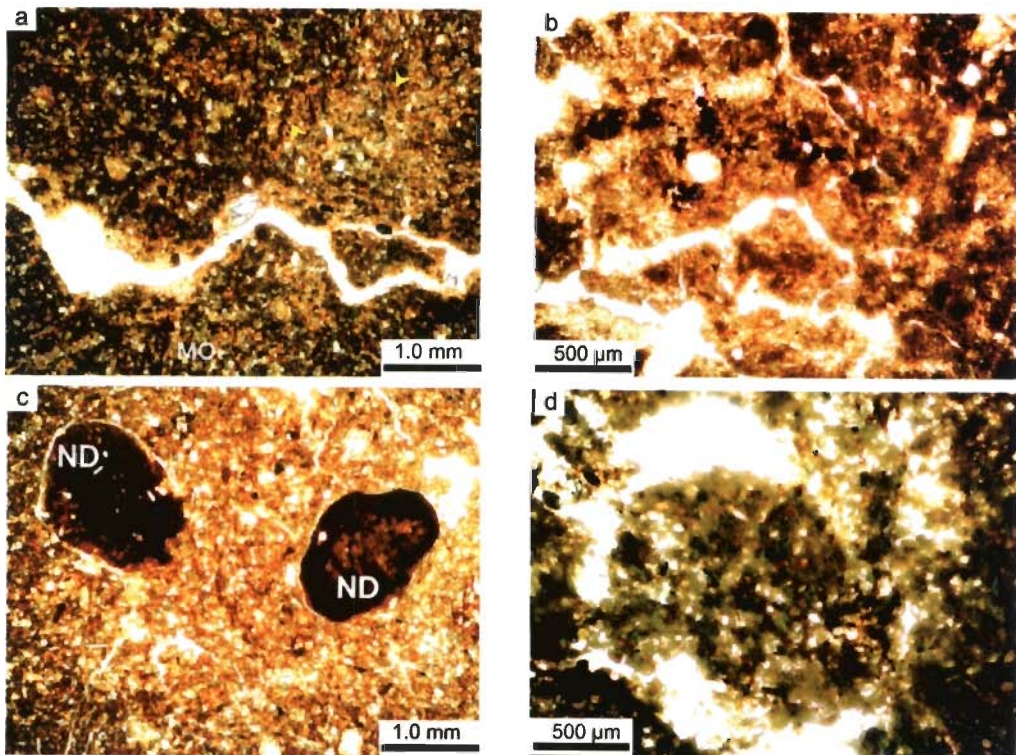


Fig. 4.10 QIMS-V (a) Thin pellicular alteration of biotite, and weakly developed reticulate b-fabric, Pedon G,(b) Moderately to well developed peds separated with chambers coated with calcetans, Pedon V-25, (c) Well impregnated Fe/Mn nodule (ND) with sharp boundaries, Pedon V-44, and (d) strongly developed rounded ped structure, serrate to smooth ped-void surface poro striated and stipple-speckled b-fabrics in groundmass, Pedon V-47.



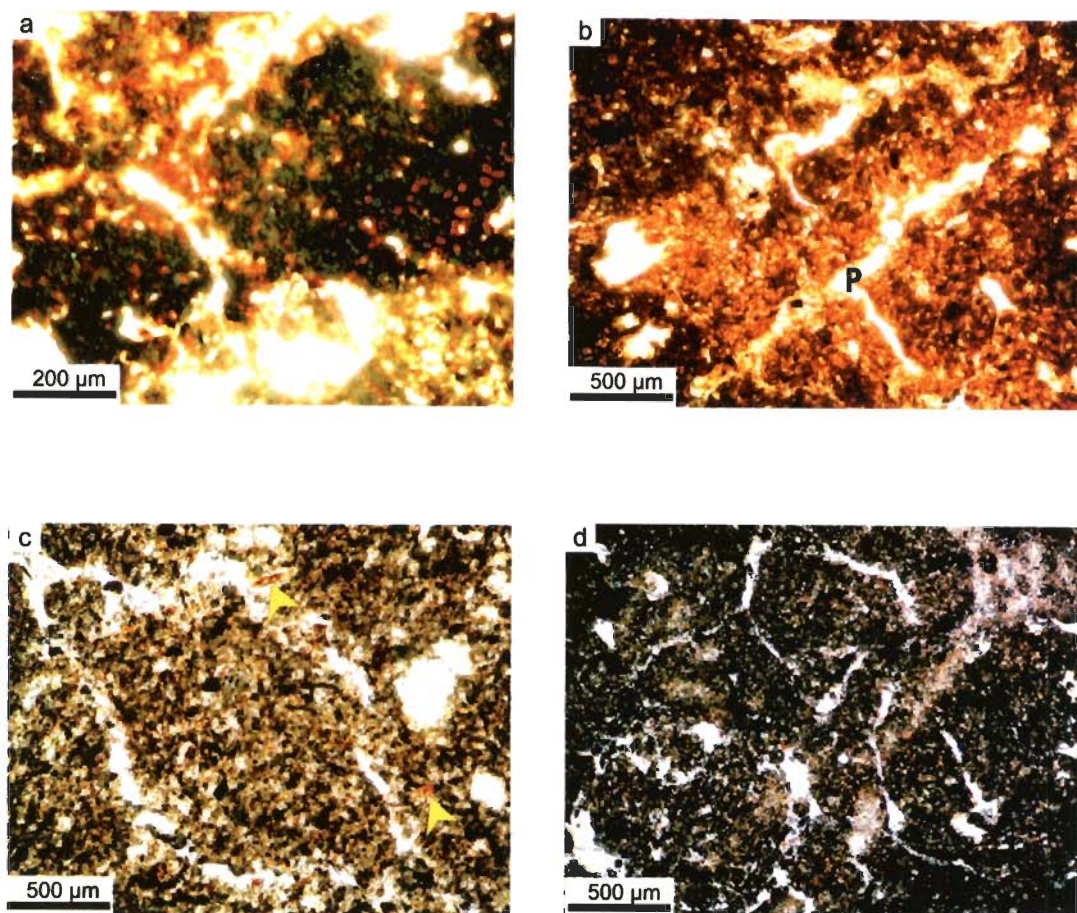


Fig. 4.11 QIMS-VI (a) Well developed peds with multi-nucleated well impregnated Fe/Mn nodule (ND), Pedon . VS-1, (b) Moderately to strongly developed prismatic structure (P), partially accommodating ped faces Pedon VA, (c) Deformed reticulated b-fabric with minute Fe/Mn nodules, and pellicular alteration of biotite released Goethite, Pedon No. V-36 (d) Very well developed peds with well accommodated ped faces, Pedon VC-3.

250 ml iii) catalyst (Cyclonox LNC) 6-7 ml and iv) hardener (Co-octoate) 3-4 drops. The mixture was stirred thoroughly and left for a few minutes, until the air bubbles were removed. The mixture was poured into the metal boxes containing the undisturbed soil samples and then the samples were evacuated for 10-12 hours for complete impregnation of soils sample. The samples were cured for at least 5-6 weeks at room temperature to allow them to be hardened.

Hard blocks of the impregnated soils were used for preparation of thin-sections. Thin-sections (9×6 cm) were prepared according to the procedure described by Jongerious and Heintzberger (1975). In order to prevent buckling and swelling of samples during cutting, kerosene oil was used as lubricant.

The slides were first ground on a lapping wheel and then by hand on a glass plate using silicon carbide and aluminum oxide powders. After obtaining a thickness of about 50-60  $\mu\text{m}$  they were studied for microstructures. Again these slides were ground on a glass plate to a final thickness of 30  $\mu\text{m}$ . and studied for pedo-features.

## **4.6 MICROMORPHOLOGICAL CHARACTERS OF SOIL**

Soil thin-sections have been described according to the system proposed by Bullock et al. (1985). Thin-sections were described in terms of micro-structure, basic mineral components, basic organic components, groundmasses and pedo-features.

### **4.6.1 Microstructures**

Micro-morphological investigation shows that QIMS-II and III member soils show very weak to moderate pedality (Fig. 4.7a, b), whereas the soils of members such as QIMS-IV to VI show moderate to well developed peds in B-horizons (Figs. 4.10b, d and 4.11c, d). In the upper and the lower horizons (A & C) soils are apedal in nature or show weak to no ped development. Channels separate the ped faces and the ped faces are non- or partially accommodating in the QIMS-II and III (Fig. 4.8d) and moderately accommodating to each other in the QIMS-IV to VI soils (Fig. 4.11d). Average ped diameter, void diameter, channel width and porosity ranges between 200  $\mu\text{m}$ -3.5 mm, 50  $\mu\text{m}$ -3 mm, 50  $\mu\text{m}$ -1.5 mm and 5-20% respectively. The ped size increases with the increase in the age. The average porosity for all the members ranges between 5-20%.

#### **4.6.2 Groundmass**

The groundmass is commonly yellowish brown, yellowish red to reddish brown and in some thin-sections it is yellowish brown to gray. The groundmass in a few thin-sections of Member QIMS-II to IV show linear accumulation of yellowish to orange colour of lepidochrosite (Figs. 4.8d, 4.10a, 4.11b) and dark brown colour of siderite (Figs. 4.9a, 4.10a, 4.11b). Soils in the piedmont zone show reddish brown colour (Fig. 4.11b) probably due to the presence of  $\text{Fe}_2\text{O}_3$  formed in the oxidizing environment due to a good drainage. The sesquioxides released by weathering of biotite get precipitated close to these grains and biotite exhibits discolouration on weathering (Fig. 4.11c). Features related to organic activities are well preserved in the soils of the younger members (Fig. 4.7b) and the plant roots are filled with micrites found in the QIMS-IV soils (Fig. 4.9d).

#### **4.6.3 Mineral Components**

Distribution of mineral components is highly variable within the soil profiles as well as among different soil-geomorphic units. Major minerals comprise dominantly quartz and feldspar and muscovite and biotite are present in minor amounts. The average grain diameter varies between 30-600  $\mu\text{m}$  for feldspar and quartz. The fine fractions are composed of fine silt sized quartz and feldspars, clay aggregates, micaceous minerals and other unidentifiable clay particles.

The QIMS-II and III soils do not show any significant alteration of primary minerals. However, in the older soils such as in QIMS-IV-VI, the degree of alterations is significantly stronger. Strong pellicular alterations of

biotite (Fig. 4.11c), irregular alteration of feldspars along the fractures (Fig. 4.10a) and fractured quartz (Fig.4.11b) are observed in the QIMS-V-VI soils.

#### **4.6.4 Pedality**

The grade of pedality is described by using terms such as apedal, weakly, moderately and strongly developed depending upon the degree of separation of peds by voids (Bullock et al., 1985). Types of peds are defined as regular blocky, sub-angular blocky and prismatic. The degree of development of pedality increases from QIMS-II to QIMS-VI soils. Soils of the younger members of the Morphostratigraphic Sequence i.e. in QIMS-II and QIMS-III are apedal (Figs. 4.7a, b, c; Figs. 4.8. a, b) to weakly developed (Figs. 4.7d; 4.8c, d) peds. However, soils in the older members (QIMS-IV-VI) are moderately to strongly developed (Figs. 4.10b, d, 4.11a-d). In the older member soils, ped faces are well accommodated (Fig. 4.10b, d), but in the younger members, the peds are partially accommodated and not-accommodated.

#### **4.6.5 Coatings**

Three types of coatings are observed: argillans (Fig. 4.8b), ferriargillans (Fig. 4.9c) and calcetans (Fig. 4.10b). Further coating type identified are typic- and hypo (Bullock et al. (1985), which deal with the morphological relation of coatings/cutans to pores and grains and aggregates. The thickness of cutans shows a gradual increase from QIMS-II to QIMS-VI soils (0-85  $\mu\text{m}$  for QIMS- II, 50-100  $\mu\text{m}$  for QIMS-III, 50-145  $\mu\text{m}$  for QIMS-IV & V and 70-165  $\mu\text{m}$  for QIMS-VI). Translocation of clay, silt and organic matter and preferred orientation of clay cutans are seen in the Oldest Member of soils.

#### **4.6.6 Voids**

Most of the soils in the study area show voids filled with  $\text{CaCO}_3$ . The size and percentage of voids decrease from the younger to older members. Though many of the voids and channels are hypocoated with calcitic materials (Figs. 4.7c, 4.8c, 4.9a, b and Fig. 4.10. a, b, d) but some of the older member soils show ferriargillan hypocoatings (Figs. 4.9b and 4.11b, d). Channel, vugh and chambers are the dominant voids in the soils. The roughness of the voids decreases from QIMS-II to QIMS-VI. The root voids are filled with both calcitic as well as ferruginous materials (Figs.4.9b, c and d).

#### **4.6.7 Coarse and Fine Ratio**

Coarse and fine ratio (c/f) were measured approximately and the c/f related distributions were expressed on the basis of the visualization of thin-sections. The range of c/f ratios are 5:95 to 50:50, 5:95 to 40:60, 10:90 to 40:60, 5:95 to 40:60 and 10:90 to 40:60 for QIMS-II to QIMS-VI soils, respectively.

#### **4.6.8 Development of b-Fabrics**

The orientation and distribution patterns of interference colours of the soil micro-mass constitute the birefringence fabric or b-fabric. The b-fabrics are described as: random- , crystallitic-, reticulate-, grano-, poro-, stippled-speckled b-fabrics There is a systematic change of b-fabric from younger to older member soils. The younger soils (QIMS-II&III) show random (Figs. 4.7a and 4.8d), grano-striated b-fabric (Figs. 4.7b and 4.8a, b) and the QIMS-V soils show stippled- speckled (Fig.4.10d), reticulate b-fabric (Fig. 4.10a). But the Oldest Piedmont (QIMS-VI) soils show deformed reticulate b-fabrics (Fig. 4.11c).



#### **4.6.9 Concretions and Nodules**

Though nodules are well recognized in the soils of all morphostratigraphic members, their abundance is high in the wet lands in the northern (OdPt-I and OdPt-II) of the study area as compared to the other parts. In the field, it was observed that Fe/Mn nodules in the younger soils are softer than their older soil counterpart. The nodules in the younger soils have diffused boundary, but those in the older soils have sharp boundaries. Multi nucleated Fe/Mn nodules are seen in the older soils (Fig. 4.10c).

#### **4.6.10 Infillings**

Most of the channels rootlets voids are filled with loose to dense calcitic material (Figs. 4.8 c &d, 4.9a, b, 4.10a, b &d, 4.11 b, c &d). Partially decomposed organic materials (Figs. 4.7b, c) and rootlet channels (Figs. 4.9c, d) are also observed. Fe/Mn coating with variable thickness (Figs. 4.8a, 4.9b, 4.10d) are observed in most of the soils.

### **4.7 SUMMARY**

According to the soil texture classification of Schoeneberger et al. (1998) most of the soil textures in the study area varies in a wide range between sandy loam to silty loam

The Clay accumulation index (C.A.I) increases systematically from QIMS-II to QIMS-VI, suggesting the increase of pedogenic clays with the increasing age of soils. Also, the younger soils have varied textures from sandy loam to silty loam classes. With increase in age soils tend to change their textures to loam probably due to breakdown of rock fragments and weathering of some minerals.

Micromorphological studies and grain size analysis of soils from different Members of the morphostratigraphic sequence show variation of features such as variation of pedality, degree of alteration of minerals, thickness of cutans, smoothness/roughness of void surfaces, development of b-fabric and mottles with the increase of age of soils.

Micromorphological investigation show that the Member QIMS-II and III show weak pedality development, QIMS-IV shows moderately pedality development and the QIMS-V to VI show strong pedality development.

Major b-fabrics observed are grano-striated, stipple-speckled, reticulate, and deformed reticulate. In general the degree of development of b-fabric in the Members QIMS-II to IV is stronger than their older soils. The groundmass of a few soils of the Members QIMS-II to IV show yellowish to orange, linear accumulation of lepidocrocite and the wet soils shows accumulation of dark brown colour due to the presence of siderite. Ped size and porosity percentage decreases from Member QIMS-II to VI soils.

In wetlands such as observed in units Young Chautang Terminal Fans-II & III and Old Yamuna Plain-II and Old Piedmont-I, low chroma soils are observed. Micromorphological investigations suggest that Fe/Mn oxide features are observed in all the horizons of such soil. Thus, in wetlands, most soils are gleyed in nature and the presence of siderite and lepidocrocite supports the inference.

The degree of alteration of minerals increases from the Member QIMS-II to QIMS-VI soils. Moderately to strongly altered feldspar grains are observed in the Member QIMS-IV to VI soils.

## **GROUND PENETRATING RADAR (GPR) STUDIES-CHAPTER-5**

---

### **5.1 INTRODUCTION**

The analysis of the geological setting is best done in outcrops, but as they usually are limited both in occurrence and in lateral extent, geophysical techniques are often used. Among them Ground Penetrating Radar has proved to be as an excellent method for high resolution imaging of the geological features in the shallow subsurface that uses radar pulses to image them. (Beres and Haeni, 1991; Olsen and Andreasen, 1995; Jol et al., 1998). This non-destructive method uses electromagnetic radiation in the microwave band (UHF/VHF frequencies) of the radio spectrum, and detects the reflected signals from subsurface structures. GPR can be used in a variety of media, including rock, soil, ice, fresh water and man-made structures. It can detect objects, changes in material, and voids and cracks. In sedimentary geology, especially in the Quaternary sediments, GPR is primarily used for stratigraphic studies, where near-continuous, high-resolution profiles aid in determining-

- (1) Stratigraphic Architecture
- (2) Sand Body Geometry, and
- (3) Correlation and quantification of sedimentary structures.

In the last few decades, GPR has been used in numerous sedimentological studies to reconstruct the past depositional environments and the nature of sedimentary processes in a variety of environmental settings with a view to assist in hydrocarbon and groundwater reservoir analogue investigations (Neal, 2004, Thomson et al., 1995; Jol et al., 1996b; Corbeanu et al., 2001). One of the more promising applications of GPR is its

use in the detection and mapping of subsurface fluids including groundwater and contaminants (Olhoeft, 1984). This is because, in the correctly processed radar profiles, at the resolution of survey, primary reflections are parallel to the primary depositional structures. GPR uses dielectric properties of materials by which it detects electrical discontinuities in the shallow subsurface (typically <50 m). By generating, transmitting, propagating, reflecting and receiving of discrete pulses of high frequency electromagnetic (EM) wave energy in megahertz (MHz) frequency range and subsequently digitally recording in a manner similar to the seismic prospecting, it maps the subsurface with a high resolution (20-25 cm in our case for 100 MHz antennae).

Keeping the above aspects in mind, radar profiles were taken across the piedmont zone, terminal fans and aeolian/fluviol plains in the study area. Also, profiles were made across the inferred faults to confirm their presence, and understand their subsurface nature and their development in relation sedimentation.

## **5.2 BASIC TECHNIQUE/PRINCIPLES OF IN GPR INVESTIGATIONS**

The GPR technique is simple and quite similar in principle to reflection seismic and sonar techniques. Digital GPR profiles are similar in appearance to seismic profiles except that GPR data are acquired by using transient electromagnetic (EM) energy reflections. The working principle of GPR is shown in Fig. 5.1. It consists of two antennas: one transmitter, which transmits short pulse of high frequency EM energy, usually in 10 to 1000 MHz range, to the subsurface, some energy is reflected back to the surface due to the changes in bulk electrical properties of different subsurface lithologies and character of subsurface interfaces. The reflected energy is detected by the

receiver and digitally stored in computer. This type of survey depends upon the position of these two antennas and the way in which they interact with the ground. If the position of the source and receiver or just the receiver is varied, the data contains the information on the spatial variation of the subsurface. The visualization of the GPR profile is the time–space representation of the subsurface, but the time is converted to depth by using measured wave velocity.

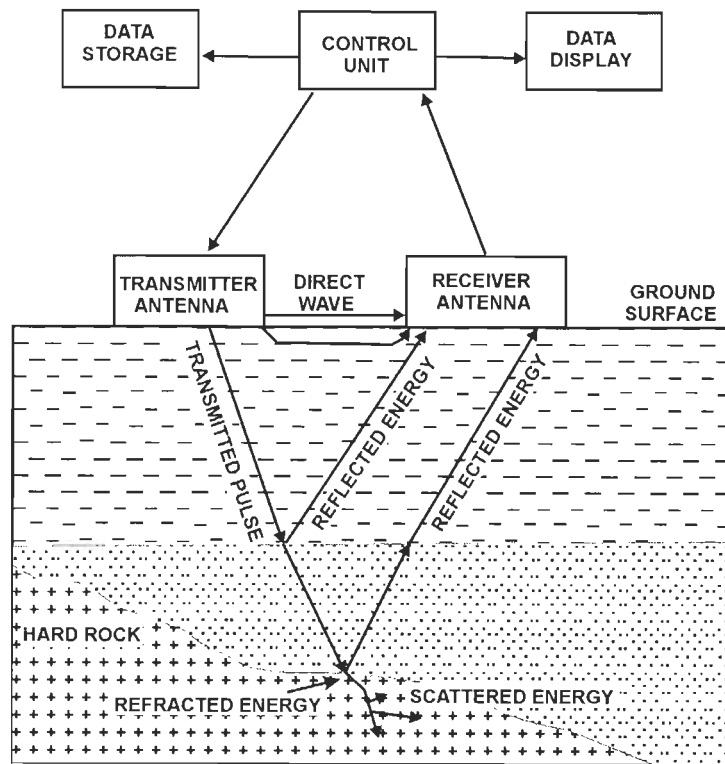


Fig. 5.1 Schematic diagram of working principle of GPR system (After Neal, 2004).

### 5.3 PROCEDURE/METHODOLOGY

GPR survey was carried out after deciding the purpose and selecting the best suitable site for the study. In the study area, both facies changes on the piedmont, terminal fans and fluvial/aeolian plains as well as structural discontinuities (faults) were studied by GPR. The exact locations of faults and

other geomorphic features were marked on the digital terrain model (DTM) and on the satellite images and their locations were transferred to the Survey of India topographic sheets for field work. In the field, GPR studies were carried out on the predetermined locations. On the terminal fans GPR profiles were taken both along, across and oblique to inferred flow direction. In case of faults, GPR profiles were taken across the inferred strike of the faults.

#### **5.4 DATA ACQUISITION PROCEDURE**

Two basic types of data collection i.e. Common Mid-Point Method (CMP) and Common Offset Method (CO) were used. Though a number of the different orientations of the source and receiver antennae can be used, for our study, surveys with perpendicular broad-side position of the antennas (Jol et al., 1996) was used. Also, in most of profiles, we used Common Offset Method, which provides good results for sedimentological studies in the subsurface (Neal, 2004).

The depth to which GPR can image below the surface is dependent upon three main factors;

- (1) The number of interfaces that generate reflections and the dielectric contrast at each interface.
- (2) The rate at which the signal is attenuated as it travels through the subsurface. It depends upon the conductivity of the subsurface material, and
- (3) The central frequency of the antennas.

As the number of interfaces increase, the proportion of energy that propagates to depth is reduced. The conductivity of the materials through which the GPR signal (EM wave) passes controls the depth of penetration. As

the conductivity increases, the material acts more like a conductor than a semi conductor. A practical consideration is that, as the frequency decreases, the depth of penetration increases and the resolution decreases, and vice versa is also true. As observed by Bristow et al. (2003), 100 MHz antennae provides the best trade off between the two aspects of depth of penetration and resolution, so this frequency antenna was used in our investigations. With this antenna, good reflections were obtained up to depths of 15 m. As the average velocity of profiles varies commonly from 0.0768 to 0.0671 m/ns with 100 MHz antenna, resolution of the GPR survey comes to 25.6 cm to 20.3 cm assuming the spatial resolution as a quarter of wave length (Reynolds, 1997).

Care was taken while acquiring the data: avoided acquiring data near hyper-tension lines or electrical poles, avoided acquiring data in heavy traffic areas as vibrations from running vehicles can contribute a good amount of noise in the data, mobile phones and other such instruments were switched off as they use electromagnetic energy like GPR, and made sure that GPR antennae were moved or towed on the plain ground without any cobbles or pebbles as they add noise to the data.

## **5.5 GROUND PENETRATING RADAR STUDIES IN THE STUDY AREA**

GPR studies were mainly carried out at 20 locations In Haryana Plains. Details of methodology like instrumentation, and techniques use in radar processing data and interpretation are given below.

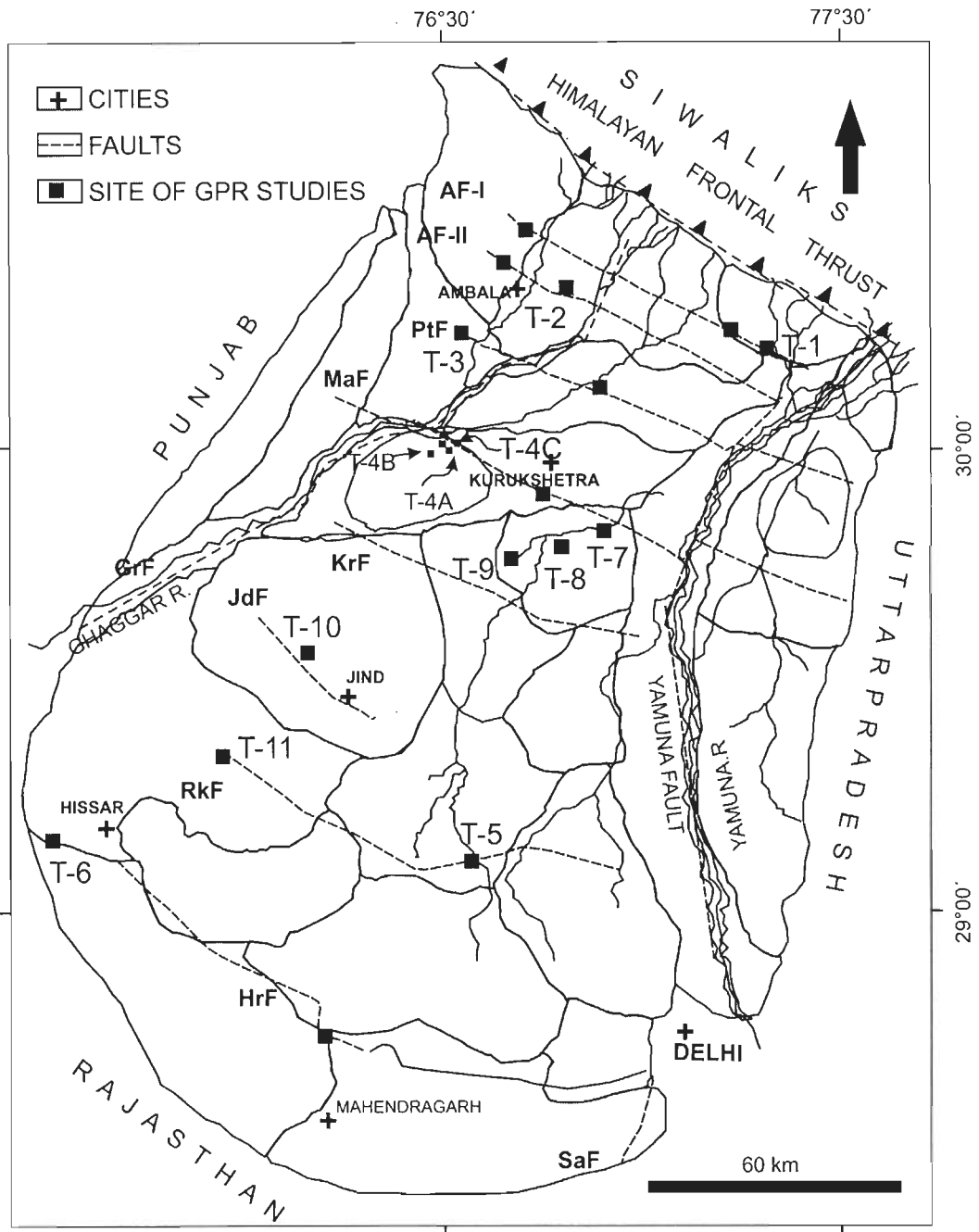


Fig. 5.2 Location of the GPR profile sites in the study area.

### 5.5.1 Instrumentation

Subsurface Interface Digital GPR system (SIR-3000), manufactured by Geophysical Survey Systems Inc (GSSI), was used in our investigations. The system comprises five main components (Fig 5.3):



- (1) Control unit,
- (2) Transmitter,
- (3) Receiver,
- (4) Antennae, and
- (5) Interface, data storage, and display module.

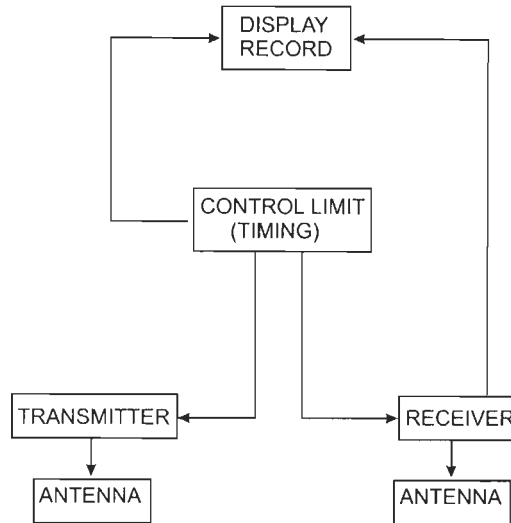


Fig. 5.3 Systematic Diagram of GPR system hardware.

Shielded antennae were used to avoid ringing inherent in the hardware (Audru et al., 2001). Data were collected in distance mode using a survey wheel (model 620, GSSI) along a profile. Data transfer from the antennae to control unit was through fiber optic cables. Automatic Gain Control (AGC) was applied while collecting the data, as it is the best way of acquiring data in a sedimentary terrain (Neal, 2004).

### 5.5.2 Interpretation and Processing of GPR Data

GPR data processing is similar to seismic data processing technique (Fisher et al., 2000; Upadhyay, 2004). The GPR data collected from sedimentary terrains do not need much processing (Jol, 2003), as the sediment bed geometries in sedimentary terrain are simple and the layers or

beds are almost horizontal in nature. Data processing involves mainly three steps-

1. Selecting an appropriate sequence of processing steps
2. Choosing an appropriate step of parameters for each processing step.
3. Evaluating output resulting from each processing step and identifying problems cause by incorrect parameter selection (Yilmaz, 1987).

Collected data were processed and plotted, using GSSI computer based RADAN software, which can apply Infinite Impulse Response (IIR), finite Impulse Response (FIR) and 2-D spatial Fast Fourier Transform filters, gain control, distance normalization, surface normalization, deconvolution, band pass filtering and hyperbola migration to the collected GPR data. Except for application of filter band width a 40/50 and 150/180 MHz as suggested by Fisher et al. (2000) for 100 MHz antenna, we tried to keep use of other processing techniques to a bare minimum, unless the data warranted it.

Interpretation of GPR profiles involves the deciphering of interference patterns rather than discrete reflections and diffractions that are characteristic of reflection seismic profiles (Gawthorpe et al., 1993).

In the present study, interpretation was made in the following steps:

- (1) Reflections caused by the waves while traveling through the air and the road materials were identified and removed from the main trace.
- (2) Origin of the reflections were identified; i.e. whether the interfaces obtained in the traces are real matching the changes expected in the subsurface, since such interfaces can be produced due to the noise and repeated reflections.

(3) Preliminary interpretations were made during and after processing the data without aid of any earlier existing data or studying the profile from trenches.

## **5.6 ARCHITECTURAL ELEMENTS, FACIES, MACROFORMS, AND RADAR FACIES**

GPR is not a universal panacea for all cases. Ground truth is still required because lithological determination is by no means unequivocal. In the study area, the GPR data were interpreted with the help of past geological history interpreted from remote sensing images. After proper processing, GPR profiles were interpreted in terms of the subsurface nature of the area. The GPR profiles were taken along, across and oblique to the inferred depositing stream directions.

### **5.6.1 Architectural Elements**

An architectural element consists of several or many types of three-dimensional bodies separated and internally subdivided by a hierarchy of bounding surfaces, and are characterised by distinctive lithofacies assemblages, external geometries and orientations (Allen, 1983). Major architectural elements observed from the present study are different types of accretions.

Accretion is the gradual accumulation of sediments by a stream. In the study area, accretions are most common features. Upstream accretion and down stream accretions are best seen in the profile taken along the flow direction of the stream. However, the lateral accretions are well recognized in the profile taken across the flow direction of the stream. Naming of the accretion depends upon the fashion of adding materials. All types of

accretions may show internally tabular cross-bedding with set thickness of up to 1 m. Following four types of accretions are recognized in the study area:

a) **Downstream accretion (DA)**: In downstream accretion beds are added in the downstream direction. These beds are internally composed of planar cross-beds, dipping in the dip direction of accretion surface or flat-bedded sands (e.g. Figs. 5.16, 5.27)

b) **Upstream accretion (UA)**: It is the adding of material in the upstream direction. Here beds are added one upon another in the upstream. Accretion surfaces dip upstream at angles of 10°-15° (e.g. Figs. 5.15, 5.29).

c) **Lateral accretion (LA)**: Lateral accretion is the accumulation of material across the stream channel laterally. This is the characteristic feature of the braid bar deposits where the bars frequently migrate laterally such as in the Brahmaputra and Kosi Rivers (Bristow, 1987, Singh et al., 1993). Lateral accretion is characterised by cross-bed dip orientations parallel to the strike of the accretion surface (Miall, 1988), typically seen in braided stream deposition or in lower part of the fluvial sequence in case of meandering streams (e.g. Figs. 5.11, 5.28).

d) **Vertical accretion in Channel (VACH)**: Within large braided river channels, braid bars are separated by anabranches, which represent deepest parts of channels, which accrete by migration of 3-D dunes, giving rise to trough cross-bedded sand, whose cosets may at places be separated by horizontal bounding surfaces. Also, parallel to sub-parallel (horizontal stratification) sand sheets may be present in the deeper parts of the channels. It can be best seen in the profile across the stream flow direction. Following

Best et al. (2003) these are included in the 'vertical accretion in channel' architectural elements (e.g. Figs. 5.16, 5.28).

e) **Vertical accretion on Bar Tops-(VABT)**: The braid bar macro-form sequences in the topmost part are at places are composed of 1.5-2 m thick accretions mainly consisting of flat-bedded or low angle sands, suggesting their probable deposition in the Upper plane-bed phase (Allen, 1983).

Considering two braid bars growing by lateral accretion by migration of sand waves/dunes up the bar from the central lowest level, two significant aspects are observed in the present area. Large braid bars in radar profiles perpendicular to flow direction show that the highest part of the bar horizontal to low-angle bedded sands. This facies continues from the bottom to the top of the bars, suggesting its deposition contemporaneous with lateral accretions on sides of the braid bar during the growth of the bar, instead of a distinct later phase of accretion on the bar top as described by Best et al. (2003). So this facies is given a name 'vertical accretion on bar top, type II (VABT-II), as compared to that described by Best et al. (2003), and called here as vertical accretion on bar top, type-I (VABT-I) (e.g. Figs. 5.7, 5.30a).

A few radar profiles show flat/low angle dipping sands in centre and lateral accretions with cross-beds showing flow directions diverging from this point in opposite directions, suggesting that a low exists between two braid bars, where flat/low angle dipping beds are deposited contemporaneous with lateral accretions on braid bars. These deposits are called vertical accretion in channel of type II (VACH-II), to distinguish them from normal in channel vertical accretion deposits of much larger lateral dimensions (cf. Best et al.,

2003), called here vertical accretions in channel of type I (VACH-I), described above.

### **5.6.2 Macroforms**

Macroforms are large-scale depositional features, products of a long-term component of a depositional system, which accumulate sediments over periods of several to many years and develop an internal consistency of facies and orientation (Jackson, 1976). In general, the most distinctive characteristic feature of the macroform is that it consists of genetically related lithofacies, with sedimentary structures showing orientations and internal minor bounding surfaces that extend from top to the bottom of the element, indicating that it developed by long term lateral, oblique, upstream or downstream accretions. A macroform is comparable in height to the depth of the channel in which it formed and in width and length is of similar order of magnitude to the width of channel. Mainly two macroforms i.e. braid bars and channels are observed in the study area.

#### *5.6.2.1 Braid bar*

Braid bars or mid channel bars are exposed sand or gravel bars that divide flow and cause a braided pattern in the streams (Allen, 1983). These macroforms are characterised by the presence of surfaces of lateral, oblique or downstream accretion and vertical accretion (discussed below), which extend, at a low angle from the top to the bottom of the deposit. In this area the braid bars are well recognized in the profiles across and oblique to the flow direction. These bars are 4-12 m in height (Figs. 5.12, 5.28) and have a convex up topographic profile. The top of these bars are cut by an erosional surface (fifth order surface, Miall, 1988), on which another sequence is lying.

The size of the braid bars of the large rivers is bigger than their small stream counterparts.

#### *5.6.2.2 Channels*

Mainly small channels with 3-4 m depth are observed towards the top of radar sequences. These may be narrow (10m wide) and wide (more than length of profile, usually >100 m). These may be filled by mud facies-II, sand or both.

The maximum height of braid bars can be taken as minimum depth of stream depositing it and a depth of 7-12 m for some sequences in the lower of profiles is interpreted. However, studies of known paleochannels show that in addition to high braid bars, at places we get 2-4 subsequences marked by lower height braid bars, but with total thickness of the same order as the maximum height of braid bars, suggesting the total thickness of these genetically related subsequences and marked by uniformity of radar reflections may be taken as minimum depth of depositing stream (Fig. 5.31).

Using the above background, three types of streams can be recognized in the present area: large rivers with depth of >7 m, medium sized river with depths of 3-7 m and small streams with depths of <3 m. At places, depths of small stream can go up to 4 m (Fig. 5.12).

### **5.6.3 Facies**

#### *5.6.3.1 Trough cross-bedding*

This facies is typically composed of trough cross-beds with foresets tangential or sub parallel to the bounding troughs. Trough cross-bedding is produced by the downflow migration of lunate dunes in both subaqueous and sub-aerial environments. The troughs have cross-cutting relationship with one

another. Individual troughs of ~3 m width and ~0.5 m depth are well recognized in upper part of profile T-11 (Fig. 5.8).

#### *5.6.3.2 Tabular Cross-bedding*

This facies is dominant in the fluvial deposits of the area. Low angle (7° to 10°) dipping foresets and 1.5 to 2.5 m in height are common. The bounding surfaces of the cross-beds dip up to 7° in the upstream direction and signify the upstream stacking of channel bars.

#### *5.6.3.3 Horizontal Bedding*

These are essentially flat/horizontal beddings in sands deposited both in the lower and upper flow regimes. Due to gross resolution of the GPR reflections, cross-laminated sands are also included in this facies. These are common in VACH-I and VACH-II architectural elements.

#### *5.6.3.4 Mud Facies*

The mud facies is recognized by the parallel or sub parallel continuous reflections (Best et. al., 2003) and lack of any other sedimentary structures. Two major types of mud facies are identified: mudfacies-I and II. Mudfacies-I represents deposition by vertical accretion in a floodplain. Mudfacies-II is confined to well-defined channels. Thickness of mud facies varies from 3 m to 6 m (e.g. Figs. 5.11, 5.12).






### **5.6.4 Radar sequences**

Following Best et al. (2003) radar sequences are identified from the GPR profiles by surfaces, which provide good reflections and are traceable over almost the whole length of the profile and have possible genetic



significance. In general two or three such sequences are observed in from most of the radar profiles.

Table 5.1 Showing annotation used in description of GPR profiles.

	Boundaries between GPR sequences
	Boundaries between GPR subsequences
	Boundary of macroforms (channels and braid bars)
	Movement along a fault
	Apparent flow direction along the profile
VACH-I	Vertical accretion in major parts of the channel (cf. Best et al., 2003)
VACH-II	Vertical accretion in channel between two braid bars
VABT-I	Vertical accretion on braid bar top as a distinct late stage phenomenon (cf. Best et al., 2003)
VABT-II	Vertical accretion on bar top contemporaneous with lateral accretions throughout the bar
LA	Lateral accretion
DA	Downstream accretion
UA	Upstream accretion

GPR profiles have been interpreted in terms of GPR sequences/subsequences. Lithofacies and faults and different annotations used to indicate these features are given in Table 5.1.

## 5.7 HARYANA REGION- LITHOFACIES

GPR studies were carried for facies analysis of piedmont zone, terminal fans and fluvial/Aeolian plains and confirmation of faults, inferred from remote sensing and G.I.S. studies.

### 5.7.1 Piedmont Zone

#### 5.7.1.1 Young Piedmont

##### Profile T-2

This GPR profile was taken near Bastoli Village (76° 15' E, 30° 20' N), 7 km northeast of Ambala City. It is 160 m in length and up to the depth of 8.5 m and almost at right angles to the Ambala fault-II (N30°-N210°) (Fig. 5.6).

Two radar sequences I and II are identified in this GPR profile. In the radar sequence-II, all the three subsequences IIa, IIb and IIc show lateral accretions. Bars in the subsequences IIc and IIb were of similar nature and height (<4 m). However, sequence IIa is finer grained (as indicated by thicker strata) than the lower subsequences and bars were of lower height (2 m). In all these subsequences, bar top may be marked by vertical accretion of type 2 (VABT-II).

The radar sequence-I shows sigmoidal bedding over the whole length of the profile in the lower part and upper part is marked by many channels filled with mud.

The sequence II was probably deposited by moderate sized stream and later sequence I was deposited by a wide, shallow stream in lower part and by numerous small width streams in upper part.

#### *5.7.1.2 Old Piedmont-II*

The Old Piedmont-II was deposited by reworking of the Oldest Piedmont in the north.

#### Profile T-3

The profile was taken near village Rurki Village (76° 33' E, 30° 40' N), 6 km northeast of Patiala City. The profile was taken along the N25° – N205° direction across the Patiala Fault, which strikes in N150° -N330° direction. It is 210 m long and the data were collected up to the 8.5 m depth (Fig. 5.7).

Mainly two GPR sequences I (1-2 m) and II (6.5-7.5 m) are identified. Sequence II is further subdivided into IIa and IIb. Subsequences IIb and IIa seem to have been deposited by lateral accretions and vertical accretions on

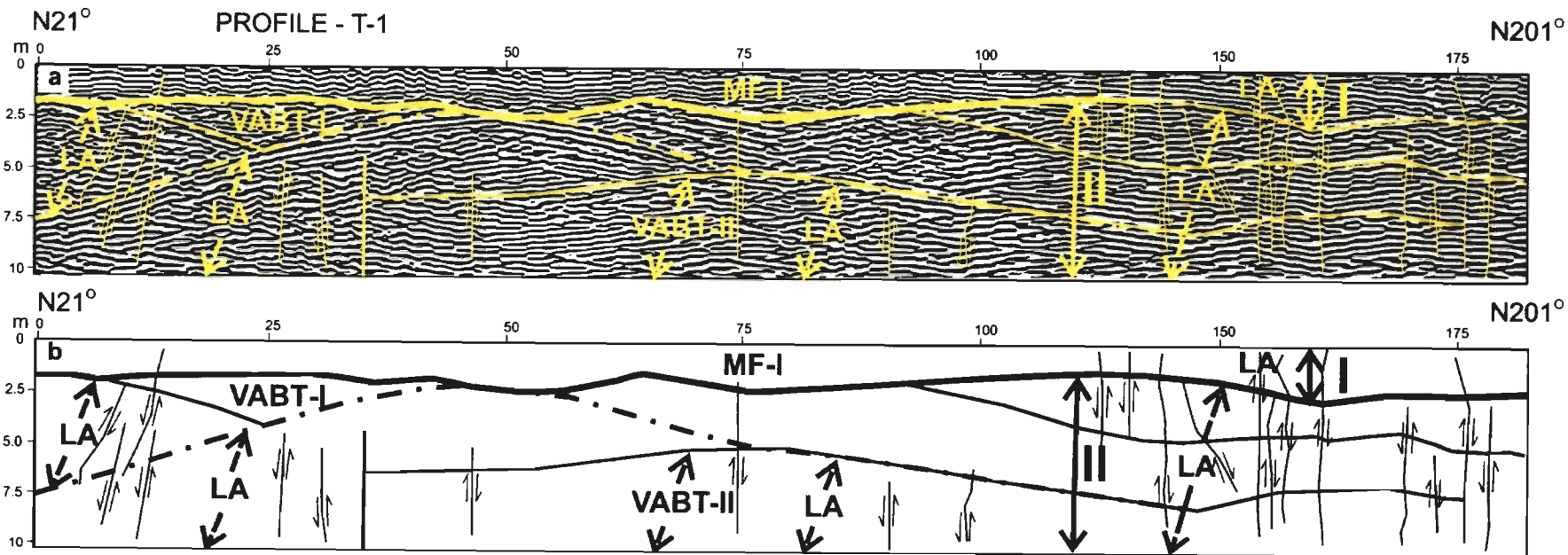


Fig. 5.4 (a) Annotated GPR profile T-1 across the Ambala Fault, showing sequences/subsequences, lithofacies and faults. (b) Outline diagram showing different features of the GPR profile T-1.

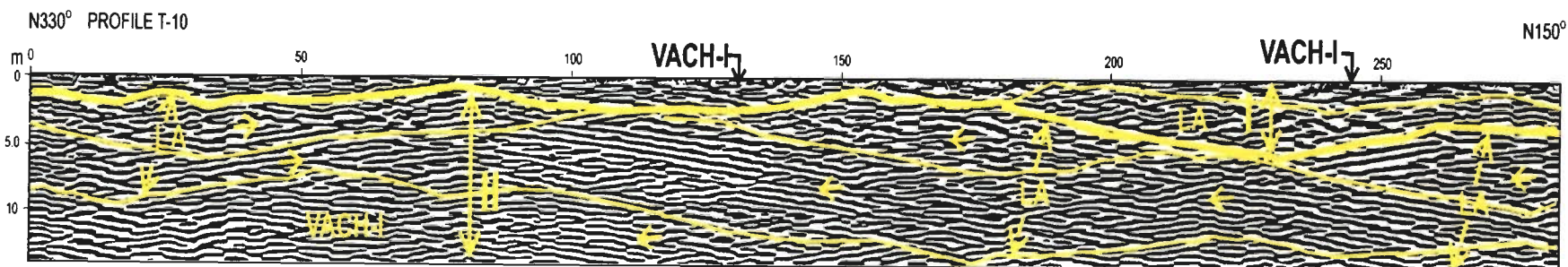


Fig. 5.5 Annotated GPR profile T-10 is from the Old Yamuna Terminal Fan near Narwana city, showing sequences/subsequences and lithofacies.

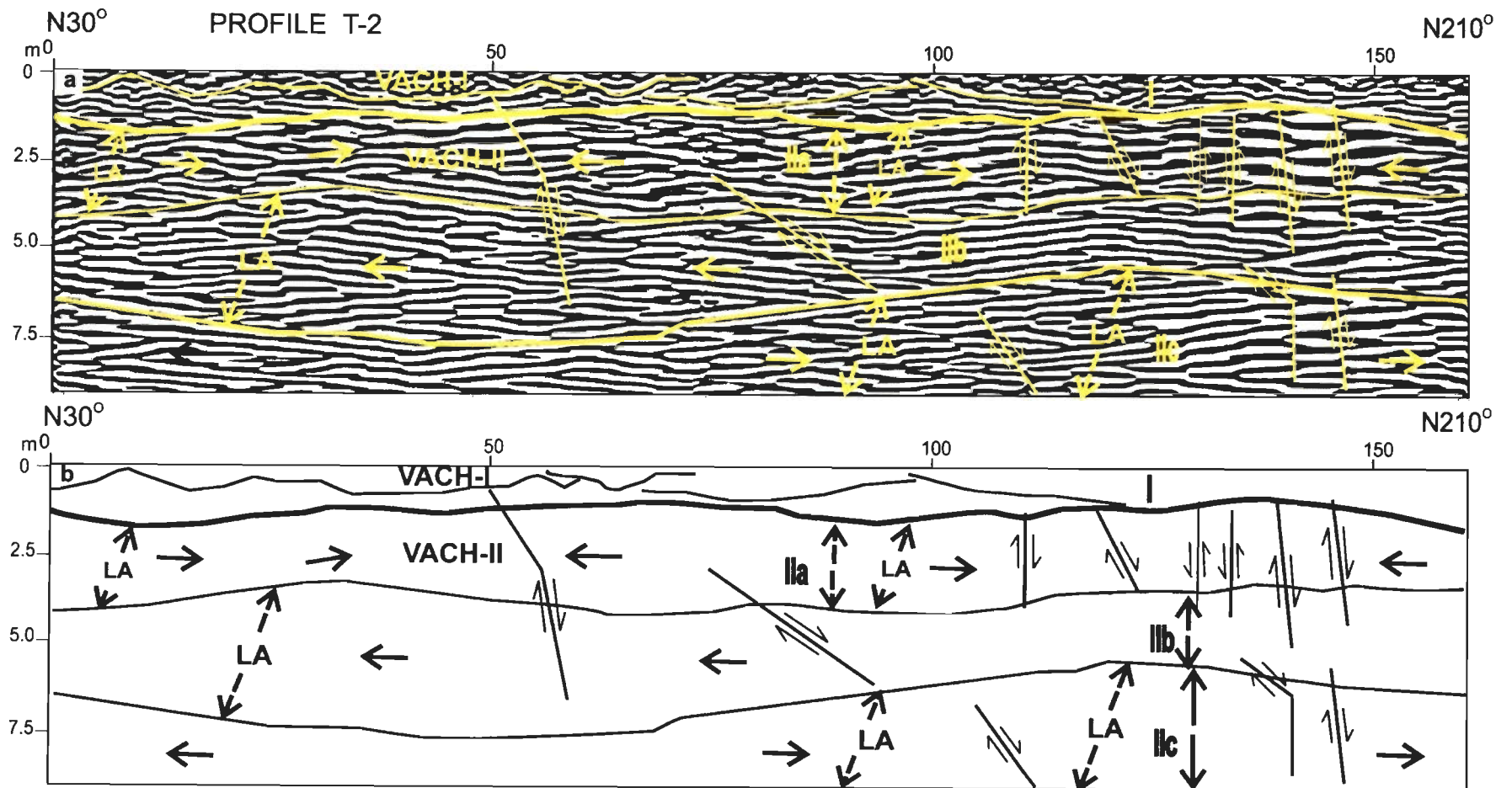


Fig. 5.6 (a) Annotated GPR profile T-2 across the Ambala Fault-II, showing sequences/subsequences, lithofacies and faults. (b) Outline diagram showing different features of the GPR profile T-2.

the bar top of type II (VABT-II). Sequence I is mainly composed of sigmoidal bedding indicating deposition by dunes/sand-waves within channel (VACH-I).

Thick (6.5-7.5 m) sequence II was deposited by the large river Sutlej. Later after shifting away of the Sutlej River, sequence I was deposited by a small stream coming out of the Oldest Piedmont.

### **5.7.2 Terminal Fans**

Three terminal fans i.e. Markanda, Young Chautang-I and Old Yamuna Terminal Fans out of nine terminal fans recognized from the Haryana plains were studied for GPR facies.

#### *5.7.2.1 Markanda Terminal fan*

Mukerji (1975, 1976) described first and used the term 'terminal fan' for the Markanda Fan, deposited in Haryana Plains, far away from Himalayan Foothills. This fan was considered to have been deposited due to the loss of stream discharge due to downward seepage and evapo-transpiration under arid to semiarid climate. Later Parkash et al. (1983) and Abdullatif (1989) described sedimentary structures of different terminal fans. Possible terminal fan deposits have been described from the ancient rocks from different parts of the world by many workers (Friend, 1978); Turnbridge, 1984; Sadler and Kelly, 1993; Kelly and Olsen, 1993). Gradual terminations of streams under semi-arid climatic region of Australia have been described as 'floodouts' (Tooth, 1999, 2000a, b). In the absence of any additional recent terminal fans being recognized, their existence has been doubted (North and Wariswick, 2007).

Three GPR profiles were carried out on this terminal fan: one (T-4C) for the Markanda fault responsible for development of the Markanda terminal fan and two (T-4A and T-4B) for study of GPR facies of this terminal fan.

#### Profile T-4A

This GPR profile was collected at a location, 0.3 km from Kanthala village, on the Kanthala-Malakpur (76° 31' E, 29° 56' N) road. The profile length is 204 m and data were recorded up to a depth of 10 m. The GPR profile was taken in N100° to N280° direction.

The profile is divided in two radar sequence I (2-3 m) and II (7-8 m) (Fig. 5.10). The II radar sequence is subdivided in two subsequences - IIa and IIb. Subsequence IIb is a large bar (max. height ~5 m) with lateral accretions on both sides. Central part of the bar exhibits vertical accretion on bar top of type II (VABT-II). Subsequence IIa represents second phase of evolution of the bar, with distinct lateral accretions and 'vertical accretion on bar top' of type I (VABT-I).

The radar sequence I exhibits mainly sigmoidal bedding, suggesting deposition from small migrating bar/dune in channel (VACH-I).

It appears that sequence II was deposited by a large river with a minimum depth of 8 m and the upper sequence I represent terminal fan deposit, formed by the Markanda River.

#### Profile T-4B

This GPR profile section was conducted at about 1 km from Kathala Village (76° 33' E, 29° 58' N) towards the Lukhi Village in the N121° to N301° direction. The profile is 180 m long and data were collected up to a depth of 16 m (Fig. 5.11).



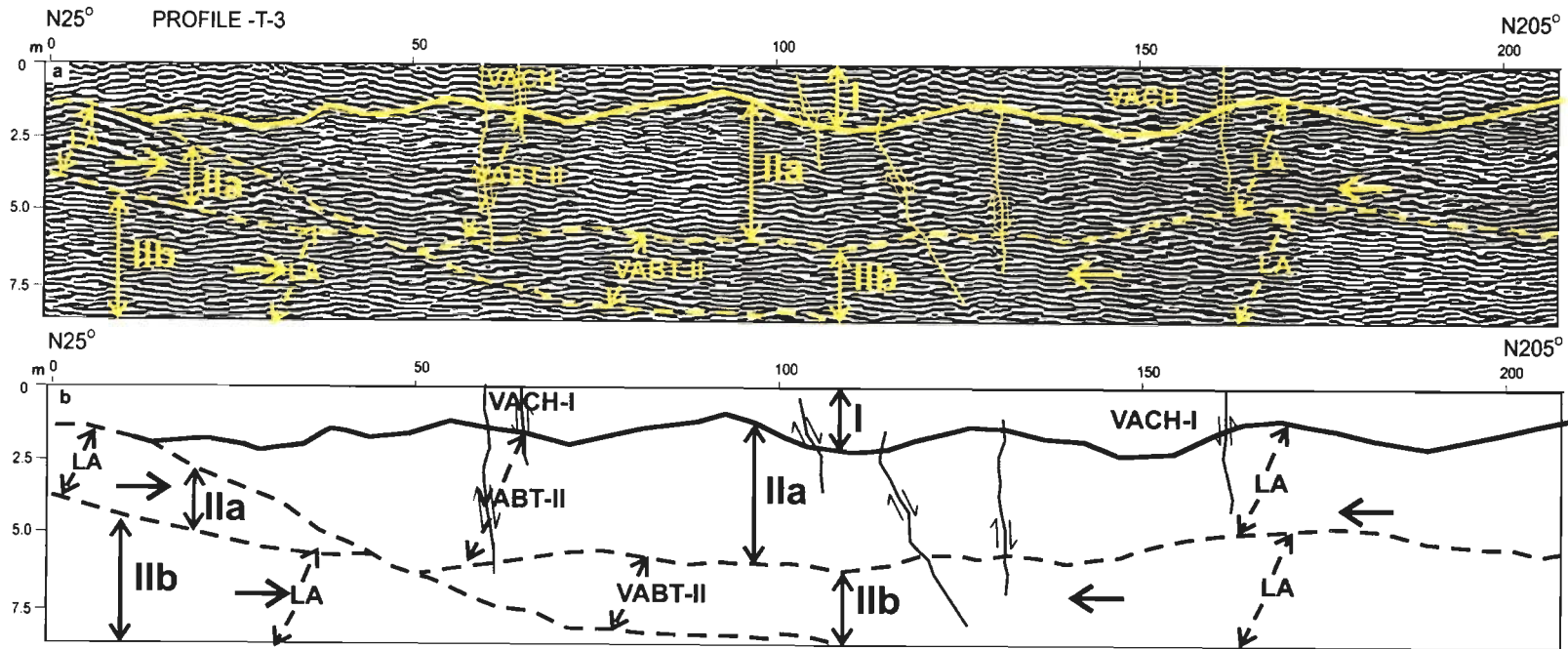


Fig. 5.7 (a) Annotated GPR profile T-3 across the Patiala fault, showing sequences/subsequences, lithofacies and faults. (b) Outline diagram showing different features of the GPR profile T-3.

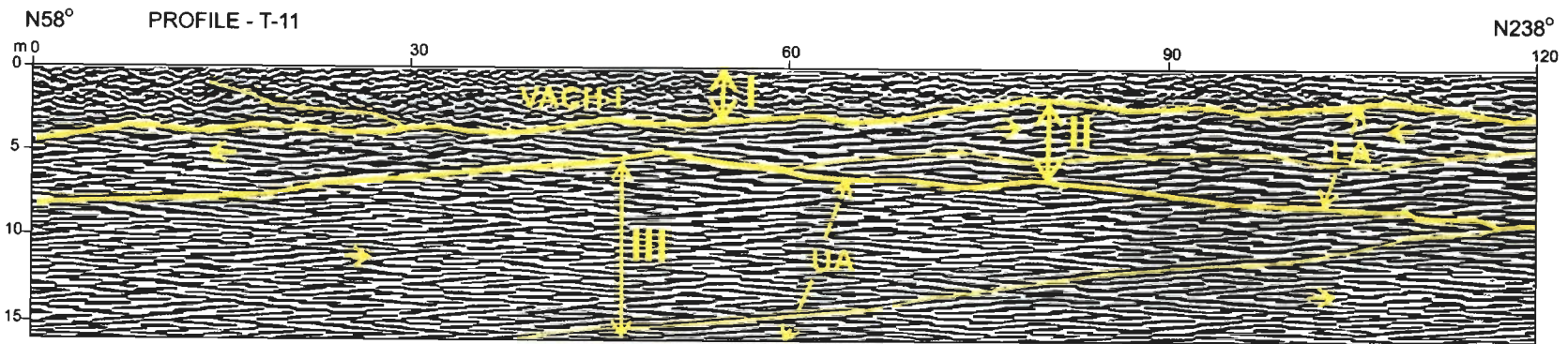


Fig. 5.8 Annotated GPR profile T-11 is from Fluvial plain near Hansi city, showing sequences/subsequence and lithofacies

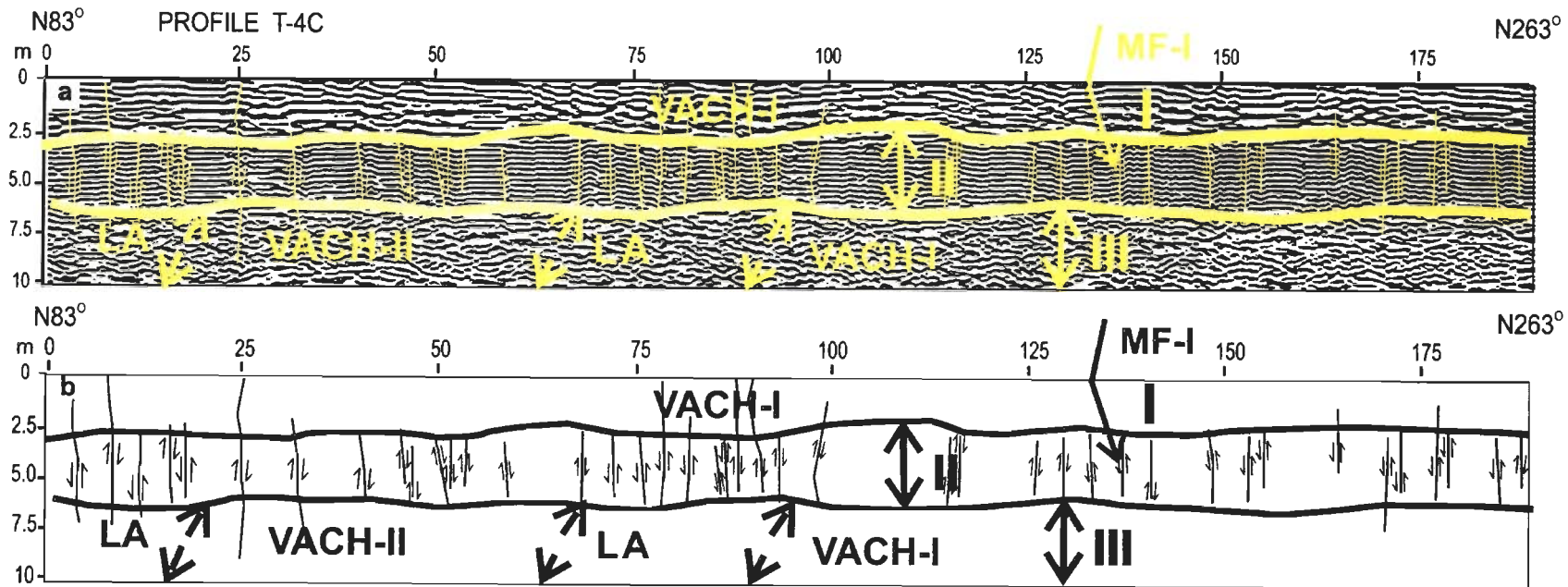


Fig. 5.9 (a) Annotated GPR profile T-4C across the Markanda fault, showing sequences/subsequences, lithofacies and faults. (b) Outline diagram showing different features of the GPR profile T-4C.

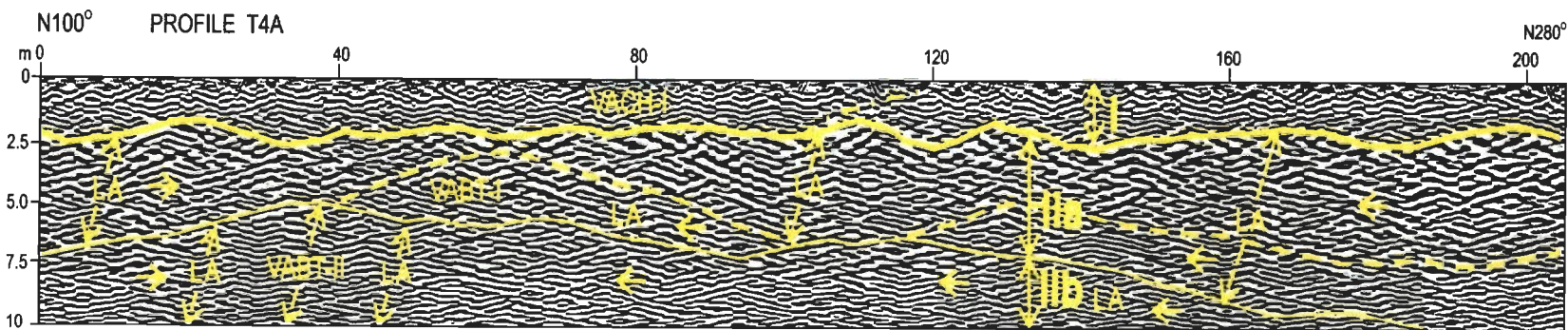


Fig. 5.10 Annotated GPR profile T-4A is from the middle part of Markanda Terminal Fan, showing sequences/subsequences and lithofacies



Two radar sequences I (2.5-3.5 m) and II (12.5-13.5 m) are identified in the profile. Both sequences are further subdivided into two subsequences i.e. Ia, Ib, IIa and IIb. Subsequence IIa show flat/low angle dipping in centre and lateral accretions on two sides with cross-beds showing flow directions diverging from this point in opposite directions, suggesting these are vertical accretions in channel of type-II (VACH-II). Subsequence IIa is marked by a bar with converging lateral accretions on the two sides and cross-beds showing flow directions towards the centre of the bar and the central portion exhibiting distinct horizontal/low angle dipping sands (VABT-II).

Subsequence Ib shows small scale cross-beds like ripple-drift cross-lamination of type A (Allen and Jopling, 1968), indicating vertical accretion in channel (VACH-I). The uppermost subsequence Ia is laterally extensive mudfacies (MF-I).

Two types of deposition i.e. by a large river in lower portion (sequence II) by lateral accretions and by vertical accretion in channel by a small river in upper part (sequence I) can be understood by relation of the profile direction with the paleo-current directions of the large river inferred earlier i.e. N89°, oblique to the profile direction and profile direction being almost parallel to the slope of the fan (flow direction) in the upper part (sequence I).

#### Profile T-4C

Profile T4C was taken for the Markanda Fault and inferred structure is discussed later. This GPR profile was taken near the Chajjupur Village (76°36' E 30 ° 02' N) in N83° to N267° direction across the Markanda fault striking in N336°, as inferred from DEM (Fig. 2.24b), 8 km north of Peowah Town and for a distance of about 180 m with data recorded up to 10 m depth (Fig. 5.9).

Three radar sequences I-III are identified. Sequence III is composed of a low height (~ 3 m) bar with lateral accretions on both sides as indicated by small scale cross-beds. However, the rest of the profile was probably marked by vertical accretion in channel-I. The sequence II is muddy nature, as indicated by uniformity of parallel reflections. Sequence I is marked by flat-bedded to slightly undulating and at places small scale crossed sands, indicating vertical accretion in channel of type I (VACH-I).

All the three radar sequences seem to have been deposited by small streams, as indicated by a low height bar in sequence III and small scale cross-beds in sequences I and III, whereas sequence II consisting of wide spread mud facies, probably deposited in a floodplain. Deposition of three thin sequences (<3m thick) close to the Markanda Fault suggests that they are probably deposited by repeated activity of the Markanda Fault by the small Markanda River.

#### *5.7.2.2 Young Chautang Terminal Fan-I*

The Young Chautang Terminal Fan-I is formed by deposition made by the River Chautang flowing presently in the N20° to N200° direction (Fig. 5.2). This is an active fan and the deposition is still going in it. This terminal fan is result of activity of the Markanda fault. It has a length of 23 km and is spread over a 183 km<sup>2</sup> area with a slope of 0.08%. The OSL date for the oldest soils on the fan is 1.5 Ka.

For facies analysis of the YgChTFn-I three GPR profile T7, T8 and T9 were taken obliquely to the flow direction of the Chautang River from the upper, middle and bottom parts of the terminal fan, respectively.

#### Profile T-7

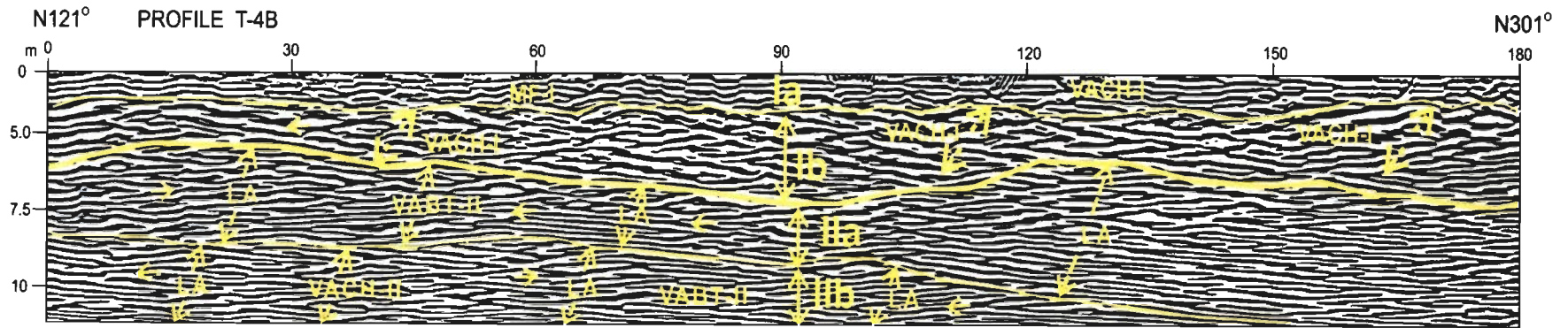


Fig. 5.11 Annotated GPR profile T-4B is from the distal part of Markanda Terminal Fan, showing sequences/subsequences and lithofacies.

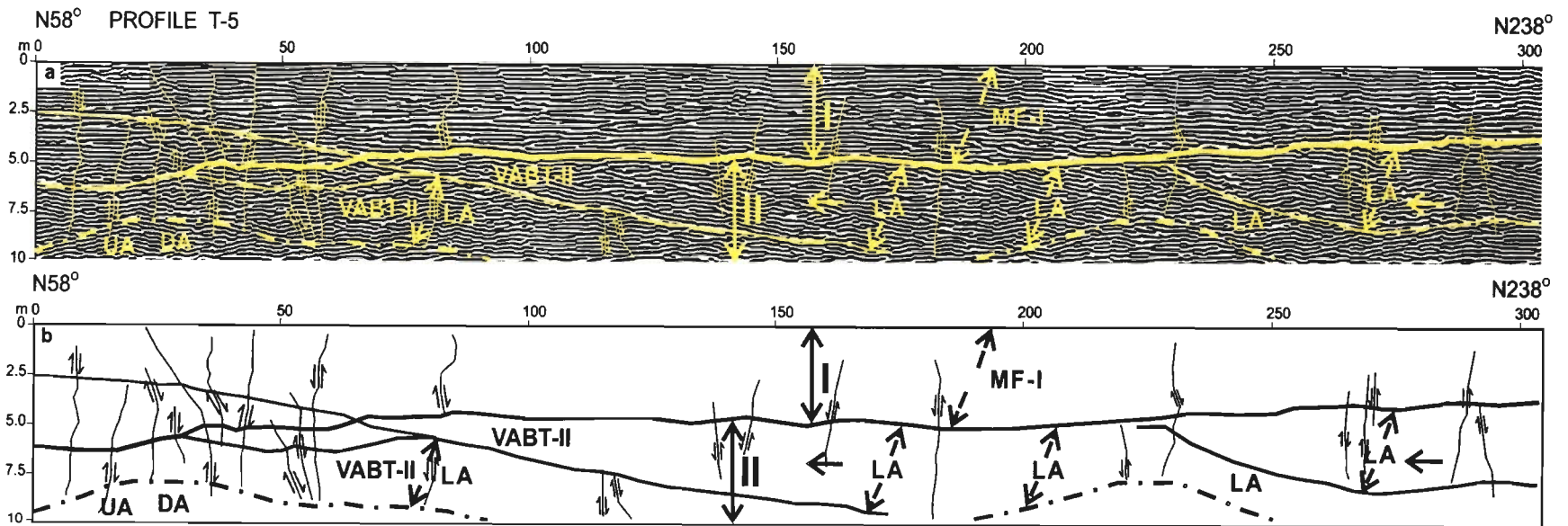


Fig. 5.12 (a) Annotated GPR profile T-5 across the Rohtak fault, showing sequences/subsequences, lithofacies and faults. (b) Outline diagram showing different features of the GPR profile T-5.

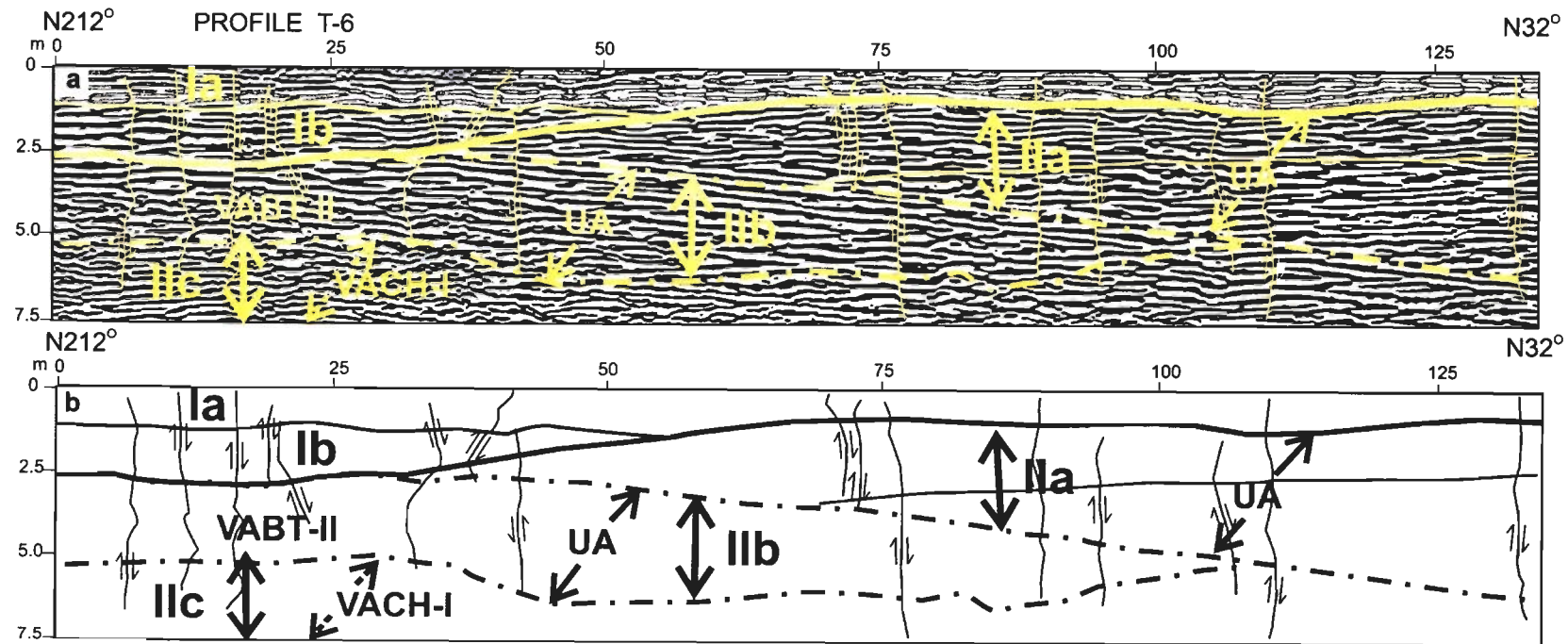


Fig. 5.13 (a) Annotated GPR profile T-6 across the Hissar fault, showing sequences/subsequences, lithofacies and faults. (b) Outline diagram showing different features of the GPR profile T-6.

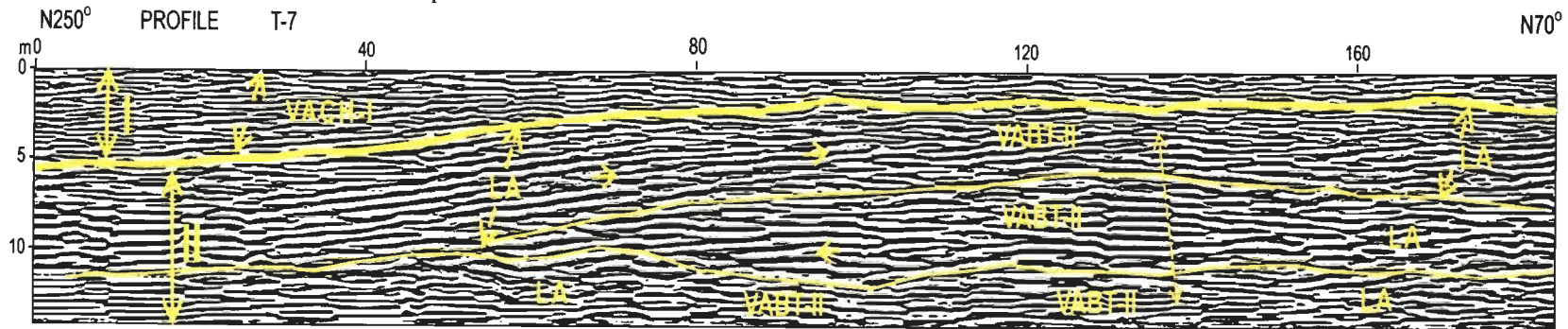


Fig. 5.14 Annotated GPR profile T-7 is from the distal part of Young Chautang Terminal Fan-I, showing sequences/subsequences and lithofacies.



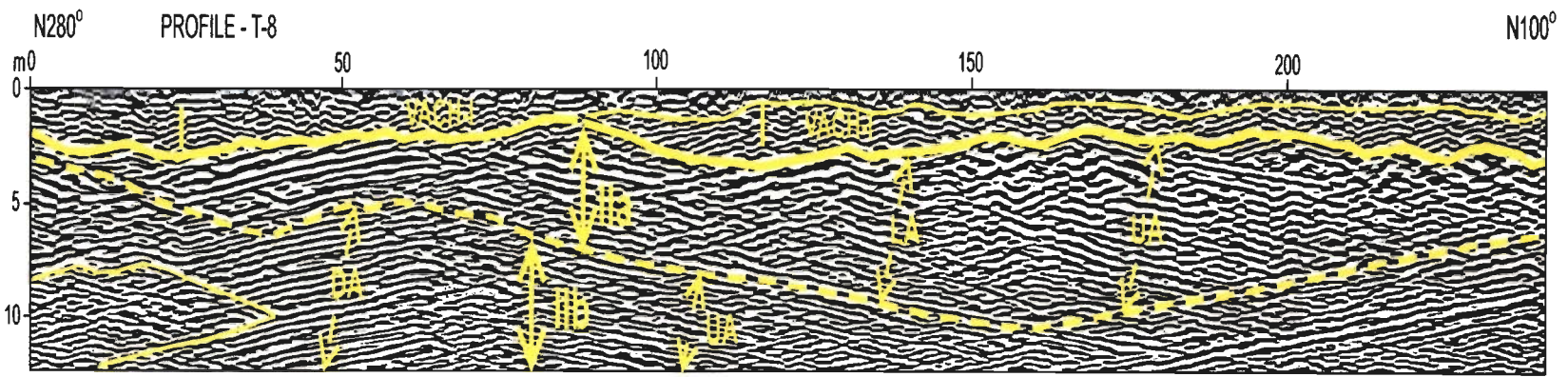


Fig. 5.15 Annotated GPR profile T-8 is from the middle part of Young Chautang Terminal Fan-I, showing sequences/subsequences and lithofacies.

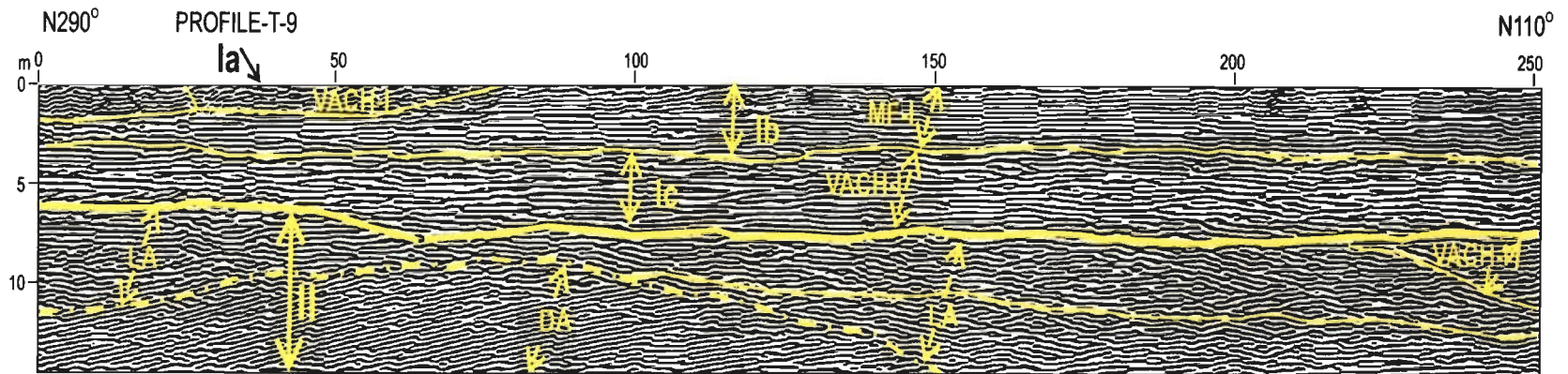


Fig. 5.16 Annotated GPR profile T-9 is from the proximal part of Young Chautang Terminal Fan-I, showing sequences/subsequences and lithofacies.

This GPR profile was taken near Nilokheri Village ( $76^{\circ} 58' E$ ,  $29^{\circ} 53' N$ ) of Kurukshetra District from  $N250^{\circ}$  to  $N70^{\circ}$  direction, at  $50^{\circ}$  to the present flow direction of the Chautang River. 170 m long profile was taken and data were collected up to a depth of 14 m (Fig. 5.14). In this profile two radar sequences I (2-6 m) and II (8-12m) are discerned.

Radar Sequence II with a thickness of 8-12 m was deposited by large bars, which grew by lateral accretions on the sides and in the central part of bar by vertical accretion on the bar top of type II (VABT-II). It took place in two distinct steps. Sequence I with a thickness of 2-6 m shows the sediment deposition by lateral accretion and vertical accretion in channel (VACH-I).

#### Profile T-8

The profile T-8 was taken near Sanbhli village ( $76^{\circ} 50' E$ ,  $29^{\circ} 49' N$ ), 14 km south of the Kurukshetra city and the profile was taken in  $N280^{\circ}$  to  $N100^{\circ}$  direction. The length of the section is 240 m and the data were collected up to 14 m depth (Fig. 5.15).

The radar sequence II which is from 11-12 m is subdivided into IIa (<4 m) and IIb (7-8 m). Both subsequences are marked by lateral accretions on sides of bars and vertical accretions on bar top of type II (VABT-II). The VABT-II is distinctly low angle sloping one.

Sequence I (2-3 m) consists of sigmoidal beds with low angle cross beds, indicating deposition by vertical accretion in a small channel.

#### Profile T-9

This GPR profile was taken from the Rasiana Village ( $76^{\circ} 40' E$ ,  $29^{\circ} 47' N$ ) 12 km northwest of Karnal from the distal part of the Young Chautang Terminal Fan-I. The profile was taken in  $N290^{\circ}$  –  $N110^{\circ}$  direction. The length

of this section is 252 m and data were collected up to a depth of 14 m (Fig. 5.16).

The two radar sequences I (6-8 m) and II (6-8 m) are observed. The lower sequence II was initiated by downstream accretion on a distinct slip face of large bar (> 5 m high). Later the bar stopped migration and lateral accretion of this took place on two sides. In the last phase vertical accretion of sandy deposit took place in a small channel on the SEE end of the profile. The upper sequence I is subdivided into three subsequences Ia, Ib and Ic. Subsequence Ic was deposited by vertical accretion in a small channel, followed by vertical accretion in wide floodplain (Subsequence Ib). The subsequence Ia represents deposition in small channel along the WSW end of the profile.

In three GPR profile T-7, T-8 and T-9 we find that lower sequences probably present deposition from a large river with a depth >6-12 m and the upper sequences represent the Chautang River (much smaller in size) fan deposit, formed at a later stage.

#### *5.7.2.3 Old Yamuna Terminal Fan*

##### Profile T-10

GPR profile T-10 was taken in direction N330° to N150°, near Narwana City on the Narwana-Kaithal road. The length of the profile is 270 m and data were collected up to a depth of 12 m (Fig. 5.5)

Two radar sequences I and II were identified in the GPR profile. Sequence II with a thickness of 10-11 m is marked by a large braid bar of similar height showing lateral accretions on both sides. Sequence I consists of sandy material and is marked by horizontal/slightly undulating stratification or even lateral accretion.

Sequence II contains a large braid bar, suggesting its deposition from a large river with a depth of >11 m. The presence of lateral accretions in the GPR profile striking N330°-N150° supports the inferred paleoflow direction of N89° for the large river. Also, later a much smaller stream led to deposition of sequence I, as a part of the Old Yamuna Terminal Fan.

### **5.7.3 Plains**

#### *5.7.3.1 Old Yamuna Plain-II*

##### Profile T-1

Profile T-1 was taken near the Rasulpur village, 3 km southwest of Bilaspur city (76° 20' E 29° 35' N). The length of the GPR profile is 180 m and it lies in the N21°- N201° direction across the Ambala Fault-I and the data were collected to a depth of 11 m (Fig. 5.4).

In the T-1 profile two radar sequences are identified: I and II. Sequence -I has a thickness of ~2 m and is characterized by a low angle parallel to low angle dipping sands (VACH-I) over the whole length of profile, suggesting a small stream with large width .

The radar sequence II with a thickness of ~9 m show a large bar (7 m height) with lateral accretions both sides and nearly flat bedding in the central part (VABT-II) in the first phase and in the later phase, only lateral accretions are observed.

Sequence II was deposited by a large river with a depth of >7 m and Sequence I with a thickness <2 m was deposited by a wide braided stream coming out of the Siwalik Hills, as observed presently.



### 5.7.3.2 Fluvial Plain

The central part of the study area is a fluvial plain marked by a number of paleochannels which can be well visualized in the DTM of the area (Fig. 2.26). The DTM indicates that the direction of paleochannels varies from N76° to N89°. Also, the Rohtak Fault disappears completely near village Khanpur (75° 50' E, 30° 10' N), 7 km north of Hansi city.

#### Profile T-11

The profile was taken in N58°-N238° direction 2km from Hansi in the Alipur village, nearly parallel to the paleoflow direction of paleochannels. The length of the GPR profile was 120 m and data were collected up to a depth of 17 m (Fig. 5.8).

In this GPR profile, three radar sequences are identified: I-III. The sequence III is about 11 m thick and is mainly consisting of upstream accretions deposits of a bar of similar height. The sequence II is composed of lateral accretions deposits with heights of bars up to 4m. The sequence I is horizontal or low angle dipping strata with trough/planar cross-beds and showing varied paleoflow directions, as indicated by small scale cross-beds and is marked by distinct changes in facies over short distances. Trough cross-bedding is present close to the NE end of the profile with troughs of ~3 m width and ~0.5 m depth.

The sequence III was deposited by a large river with a depth of >11 m, However, later main river shifts away and a small stream takes over which follows lows between the bars of large river and deposition by lateral accretion (sequence II) is a major process. The phase III is probably marked by

reworking of the alluvial sands and their redeposition with varied flow direction.

#### 5.7.3.3 Aeolian Plain

The Aeolian Plain is a flat area dotted with low height (2-3 m) Aeolian dunes at places.

#### Profile T-6

Profile T-6 was carried out near Balsamand village ( $76^{\circ} 02' E$   $29^{\circ} 20' N$ ), close to an abandoned channel (Fig. 5.13). The length of the profile is 130 m and the data were collected up to a depth of 7.5 m. The direction of the profile is from  $N212^{\circ}$  to  $N32^{\circ}$ . In this profile, two sequences I (1.25- 2.5 m) and II (5-6.25 m) are identified. Sequence II is further subdivided into three subsequences IIa, IIb and IIc. Sequence II first starts with a low height (~ 2.5 m) bar (IIc), which later grows by upstream accretion in two steps to a height of about 6.25 m (IIb and IIa). Sequence I is subdivided into two subsequences Ia and Ib. Subsequence Ib is discontinuous and confined to a small channel (max, depth 1.2 m), Subsequence Ia is sheet sand deposit of 0.6-1.2 m thickness without any mud.

Sequence II was deposited by a large river with a depth of  $>6.25$  m. Subsequence Ib was deposited by a small stream following lows created by bars in the large river. Subsequence Ia with uniform thickness of 2.5 m of dry sand represents the aeolian sheet deposit.

### **5.8. HARYANA REGION -FAULTS**

Eleven faults have been identified in using remote sensing and GIS techniques and out of these two faults i.e. the Ghaggar and Yamuna Faults are transverse faults whereas all others are longitudinal parallel to the HFT

Table (2.4). The GPR studies of 6 major transverse faults have been carried out and discussed below.

### **5.8.1 Ambala Faults I and II**

Ambala faults I and II run parallel to each other in the northernmost part of the study area in the piedmont zone. The DEM of these faults suggests that the 'older' Piedmont in the north is being uplifted along Ambala-I Fault and the 'younger' piedmont is being deposited in the south and further 'younger' Piedmont is also being uplifted along the Ambala-II Fault and a few fans are being deposited further south. Probably all this happened over a short period and our limited number of dates are not able to bring out these differences. Five GPR profile were carried out in different places over these fault for their confirmation: three for the Ambala Fault-I and two for the Ambala-II Fault. The GPR profile taken just below the Young Piedmont (YgPt) for the Ambala Fault-I (Profile T-1) and the profile T-2 done northeast of the Ambala city for the Ambala Fault-II are discussed here (Figs. 5.4, 5.6).

#### Profile T-1

In this profile across Ambala Fault-I we can see a number of fault among which 9 are the major faults. Faults are concentrated largely in two ends of the profile. Throw of the maximum number of the fault is towards south with a few showing throw in opposite direction and faults are mainly nearly vertical (Fig. 5.4).

#### Profile T-2

In T-2 GPR profile across Ambala Fault-II, eleven faults are deciphered, and most of which are concentrated in the SWS corner. Six faults are mainly confined to sequence I and three to subsequence IIC. Most of the

faults show downthrows sides towards the southwest direction except a few, which show downthrow in the opposite direction. Most the faults are nearly vertical and three faults are inclined 10-25° (Fig. 5.6).

### **5.8.2 Patiala Fault**

The Patiala fault runs in the N156°-N336° direction and passes just north of Patiala city, causing offset of the Ghaggar River and convergence of smaller streams coming out of the piedmont zone. This fault continues east of the Yamuna River into Uttar Pradesh and give rise to Katha terminal fan formed by the Katha River. Two GPR profiles were carried out across this fault, one near the Patiala city and other near Shahabad city. The section near the Patiala city is interpreted and discussed here (Fig. 5.7).

#### Traverse T-3

In the GPR profile T-3, six faults are identified: three major faults exhibit large displacements, while three faults cause minor displacement. Two of the faults extend up to a depth of 6 m, while others extend only up to a depth of 2.5-5 m. The throw of the 4 faults is towards the south and two showing northward throw.

As described earlier, mainly two GPR sequences I and II are identified. Sequence II is further subdivided into IIa and IIb. Subsequence IIa thickens to SWS between 10 m and 50 m marks, showing effect of activity of faults contemporaneous with sedimentation.

### **5.8.3 Markanda Fault**

The Markanda Fault passes through Kurukshetra town and is responsible for the development of the Markanda Terminal Fan and Young Chautang Terminal Fan-I. Field observations suggest that the fault is active

and nascent one, with distinct surface displacements of up to 12 m at places, which die out gradually laterally (Fig. 5.9). A number of such segments are present within the traceable fault length of 136 km. One GPR profiles was taken across the fault (Fig. 5.2).

#### Profile T-4C

As mentioned earlier, in this profile, three main radar sequences are identified I (2-3 m), II (3.5-4.5 m) and III (3.5-4.5 m) (Fig 5.9). Radar sequence II is most affected by faults followed by sequence I. In sequence II, 7 faults exhibit large displacements and the rest of the show small displacements. Most of the faults show downthrow in southwesterly direction except a few, which show throw in opposite direction.

#### **5.8.4 Rohtak Fault**

The Rohtak fault extends in N154°-N341° direction in the central part of the study area. This fault approximately defines the boundary between the Young Chautang Terminal Fan-I and II. Soils of the southern block are much more saline and waterlogged (Fig. 2.9) as compared to those of the northern block. This fault shows throw of the 11 m and is traceable up to a distance of 122 km.

#### Profile T-5

Only one GPR profile T-5 was taken across this fault near the village Gopalpur (76° 58' E 29°48' N), 5 km northwest of Rohtak city. The profile was taken in N58°-N238° direction (Fig. 5.12) across the fault and the length of the profile was 305 m and data were collected to a depth of 10 m. Two radar sequences are deciphered from the profile. Twenty-five faults are identified from the profile. Most of the small faults are confined to the sequence-II and

only one is observed in the sequence-I and six faults extend from sequence I to II. Most of the faults are normal in nature and show throw towards south, except a few, which show throw towards north.

#### **5.8.5 Hissar Fault**

The Hissar fault is in the southernmost part of the study area and acts as a boundary between the Haryana plains and the Aravalli Hills in the southeastern region near Gurgaon for a distance of 67 km, and displaces alluvial/aeolian sediments in northwestern region (e.g. near Hissar city) (Fig. 2.23) over a distance of 90 km. This is the only fault having downthrow side towards northeast in the study area and all the other faults have throw towards southwest. One GPR section was investigated across this fault for the confirmation (Fig. 5.13).

#### Profile T-6

In this profile, 16 faults are identified out of which 7 faults extend from the surface to the base of the profile i.e. from sequence I to II. Nine other faults either start from the surface or the center of the sequence but do not continue down to the bottom of profile. Most of the faults have their downthrow in the northern side direction except a few that have downthrow towards the southern side (Fig. 5.13).

Near the 30 m mark in the profile, Subsequence IIa starts, subsequence IIb thickens by one meter and subsequence IIc goes down by about 1 m due to faulting in this region towards the NE end.

#### **5.9 GANGA-YAMUNA INTERFLUVE- SET-UP**

Apart from the GPR studies in the Haryana plains, an attempt is made to carry similar investigations in the adjoining Ganga-Yamuna Interfluve. The

Ganga-Yamuna Interfluvium constituting the western most part of the Gangetic plain was systematically studied using digital image processing of satellite images, field and laboratory studies including micromorphology and luminescence dating of soils led to identification of thirty-three soil-geomorphic units. These soil-geomorphic units were classified into five members of morphostratigraphic sequence: QGMS-I (<1.7 ka), QGMS-II (1.7-3.6 ka), QGMS-III (3.6-6.5ka), QGMS-IV (6.5-9.5 ka) and QGMS-V (>9.5 ka). Major geomorphic features identified from the area were (i) plains associated with rivers (Young and Old plains of Yamuna and Ganga Rivers), (ii) piedmont plain (Young and Old Piedmonts in the northern regions along the Himalayan foothills), (iii) terminal fans (East-, West- and Middle Muzaffarnagar Fans, Khurja-Aligarh Fan, Iglas-Raya Fan, Bhagpat Fan, Karhal-Bidhuna fan, Muhammadabad-Bhilaur Fan and Saurikh- Rasulabad Fan); (iv) Paleochannels (Yamuna and Ganga Paleochannels within the Ganga-Yamuna Plain); and (v) aeolian ridges (exposed in patches near Aligarh, west of Muzaffarnagar) and over paleochannels (Fig. 5.17). Faults in this area were first identified and mapped by Khan et al., (1996) and Kumar et al. (1996), mainly on the basis of remote sensing and photo analysis. Later Parkash et al., (2001) classified the faults in the Indoganic plain as longitudinal faults.

Previously Bhosle et al. (2006) first used GPR technique on a limited scale to confirm the Muzaffarnagar fault and Solani Fault in the Ganga- those running along the major bounding rivers- Ganga and Yamuna while those fault which are perpendicular to the longitudinal faults as transverse fault. On the basis of geomorphic expressions in the present area, Bhosle et al. (2006)

identified seventeen faults in the Yamuna Interfluvial region. We have been made to

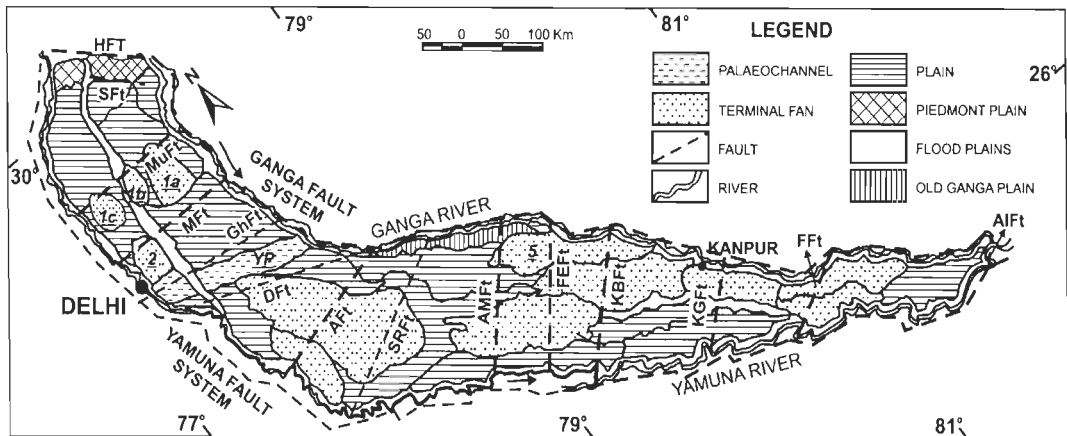


Fig. 5.17. Structural map of the Ganga, Yamuna & Doab region showing important fault locations and their associated Terminal Fans, Piedmont Plain, Flood Plains, Paleochannels and Old and Young River Plains of Ganga and Yamuna Rivers. After Bhosle et al., (2008).

confirm and know their subsurface nature 5 transverse faults and analyze the lithofacies of three terminal fans and Ganga paleochannels, using GPR in the present area.

In the present study, we have re-scanned the MSS images and Wifs data of March, 2000 (Figs. 5.18 a & b) of the Interfluvial region and carried out GPR survey in 17 sites (Fig. 5.19c) and also a new fault i.e. Jhaberera Fault of limited extent and a new terminal fan called Iqbalpur Terminal Fan are identified. This terminal fan overlies one of the Ganga Paleochannels.

## 5.10. GANGA-YAMUNA INTREFLUVE – GPR LITHOFACIES

### 5.10.1 Paleochannels

Large paleochannels of the Ganga and Yamuna Rivers in the Ganga-Yamuna Plain with widths of 2.5-15 km were described by Kumar et al., (1996) and Bhosle et al., (2008). The Ganga paleochannels have been studied by two GPR profiles at Barla and Deoband. Other two profiles done



over Iqbalpur Terminal Fan overlying the Ganga Paleochannel also show GPR facies of the paleochannel, which are discussed later.

#### Barla Profile D-17

The Barla profile was carried in for a distance of about 95 m in N5°-N185° near Barla village (77° 35' E, 29° 37' N). Data were collected up to a depth of about 9 m (Fig. 5.31).

GPR profile consists of two sequences I (2-3 m) and II (6-9 m). Sequence II started with a large braid bar with a height of >6 m. Later a thinner sand bed was deposited by lateral accretions along sides of small bars (< 2 m high). Sequence I is marked by vertical accretion with distinct lateral accretions at places.

The sequence II was deposited by a large river (Ganga River) with a depth of >9 m). As the channel was being abandoned, first smaller channels flowing along topographic lows created by the presence of bars took over. In the last phase a wide shallow stream was flowing in area deposited sequence-I.

#### Deoband Profile D-4

Profile D-4 was carried out near Deoband town (77° 39' E, 29° 32' N) for a length of 200 m up to a depth of 16 m in the direction N88° -N268° (Fig 5.21).

The profile consists of two sequences I (2-3 m) and II (12-13 m). Sequence II is further divided into three subsequence IIa, IIb and IIc. All these subsequence were deposited as lateral accretions on sides of braid bars, though bars in subsequence IIa are smaller in height than IIb and IIc.

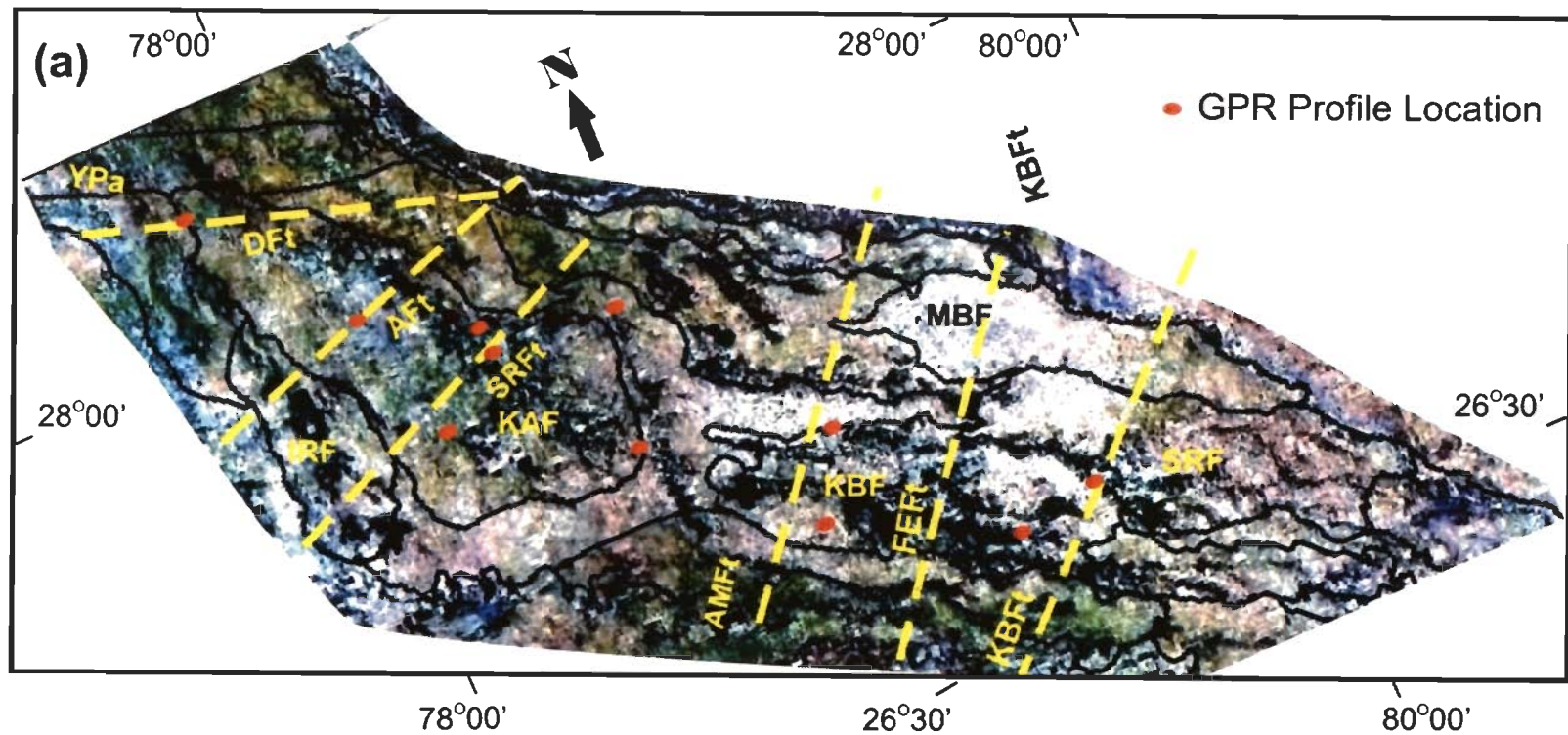


Fig. 5.18 (a) Shows soil geomorphic units, faults and GPR location superimposed on IRS 1D False colour Composite of Wifs data of March, 2000. Abbreviations for different faults and soil-geomorphic units given in Fig. 18c.

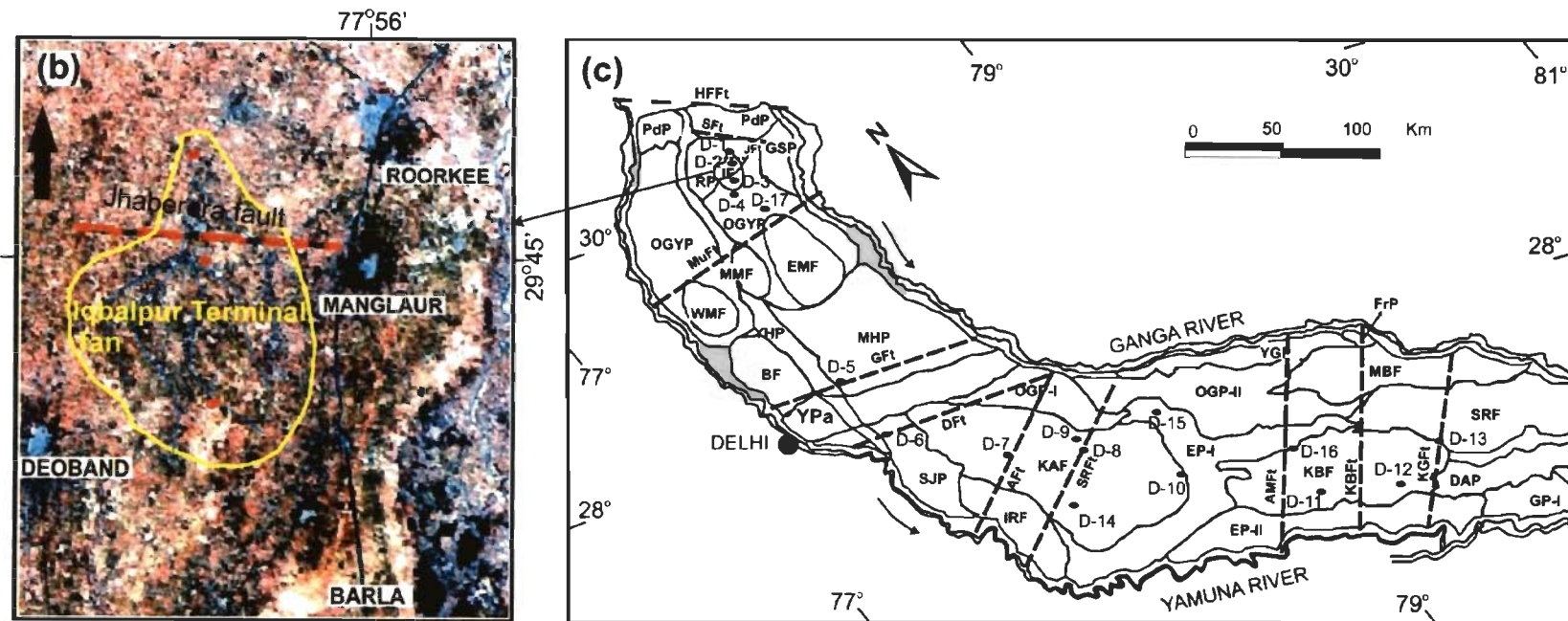


Fig. 5.18 b) Show the Landsat MSS image (band combination 1-4-2) of the Iqbalpur Terminal Fan showing GPR points location and the Jhaberera Fault c) Ganga Yamuna interfluvial marked with soil geomorphic units faults and GPR locations.

Abbreviation used for Faults- HFFt-Himalayan Frontal fault, Sft Solani Fault MuFt- Muffaranagar Fault, Gft- Ghaziabad Fault, DFt Delhi Fault, KAF- Aligarh Fault, SRft- Sikandra Rao Fault, AMFt- Aliganj-Mianpuri Fault, KBFt- Kannauj-Bidhuna Fault, Kanpur-Ghatampur Fault. Abbreviation used for the soil geomorphic units- PdP- Piedmont plain, RP- Roorkee Plain, GSP- Ganga-Solani Plain, OGY, Old Ganga Yamuna plain, EMF- East Mujaffarnagar fan, YHP- Young Hindon Plain, MHP-Meerut Happur Plain, Bf- Baghpat fan, YPa- Yamuna Paleochannel, SJP, Sikandra Rao-Jewar Plain, KAF-Khurja Aligarh fan, IRF-Iglas-Raya fan, OGP-I&II- Old Ganga Plain-I & II, EP-I & II- Etawah Plain -I & II, KBF- Karhal-Bidhuna fan, KF-Kanpur fan, SRF-Sirathu fan.

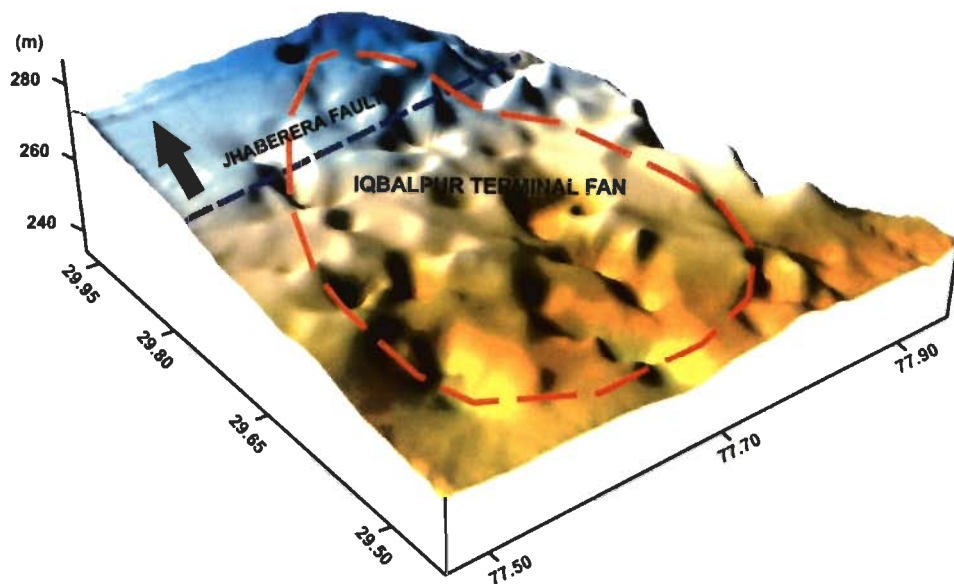


Fig. 5.19. DEM of the Iqbalpur Terminal fan and the Jhaberera fault region.

Sequence I represents vertical accretion in a shallow (< 3m depth), wide stream.

Very similar to Barla profile, lower sequence II was deposited by a large stream (Ganga River) with a minimum depth of 13 m (Subsequences IIa, IIb and IIc). Later probably a shallower stream took over and the upper sequence I seem to have been deposited by a still smaller wide stream.

### 5.10.2 Terminal Fans

Most of terminal fans recognized from the Ganga-Yamuna Interfluvium can be categorized on the basis of nature of streams/drainage on the terminal fan into two types viz. fans formed by braided streams and fans deposited by streams with distributary pattern, Iqbalpur Terminal Fan seems to have been deposited by a braided stream. However, Khurja-Aligarh, Karhal-Bidhuna and Muhammadabad-Bhilaur Terminal Fans are overlain by streams showing distributary pattern (Fig. 6 of Bhosle et al., 2008).

#### 5.10.2.1 Iqbalpur Terminal Fan

This terminal fan is newly recognized in this region and is located on the Old Ganga-Yamuna Plain and is formed by a stream originating in the piedmont zone. This terminal fan formed due to the activity of the Jhaberera Fault.

It covers an area of 76 km<sup>2</sup> and has a radius of ~16 km (Fig 5.19). The Jhaberera fault passes from the Jhaberera village and can be traced up to Manglaur town. A soil sample from this terminal fan gives an OSL age of 1.8 Ka. Though it has only 15 km of surface expression, it may be an extension of the Patiala Fault, which forms the Katha Terminal fan in nearby Saharanpur region.

Three GPR profiles were carried out on this terminal fan: one near the top at Iqbalpur village (D-1), one from the middle at Jhaberera village (D-2) and one near the base of the fan near Zabardastpur village (D-3). Here only D-2 and D3 profile are described.

#### Profile D-2

Profile D2 was taken at the Jhaberera village (78° 55' E, 28° 37' N), 11 km southwest of Roorkee city. The direction of the profile is N355°-N175°. The length of the profile is 160 m and the data were taken up to a depth of 14 m (Fig. 5.30b). Two radar sequences I and II are identified in this profile. Sequence II with thickness of ~10 m is further subdivided into three subsequences IIa, IIb and IIc. Subsequence IIb and IIc were deposited by lateral accretions on sides of braid bars and vertical accretion on bar top of type II (VABT-II). Subsequence IIa seems to be a result of vertical accretion in channel (VACH-I). Sequence I is also subdivided into Ia and Ib. Subsequence Ib is a result of lateral accretions on sides of a low height (<3 m) braid bar in

wide stream and Ia represents vertical accretion in a low width small stream along northeastern end of the profile.

Sequence II was deposited by a large river, of whose paleo-channel lies below terminal fan. Sequence I is part of a terminal fan, deposited by a small stream.

### Profile D-3

Profile D3 was carried out in direction N225-N45 for a length of 300m and up to a depth of 17 m near village Zabardastpur (Fig. 5.30c).

Profile D3 is composed of two sequences I (1.0-3.25 m) and II (11.75-14 m). Sequence II is further subdivided into three sequences: IIa (<3.5 m), IIb (4.0-7.5 m) and IIc (>6.0 m). Subsequence IIc consists of nearly flat beds or unidirectional cross-bedded units, indicating vertical accretion in channel. Subsequence IIb is marked bilateral accretion on sides of low height braid bars and vertical accretion on low lying areas between bars (VACH-II). Subsequence IIc represents vertical accretion in a small channel. Sequence I is marked by vertical accretion of mud in floodplain (MF-I), followed by vertical accretion of sandy material in small width streams, entrenched into the lower mudfacies.

The lower sequence II was deposited by a large river with depth of >14 m and upper sequence I was deposited as a part of Iqbalpur Terminal Fan.

#### *5.10.2.2 Khurja-Aligarh Terminal Fan (KAF)*

Khurja-Aligarh Terminal Fan was first described by the Bhosle et al., (2006). The length of this terminal fan is 149 km and it covers an area of 1980 km<sup>2</sup>. It shows a slope of 16.3° in SEE direction. Five GPR profiles were taken on this terminal fan, two of there were for the confirmation of the Aligarh and



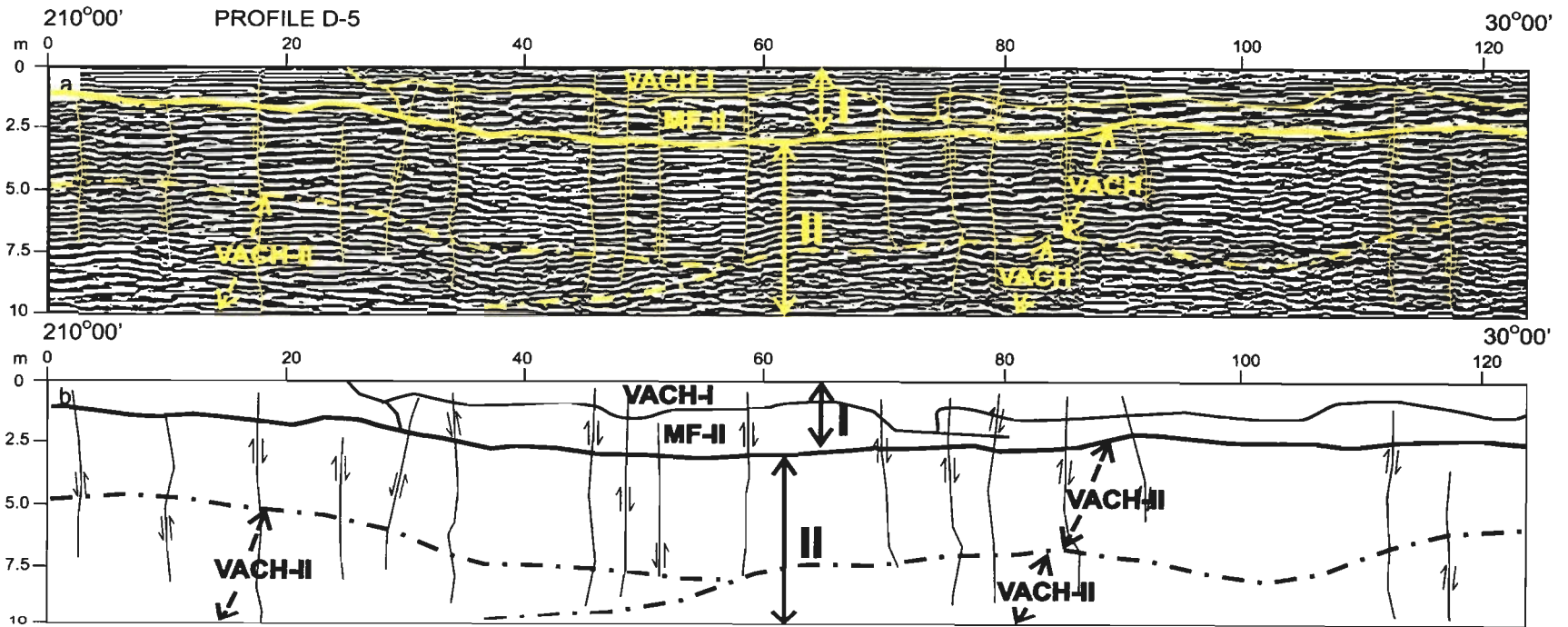


Fig. 5.20 (a) Annotated GPR profile D-5 across the Gaziabad Fault, showing sequences/subsequences, lithofacies and faults. (b) Outline diagram showing different features of the GPR profile D-5.

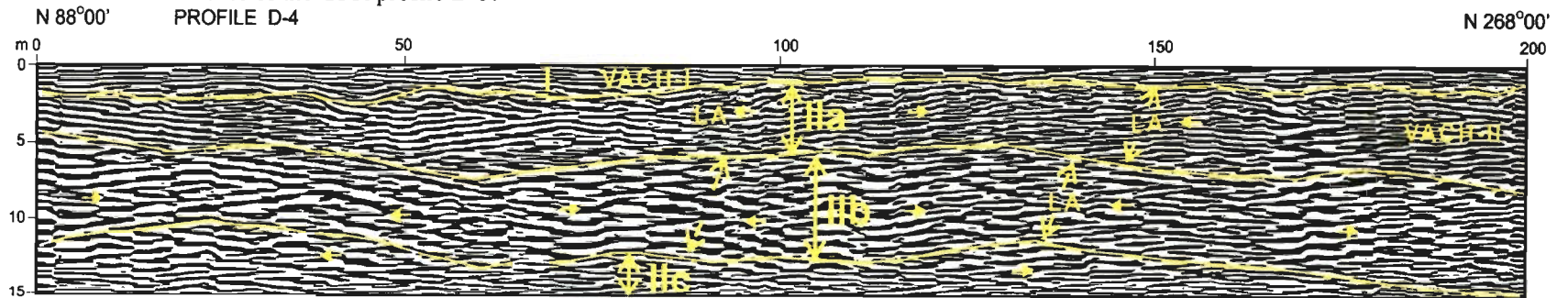


Fig. 5.21 Annotated GPR profile D-4 from Deoband area over a Ganga River paleochannel, showing sequences/subsequence and lithofacies

Sikandra Rao Faults and three of the GPR profiles were taken to study the architecture of the KAF.

#### Profile D-7

GPR profile D-7 was taken near Aligarh city in Rustampur village ( $77^{\circ} 08' E$ ,  $28^{\circ} 00' N$ ) (Fig. 5.22). The length of the profile was 195 m in direction  $N290^{\circ}$ - $N110^{\circ}$  and the data were collected up to a depth of 9 m.

In profile D-7, three radar sequences are identified: I-III. Radar sequence-III is mainly a sandy bed formed by vertical accretion in a wide channel (VACH-I) with a depth of  $>6.25$  m. Accretion was by migration of small dunes/sand waves. Sequence II ( $<4.5$  m) was deposited in two overlapping channels by vertical accretion (VACH-I). Sequence I represents mainly mud deposited by vertical accretion in a wide floodplain (MF-I), except for the SEE end, where deposition was by lateral accretion in a small channel.

Sequence III was probably deposited by a moderate to large stream with a depth of  $>6.25$  m. Sequences II and I are the Khurja-Aligarh fan deposits formed by a small stream with depth of  $<4.5$  m.

#### Profile D-9

Profile D-9 was taken on Akarabad-Pilakhani road, 2 km from Akarabad ( $78^{\circ}17' E$ ,  $27^{\circ}47' N$ ) near Village Jirauli. Length of the GPR profile was 190 m (Fig. 5.25). Two radar sequences are identified: I (1.5-4.0 m) and II (13-14.5 m). Sequence II is further divided into 3 subsequences: IIa (1.75-7 m), IIb (2-6 m) and IIc ( $>9$  m). Subsequences IIa to IIc were deposited by lateral accretion along sides of braid bars and vertical accretions on bar top of type-II (VABT-II), The sequence I was initially deposited as floodplain deposit



(MF-I) and later small channels appeared, in which vertical accretion of sandy material took place.

Sequence II was initially deposited (IIc) by a large river with a depth of > 9 m. However, later thinner subsequences IIb-IIa were deposited by a moderate sized stream with a depth of <7 m. Sequence I was deposited by a small sized stream with a depth of <4m as a part of the Khurja-Aligarh fan.

#### Profile D-10

This Profile was carried out has been done near distal part of the edge of the Khurja-Aligarh Terminal Fan, near in village Nidhauri (78°35' E, 27°32' N), 3 km southwest of Etah city. The topography of this area shows it's a low lying area and much of the area is affected by the floods during the rainy season. The profile was carried out in direction N38°-N218° for a length of 85 m and data were collected up to a depth of 9 m. In this profile, two sequences I and II are identified on the basis of thickness of individual reflections (Fig. 5.33) Each of Sequences I and II is further subdivided into two subsequences Ia (2-2.5), Ib (2-2.75 m) and IIa (1.5-3.25 m), IIb (>2.25 m), respectively.

Subsequence IIb was deposited by lateral accretions away from a central area, where vertical accretion of type II (VACH-II) took place. In subsequence IIa mainly vertical accretion in channel of type I (VACH-I) took place. Though subsequence Ia (2.0-2.5 m) is marked by parallel reflection throughout the profile, field observations indicated active deposition of sand on the terminal fan (VACH-I) at the location of the profile. Deposition of subsequence Ib processes similar to those of Ia.

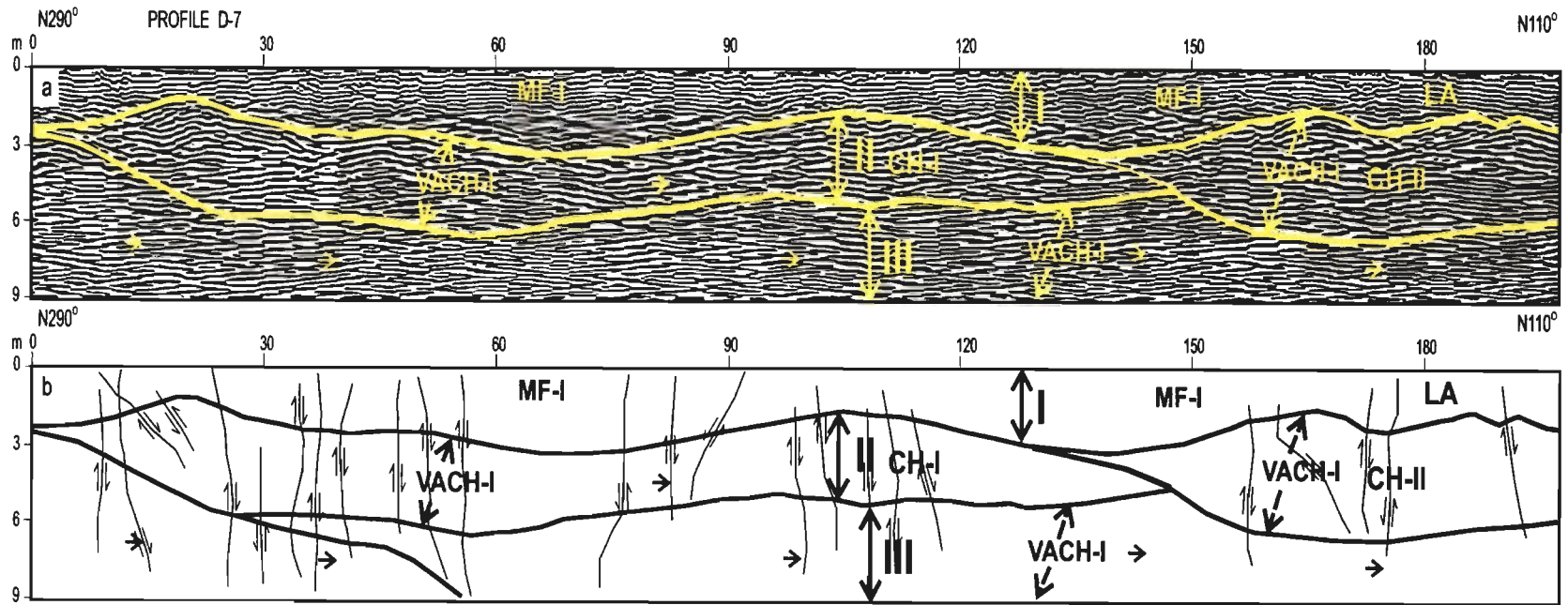


Fig. 5.22 (a) Annotated GPR profile D-7 across the Aligarh Fault, showing sequences/subsequences, lithofacies and faults. (b) Outline diagram showing different features of the GPR profile D-7.

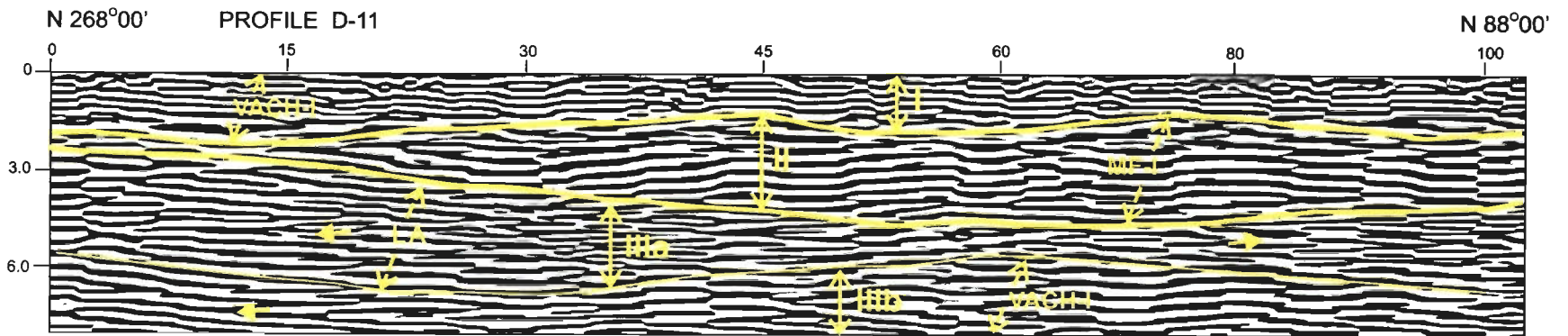


Fig. 5.23 Annotated GPR profile D-11 from the Karhal-Bidhuna Terminal Fan, showing sequences/subsequence and lithofacies

Sequences II was deposited by a moderate sized stream (depth of >5.5 m). Sequence I, a part of the terminal fan was deposited in two subsequences by a small stream in two phases by probably a small stream (depth < 3m).

#### Profile D-14

This profile was taken from Veernagar (15 km to Hathras and 3 km from Awa city) on the Etah-Agra road (78°12' E, 27°37' N). The direction of the profile is N38°-N258°, the length of the profile is 100 m and the data were collected to the depth of 9 m.

The GPR profile shows two radar sequences: I (3.0-4.0 m) and II (>6 m) (Fig. 5.34). Sequence II is subdivided into subsequences IIa (1.5-4.25 m) and IIb (>4.25 m). Subsequences IIa and IIb were deposited by vertical accretions in channel (VACH-I). Sequence I is characterized by the lateral accretions on two sides of a large braid bar. The sequence-I shows sandy deposition with thicker stratification as compared to sequence II. This is probably due to the presence of finer grained material in sequence I, as compared to sequence II.

Sequences II was deposited by a slowing down, moderate size stream with a depth of >6 m. Sequence I seems to be a part of the Khurja-Aligarh terminal fan, and deposited by a small stream with a depth of ~4 m.

#### Profile D-15.

This profile was carried in direction N290 ° -N110 ° for a distance 100m near village Kareempur (78°42' E, 27°27' N). Data were collected up to a depth of about 17 m. Three sequences were recognized: I (<2 m), II (4-8 m) and III (9-12 m). Sequence III starts with bar of height of about 5 m, which is marked by good downstream accretion deposits. Later it grow by upstream,

downstream and bar top accretion (VABT-I). Sequence II was initially deposited by lateral and vertical accretion in channel (VACH-I) followed by mudfacies deposition in a wide floodplain. Sequence I is a floodplain mudfacies deposit with a few small incised channels filled with vertical accretion deposits.

Sequence III represents large stream deposits with a depth of up to 12 m and sequence II and I are Aligarh-Khurja terminal fan deposited by a small stream.

#### *5.10.2.3 Karhal Bidhuna Terminal Fan*

Three GPR profiles have been carried out in this terminal fan.

##### Profile D-11

Profile D-11 was carried out Karhal-Mainpuri road, 2.4 km from Karhal village in N268°-N88° direction up to a depth of 9 m (Fig. 5.23). Profile is divided into three sequence: I (1.5-2.5 m), II (0.75-4.25 m) and III (>6.75 m). Sequence III starts with vertical accretion in a stream (IIIb) and later it develops a large braid bar of >6.75 m height by lateral accretion. Sequence II represents mud deposition in an abandoned stream (MF-II). Sequence I is sandy in nature and forms a channel-fill (VACH-I), as observed in field and represents vertical accretion in a wide stream.

Field observations indicate that mudfacies of sequence II & I is very extensive and indeed it is MF-I facies. Sequence I is channel filled with VACH-I deposit, Sequences I and II are terminal fan deposits and sequence III was deposited by moderate sized stream.

##### Profile D-12

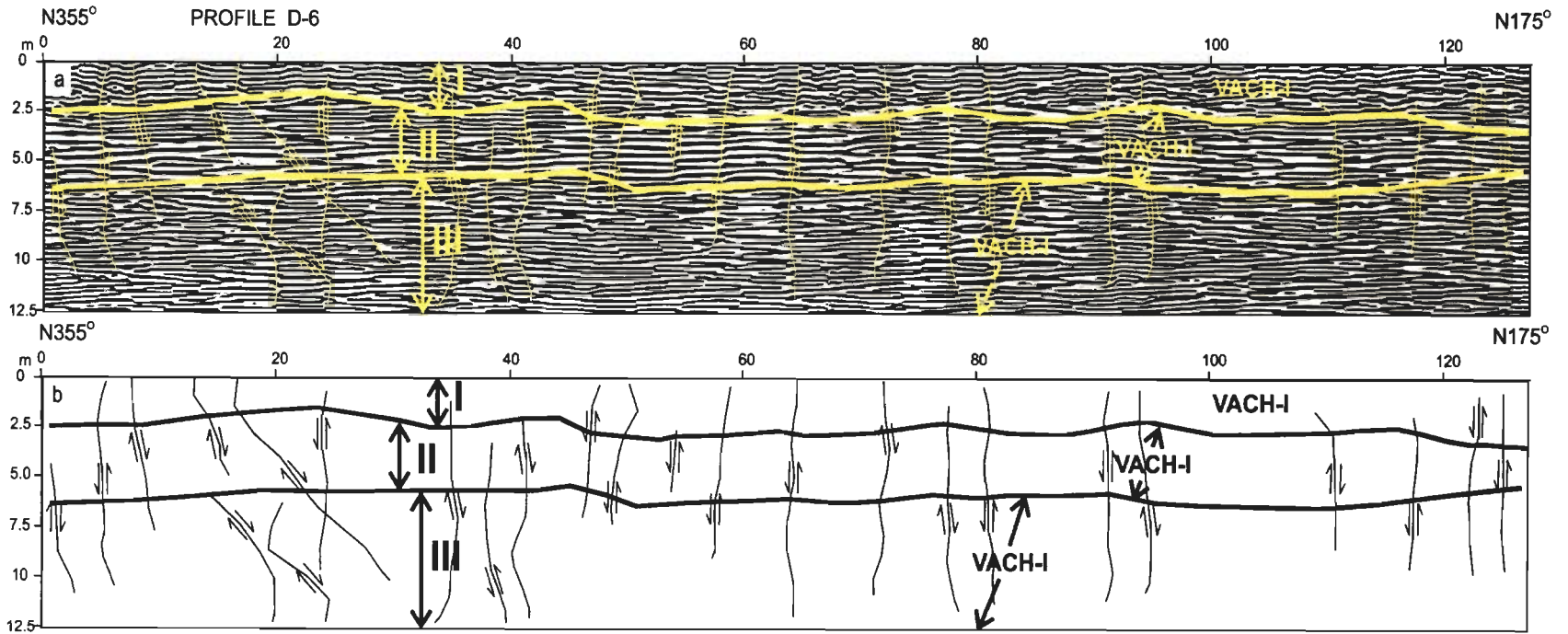


Fig. 5.24 (a) Annotated GPR profile D-6 across the Delhi Fault, showing sequences/subsequences, lithofacies and faults. (b) Outline diagram showing different features of the GPR profile D-6.

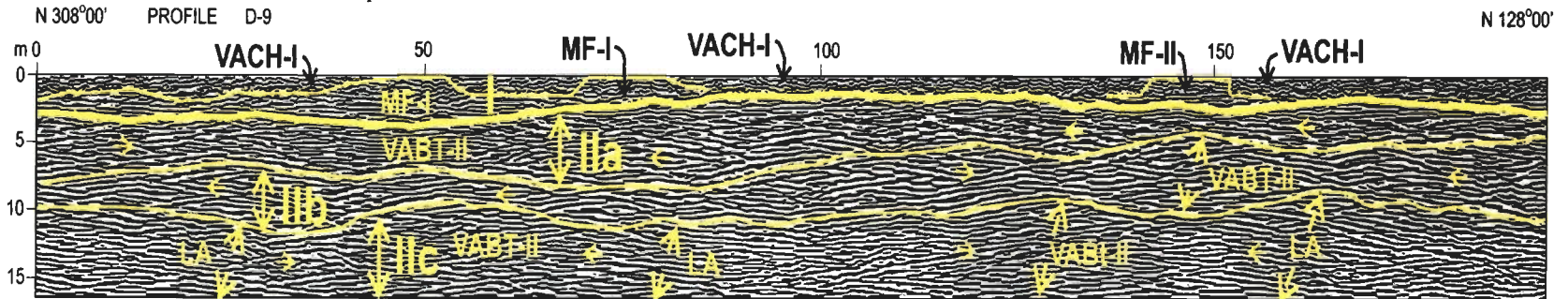


Fig. 5.25 Annotated GPR profile D-9 from the Akarabad area on the Aligarh-Khurja Terminal Fan, showing sequences/subsequence and lithofacies.



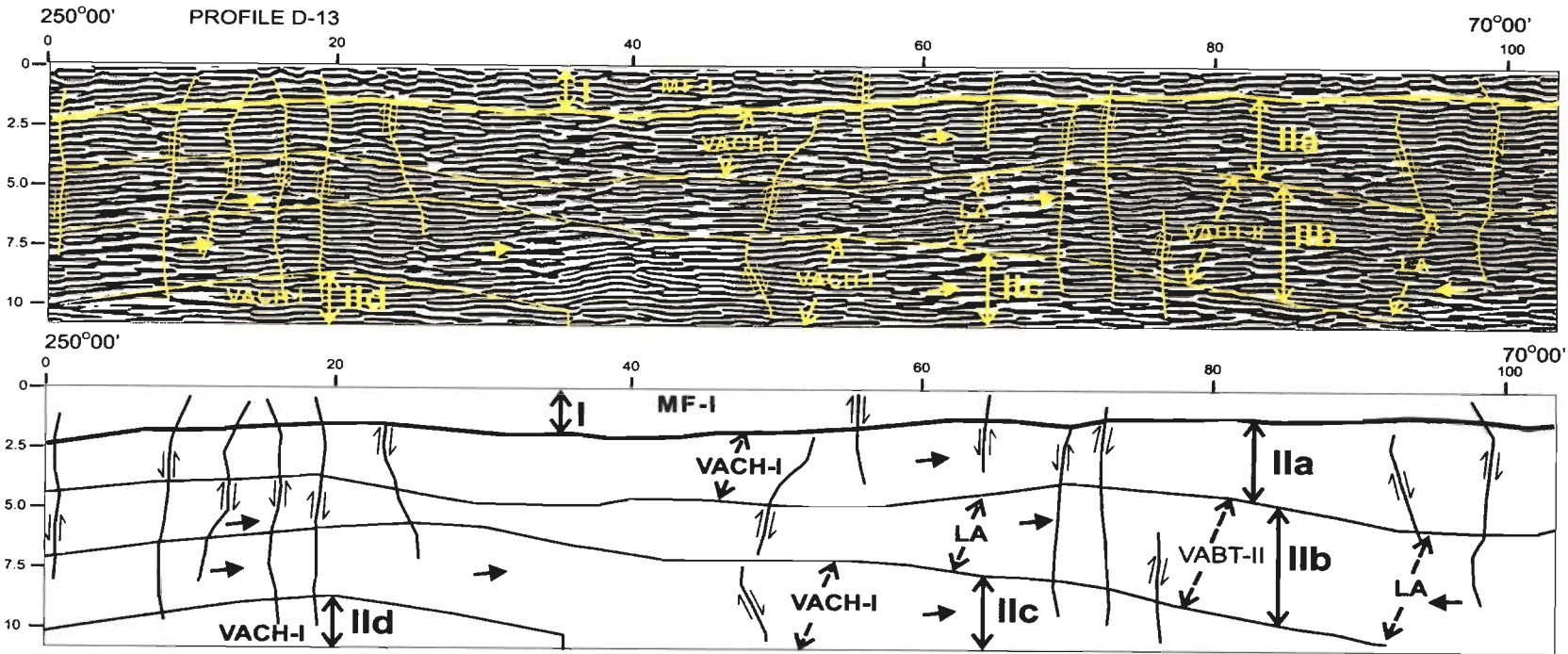


Fig. 5.26 (a) Annotated GPR profile D-13 across the Kanpur-Ghatampur Fault, showing sequences/subsequences, lithofacies and faults. (b) Outline diagram showing different features of the GPR profile D-13.

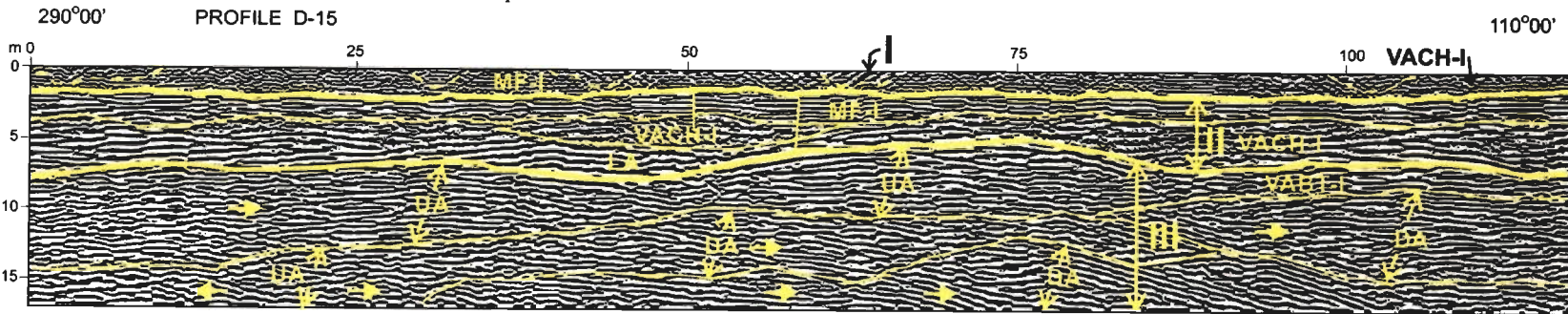


Fig. 5.27 Annotated GPR profile D-15 is from the central part of Aligarh-Khurja Terminal Fan, showing sequences/subsequence and lithofacies.

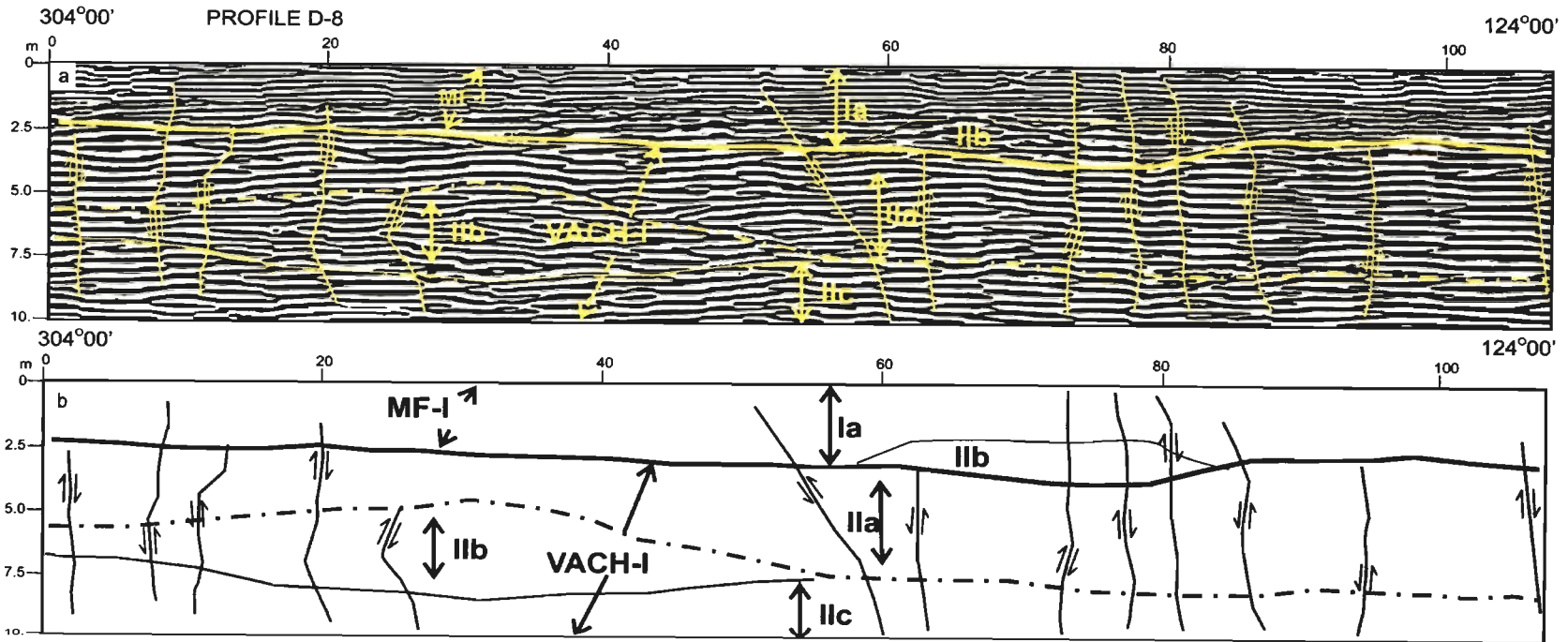


Fig. 5.28 (a) Annotated GPR profile D-8 across the SikandraRao Fault, showing sequences/subsequences, lithofacies and faults. (b) Outline diagram showing different features of the GPR profile D-8.

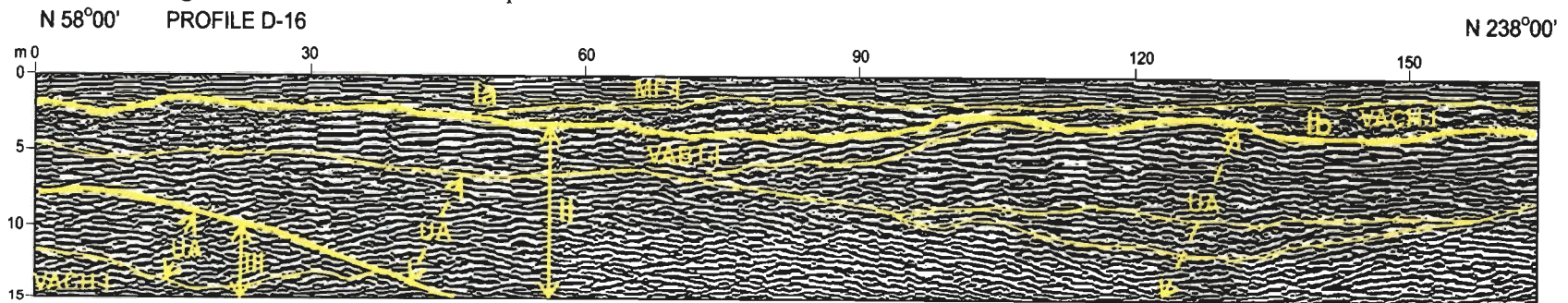


Fig. 5.29 Annotated GPR profile D-16 is from the Karhal-Bidhuna Terminal Fan, near Mainpuri Town, showing sequences/subsequence and lithofacies

Profile D-12 was carried out on Bharthana-Bidhuna Road, 20 km from Bidhuna in N78°-N258° direction up to a depth of 9 m and for a length of 120 m (Fig. 5.32). The profile is composed of two sequence I (1.75-3.25 m) and II (>5.75m). Sequence II is further subdivided into three subsequences IIa, IIb and IIc with thicknesses of 0.25-3.0 m, 1.5-3.0 m, >1.5 m respectively, which are marked by vertical accretion of sandy material in shallow parts of a large stream. Sequence I is mainly muddy sequence representing vertical accretion in a wide floodplain (MF-I), except that the lowermost part may represent lateral accretion in a small stream.

#### Profile D-16

GPR profile was carried near U.P. State Irrigation Department Offices, Mainpuri in direction N58°-N238° up to a depth of 15 m (Fig. 5.29). The profile consists of three sequences I-III. Sequence III starts with vertical accretion in a large stream and quickly develops a large bar of height ~7 m by upstream accretions and presumably on accretions on downstream as well. In later stage (Sequence II) bar grows to height of up to 12 m by upstream accretions on side of the braid bar and vertical accretion on bar top (VABT-I). Lower part of sequence I (Ib) consists sand deposited as vertical accretion in narrow channels (VACH-I), followed by mudfacies deposited by vertical accretion in a floodplain (MF-I).

Deposition was in a large stream with a depth of ~12 m (sequences II and III). Sequence I started by vertical accretion in shallow small channels and later deposition by vertical accretion of mud in a large floodplain by a shallow stream took place as part of the Karhal-Bidhuna Terminal Fan.



#### 5.10.2.4 Kanpur Terminal Fan

##### Profile D-13

GPR profile D-13 was carried out near Bella village ( $80^{\circ} 13' E$ ,  $26^{\circ} 17' N$ ). The profile is about 110 m long, ~11 m deep and in direction  $N250^{\circ}$ - $N70^{\circ}$  (Fig. 5.26). The profile shows mainly two sequences I (1.25-2.25 m) and II (8.5-9.5 m). Sequence II is further divided into four thin subsequence IIa (2.0-4.75 m), IIb (0.75-5.0 m), IIc (3.-3.5 m) and IId ( $<2.0$ m). All these subsequences (IIa-IId) represent vertical accretion in a large stream. Sequence I, a part of the Kanpur Terminal Fan is mainly a wide spread mudfacies (MF-I), with minor lateral accretion in lower part at the eastern end.

Sequence II seems to have been deposited in large river. However, sequence I first starts with lateral accretion in small stream and later vertical accretion of mudfacies in a wide floodplain takes place.

### 5.11 GANGA-YAMUNA INTERFLUVE - FAULTS

#### 5.11 1 Ghaziabad Fault

This fault was first deciphered by (Kumar et al., 1996; Parkash et al., 2000) and was named as Faridabad Fault, but later Bhosle et al. (2006) found that it is passing through north of Ghaziabad city and named it as Ghaziabad fault on basis of drainage pattern changes in inland streams, DEM of the area and even changes in channel widths of the Ganga and Yamuna Rivers.

##### Profile D-5

GPR profile was taken in Ayadnagar area ( $77^{\circ} 52' E$  –  $28^{\circ} 39' N$ ), 10 km south of Hapur city in the  $N30^{\circ}$ - $N210^{\circ}$  direction across the fault and length of the profile was 125 m and the data were collected up to a depth of 10 m (Fig. 5.20). GPR profile shows at least 18 faults, out of which nine faults

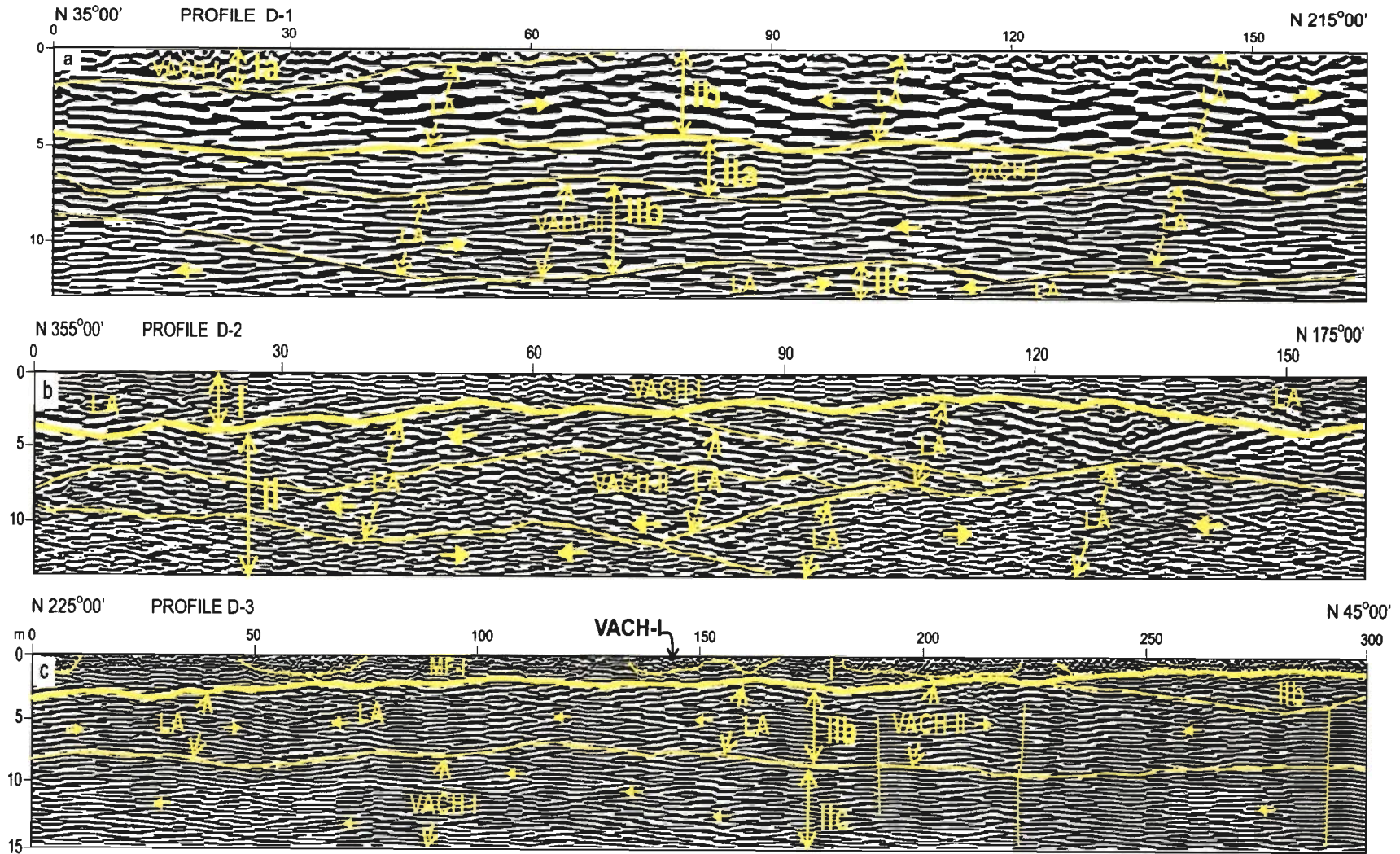


Fig. 5.30 Annotated GPR profiles (a) D-1 from the proximal area (Iqbalpur village), (b) D-2 from central part (Jhaberera Village) and (c) D-3 from (Zabardastpur Village) distal part of Iqbalpur Terminal fan, respectively, showing sequences/subsequence and lithofacies.

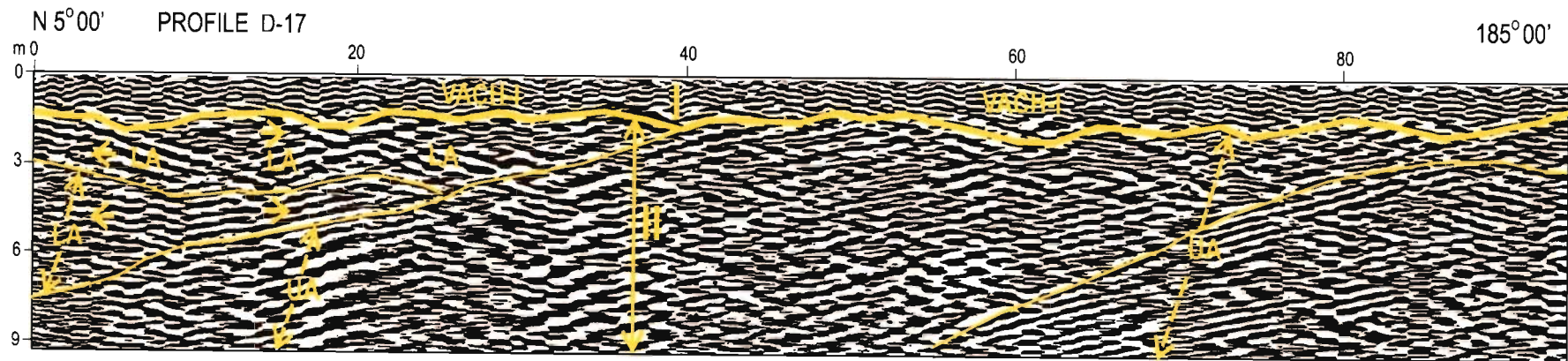


Fig. 5.31 Annotated GPR profile D-17 over the Ganga Paleochannel near Barla village, showing sequences/subsequence and lithofacies.

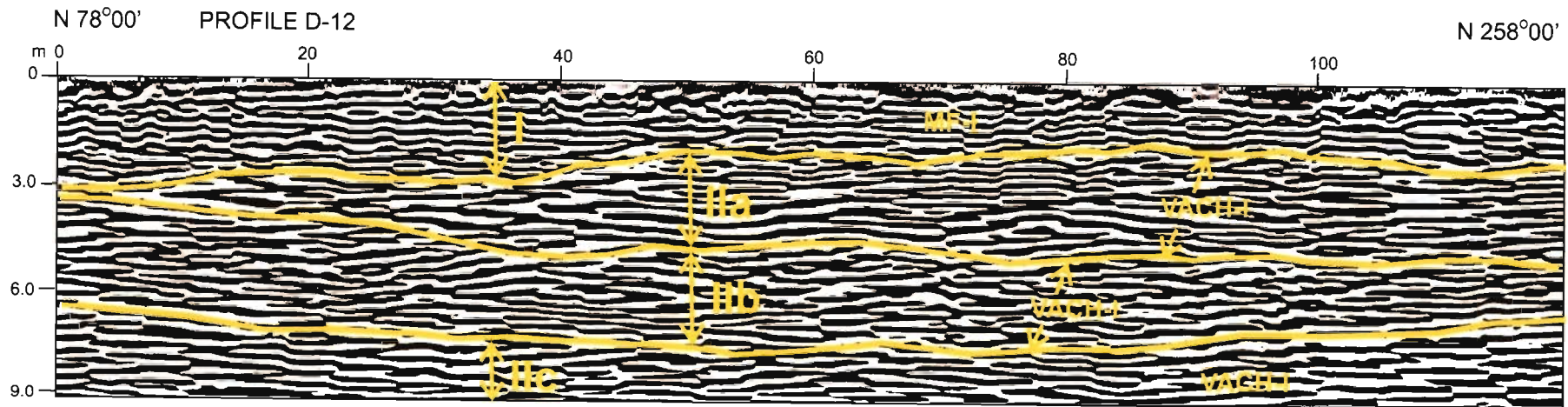


Fig. 5.32 Annotated GPR profile D-12 from the Karhal-Bidhuna Terminal Fan, showing sequences/subsequence and lithofacies.



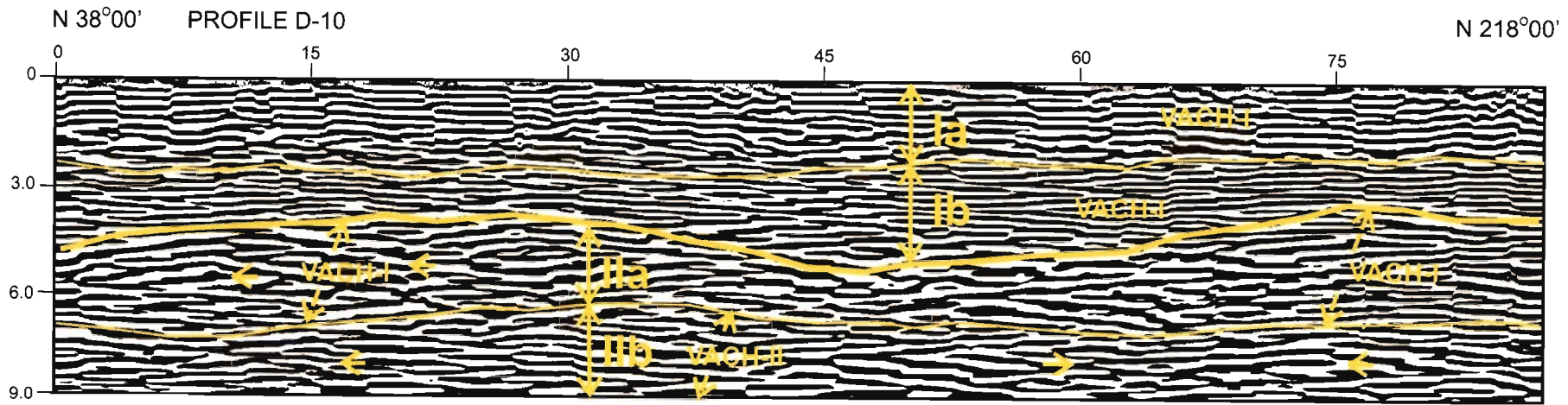


Fig. 5.33 Annotated GPR profile D-10 near Nidhauri village on Aligarh-Khurja Terminal Fan, showing sequences/subsequence and lithofacies

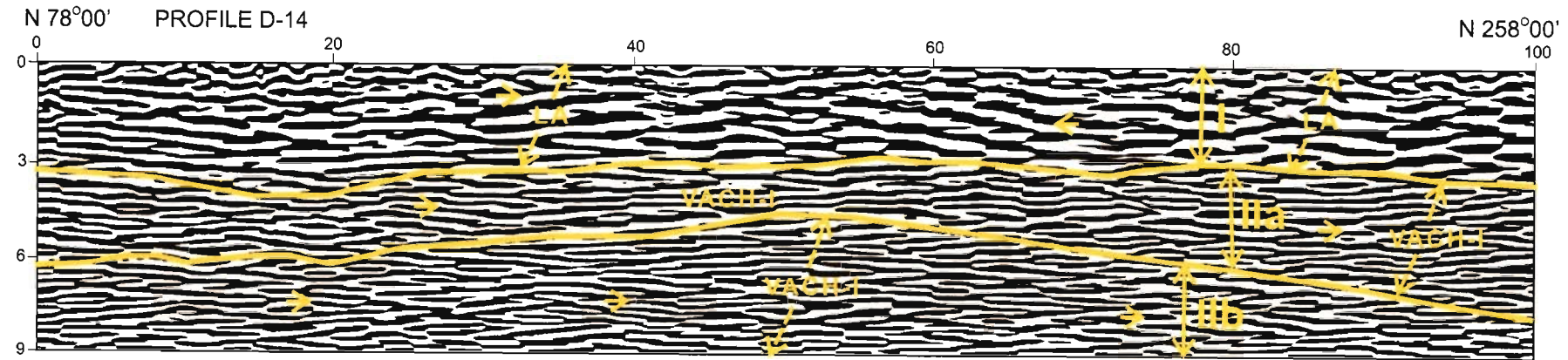


Fig. 5.34 Annotated GPR profile D-14 from the Aligarh-Khurja Terminal Fan, showing sequences/subsequence and lithofacies.

extend from the surface to the bottom of the profile. Throws of 12 faults are towards SWS end, and the rest have throw towards NEN end, confirming inference from the DEM.

### **5.11.2 Delhi Fault**

The Delhi Fault is first introduced by Bhosle et al. (2006) and it strikes in NWW-SEE direction passing close to Nation Capital Region of Delhi. GPR profile confirms its presence. It has downthrow in the ESE direction and joins with the Aligarh Fault in its eastern end. For the study of this fault a GPR profile was taken across the fault in the direction  $N355^{\circ}$  - $N175^{\circ}$  near Dastara village ( $77^{\circ} 52'$  E –  $28^{\circ} 43'$  N), 12 km east of Khurja city (Fig. 5.24).

#### Profile D-6

The length of the profile is 125 m and the depth of the data collected is 12.5 m. The profile shows 25 faults, out which 11 faults extend from the surface to the bottom of the profile while rest run for short thickness of the profile. Thirteen faults have a downthrow towards northerly direction and whereas 12 have towards south. However, field work showed a downthrow of a couple of meters towards NE, So the GPR investigation confirm the presence Delhi fault, but results about throw direction are not unequivocal.

### **5.11.3 Aligarh Fault**

As the name suggests this fault passes closed to Aligarh city. It extends across the Interfluve width up to the Ganga and Yamuna Rivers in the NEE and SWW direction, respectively (Fig. 5.22). This fault was first deciphered by the Kumar et al., (1996) and Khan et al., (1996) on the basis of changes in the sinuosity of the Ganga and Yamuna Rivers and correlation of the tube well lithologs, respectively. Later Bhosle et al., (2006) studied this

fault by DEMs and changes in inland streams across this fault. This fault also leads to development of the Khurja-Aligarh Terminal Fan.

#### Profile D-7

In this profile, 24 faults are deciphered, out of which 8 faults extend from surface to the bottom of the profile, while others start from the surface and extend to the radar sequence II only. Most of the faults show their throw in the in the SEE direction, as inferred from the DEM, and only a few exhibit throw in the opposite direction. Most of the faults are nearly vertical in nature.

#### **5.11.4 Sikandra Rao Fault**

##### Profile D-8

GPR profile D-8 was carried out in direction N304° -N124° up to a depth of 10 m and a length of about 110 m on Etah-Aligarh road, 20 km before Akkrabad (Fig. 5.28).

In profile D-8, 14 faults are identified and out of these nine faults show downthrow towards SE and 5 have downthrow towards NW end of the profile. Thus, most of the downthrows are in the direction, as observed from most other faults of the area. Majority of the faults are near vertical.

#### **5.11.5 Kanpur-Ghatampur Fault**

##### Profile D-13

In profile D-13, in all 15 near vertical faults are observed, out of which 10 show downthrow towards SEE end and rest in the opposite direction. These results confirm the downthrow direction obtained from the DEM (Bholse et al., 2008) (Fig. 5.26).

## 5.12 SUMMARY

### 5.12.1 Haryana Region

Radar Lithofacies studies indicate that except for profiles T-4C, all other profiles in Haryana plains show existence of large river with depth of >7 m depositing lower parts of sequences and upper parts being deposits of wind reworking/ or terminal fan/ young piedmont sediments. Except for profile T-9 taken approximately in direction of major river inferred from the DTM, all other profiles are oblique to paleo-flow directions determined for other locations. The presence of upstream accretion on a large scale in the profile and mainly lateral accretions being present in the lower thick parts of all other profiles supports the inference of paleo-flow directions (ENE, NE), determined from the DTM.

The presence of three thin sequences in profiles T-4C may be due to the activity of the Markanda Fault, which is present closeby.

The presence of lower thick profiles (usually 7-13.5 m) in Haryana are similar to that (6.5-7.5 m) present in lower part of profile T-3, interpreted as a large Sutlej River paleo-channel. It supports the inference of the presence of a large river over most of Haryana plains in recent past.

The GPR profiles across 5 out of six faults inferred from remote sensing and GIS studies confirm the presence of these faults. Also, these faults are not single faults, but are sets of a number of faults, and majority of faults show downthrown side in direction inferred from the DEMs, and the rest show downthrow in the opposite direction. Faults in individual sets are not present throughout the studied profile, but most of them continue for a part of the depths studied.

The Patiala and Hissar Faults show effect of activity of faults contemporaneous with sedimentation by thickening of beds on downthrown blocks (profiles T-3 and T-6).

### **5.12.2 Ganga-Yamuna Interfluve**

Lithofacies studies of the Ganga Paleo-channels at Iqbalpur and Barla suggest that a large river with a depth of >7 m deposited sequences >14 m thick. These sequences were sometimes deposited by lateral accretions on sides of large bars >6 m high. Two to four sequences with commonly thickness of <4 m may be present in these deposits. The subsequences were also deposited by lateral accretions on lower height braid bars and some times by vertical accretions in channels.

Terminal fan deposits in the lower part consist of channels filled with vertical accretion deposit (VACH-I)(D-7, D-10, D-16) lateral accretion sands (LA) (D-1, D-14, D-12, D16, D-13), overlain by wide spread floodplain mudfacies (MF-I) (D-3, D-9, D-11, D-12, D-13) and the top part is commonly composed of narrow to wide shallow channels filled with VACH-I (D-1, D-3, D-7, D-9, D-11). Rarely as in profile D-10, two subsequences of <2.75 m thickness each with vertical accretions may form terminal fan deposit. The tops of terminal fan deposits exhibit moderate to weak soil development.

Litho-facies analysis also brings out the lower part of sequences observed in GPR profiles were deposited mainly by moderate sized streams with depths of 5-7 m (profiles D-7, D-10, D14, D-11, D-12). However, at a few places, the lower parts of profiles seem to have been deposited by large steams with a depth of 7-13 m (profiles D-9, D-16, and D-13). However, more



detailed work needs to be done to trace the course of the large stream inferred here.

Five faults inferred from DEMs and drainage pattern changes (Bhose et al., 2006b) were investigated by GPR technique and their presence was confirmed. Usually these faults consist of a set of a number of small, near vertical faults and most of these show downthrow towards directions indicated by DEMs, except for Delhi Fault, in which case almost equal number of faults show throws in opposite directions.

**6.1 INTRODUCTION**

The Haryana Plains form a drainage divide between the Indus and Gangetic drainage systems. Also, the Indo-Gangetic Plains have been known to be tectonically active since Mid Miocene and the Gangetic Plains have been shown to be fairly tectonically active during the Holocene Period. Thus the possibility of the Haryana Plains being tectonically affected during the Holocene Period is high. The Haryana Plains form a transitional zone between the sub-humic Himalayan regions and the Thar Desert region just to the southwest. Thus effects of climatic changes in the recent past are likely to be recorded in sediments of this region. Lastly Haryana is known to be host to the Vedic Civilization, which was intimately related to the Sarasvati, the Lost River. The Yamuna River, flowing through Haryana Plains, forming a major tributary of the Sarasvati, (flowing along the presently small, ephemeral Ghaggar River) has been suggested by a number of archaeologists, but geological evidence for the same is still to be worked.

Keeping the above points in view, Haryana region was mapped for its soil-geomorphic units, using remote sensing digital data, field checking of these units, study of typical pedons from each unit for their morphological features, collection of soil samples for granulometric and micromorphological studies and dating of C-horizons of soils. Digital elevation models and changes in modern/paleo-drainage were used to locate faults, which were confirmed by Ground Penetration Radar studies. Attempt was made to investigate subsurface lithofacies using GPR to infer the absence/presence of

the large Yamuna River in Haryana in recent past. Also, drainage evolution of the Haryana region was worked out.

## 6.2 METHODOLOGIES USED

### 6.2.1 Remote Sensing and Geographic Information SYSTEM (G.I.S.) Studies

Remote sensing and G. I. S. techniques to map soils in the Upper Gangetic Plain have used with success by Singh et al. (2006) and Bhosle et al. (2008). As regional studies in the study area are limited (Singhai et al., 1991), our study is an attempt in this direction. The following LANDSAT satellite Multi Spectral Scanning (MSS) data freely accessible from site [www.glc.f.umd.edu/](http://www.glc.f.umd.edu/) have been used in the present investigations:

Image-MSS	path/row	Date
a) WRS-P/R-1	158/039	23 Feb 03.
b) WRS-P/R-1	158/040	31 Jan 03.

The False Color Composite (FCC) was generated by coding bands 4, 3 and 2 as red, green and blue for MSS images, respectively. LANDSAT data are already geo-referenced in UTM co-ordinates and was converted into polyconic and geographic projections, as required.

### 6.2.2 Digital Elevation Models (DEMs) and Digital Terrain Models (DTMs)

Though SRTM (Shuttle Radar Topographic mission) images provide digital elevation data of 90 m resolution, but it is not useful for the present study due to its low vertical resolution  $\pm 6$  m. So Digital Elevation Model (DEM) was prepared by manually digitizing the point heights from the Survey of India topographic sheets, which have resolution of  $\pm 2$  m (*Pers. commun.* with Mr. R.P. Jhalina, Survey of India). First the topographic sheets were geo-

referenced with the same co-ordinates as that of the MSS image. A total of 6579 points were taken from 105 number of 1:50,000 scale topographic sheets by using Arc View 3.2a, G.I.S. software and a DEM was prepared by using Linear rubber stretching interpolation method in ERDAS IMAGINE-8.5 software. 2-D topographic profiles (cross-sections) are generated from these DEMs were useful to find out the amount of throw of normal faults and the regional as well as the local slope across the faults. Then the MSS image was draped upon the prepared DEM and a DTM was prepared for regional overview of the area. Lower and higher vertical exaggeration of 600 and 1200, respectively, were used to prepare DTMs to identify lineaments, and faults and land forms, respectively. These DEMs can be generated for any desired viewpoint and view angles.

However, DEMs of small areas around the possible faults and related terminal fans were prepared using krigging interpolation method of SURFER-8 program (Golden Software, Inc., 2003) (Figs. 2.6, 2.7, 2.24, 2.25 and 2.26) The details of the DEMs are given in the Tables 2.1 and 2.4. For DEM construction by SURFER-8 software, x-axis and y-axis of lengths of 6" for representing 1/2° are taken and the Z-axis is taken as default value. Normally Z-axis value of 1" or 0.75" is taken representing a height difference of 25 to 30 m. to produce a near realistic DEM, which translates into a vertical exaggeration about 400 to 600 times (Tables 2.1, 2.4). Also, best possible viewing position and sun setting were used in construction of DEMs. DEMs thus obtained, show some artifact features like 'cliffs' in our case, which are indicative of faults (Bhosle et al., 2009).

### **6.2.3 Luminescence Dating of Soils**

Fifty three samples were dated from all 25 soil geomorphic units. In most of the sample signal show a linear increase with the dose (Fig. 3.4). This leaves no or least uncertainty in extrapolation in the paleodose based on the additive growth technique. Table (3.1) provides the experimental data including the paleodose, dose rate and age of the samples.

### **6.3 IDENTIFICATION OF GEOMORPHIC FEATURES AND SOIL-GEOMORPHIC UNITS**

Using the elements of the image interpretation as described by Gupta (1991) like tone, texture, pattern, size, shape, site/association, twenty five soil-geomorphic units were identified and mapped (Fig. 2.3). Also, a number of landforms like river floodplains, piedmont, paleochannels, and terminal fans, old river plains and aeolian plain and structural features like lineaments and faults were identified and mapped.

### **6.4 FIELD INVESTIGATIONS**

For the determination of different soil morphological properties of various soil-geomorphic units mapped by remote sensing, to confirm various geomorphological and structural features and to identify the possible locations for Ground Penetrating Radar (GPR) studies, detailed field work was carried out. Also, boundaries of the soil-geomorphic units and properties like salt efflorescence and water-logging conditions of the identified soil-geomorphic units were cross-checked in field.

The field work was planned in such a way that the whole area was properly covered (Fig. 2.2). Fifty-six pedons from the different soil-geomorphic units were studied in detail in the field for their soil morphology. Loose

samples were collected from each horizon and sub-horizons for grain size analysis and undisturbed samples were collected in tin boxes for soil-micromorphological studies. Samples from C-horizons of each pedons were collected in one end closed iron pipes for Optical Stimulated Luminescence (OSL) dating (Chapter-3).

## **6.5 MAJOR LANDFORMS IN THE STUDY AREA**

Using the satellite images, topographic maps, DEMs, DTMs and detailed field work, major landforms like floodplains of rivers, aeolian plains, old fluvial plains, piedmont zone and terminal fans are identified (Fig. 2.3).

### **6.5.1 Fluvial Plains**

Depending upon IRSL ages, thirteen plains have been identified: Yamuna and Ghaggar floodplains, Old Yamuna Plain-I, Old Yamuna Plain-II, Old Yamuna Plain-III, Fluvial Plain, Fluvial-Aeolian Plain, Old Sutlej Plains-I & II and Katha Plains I&II.

#### *6.5.1.1 Floodplains*

Two major rivers i.e. the Ghaggar and Yamuna have 7 km and 9 km wide floodplains on the average, respectively. Other small inland streams on the interfluvial are ephemeral in nature and have small discharges and narrow floodplains (<1.5 km). They flow in southwesterly direction, following the regional slopes. Since the floodplains are occasionally inundated during rainy season, they are marked by A/C horizons mainly. The floodplains of rivers have not been studied in detail in the present study.

6.5.1.1.1 Ghaggar Floodplain: The River Ghaggar originates from the Siwalik Ranges and flows in the southwesterly direction. The average annual

flow of the Ghaggar is  $2.159 \times 10^6 \text{ m}^3$  (Duggal, 1977). The floodplain of this river is narrow in the northeast and gradually widens up to 13 km in the Kurukshetra and Hissar districts and the river loses itself in the Thar Desert of Rajasthan.

Manchanda (1981) divided the Ghaggar plains into three zones i.e. upper, middle and lower. The upper part mainly lies in the Union Territory of, Chandigarh, Ambala and Kurukshetra districts. This zone does not have problems of salinity, alkalinity or drainage. The middle zone mainly lies in parts of Kurukshetra and Narwana Districts. Here the river has meandering nature and a number of levees, bars and abandoned channels are observed. This gently sloped floodplain is poorly drained, causing salinity at places and development of mottles. The dominant soils types are Ustochrepts, Ustipsamments and Haplaquepts.

The lower reaches of the southern floodplain show salinity and alkalinity in general. Development of  $\text{CaCO}_3$  concretions are reported in this floodplain by Ahuja (1981). In these reaches, a narrow active floodplain with a width of 0.3-0.7 km and older one with a width of 8-13 km are identified in the MSS image. Major soil types are Ustochrepts and Ustipsamments.

6.5.1.1.2 Yamuna Floodplain: The River Yamuna crosses the Doon valley and breaks through the Siwalik Range along the Paonta Fault (Rao et.al., 1974). After the river enters the plains, it flows through a large 'valley' that extends up to Delhi. This valley with a width of 10-25 km is incised into the older alluvium by several meters. The river forms a narrow active floodplain within this 'valley' and region beyond the floodplain is covered by older soils (Old Yamuna Plain-I). The Yamuna has a braided character up to a

distance of 35 km after entering the plains and later it meanders through a wide floodplain. The width of floodplain is about 8 km in Bilaspur district and widens up to 13 km in Karnal and Sonapat districts, further narrows down to 6 km in Gurgaon district. The 'valley' continues up to Mathura and further downstream narrow floodplain of the river is deeply entrenched. The landscape aspects of the active floodplain are related to the channel remnants of the former river courses and related features like levees, basins, channel bars and the abandoned channels.

#### 6.5.1.2 Old Sutlej Plains –I and II

These plains lay just northwest of the Ghaggar floodplain and are a part of the old Sutlej plains. The River Sutlej shifted northwestward from a position of being a tributary to the Ghaggar River earlier than 1700 B.C. and this is evidenced by the presence of a number of paleo-channels (Fig. 2.4), starting from Ropar, where the Sutlej enters the plains (Pal et al., 1982). These plains basically consist of coarse sand along the paleo-channels and silt and clay in the intervening areas. As seen in the old (pre 1937) topographic maps, sands of the paleo-channels were heaped into elongated mounds, which have been removed in the last two decades. This plain is marked by abundance of impure calcareous irregular concretion i.e. '*kankar*'. Soil development is moderate in southern part and it decreases northward to very weakly developed soil. The diagnostic horizons observed in this area are, cambic, salic, calcic and argillic and nitric (Sehgal et al., 1968, Sehgal, 1974; Sidhu et al., 1976; Anand et al., 1977 and Sharma et al.; 1978). Major soils are Ustochrepts, Ustipsamments, Haplaquepts and Natrustalfs. Based on



IRSL ages, the Sutlej Plains in the study area have been divided into the Old Sutlej Plain-I (3.9 Ka) and Old Sutlej Plain-II (2.7 Ka), respectively.

#### 6.5.1.3 Yamuna Plains

Three Yamuna Plains viz. Old Yamuna Plain –I, Old Yamuna Plain-II, and Old Yamuna Plain-III are identified in the present study.

The Old Yamuna Plain-II forms an elongated region running at the base of the Piedmont zone in approximately E-W direction and covers an area from the present Yamuna course to the Ghaggar course. This plain is traversed by numerous small streams coming out of the Piedmont zone. This plain is characterized by two soil profiles at places, the older profile being well-developed and with an age of 4.0 Ka age and the younger profile is moderately developed and is of 2.8 Ka age. Soils in this unit are classified as Typic Ustochrepts, Typic calciorthids and Typic Torripsamments.

The Young Yamuna Plain-III lies just south of the Old Yamuna Plain-II (Figs. 2.4, 2.18). Moderately to weakly developed soils in this unit are developed on the sandy parent materials and shows salt efflorescence. Calcrete concretions are fairly common. The soils are mostly sandy loam and classified as Typic Ustochrepts, Aquic Comborrhthids, Typic calciorthids and Typic Torripsamments.

The Old Yamuna Plain-I is an elongated plain along the Yamuna River, strikes in NE-SE direction and this unit continues beyond the study area up to Mathura (UP). This plain is confined within the 13-15 m cliffs of the Yamuna Faults (Figs. 2.25 c, d). This plain is dominated by the geomorphic elements like the paleochannels and ox-bow lakes. The sandy character of the plain is well reflected by lighter tone in the MSS image. Numerous small streams are

now active in this plain and deposition is mainly confined in their floodplains. Soils in this plain are moderately developed and classified as Typic Ustochrepts, Typic calciorthids and Typic Torripsamments.

#### *6.5.1.4 Old and Young Katha Plains*

The plain Old Katha Plain (OdkPn) and Young Katha Plain (YgKaPn) is formed by the tributary of the Yamuna River flowing in this area (Ganga-Yamuna interfluve) known as Katha River. The OdkPn soils are weakly developed, and show little salt efflorescence. Due to low lying condition, the area appears as wet in the satellite image by darker tone. The soils are mostly sandy loam and classified as Typic Ustochrepts, Aquic Camborthids,

Young Katha Plain is marked by the presence of number of abundant paleochannels and show weakly developed soil on the sandy parent materials and is classified as Typic Ustochrepts

#### *6.5.1.5 Fluvial Plain*

Soils in this plain are weakly developed due to an arid climate, Morphologically this plain is marked by the major landforms like bars, old levees, relict channel courses, salt-affected plains and basin plains. Typical soils in the area are Typic Camborthids and Typic Ustochrepts.

#### *6.5.1.6 Fluvio-Aeolian Plain*

Fluvio-Aeolian Plain is situated in the west-central part of the study area. Soils occur dominantly on the fluvial plains modified by aeolian activities by the westerly winds from the adjacent Thar desert. The moisture regime is ustic to aridic with annual rainfall not exceeding 350-400 mm. This area is marked by large numbers of paleochannels (Fig 2.9) filled with the sandy materials, indicating a strong fluvial activities in the past. Dominant soils of

this area are sandy and calcareous, occurring on gently sloping plains, with sand at places are being reworked into dunes. The soils in this unit are classified as Typic Torripsamments.

### **6.5.2 Piedmont**

The piedmont zone is marked by steep slopes (average slope =0.6%), elongated in the east-west direction and lies at the Siwalik ranges with a length and width of 140 km and 54 km, respectively (Fig. 2.4). This zone is marked by parallel and sub-parallel drainage system. Most of the large streams join the bounding rivers at acute angles. This zone is marked by coarse sediments i.e. sand and gravels deposited by the streams coming out the Siwalik Ranges. On the basis of the degree of soil developments and IRSL ages, four soil-geomorphic units are identified within this zone: Oldest Piedmont (OdPt), Old Piedmont-I (OdPt-I), Old Piedmont-II (OdPt-II) and Young Piedmont (YgPt).

#### *6.5.2.1 Oldest Piedmont*

The Oldest Piedmont lies west of the Ghaggar River, extends southwards from the foot of the Siwalik Ranges and has a maximum width of about 40 km. It has the thickest (~1.7 m) soil cover, which is eroded at places. This unit is well drained with parallel to sub-parallel drainage towards west and southwest. The streams in this unit are incised in nature and have narrow floodplains. Soils in this unit are sandy to loamy in nature and classified as Udic Ustochrepts. The OSL age of this unit varies from 7.6 to 9.8 Ka and it is the oldest soil-geomorphic unit in this area.

#### *6.5.2.2 Old Piedmont-I*

Old Piedmont-I covers the maximum area in the piedmont zone. Well distributed drainage system of the area is marked by southwest flowing streams like the Sarasvati, Chautang and Markanda streams. These streams are characterized by their incised courses and are transporting gravelly and sandy sediments. Soils are well-developed. Sediments eroded from this piedmont are being spread over the Old Yamuna Plain-II. Smaller streams have removed the soil cover at places. Soils here are classified as coarse loamy to fine loamy Udic Ustochrepts.

#### *6.5.2.3 Old Piedmont-II*

This unit is in the south of the Oldest Piedmont and was deposited as a result of streams flowing from the Oldest Piedmont, as suggested by some paleochannels. As compared to the Old Piedmont-I, the moisture content of this unit is more as suggested by a darker tone in the MSS image. Soils in this unit are moderately developed and are mainly Ustorthents.

#### *6.5.2.4 Young Piedmont*

Young Piedmont forms a small portion in the northeastern part of the study area bordering the Siwalik Ranges. This is formed by the streams descending from the Siwalik Ranges, which turn eastwards to meet the River Yamuna. Alluvial fans formed by the small streams overlap each other in this unit (Fig 2.4). Soils in this area are very weakly developed and are well drained. In some areas mottling is reported. Soils from this area are classified as Ustifluent and typic Ustochrepts. The Young Piedmont is also observed east of the Yamuna River.

### **6.5.3. Aeolian Plain**

The Aeolian Plain is the southernmost soil-geomorphic unit of the study area with an age of 4.4-4.7 Ka. This unit is influenced by hot winds and frequent dust storms from the neighboring Thar desert. On the whole it is a flat aeolian plain dotted with isolated low height (<2 m) dunes at places.

Dominant soils are loose sands on dunes and are classified as Typic Torripsamments. The inter-dunal soils are moderate to poorly drained, calcareous and coarse-loamy. They are classified as Typic Camborthids. They are generally alkaline in nature. Calcrete precipitation is present in the pore spaces of the sediments.

### **6.5.4 Terminal Fans**

Out of eight terminal fans identified in the study area, the Sonipat and Karnal terminal fans in the eastern-central part of the study area are slightly at higher topographic level than adjoining areas. All the fans are slightly convex upward in nature and their distal boundaries are not clear. Geometric aspects like length, perimeter, slope, related fault and the area of the fans are given in Table (2.1). The largest fan identified is the Old Yamuna Terminal Fan in the western-central part of the study area. All the terminal fans have formed due to activity of different faults across some streams. Most of the terminal fans in the study area were formed by the rivers, which used to flow in the recent past. The Sonipat terminal fan is supposed to be formed by the Burhi Yamuna River, which is now a minor stream in the area. Similarly the Old Yamuna terminal fan was formed by the Paleo-Yamuna River, which used to flow in this area. The Chautang River formed four terminal fans (Young Chautang terminal fans I-IV) due to activity of different faults at different times. The

Young Chautang Terminal Fan-I shows dichotomic drainage for numerous paleochannels over its surface.

#### **6.5.5 Aravalli Hills and Pediments**

This unit consists of low altitudes (<775 m) ridges in the southwestern and southernmost part of the study area. At places, the Aravalli Hills have been eroded to form undulating hillocks and pediments, especially along the marginal regions of these hills. It is covered by sandy to fine loamy loess brought in from the Thar Desert in the south. The subsoil water is brackish. Calcium carbonate nodules are found at a depth of 1-2 m depending upon the thickness of the sand cover. Soils in general are classified as Typic Camborthids, Typic Torripsamments, Typic Torrifluents, and Typic Haplaquepts.

#### **6.5.6 Aravalli Piedmont**

The Aravalli Piedmont mainly lies northeast of the Aravalli Hills and Pediments unit. It has been constructed by the monsoonal streams like the Dohan, Kali Nadi and Sahibi Nadi, draining from the Aravalli Hills. Major part of the unit is occupied by a fan formed by the Sahibi River. Almost all the sediments brought by these streams are reworked by the aeolian activity during the dry months. Major soils in the area are Typic Camborthids and Typic Torripsamments. Its age is 2.7 Ka.

#### **6.5.7 Paleochannels in the study area**

The available January to March MSS images were not very useful for locating paleochannels. However, images taken from Googleearth probably of post-monsoon months, bring out numerous paleochannels with distributary

pattern in southern half of the study area (Fig 2.9). Distributary paleochannels are observed to be flowing from approximately NE direction, suggesting that some remnant channels of the Yamuna River may have been responsible for their formation. Many of these paleochannels are now occupied by modern canals. Well-defined paleochannels are observed in the Young Chautang and Old Yamuna terminal fans. However, the Young Chautang terminal fan-I may have been formed by contributions from the Chautang and some distributary of the Yamuna rivers.

In MSS image, salt efflorescence pattern also brings out the presence of paleochannels flowing from the NE and N in the Karnal and Young Chautang terminal fans, respectively.

## **6.6 MORPHOSTRATIGRAPHY OF THE STUDY AREA**

In the present study, MSS images along with DEMs and DTMs (Sec. 2.2.2) were used to identify twenty-three soil-geomorphic units. Also, optical luminescence dating was carried out for C-horizons of soils in different soil-geomorphic units to provide absolute ages. Based on the OSL ages, six members (QIMS-I to VI) (Quaternary Indus Morphostratigraphic Sequence) of a Morphostratigraphic Sequence are identified (Frye and William, 1962. in Fairbridge, 1968, p. 915): QIMS-VI 9.86-5.38 Ka, QIMS-V- 5.38 -4.45 Ka, QIMS-IV- 4.45 - 3.60 Ka, QIMS-III - 3.60 -2.91 Ka, QIMS-II - < 2.91-1.52 Ka and QIMS-I - < 1.52 Ka.

## 6.7 SOIL MORPHOLOGY OF DIFFERENT MEMBERS OF MORPHO-STRAITIGRAPHIC SEQUENCE

### 6.7.1 Member QIMS –VI

This is the oldest member of the study area and includes only one soil- geomorphic unit, i.e. the Oldest Piedmont. This unit is present in the extreme northwestern portion and covering approximately an area of 630 km<sup>2</sup>. In north, it is separated by the Himalayan Frontal Thrust from the Siwalik Hills and is elongated and parallel to Ghaggar River, which flows along the eastern boundary of the unit (Figs. 2.3, 2.4 and 2.10). It is well drained by the seasonal streams originating in the Siwalik Ranges and the Ghaggar River and its tributaries like the Chola Nadi, Siswa Nadi and Buoki Nadi, but shows low drainage density. Soils in this member are moderate to well develop with sub-angular blocky and prismatic structures. The matrix colour varies from 10YR3/2 (very dark grayish brown) to 10.YR 6/4(light yellowish brown). The thickness of B-horizon varies from 80-65 cm and that of the solum varies from 95-135 cm. The detailed description of soil properties is given in Table 2.3. The pores size gradually decreases from upper to lower part of profiles from fine to very fine. Roots are medium in the upper A and B horizons and become finer with depth and absent in the C horizon. Thick clay cutans are observed in B-horizons. Hard, dark brown (7.5YR3/3) Fe-Mn nodules are well distributed in the B-horizons. pH varies between 6.2-7.4, indicating slight acidic to mildly alkaline nature of the soils. Absence of effervescence on being treated with hydrochloric acid indicates the soils in this unit are free of carbonates. Texture of the soils varies from sandy loam to loamy sand class (Fig. 2.12).



### **6.7.2 Member QIMS –V**

This member covers the major part of study area and includes six soil geomorphic units i.e. Old Piedmont-I, Old Piedmont-II, Aeolian Plain, Aravalli Hills and Pediment Plain, Karnal Terminal Fan and Fluvial Plain are distributed in the northern, southern and central parts (Fig. 2.10).

The soils in this area are moderate to strongly developed having sub-angular blocky structures. Thickness of B-horizon varies from 34 to 96 cm and that of the solum varies from 65-119 cm. Common medium and distinct mottles and Fe-Mn nodules (7.5YR3/3) are well distributed, in the B- and C-horizons of OdPt-I, OdPt-II, and ArHPn. Medium thick clay cutans are well distributed in the B-horizons. Due to low lying nature, soils in the OdPt-II show gleying affects. The colour of the soils varies from light yellowish brown (10YR6/2) to dark brown (10 YR4/3m). Variation of pH from 5.89-7.5, indicates medium acidic to mildly alkaline nature of soils. Texturally, the soils in this member vary from sandy loam to loamy sand and in Karnal Terminal Fan and Aeolian Plain, the soils show sandy texture (Fig. 2.13) as developed in Old Piedmonts-I and II and Karnal Terminal Fan, respectively. Fine to very fine roots are observed in the A- and B-horizons, but the C-horizon shows absence of roots. The soils of this member are free of carbonates except the Aeolian Plain, which shows moderate effervescence.

### **6.7.3 Member QIMS –IV**

This member consists of six soil geomorphic units i.e. Old Sutlej Plain-I, Old Yamuna Plain-I, Old Yamuna Plain-II, Old Yamuna Plain-III, Markanda Terminal Fan and Fluvial-Aeolian Plain. Most soil geomorphic units in this member represent the old plains of the Yamuna and the Sutlej Rivers (Fig.

2.10). In most parts of these units, abandoned channels can be clearly visualized in the field, which are filled with the alternating sand and mud beds. The soils in this member area are moderately developed. The B-horizon thickness varies from 22 to 75 cm. The soils of this member show sub-angular blocky as well as prismatic structures along with the Fe-Mn and calcium carbonates nodules. Medium thick clay cutans are well distributed in the B-horizon and the BC horizons are marked by patchy thin clay cutans. The colour of the soil varies from dark grayish brown (10YR5/2) to dark brown (10YR4/3). The C-horizon is marked by absence of roots. Many medium and prominent mottles (10YR4/3) are well distributed in the B-horizons, but the BC and C-horizons are marked by the presence of dark brown (10YR4/1.5) Fe-Mn nodules. CaCO<sub>3</sub> nodules are seen in the C-horizons of the Fluvial-alluvial Plain in the southern part of the area. Texturally the soils in this member fall in the sandy loam to sandy clay classes (Fig. 2.14). Variation of pH from 5.4 - 7.12 indicates the soils are strongly acidic to neutral in nature. Gleying is observed in the Old Yamuna Plains-I & II soils due to its low lying nature.

#### **6.7.4 Member QIMS –III**

This member of the morphostratigraphic sequence includes five soil geomorphic units i.e. Old Yamuna Terminal Fan, Sonipat Terminal fan, Old Katha Plain, Young Katha Plain and Katha Terminal Fan. These units are well distributed in the west-central and eastern part of the study area (Fig. 2.10).

Soils found in this member are moderate to weakly developed with subangular blocky structures. The B-horizon thickness varies from 26-61 cm and that of the solum varies from 53-96 cm. The matrix colour varies from pale yellowish brown (2.5YR7/4) to dark brown (10YR4/3) in colour. Many

medium distinct mottles (10YR4/3) are well distributed in the B horizons of Old and Young Katha plains, but the same in the Sonipat and Karnal Terminal Fans are fine and faint. Fe-Mn concretions of light yellowish brown colour (10YR6/3) are reported from the units in the Old Katha Plain, Young Katha Plain and Katha Terminal Fan. Patchy, thin clay cutans are observed in the Old Katha Plain and in some pedons of the Young Katha Plain, but all other soil-geomorphic units don't show any significant clay illuviation features. The pH varies from 5.98-7.2 indicating medium acidic to neutral nature of soils. Texturally the soils in this member fall in the sandy to sandy loam classes (Fig. 2.15).

#### **6.7.5 Member QIMS –II**

This member includes six soil-geomorphic units i.e. Young Chautang Terminal Fans-I-IV, Sahibi Fan, Young Piedmont and Old Sutlej Plain-II (Fig. 2.4). Most of the units in this member were deposited in the form of terminal fans by the activity of Markanda, Karnal & Rohtak faults. However, the Young Piedmont in the northernmost region has been deposited by the activity of the Himalayan Frontal Thrust (HFT), by the various ephemeral rivulets rising from the Siwalik Ranges. The Old Sutlej Plain-II in the west was deposited by the Sutlej River.

Soils in this member are weakly developed and the B-horizon thickness varies from 13-47 cm and the Ap horizon is much thicker comparatively. The pH varies from 6.9-7.89, indicating that the soils in this unit vary from neutral to moderately alkaline nature (Fig. 2.16).

Patchy thin clay cutans are observed in some pedons of the Young Chautang Terminal Fan-II and other units on this member don't show any clay

illuviation features. Fine faint mottles are observed in this member. The matrix colour varies from dark grey 2.5Y4/1 to dark grayish brown 2.5Y4/2. Roots are common and fine.

Soils in the Old Sutlej Plain-II consist of sandy material occurring along the paleo-channels and silt and clay cover the intervening areas between the paleo-channels. This plain is marked by the abundance of calcareous material in the form of irregular concretions (called *kankar* locally) and in this area salt efflorescence is also common (Appendix-2) The soil matrix colour varies from brown (7.5YR4/4) to yellowish brown (2.5Y6/3). The animal activity is present in considerable amount and calcareous nodules predominant in the C-horizon (Fig. 2.16).

Soils in the Young Piedmont show a typical colour yellowish brown (2.5Y6/3) to dark yellowish brown (2.5Y3/3) and are dominated by the fine and very fine sand and their texture varies from sandy to sandy loam classes (Appendix -2). The matrix colour varies from dark olive brown (2.5Y3/3) to light olive brown (2.5Y5/4). Fe-Mn and calcium carbonate concretion are commonly observed in this unit.

## **6.8 GRAIN SIZE ANALYSIS AND MICRO-MORPHOLOGY OF SOILS**

### **6.8.1 Grain Size Analysis, and pH and EC Studies**

A total number of 96 soil samples from typical profiles of different soil-geomorphic units (Fig.2.10) were investigated for the particle size distribution and to determine the soil texture and the amount of clay present in the soils (Catt, 1986, 1990). Soil textures have been used to work out the nomenclature of soil horizons and the classification of soil profiles (Appendix-2).

Variation of pH is given in Appendix-2. In individual pedons, there is no definite order of increase or decrease of the pH value with depth. All the members of the morphostratigraphic units show neutral to moderately alkaline nature except the Old Katha Plain (QIMS-III), which is slightly acidic in nature. Similarly soils of all the three Old Yamuna Plains (OdYPn-I-III) and the Old Piedmonts show neutral to slightly acidic in nature.

Results of the EC values of individual pedons are given in Appendix-2. These data show that soils of all the morphostratigraphic sequence members are non-saline in nature, except the Karnal Terminal Fan, Old Piedmont-II, I, Chautang Terminal Fan-II, which are mildly to moderately saline, as indicated by their EC values.

Textural classes were determined from the particle size data according to Schoeneberger et al. (1998) by plotting sand, silt and clay percentages in a combined texture triangular diagram (Fig 4.4(a), 4.5(a & b), 4.6(a & b)). The results of the particle size are given in Appendix-2. Particle size distributions show that the texture of most of the soils of the study area varies in a wide range between sandy loam to silty loam and become heavier especially in B-horizon with increasing soil development. However, the QIMS-III soils have a larger range of textural variation from loamy sand to silty loam class (Fig. 4.5 b).

The QIMS-I soils include the active floodplains of the rivers Yamuna, Sutej and Markanda and show very weakly development soils and were not studied in details. The QIMS-II soils do not show any significant change in sand, silt and clay percentage with depth, which suggests fluvial processes of deposition varied only in a small range (Fig. 4b). Plots of the total clay content

with pedogenic clay content are shown in the (Fig. 4.3) and the degree of illuvial translocation has been assessed by calculating clay accumulation index (C.A.I) of Levine and Ciolkosz (1983). The clay accumulation index (C.A.I) for QIMS-II, QIMS-III, QIMS-IV, QIMS-V and QIMS- VI vary from 227-484, 166-485, 186-714, 300- 855 and 885-1147, respectively. Clay accumulation index (C.I.A) increases systematically from QIMS-II to QIMS-VI suggesting the increase of pedogenic clays with the increasing age of soils. Also, the younger soils have varied textures from sandy loam to silty loam classes. With increase in age soils tend to change their textures to loam probably due to breakdown of rock fragments and weathering of some minerals.

### **6.8.2 Micromorphology**

A total of 54 typical thin-sections have been studied from 20 soil profiles of different morphostartigraphic sequence members of the study area and have been described in the Appendix-3.

Micromorphological investigation shows that QIMS-II and III member soils show very weak to moderate pedality (Fig. 4.7a, b), whereas the soils older members such as QIMS-IV to VI show moderate to well developed peds in B-horizons (Fig. 4.10b, d and 4.11c, d). In the upper and the lower horizons (A & C) soils are apedal in nature or show weak to no ped development.

Channels separate the ped faces and the ped faces are non- or partially accommodating in the QIMS-II and III (Fig.4.8d) and moderately accommodating to each other in QIMS-IV to VI soils (Fig.4.11d). Average ped diameter, void diameter, channel width and porosity ranges between 200  $\mu\text{m}$ -3.5 mm, 50  $\mu\text{m}$ -3 mm, 50  $\mu\text{m}$ -1.5 mm and 5-20% respectively. The average

porosity for all the members ranges between 5-20%. Micro-morphological investigation show that the Member QIMS-II and III show weak pedality development, QIMS-IV shows moderately pedality development and the QIMS-V to VI show strong pedality development.

Major b-fabrics observed are grano-striated, stipple-speckled, reticulate, and deformed reticulate. In general the degree of development of b-fabric in the Members QIMS-II to IV is stronger than their older soils. The groundmass of a few soils of the Members QIMS-II to IV show yellowish to orange, linear accumulation of lepidocrocite and the wet soils shows accumulation of dark brown colour due to the presence of siderite. Porosity percentage decreases from Member QIMS-II to VI soils.

In wetlands such as in Young Chautang Terminal Fans-III & II and Old Yamuna Plain-II of the study area, low chroma soils are observed. Micromorphological investigations suggest that Fe/Mn oxide features are observed in all the horizons of such soils. Thus, in wetlands, most soils are gleyed in nature and the presence of siderite and lepidocrocite supports the inference.

## **6.9 SOIL SALINITY IN THE STUDY AREA**

Nearly 60% of the geographical area of Haryana state is underlain by saline ground water. The intra-basin transfer of surface water in the early sixties for irrigation has disturbed the hydrodynamic equilibrium resulting in water-logging and salinization in large parts of the state. The existing inland drainage basin conditions did not permit the disposal of effluent drainage resulting in the continuous increase in the salinity (Singh et al., 2004).

The Rohtak region can be easily demarcated on the images indicating the excessive white patches, which are the result of the high salt efflorescence, resulting in high reflectivity. Similarly in the southern part of Haryana the presence of the excessive canal irrigation has resulted in the water-logging on a wide scale and thus increasing in the soil salt content (Fig. 2.8).

## **6.10 LINEAMENTS**

The DTM generated from DEM with vertical exaggeration 600 of by ERDAS IMAGINE 8.5 software brings out clearly two sets of lineaments D-I and D-II, striking in NE and ENE directions respectively. D-I stands for the Drishadvati River, which used to flow this area. The lineament D-II seems to younger than D-I, as the area showing this lineaments cuts across the D-II Normally lineaments are interpreted as structural features. However, in the present case, both these lineaments are considered to have been created by the Drishadvati River, which shifted its position from D-I to D-II over a short period, as oldest soils in regions of both lineaments D-I and D-II have similar age (Fig. 2.17).

## **6.11. MAJOR STRUCTURAL FEATURES OF THE STUDY AREA**

### **6.11.1 Methodology Used to Identify Faults**

Faults were identified in the four steps by following suggestions made by Singh et al. (2006), Bhosle et al. (2008) and Bhosle et al. (2009) with some modifications, given below. First drainage is examined from topographic maps. Offset and convergent drainage and drastic change in width or direction of a river over a short distance, were taken to indicate possible faults. In second step, the DTM obtained by draping Landsat image over a



DEM, generated by using ERDAS IMAGINE software with a high vertical exaggeration was helpful in identifying and mapping Himalayan Frontal Thrust and Ghaggar, Yamuna, Markanda, Jind, Rohtak and Hissar Faults. This step was not used by earlier workers. In third step, we prepared profiles in directions roughly at right angles to faults already recognized in steps (i) and (ii) throughout the whole study area using the DEM already prepared by ERDAS software. Breaks slopes in the profiles and lateral continuity of these breaks over 10's of kilometers were taken to further confirm the possibility of the presence of a fault. In this process, we paid special attention to boundaries of soil-geomorphic units, which may lie along faults. Later we prepared DEMs using SURFER 8 software with a very high vertical exaggeration using kriging extrapolation technique for areas of interest. Artifact 'cliffs' in such DEM were taken indicative of faults (Bhosle et al., 2009). Terminal fans were identified from Landsat images and these were invariably associated with faults (Table 2.4), as observed earlier by Singh et al., (2006) and Bholsle et al., (2008). In the last step, GPR was used in the field to confirm and to know subsurface nature of the all the major faults identified above.

Based above techniques, eight faults and five tectonic blocks are identified.

### **6.11.2 Faults**

Parkash et al. (2001) classified the faults in the Indo-Gangetic Plain as longitudinal (parallel to the Himalayan trend) and transverse (at large angles to the Himalayan trend). In the study area, the Himalayan Ranges trend in the NW-SE direction. So Ambala-I and II, Markanda, Patiala, Jind, Rohtak and

Hissar Faults run almost in NE-SW direction, sub-parallel to the Himalayan trend, are longitudinal in nature, whereas the faults bounding the study area i.e. Ghaggar and Yamuna Faults are transverse in nature (Fig.2.18). The Ghaggar fault consists of a number of segments and as a whole it shows a curvilinear trend with convexity towards the southeast. Similarly the Yamuna faults follow a curvilinear pattern with convexity to the southwest that controls the course of the Yamuna River.

#### *6.11.2.1 Ambala Faults-I and II*

The Ambala Fault-I and II are sub-parallel, strike in NW-SE direction, and are traceable for distances of 78 and 90 km, respectively. These faults have throws of 7-11 m (Figs. 2.20, 2.23b, 2.28). The Ambala-I Fault forms the southern boundary of the Young Piedmont in the northeast corner of the study area. This also causes offsetting of small tributaries of the Ghaggar and its tributaries like the Chola Nadi, Siswa Nadi and Buoki Nadi. The Ambala Fault- II forms boundary of the Old Piedmont-I with the Old Yamuna Plain-II for a distance of 30 km.

#### *6.11.2.2 Patiala Fault*

The Patiala fault bounds the Old Piedmont-II on the southern side and is traceable for a distance of about 104 km with a throw of 11 m (Figs. 2.20, 2.23a). Also, this fault causes an offset of the Ghaggar River by ~1.5 km and convergence of the Ghaggar and its tributary. This fault is traceable on the eastern side of the Yamuna River, passes close to Saharanpur city and leads to formation of the Katha Terminal Fan (Fig. 2.6).

#### *6.11.2.3 Markanda Fault*

The Markanda Fault is traceable over 136 km in the study area; it passes through Kurukshetra cities and causes convergence of the Markanda and Ghaggar Rivers. Also, this fault has caused the formation of the Markanda and Young Chautang Terminal Fan-I. It continues across the Ghaggar and Yamuna Rivers, to the west and east respectively, as seen in the DEM and DTM (Figs. 2.24b, 2.26). It continues east of the Yamuna River with a northerly offset of 3 km. The DEM shows that northern block is upthrown block with an average throw of around 12 m (Fig 2.20). Narrowing of the floodplains of the Ghaggar and Yamuna Rivers downstream of this fault are observed.

#### *6.11.2.4 Karnal Fault*

The Karnal Fault strikes along ESE-WNW direction and can be traced up to a distance of about 81 km. It starts in the Old Yamuna Plain and extends in NW direction near the Kaithal city forming three important fans: The Karnal Terminal Fan, Young Chautang Terminal Fan-III and the Old Yamuna Terminal Fan (Figs. 2.25c, 2.26). The throw of this fault is 7 m towards southwest. Also, it forms southern boundary of the Young Chautang Terminal Fan –I. Time of activity of faults are 2.9-3.2 (Eastern part), 2.3-2.4 (central part) and 4.7 (western part) (Table 2.4).

#### *6.11.2.5 Rohtak Fault*

The Rohtak Fault strikes roughly NW-SE and is traced over a distance of 122km and passes through the Rohtak city and extends up to Sonipat district. The DEM of the region around the fault shows that the northern block of it is an upthrown side with a throw of 11 m in the Rohtak area (Fig. 2.20, 2.24a). This fault approximately defines the boundary between the Young

Chautang Terminal Fan-II and III. Soils of the western block are much more saline and waterlogged (Fig. 2.8) as compared to those of the eastern block.

#### *6.11.2.6 Jind Fault*

The Jind fault is shortest of all the identified faults and is traceable over a distance of 35 km only in the western-central region of the study area and strikes in NW-SE direction. Over major part of its length, it has a throw of around 7 m (Fig. 2.25b). After an exceptionally wet rainy season in this semiarid region, paleochannels north of this fault were filled with water in the year 2000 and their abrupt ending against this fault helped to identify this fault (Fig. 2.22). Probably its eastward extension caused the development of the Young Chautang Terminal Fan-III during the period 2.1-2.4 ka.

#### *6.11.2.7 Hissar Fault*

This Fault runs from region near Gurgaon up to Hissar strikes in a NW-SE direction for distance of about 157 km and is the longest fault in the study area. It is in the southernmost part of the study area and acts as a boundary between the Haryana plains and the Aravalli hills in the southwestern region near Gurgaon for a distance of 67 km, and displaces alluvial/aeolian sediments in northeastern region near Hissar (Fig. 2.23c) over a distance of 90 km. This is a major barrier to the Aeolian transport of sand from the Thar desert in the south. The DEM of region around the fault indicates that the western block is the upthrown block, and thus it is antithetic to the rest of the longitudinal faults, described above. The northern block is less saline comparatively to the southern block across this fault. In the southern portion of Haryana state, small streams originating in the Aravalli flow northward and the Sahibi River from this group forms a fan (ShFn).

#### *6.11.2.8 Yamuna Faults*

The Yamuna fault system has a curvilinear shape with convexity towards the southwest. It strikes in almost NNE-SSW direction in the northern part, and strike changes to N-S direction in southern part of the study area. The fault forms a continuous ridge on the western side of the Yamuna plains and western side is upthrown block, as shown by the DEM (Fig. 2.24 c, d)

#### *6.11.2.9 Sohana Fault*

The Sohana fault strikes in N-S direction and it starts from Gurgoan, Faridabad region and ends near Delhi (Fig. 2.25a). It marks boundary of the Aravalli Formation with alluvium. As it joins the Yamuna faults in the north, it could be an extension of a segment of this fault system. Sohana water hot spring is located along this fault.

#### *6.11.2.10 Ghaggar Fault*

The Ghaggar fault is curvilinear in nature, with convexity towards SE. It starts in the Old Piedmont region, where it strikes N-S and further west it takes NE to SW direction and ends near Hanumangarh district in Rajasthan. The downthrow is towards NW. The Ghaggar River flows along this fault. This fault was first recognized by Manchanda (1981).

### **6.11.3 Tectonic blocks**

Five tectonic blocks are identified in the study area. These tectonic blocks are bounded by the transverse as well as longitudinal faults.

#### *6.11.3.1 Piedmont Block*

The Piedmont block is bound by the Himalayan Frontal Fault in the north, the Markanda Fault in the south. The block is marked by the presence

of the different piedmonts (oldest, old and young piedmonts), identified on the basis of ages and the degree of development of soils.

#### *6.11.3.2 Jind-Rohtak Block*

The Jind-Rohtak block is present in the central part of the study area between the Piedmont Block and the Aravalli block in north and south, respectively. The major portion of this block is covered by of the terminal fans (3.5 to 1.5 Ka), formed by the activity of the Karnal and Markanda Faults. Most of the area in the south is marked by the presence of a number of paleochannels. The block is characterized by weakly to moderately developed soils.

#### *6.11.3.3 Aravalli Block*

This block is overlain low hills of Aravalli Formations. The soil in this area is medium to well developed with an age of 5.3 - 4.4 Ka.

#### *6.11.3.4 Punjab Block*

This Punjab Block lies on the northwestern side of the Ghaggar Fault (Manchanda 1981., Singhai et al., 1991). This block is marked by numerous paleochannels starting from Ropar, where the River Sutlej enters the plains from the Siwalik Ranges, suggesting that these were formed as a result of northwestward migration of the Sutlej River (Pal et al., 1982). This block is marked by moderately developed soils in the southern portion and weakly-developed in the northern part.

#### *6.11.3.5 Saharanpur Block*

This block lies on the eastern side of the River Yamuna in the Uttar Pradesh state and is separated by the Yamuna fault from the Haryana Plains. Soils in this area are moderately developed with an age of 3.5-4.4 ka. On this

block the Katha terminal fan is observed, which developed due to activity of an extension of the Patiala fault.

## **6.12 DISTRIBUTION OF EARTHQUAKES**

Major part of Haryana state falls under seismic Zone-IV (<http://asc-india.org/seismi/seis-cdh.htm>). Most earthquakes in this region are shallow, though a few earthquakes from this region with intermediate depth have been recorded. Earthquake epicenters from the study area were plotted on the map showing faults. We find that the region between the Rohtak and Hissar faults is the most active. The Rohtak Fault seems to be most active followed by Hissar fault. Also, the activity of the Jind fault and Ambala fault-II possibly created a few earthquakes. Local people of Jind town tell of frequent tremors, probably caused by the Jind fault.

## **6.13 GPR STUDIES**

### **6.13.1 Haryana Region**

Radar lithofacies studies indicate that except one, all other profiles in Haryana plains show that the lower of radar profiles were deposited by a large river with a depth of >7m and upper parts were deposited by wind reworking or as terminal fan/ young piedmont sediments. Except for profile T-10 taken approximately in direction of the major river inferred from the DTMs/DEMs (Fig. 2.26, 2.23, 2.24, 2.25) all other profiles are oblique to paleoflow directions. The presence of upstream accretion on a large scale in this profile and mainly lateral accretions being present in the lower thick parts of all other profiles supports the inference of paleoflow directions determined from the DTM.

The presence of lower thick profiles (usually 7-13.5 m) in Haryana, similar to that (6.5-7.5 m) present in a profile over a large Sutlej River paleochannel, supports the inference of the presence of a large river over most of Haryana plains in recent past.

The GPR traverses across 5 out of six faults inferred from remote sensing and GIS studies confirm the presence of these faults. Also, these faults are not single faults, but are sets of a number of faults, and majority of faults show downthrown side in direction inferred from the DEMs, and the rest show downthrow in the opposite direction. Faults in individual sets are not throughout the studied profile, but most of them continue for a part of the depths studied. The Patiala and Hissar Faults show effects of activity of faults contemporaneous with sedimentation by thickening of beds on downthrown blocks.

### **6.13.2 Ganga-Yamuna Interfluvium**

The Ganga-Yamuna Interfluvium is marked by many paleochannels of the Ganga and Yamuna rivers in the northern region, close to which many Late Harappan sites are found. However, central and distal parts of Interfluvium are mainly covered by terminal fan deposits.

Lithofacies studies of the Ganga Paleochannels at Iqbalpur and Barla suggest that a large river with a depth of >7 m deposited sequences >14 m thick. These sequences were sometimes deposited by lateral accretions on sides of large bars >6 m high. Two to four subsequences with common thickness of <4 m may be present in these deposits. The subsequences were also deposited by lateral accretions on lower height braid bars and some times by vertical accretions in channels.



A model for terminal fan deposition from studies in the Ganga-Yamuna Interfluvium is presented. It consists of lower part comprising channels filled with vertical accretion deposit /lateral accretion sands, overlain by wide spread floodplain mudfacies and commonly further overlain at the top by many, narrow (rarely wide) shallow channels filled with vertical accretion deposits . Rarely, two subsequences of <2.75 m thickness, each composed of vertical accretions may form terminal a fan deposit. The tops of terminal fan deposits exhibit moderate to weak soil development.

Lithofacies analysis of the region in central reaches of the Interfluvium, mainly marked by terminal fans, brings out that the lower part of sequences observed in GPR profiles were deposited mainly by moderate sized streams with depths of 5-7 m. At a few places, the lower parts of profiles seem to have been deposited by a large river with a depth of 7-13 m. However, more detailed work needs to be done to trace the course of the large river inferred here.

Five faults inferred from DEMs and drainage pattern changes (Bhosle et al., 2008) were investigated by GPR technique and their presence was confirmed. Usually these faults consist of a set of a number of small, near vertical faults and most of these show downthrow towards directions indicated by DEMs, except for Delhi Fault, in which case almost equal number of faults show throws in opposite directions.

## **6.14 INTERPRETATION AND INTEGRATION OF DATA**

### **6.14.1 Role of climate in the Development of the Geomorphology and soils and Cultural Changes**

Some broad ideas about climatic changes during the Holocene in the present and adjoining Gangetic plains are available. Goodbred and Kuehl (2000) and Goodbred (2003) studied oceanic cores from the Bay of Bengal and Sharma et al. (2004) studied lacustrine cores from the Upper Gangetic Plain and came to the conclusion that the earlier half of the Holocene was marked by very wet and warm climate and in the later half the climate turned wet and warm. Also, studies of lacustrine sediments from the semi-arid marginal part of the Thar Desert by Singh et al. (1972, 1974, 1990) show that the periods >10,000, 10,000-5,000 and 5,000-3,000 yrs. B.P. were marked by cold and severe dry climate, slightly wetter phase and wet phases. Later drier conditions came in and continued with minor modifications till present.

Our soil-geomorphological studies indicate that since about 4.1 Ka terminal fans related to faults, formed by streams with distributary pattern have developed. As discussed later, period 4.1-3.8 Ka was a time of tectonic activity, which also caused shifting away of the Yamuna from the Haryana plain due to its uplift and forming upland, followed by development of many terminal fans due to activity of longitudinal faults. Thus role of any climatic changes is ruled out in this major change in drainage pattern of the area.

However, initiation of drier climate at about 3000 B.C., as suggested by reviews above, is considered to have caused lower discharge of rivers including that of the Sarasvati River and led to dispersal of Harappan culture from the Sarasvati Valley to north into the Indus Valley and to east.

#### **6.14.2 Structure of the Area and Nature of Faults**

All the six faults in Haryana plains are parallel to the Himalayan/Haryana Plain Basin trend and are thus longitudinal in nature. These are have normal nature at least up to a depth of 12 m. Southernmost Hissar Fault is very similar to Southern Boundary Fault (Parkash et al., 1991), between the southern Peninsula. Both are normal faults and have northerly downthrow direction. Structural features of Haryana Plains are entirely different form adjoining Upper Gangetic Plain, where surficial structural features have been worked out in fair detail (Singh et al., 2006; Bhosle et al., 2008). From tilting of large blocks in these plains, major compression from southwest has been inferred.

The major faults (Yamuna fault, Deoha-Ganga Fault, Ghaghara Fault) trend N-S or NNE-SSW in the northern region; turn N-S in the central region and take easterly to ESE direction in the south, thus giving these faults a curvilinear shape. Finite element modeling of stress conditions of the region, with compression from SW and confining of basin in west by N-S trending subsurface Aravalli Ridge and southern Peninsula in the south with E-W trending contact produced a stress a pattern very similar to the major faults, which were called as longitudinal faults (Parkash et al., 2000). More recent finite element modeling for the Gangetic plain and Haryana plains produces a stress pattern with major deformation contours in Haryana running parallel to Himalayan trend (Fig. 6.1) (Das et al., 2008). This is due to the fact that Haryana basin is much narrower than Upper Gangetic Plains. Also, Himalayas striking WNW- ESE by the side of the Gangetic Plains, take a turn along NW-SE west of the Yamuna River. Thus SW compression almost

impinges perpendicular to basin/Himalayan trend, forming Himalayan-trend parallel longitudinal faults in Haryana plains.

Major faults of the Haryana Plains are longitudinal in nature and formed by compression from a direction perpendicular to them. Most probable explanation is that they (except for Hissar fault) are imbricates of the Himalayan Frontal Fault and thus these are basically thrusts in nature. Their near normal character in the shallow subsurface as observed in GPR profiles is probably due to the fact these thrusts are curved in nature and these are nearly normal near the surface (Fig 6.2).

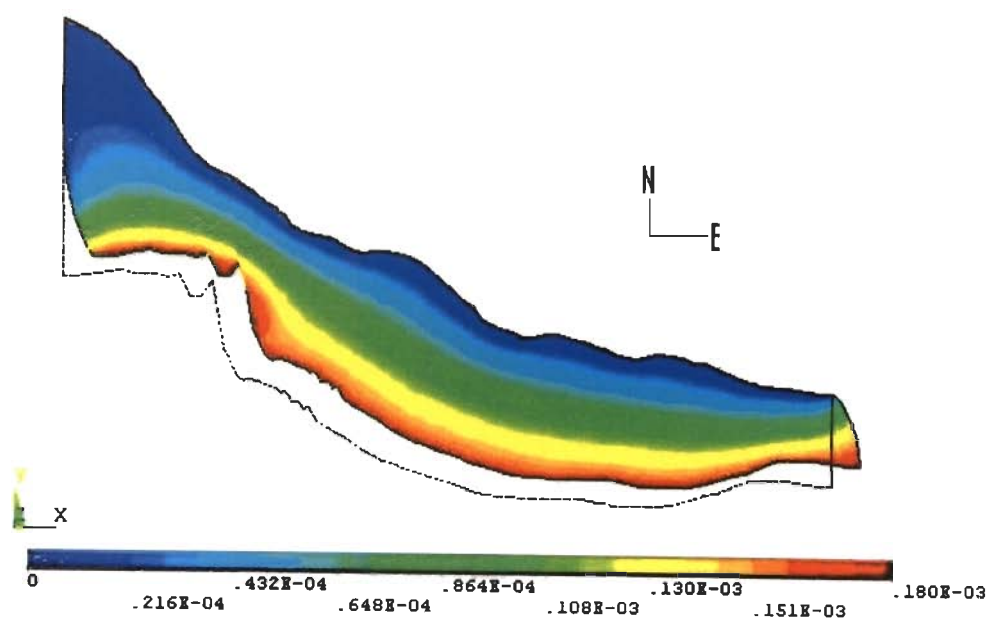


Fig.6.1 Displacement pattern in the in case where the northern boundary is fixed. Compression is from SW. (after Das et al., 2009)

### 6.14.3 Tectonics, Sedimentation and Terminal Fans

Mukerji (1976) first introduced the name and described morphology of a terminal fan (Markanda Terminal fan) from the Haryana plains. It was Mountain front, due to the loss of discharge due to evapotranspiration under considered to have formed in the plain area, away from the Himalayan

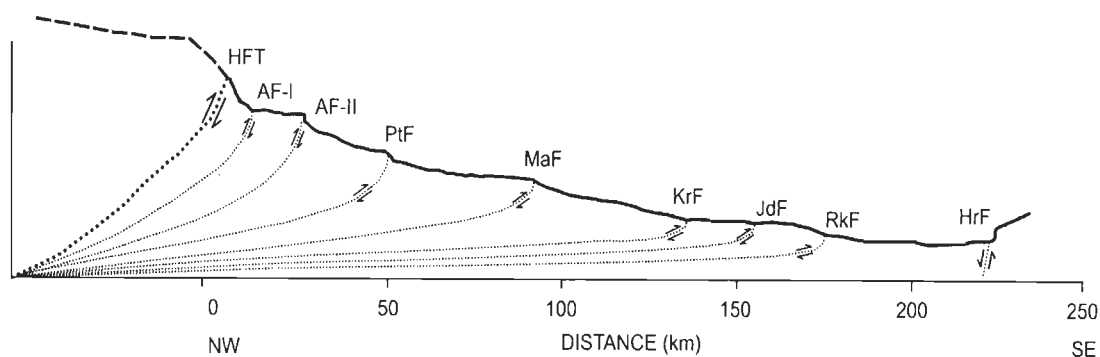


Fig. 6.2 Diagrammatic sketch showing different longitudinal faults in the Haryana plain as imbricates of the HFT (Himalayan Frontal Thrust).

semiarid climate. Parkash et al., (1983) described sedimentary sequences from shallow trenches on this terminal fan. Later Abdullatif (1989) described terminal fan of the Gash River, marked by a distributary pattern, before its disappearance into the desert from Sudan. However, later terminations of ephemeral streams from Australian semi-arid region have been described as 'floodouts' (Tooth, 1999, 2000a), channel-fans (Packard, 1974, *in* Bull, 1997) and 'erosion cells' (Bourke and Pickup, 1999). But nothing like terminal fans could be observed.

In view of non-reporting of 'terminal fans' for so many years from other parts of the world and various type of stream terminations in Australian semiarid/arid areas other than terminal fan, the existence of 'terminal fan' as being significant geomorphic features was doubted (North, 2007, Tooth, 2000b). Singhai et al. (1991) had noted the Markanda Terminal Fan formed at least partly due to a small relief created by a fault in its proximal region (now recognized as Markanda fault). Later many terminal fans related to faults have been recognized from dry subhumid Ganga-Yamuna interfluvium and sub-humid Ganga/Deoha- Ghaghara Interfluvium (Singh et al., 2006; Bhosle et al., 2008).

North (2007) has attached a great significance to the presence of distributary stream in formation of terminal fans. In our case, except for the Young Chautang Terminal Fan-I in Haryana Plains and Iqbalpur Terminal Fan in Ganga-Yamuna Interfluve, all other terminal fans in these two areas with semiarid climate were deposited by streams with distributary system. However, the sub-humid Deoha/Ganga-Ghaghara interfluve is marked by terminal fans deposited by braided streams. Thus terminal fans formed by distributary stream system seem to be related to semiarid climate, with a few exceptions.

Singh et al. (2006) and Bhosle et al. (2008) found that all the terminal fans in the major parts of the Upper Gangetic Plains were formed by involvement of the whole of the inland streams on the downthrown blocks of normal faults. However, more recently Pati (2008) studied the Middle Gangetic Plains and found that splays from a large river like Gandak could also generate 'splay terminal fans' on the downthrown sides of some normal faults. In fact, the Markanda Terminal Fan could be splay terminal fans, as the Markanda River flowing in southerly direction is constrained to flow westwards by the E-W trending Markanda Fault, Markanda Terminal Fan, probably developed on the downthrown block on the south of the Markanda fault by splays from the Markanda River. In the same way, Old Yamuna Terminal Fan developed on downthrown block south of the Karnal Fault by splays from the Yamuna River, in the process of withdrawing from this area. Similarly, splays from the Yamuna River, when it flowing along modern Chautang river course could have created Karnal (splay) Terminal Fan across the Karnal Fault and Sonipat (splay) Terminal Fan may have been developed by splays from the

Yamuna River from its present position. Thus mainly the Young Chautang Terminal Fans-I-IV were formed by involvement of the whole of the Chautang river.

#### 6.14.4 The Lost Sarasvati and Drishadvati Rivers Evolution of Drainage in the Haryana Region

As is obvious from soil-geomorphic map, even if the Yamuna had flowed through Haryana Plains, its deposits were covered by later terminal fans deposits, so obvious surficial evidences of the presence of this large river are not expected.

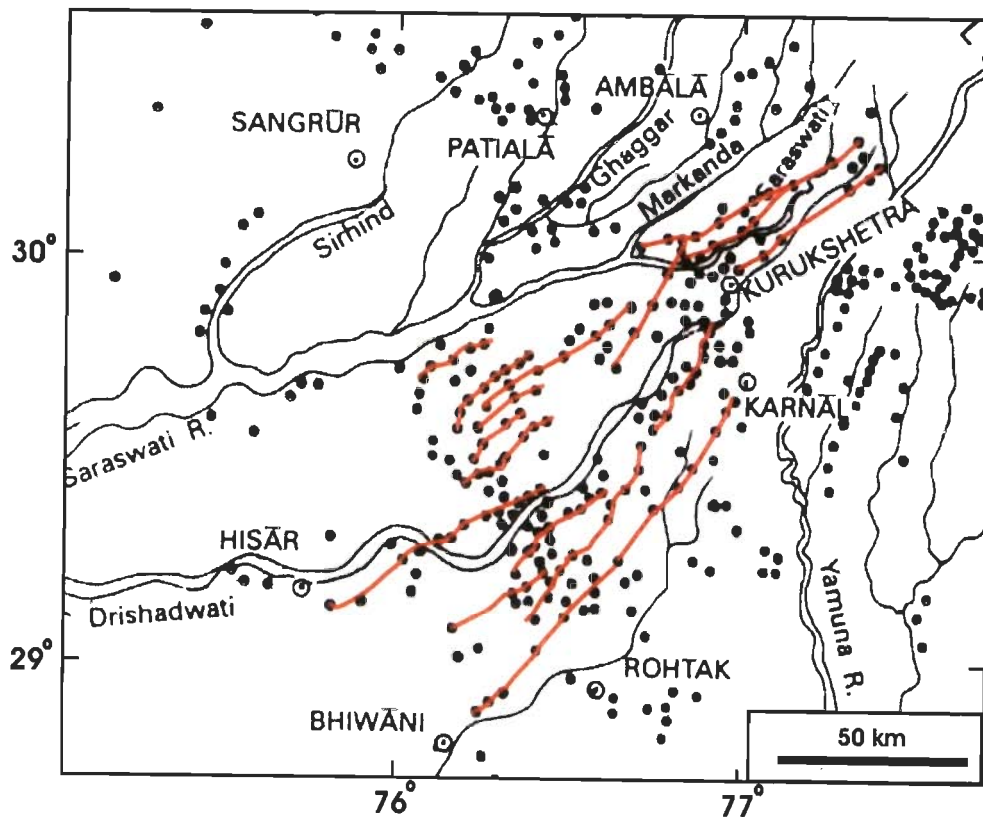


Fig. 6.3 The Proto-historic sites lie in straight lines (marked in red), which on northward extension meet the modern Yamuna River, suggesting that the Proto-Yamuna River flowed through these regions in those times (modified after Valdiya (2002)).

In Jind-Rohtak Block (Fig. 2.27), archaeological sites of pre-Harappan to post-Harappan period follow straight lines trending NE-SW (Fig. 6.3) also show

proto-Yamuna flow. Since these cultures were essentially riverine in nature it is very likely that the rivers were flowing in these directions during these periods. Indication of flow of the large Yamuna River in the same NE-SW direction from lineament map confirms this aspect. But major confirmation of the Yamuna River flowing through Haryana Plains comes from GPR studies of the subsurface lithofacies, suggesting the presence of a large river in the area in the recent past. Different types of accretions lithofacies in the GPR profiles seem to confirm the directions of large river, suggested by lineament map.

The Young Piedmont lying just east of the Yamuna River lies between 288-325 m amsl elevation, though the adjoining Old Piedmont-I has much higher elevation (282-369 m amsl). Differences in elevation of the two units are explained as follows. As the Old Piedmont-I (including Young Piedmont) was getting uplifted between the Ambala Fault-I and HFF, the large Yamuna River moved around after entering the plains and its erosion was able to keep pace with the uplift of HFF-AF-I block in the Young Piedmont region and this region was kept at a much lower level. Such a situation prevails close to points of entry of all the large rivers into the Indo-Gangetic Plains. Only after shift of the Yamuna River from Haryana to the present course, smaller streams from the Siwalik Ranges could deposit a thin layer of the low level Young Piedmont in this area. The flow of the Yamuna through the region of the Young Piedmont implies that it was flowing through the Haryana plains.

Integration of our work with available archaeological information can be used to reconstruct changes in the course of the Yamuna River in the



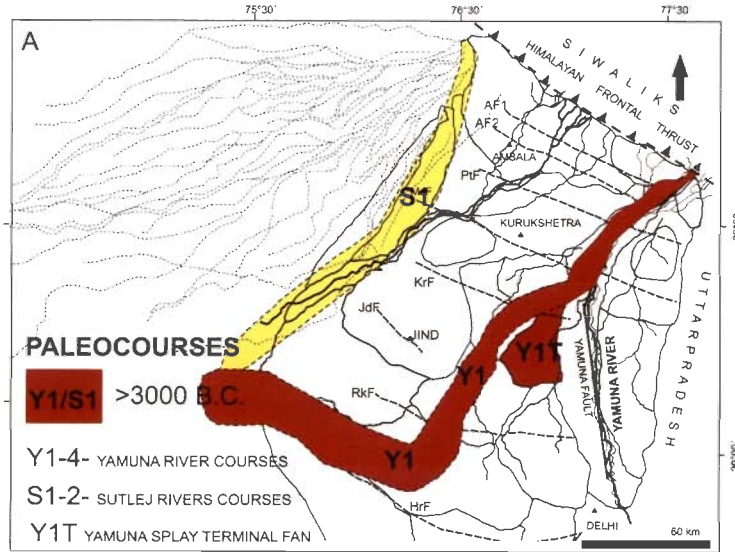
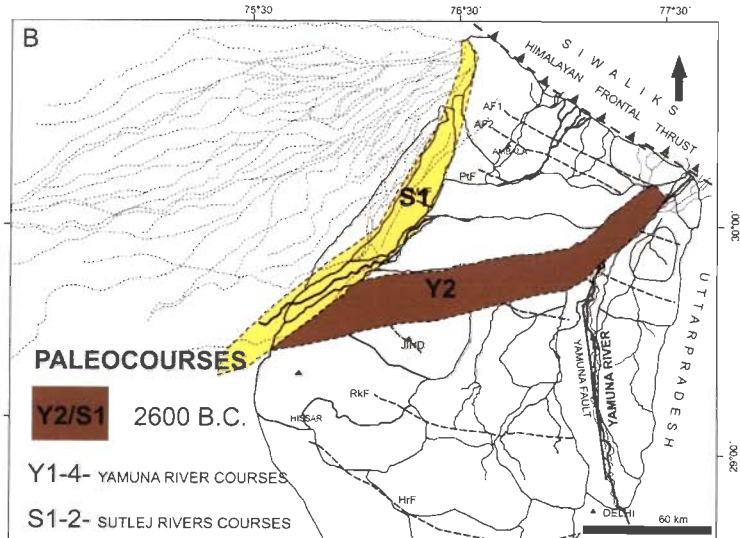
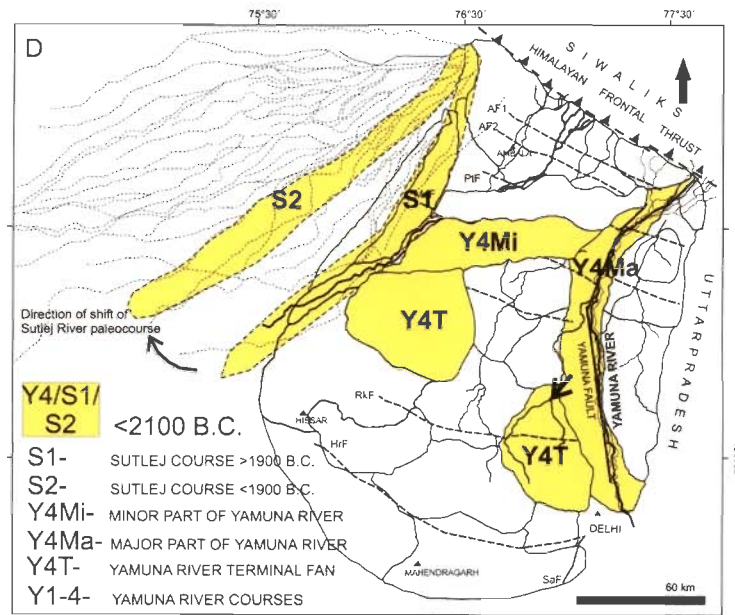
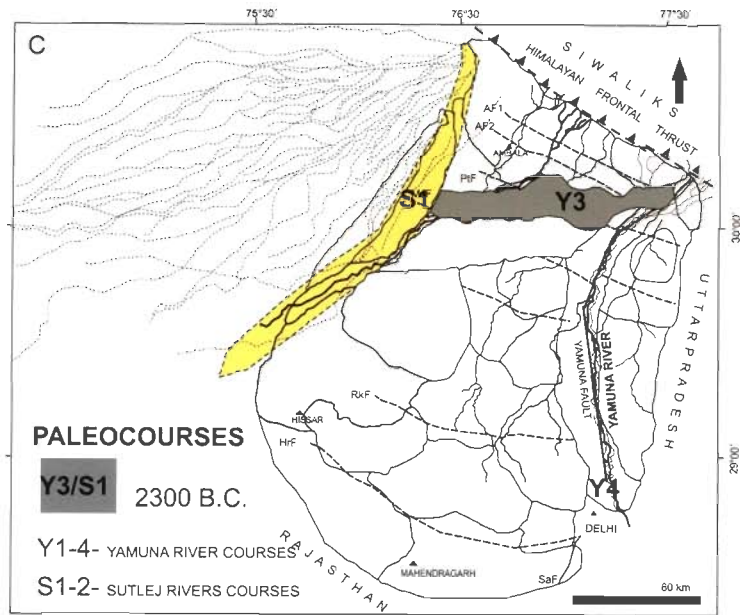


Fig 6.4 Schematic diagrams showing shifting of the Rivers Yamuna and Sutlej since about 3000 B.C.

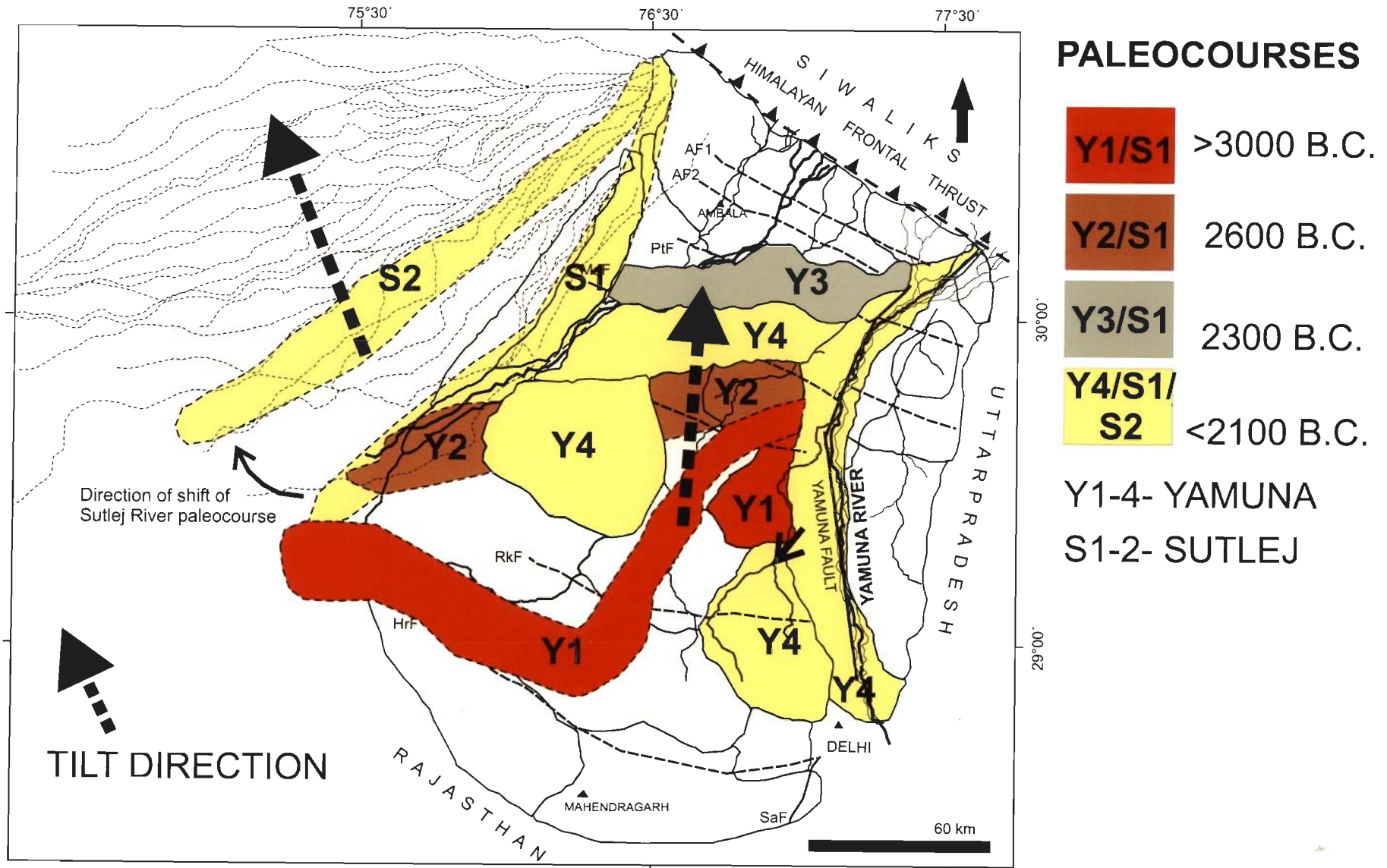


Fig. 6.5 Evolution of drainage in the Haryana plains and adjoining area during period 3000 B.C to 1900 B.C.

Haryana Plains (Fig.6.4), as suggested earlier by Wilhemy (1969), the Yamuna flowed along the modern Chautang River, forming the Drishadvati River. It was entering the Haryana Plains near Karnal, as indicated by lineaments. As Pre-Harappan (Vedic Civilization) sites are concentrated along the Jind-Hissar-Rohtak triangle on the Drishadvati course and age of the Vedic Civilizations is >3000 B.C. (Radhakrishna, 1999), it is likely that the Chautang River course is oldest course of the Yamuna in the Haryana Plain. Splays from the Drishadvati created Karnal Terminal fan.

As we can see from the soil-geomorphic map (Fig. 2.10), from the Rohtak-Jind-Hissar triangle of Pre-Harappan culture, towards northwest, we have younging sequence – Fluvial plain and Old Yamuna Plains II and III, suggesting that the Yamuna shifted northwestward through these plains in stages. The second stage was of lineament D-II in the Fluvial Plain (4.6-4.9 Ka), when the River Yamuna entering the Yamuna Plains from still more northerly position. In next stage the Yamuna occupied Old Yamuna Plain-II. In the last stage (<4.1 Ka), the major part of the River Yamuna shifted to the Old Yamuna Plain-I and a small part flowed through Old Yamuna Plains-III, till about 3.0 Ka to form the Old Yamuna Terminal fan. The Sutlej River started shifting by 3.9 Ka and soon became an independent river, instead of being a tributary of the Ghaggar (Sarasvati) River, though a minor part of it flowed through the Old Sutlej Plain-II till about 2.75 Ka.

The cause of the systematic shifting of the Yamuna towards northwest is probably tilting of the Haryana Plains towards north. A fault along the northern boundary of the Old Yamuna Plain-II and tilt around this fault would have explained the whole story nicely and it needs to be checked. Also, the Sutlej River started shifting northwestward almost at the same time due to tilting of the Panjab

block towards NNW (Singhai et al., 1991). Thus major changes in drainage pattern in the Haryana and Panjab led to complete disruption of supply of perennial flow of two major rivers (Yamuna and Sutlej) into the Ghaggar River (Sarasvati River), which caused northward and eastward movement of the Late Indus Valley (Harappan) civilization. Cause was tectonic one: involving tilt and uplift of Haryana block and tilt of the Panjab block.

Period of 3.8-4.1 Ka was very crucial in shifting of the Yamuna river, The Old Yamuna Plains-I & III are approximately of this age, suggesting either the shift in the river from Old Yamuna Plains-II to III to I took place in short period, or the river had its discharge distributed into two streams, one into Haryana Plain (Old Yamuna Plain-III) and one into the present setup in Uttar Pradesh State. This situation is very similar to the River Noa Dihing in easternmost part of Assam state (India), which also divides itself into two streams (Noa Dihing and Kaikhe Rivers) on entering the plains from the Naga Hills. During this period, Old Yamuna Terminal fan developed, when the depleted Yamuna River was flowing through the Old Yamuna Plains-III and the Sonipat Terminal developed by splays from the Yamuna River, after it had shifted to the Old Yamuna Plain-I.

After shifting away of the main Yamuna River from the Haryana Plain, activity of the Markanda Fault gave rise Markanda Terminal Fan at about 3.4 Ka and activity of Markanda, Jind, Karnal and Rohtak faults at different time gave rise to the Young Chautang terminal Fans I- IV.

## **6.15 CONCLUSIONS**

- i. Major landforms recognized from the Haryana and adjoining areas are Piedmont, Fluvial Plains (Old Yamuna Plain –I-III, Old Sutlej Plans I-II, Old and

Young Katha Plains), Aeolian Plain, Terminal Fans, Aravalli Hills and Pediments and Aravalli Piedmont.

- ii. Based on the degree of soil development and OSL ages, individual landforms were further subdivided into soil-geomorphic units e.g. Piedmont into Oldest Piedmont, Old Piedmont-I and II and Young Piedmont. In all 25 soil-geomorphic units were identified. Based on the OSL ages, this soil-geomorphic unit was grouped into six members (QIMS-I to VI) (Quaternary Indus Morphostratigraphic Sequence) of a Morphostratigraphic Sequence:  
QIMS-VI 9.86-5.38 Ka, QIMS-V- 5.38 -4.45 Ka, QIMS-IV- 4.45 - 3.60 Ka, QIMS-III - 3.60 -2.91 Ka, QIMS-II - < 2.91-1.52 Ka and QIMS-I - < 1.52 Ka.
- iii. Though there is in general increase in the degree of soil development from member QIMS-I to QIMS-VI soils, soils developed on sandy parent material show much less development than the soils developed in loamy parent material, even of similar ages.
- iv. Six sub-parallel, E-W trending longitudinal faults i.e. Ambala Faults-I and II, Markanda Fault, Patiala Fault, Jind Fault, Rohtak Fault and Hissar Fault are identified using drainage, paleo-drainage, DEMs and DTMs. In DEMs, these faults show downthrown sides to the south, except for Hissar Fault, which exhibits downthrow towards north.
- v. DEMs prepared by ERDAS software indicate NE-SW trending lineaments, which are interpreted to indicate direction of past flow of the Yamuna through these plains.
- vi. Using GRR studies, all faults except the Jind Fault have been confirmed and found to consist of a set of a number of faults, and all of them show downthrow in directions, suggested by DEMs.

- vii. GPR Lithofacies investigations of Haryana region indicate a large river (Yamuna River) was present over major parts of Haryana Plains at different times during the Holocene, whose deposits are present at shallow depths. The river had a depth of >7m.
- viii. Combining archaeological information with our data, two phases in geomorphological evolutionary history of the Haryana region can be deciphered:
- a. In first phase of 3000 B.C. to about 2200 B.C., the Yamuna was first flowing along the Chautang River course forming the Drishadvati River, it migrated northwestward slowly due to tilting of the Haryana plains towards NW. Then it shifted to its present position by 2100 B.C., though a minor flow through the Old Yamuna Plain formed the Old Yamuna Terminal Fan at about 1000 B.C. and Sonipat Terminal Fan developed by splays from the Yamuna River in its modern setting. The Sutlej River also started shifting by 1900 B.C. and soon became an independent entity, from a tributary of the Ghaggar (Sarasvati) River.
  - b. In second phase, different longitudinal faults became active and some more terminal fans (Markanda Terminal Fan and Chautang Terminal Fans-I-IV) were deposited due to their activity.
- ix a) GPR Lithofacies studies of the paleo-channels of the Ganga in the proximal part of the Ganga-Yamuna Interfluvium suggest a depth of river more than 7m.
- b) Model of terminal fan sedimentation, obtained from GPR studies suggest that the terminal fan consists of the lower part comprising channels filled with vertical accretion sands/lateral accretion sands, overlain by wide spread floodplain mudfacies and commonly further overlain at the top by many narrow

(rarely wide) shallow channels filled with vertical accretion deposits. These deposits at the top are pedogenised.

c) Also, terminal fan deposits in the middle reaches of the Interfluvium are underlain by a paleo-channel of a large river at places.

x. Major upheavals in the Proto-history of the NW India took place at about 3000 B.C. and 2000 B.C., causing major migrations of population at those periods. The one at 3000 B.C. was probably caused by a climatic change to slightly drier condition. However, our studies indicate the second major upheaval at about 2000 B.C. leading to breakdown of the drainage of 'Lost Sarasvati River' was a tectonic one, because of tilting of Panjab block causing shifting away of the major tributary Sutlej River and uplift of the Haryana Block leading to shift of the second tributary Yamuna River, from Haryana to the present position.

## BIBLIOGRAPHY

- Abdullatif, O.M., 1989. Channel-fill and sheet flood facies sequence in the ephemeral terminal River Gash. Kassala, Sudan. *Sediment. Geol.*, 63: 171-184.
- Agarwal, R.K., 1977. Structure and Tectonics of Indo-Gangetic Plains. *Geophysical Case Histories of India. Assoc. Explor. Geophys., Hyderabad, India*, 1 9-46.
- Ahuja, R.L., Garlapuri, V.N., Manchanda, M.I and Khanna, S.S., 1978, Physiography and Soil association of Haryana. *J. Indian. Soc.. Soil. Sci.*, 26(3): 261-267.
- Ahuja, R.L., 1981, Pedogenic characteristics of the Ghaggar River basin of Himalaya. (Unpubl.) Ph.D thesis, Haryana Agriculture Univ., Hissar, 309p.
- Ahuja, R.L. and Mahendra Singh., 1983, A report on Soils of Hissar districts and management., Deptt. of Soils, Haryana Agriculture Univ. Publ., 75 pp.
- Aitken, M.J. 1985. *Thermo-luminescence Dating*, Academic Press, London, 359p.
- Aitken, M.J., 1998. *An Introduction to Optical Dating*. Oxford University Press, 267p.
- Allen, J.R.L., 1983. Studies in fluvial sedimentation: bars, bar-complexes and sandstone sheets (low sinuosity braided streams) in the Brownstone (L. Devonian), Welsh Borders. *Sediment. Geol.*, 33: 237-293.
- Anand R.R. and Sehgal, J.L., 1977, Nature and distribution of clay minerals in relation to different landscapes of some soils of Malwa alluvial, plain (Punjab). *Fertil, Technol.*, .14: 66-69.
- Audru, J.-C., Bano, M., Begg, J., Berryman, K., Henrys, S., Niviere, B., 2001. GPR investigations on active faults in urban areas: the Georisc-NZ project in Wellington, New Zealand. *Earth Planet. Sci.* 333: 447– 454.
- Bajpai, V.N., 1989. Surface and subsurface evidence of neotectonics and aquifer disposition in central Gangetic alluvial terrain of Kanpur-Unnao region in Uttar Pradesh, India. *Photonirvachak*, 17(2): 47-53.
- Bakhiwal, P.C. and Grover, A.K., 1988. Signature and migration of Sarasvati River in the Thar desert, Western India. *Rec. Geol. Surv. Ind.*, 116; 3-8.
- Beres, M., Haeni, F.P., 1991. Application of ground-penetrating radar methods in hydrogeologic studies. *Groundwater*. v.29, p. 375– 386.



Best, J.L., Ashworth, P.J., Bristow, C.S., Roden, J., 2003. Three dimensional sedimentary architecture of a large, mid-channel sand braid bar, Jamuna River, Bangladesh. *J. Sediment. Res.* 73: 516–530.

Bhandari, R.C., Curtis.L.F. and Shukla, U.C., 1976, Visual interpretation of Landsat Imagery of Central and Southern districts of Haryana state, *J. Indian. Soc. Photo-interpretation*, 4: 37-41.

Bhargava, G.P. and Pal, D.K., 1985. Clay illuviation in a sodic soils of north-western part of Indo-Gangetic alluvial plain, *Clay Research*, 4(1): 7-13.

Bhat, G.M and Bhat, G.D. 1997. Stratigraphy and depositional environments of Late Permian carbonates, Kashmir Himalaya. *Geology in South Asia-II*, Geological Survey and Mines Bureau, Sri Lanka, pp. 205-223.

Bhatia, K.B. and Khosla, B.C., 1977. Sub-recent ostracodes from Tehsil Charki-Dadri, distt. Mahendragarh, southern Haryana., *J. Palaeon. Soc. India.*, .20: 333-338.

Bhatia, S.B. and Singh, N., 1988. Middle Holocene paleoclimatic and palaeoenvironmental events in southern Haryana. *Bull. Ind. Nat. Sci.. Acad.*, v.54,p 574-584

Bhosle, B.N., 2006. Holocene evolution of the western Gangetic Plain, India. (Unpubl.) Ph.D Thesis, Department of Earth Sciences, Indian Institute of Technology, Roorkee, India, 220p.

Bhosle, B., Parkash, B., Awasthi, A.K., Singh, V.N., Singh, S., 2006. Remote sensing-GIS and GPR studies of two active faults, Western Gangetic Plains, India. *J. App. Geophys.* , 61(2): 155-164.

Bhosle, B., Parkash, B., Awasthi, A.K., Singh, S. and Khan, M.S.N. 2008. Role of extensional tectonics and climatic changes in geomorphological, pedological and sedimentary evolution of the Western Gangetic Plain (Himalayan Foreland Basin), India. *Himalayan Geology*, 29 (1):.1-24.

Bhose, B. Parkash, B., Awasthi, A.K. and Pati, Pitambar, 2009. Use of digital elevation models and drainage patterns for locating active faults in the Upper Gangetic Plain, India. *Intern. J. Remote Sens.*, 30 (3): 673-691.

Bhumbla., D.R. and Dhingra, D.R., 1964. Micronutrient status of saline and alkaline soils of the Panjab, *J. Indian Soc. Soil Sci.*, 12(4): 255-260.

Bourke, M.C., and Pickup, G., 1999, Fluvial form variability in arid Central Australia, In Miller, A.J., and Gupta, A. (Eds.), *Varieties of Fluvial Form*: Chichester, U.K., John Wiley & Sons; 249–271.

Bristow,C.S. 1987. Brahmaputra River : Channel migration and deposition ,in Ethridge.F.G.,Flores,R.M. and Harvey, M.D. (Eds.), *Recent Developments in Fluvial Sedimentology*: SEPM, Special Publication, 39:. 63-74.

Bristow, C.S., Jol, H.M. (Eds.), 2003. Ground Penetrating Radar in Sediments. Geol. Soc. London Spec. Publ., vol. 211p.

Bull, W. B., 1997. Discontinuous ephemeral streams. *Geomorphology*, 19: 227-276.

Bullock, P., Fedoroff, N., Jongerius, A., Stoops, G. and Tursina, T., 1985. Handbook for Soil Thin-Section Description. Waine Res. Publ., U.K., 152p.

Catt, J.A., 1986. Soils and Quaternary Geology. Monographs on Soil and Resource Surveys, 11, Clarendon, Oxford, 267p.

Catt, J.A., 1990. Paleopedology Manual. *Quat. Intern.*, 6: 1-95.

Center, W.J., 1880. Note on alkali or rieh soils and saline well water. *Rec. Geol. Surv. India.*, 43: 253-273.

Chopra, S. and Thusu, J. L., 1988. A note on the avulsion of Ghaggar river in the Alluvial Plains of Punjab and Haryana, Northwest India, *J. Ind. Soc. Remote Sens.*, 2: 46-77.

Complete study report on perspective landuse for Haryana State. Central Ground water Board (C.G.W.B June (2004) S. no. 24, ref. 1223.

Computer Simulation Model for Ground Water Basins. Central ground water Board (CGWB Aug 2008), Chandigarh, S. no. 34, ref. 223.

Corbeanu, R.M., Soegaard, K., Szerbiak, R.B., Thurmond, J.B., McMechan, G.A., Wang, D., Snelgrove, S., Forster, C.B., Menitove, A., 2001. Detailed internal architecture of a fluvial sandstone determined from outcrop, cores, and 3-D ground penetrating radar: example from the middle Cretaceous Ferron Sandstone, east-central Utah, *Am Assoc. Petrol. Geol. Bull.*, 85: 1583-1608.

Courty and Fedoroff, N., 1985. Micromorphology of recent and buried soils in a semi-arid region of N-W, India., *Geoderma*, 35: 287-332.

Cunningham, A., 1877, *The Ancient Geography of India.*, Reprinted .1979 by Indological Book House., Varanasi.

Das, Bhaswati, 2008). Finite element modeling for the Indo-Gangetic plain, (Unpub.) M.Tech Dissertation, Deptt. of Earth Sciences, IIT Roorkee.

De Sigmond, A.A.J., 1927, Classification of alkaline and salty soils., *First Intern. Congr. Soil. Sci. Proc.*, 1: 330-340.

Dey, N.L., 1927. *The Geographical Dictionary of Ancient, and Medieval India*, Reprinted, 1979., Cosmo. Publ., N.Delhi.

Dhankar, Jain, R.P., Lai, S.P., Rana, T., K.P.C and Pandey, S., 1983. Geomorphology, Soils and Landuse of Haryana., Publ. Nat. Bur. Soil Surv. and Landuse Planning; Nagpur,

Duggal, S.L., 1977. Water Resources of Haryana., Haryana Agricultural University Hissar.

Fairbridge, R.W. (Ed.), (1968). Encyclopedia of Geomorphology, Encyclopedia of Earth Sciences Volume 3. Reinhold Book Corp., New York, 1295p.

Fisher, C. S., Stewart, R.R. and Jol, H. M., 2000. Processing Ground Penetrating radar. Proceedings of Eighth International Conference on Ground Penetrating Radar, University of Queensland.

Franklin, A.D., 1998. A kinetic model of the rapidly bleaching peak in quartz thermo-luminescence. *Radiat. Meas.*, 29(2): 209-221.

Friend, P.F., 1978, Distinctive features of some ancient river systems, in Miall, A.D. (Ed.), *Fluvial Sedimentology*, Can. Soc. Petrol. Geol. Mem. 5 531-542.

Friend, P.F., 1998. General form and age of the denudation system of the Himalaya. *GFF.*, Part-II, 120(2): 231-236.

Galehouse, J.S., 1971. Sedimentation analysis. In: Carver, R.E. (Ed.), *Procedures in Sedimentary Petrology*, Wiley-Inter science, London: 69-94.

Garlapuri, V.N., 1984, Geomorphology of Haryana State., Proc. of fifth Asian Conference on Remote Sensing (Nov. 15-18) (ACRS). Kathmandu, Nepal., 8-1-9.

Gawthorpe, R.L., Collier, R.E.L., Alexander, J., Leeder, M., Bridge, J.S., 1993. Ground penetrating radar: application to sandbody geometry and heterogeneity studies. In: North, C.P., Prosser, D.J. (Eds.), *Characterization of Fluvial and Aeolian Reservoirs*. Geol. Soc. Lond. Spec. Publ., 73: 421-432.

Geddes, A., 1960.. The alluvial morphology of the Indo-Gangetic Plain: Its mapping and geographical significance. *Trans. Int. Geog.*, 28: 253-276.

Geological Survey of India, Calcutta: 26-27. (Please make changes in text and seismotectonic map caption and quote this as Narula et al., (2000).

Gerrard, J., 1994. The landslide hazard in the Himalayas - geological control and human action. *Geomorphology*, 10(1-4): 221-230.

Godfrey-Siith, D.I., Huntley, D.J and Chen, W.H., 1988. Optical dating studies of quartz and feldspar sediment extracts. *Quat. Sci. Rev.*, 7:373-380.

Goodbread, Jr., S.L. and Kuehl, S.A., 2000. Enormous Ganges-Brahmaputra sediments discharge during strengthened early Holocene monsoon. *Geology*, 28: 1083-1086.

Goodbread Jr., S.L., 2003. Response of the Ganges dispersal system to climate change: a source-to-sink view since the last interstade. *Sedimentary Geology*, 162: 83–104.

Govindrajan, S.V., 1970. Soil Map of India., All India Soil and Landuse Survey (IARI), New Delhi.

Goyal, V.P., 1981. Landform soil-relationship and pedogenic characterisation of the soils of a part of southern Haryana., (Unpubl.) Ph.' D. Thesis, Haryana Agri. Univ., Hissar.

Gupta, R.P., 1991. Remote Sensing Geology. Springer-Verlag, Berlin, Heidelberg, 356p.

Gupta, S.P., Asthana, S and Nath, A., 197. Painted Greyware sites in relation to old river beds in Rajasthan, In: Agarwal, D.P. and Pande, B.M , (Eds.), Ecology and Archaeology of Western India, Concept Publ. Co. Delhi: 79-92.

Huntley, D.J., Godfrey-Smith, D.I. and Thewalt, M.L.W., 1985. Optical dating of sediments. *Nature*, 313(10): 105-107.

Hutt. G, Jaek, I. and Tchonka J.,1988. Optical dating: K- feldspar optical response stimulation spectra *Quat. Sci. Rev.*, 7: 381-386.

Indras., 1967, Lost Saraswati, Sardar Patel University, Vallabh Vidhyanagar, p.

Jackson, R.G., 1976. Sedimentological and fluid-dynamic implications of the turbulent bursting phenomenon in geophysical flows. *J. Fluid Mech.* 77: 531–560.

Jol, H.M., Smith, D.G., Meyers, R.A., 1996a. Digital Ground Penetrating Radar (GPR): a new geophysical tool for coastal barrier research (examples from the Atlantic, Gulf and Pacific coasts, USA. *J. Coast. Res.* 12: 960– 968.

Jol, H.M., Smith, D.G., Meyers, R.A., 1996b. Three dimensional GPR imaging of a fan-foreset delta: an example from Brigham City, Utah, U.S.A. *Proceedings of GPR '96: 6th International Conference on Ground Penetrating Radar*, September 30–October 3. Tohuko University, Sendai, Japan: 33– 37.

Jol, H.M., Bristow, C.S., 2003. GPR in sediments: advice on data collection, basic processing and interpretation, a good practice guide. In: Bristow, C.S., Jol, H.M., eds., *Ground Penetrating Radar in Sediments*. *Geol. Soc. London Spec. Publ.* 211: 9 –27.

- Jongerius, A. and Heintzberger, G., 1975. Methods in Soil Micromorphology; A technique for the preparation of large thin sections, Soil Survey Paper No. 10, Netherland Soil Surv. Inst., Wageningen, 152p.
- Joping, A.V. and Walker, R.G., 1968. Morphology and origin of ripple-drift cross-lamination, with examples from the Pleistocene of Massachusetts. *J. Sediment. Res.*, 38(4): 971-984.
- Joshi, J. P., Madhubala., Jas Ram., (1984). The Indus civilization: A reconsideration on the basis of distribution maps. In: *Frontier of the Indus civilization*, B.B Lal and S.P Gupta (Eds), Books and Books, New Delhi, pp. 511-539.
- Kapoor, B.S., Singh,, H.B., and Goswami, S.C., 1981, Distribution of illite in some alluvial soils of the Indo-Gangetic plain. *J. Indian Soc. Soil. Sci.*, 29: 572-574.
- Kar, A. and Ghose, B., 1984. The Drishadvati river system of India- an assessment and new findings. *Geogr. J.*, 150:122-229.
- Kaushik, R.N and Shukla, U.C., 1977. A study on the development of salt-affected soils in a typical area., *J. Indian Soc. Soil. Sci.*, 25:276-283.
- Keith, A.B., 1922, The age of the Rigveda, In: Rapson, F.J. (Ed.) *The Cambridge History of India.*, Reprinted (1962), .S.Chand & Co, N.Delhi.: 69-101.
- Kelly, S.B., and Olsen, H., 1993. Terminal fans—a review with reference to Devonian examples: *Sediment. Geol.*, 85: 339–374.
- Khan, A.U., Bhartiya, S.P. and Kumar, G., 1996. Cross-Faults in Ganga Basin and their surface manifestations. *Geol. Surv. Ind., Sp. Publ.*, 21(2): 215-220.
- Khanna, S.S., Ahuja, R.L., Manchanda, M.L., Sangwan, B.S and Gpyal, V.P., 1977, Soil-landscape relationship of the dune infected PreCambrian pedepain area in S-W part of Haryana., *Ann. Arid Zone*, 16: 201-212.
- Kochhar, N., 1984. Malani Igneous suite: Hot spot magmatism and carbonatiszation of Northern part of India Shield. *J. Geol. Soc. India*. 25: 155-161.
- Kooistra, M.J., 1982, *Micromorphological Analysis and Characterisation of -70. Benchmark Soils of India, Parts I & II.*, Netherland Soil Survey Inst. Wageningen.
- Krishnan, M.S., 1952, *Bull. Natl. Inst. Sci. India*. pp. 1-19.
- Kristof, S.J and Zachary,A.L., 1971. Mapping soil types from multi spectral data, *Proc. 7th Intern. Symp. on Remote Sensing of Environ.*: 2095-2109.

Kumar, S., 1991. A Holocene soil chronoassociation and neotectonics in the Western Gangetic Plains, India. Ph.D. Thesis (unpubl.), Dept. Earth Sc., Univ. of Roorkee, India, 292p.

Leather, J. W., 1897, Reclamation of salt-rich or user lands., *Agri.Ledger.* 7, 9, 13, 37.

Levine, E.L. and Ciolkosz, E.J., 1983. Soil development in till of various ages in northern Pennsylvania. *Quat. Res.*, 19: 85-99

MacBeth Division of Kollmorgen Instruments Corp. 1975. Munsell Soil Color Charts, Baltimore, MD.

Manchanda, M.L and Khanna, S.S., 1979, Soil salinity and landscape relationships in part of Haryana, India. *J. Indian Soc. Soil. Sci.*

Manchanda, M.L and Hilwig, F.W., 1981, Visual interpretation of, computer transformed Landsat Imagery for salt-affected areas of part of Haryana., *Photonirvachak.*, Ind. J. Photo-Inter. and Remote Sensing., 9 No.2.

Manchanda, M.L and Hilwig, F.W., 1983, Micromorphological studies of Indo-Gangetic alluvial plain developed under different climatic conditions., *J. Indian. Soc. Soil. Sci.*, 31: 73-84.

Manchanda, M.L and Iyer, H.S., 1983. Use of Landsat imagery and aerial photographs for delineation and characterisation, of salt-affected soils of part of N-W India., *J. Indian. Soc. Soil .Sci.*, 31: 263-271.

Manchanda, M.L and Khanna, S.S., 1981, Identification of new sub-groups for Taxonomical classification of salt-affected soils of a part of Haryana. , *J. Indian Soc. Soil Sci.* 29(2): 241-248.

Manchanda, M.L., 1981, Study of Landsat imagery and aerial photographs for evaluation of salt-affected soils of part of north-west India, M.Sc. Diss., Deptt. of Soil Survey, Inter. Inst. for Aerial' Survey and Earth Sciences, Enschede, p.

Medlicott, H.B., 1878, The reh soils of the upper India. *Rec. Geol. Surv. India.* 13:273-276.

Menzies, J. (ed.), 1995. *Modern Glacial Environments: Processes, Dynamics and Sediments.* Butterworth-Heinemann Ltd., Oxford, UK, 621 p.

Miall, A.D., 1988. Reservoir heterogeneities in fluvial sandstones: lessons from outcrop studies. *Bull. Am. Assoc. Petrol. Geol.*, 72: 682-697.

Middleton, G.V. and Neal, W.J., 1989. Experiments on the thickness of beds deposited by turbidity currents. *Journal of sedimentary petrology*, 59(2): 297-307.

Miedema, R., Th. Pape and Van der Wall, G.J., 1974. A method to impregnate wet soil samples, producing high-quality thin sections. *Netherland. J. Agric. Sci.*, 22: 37-39.

Mohindra, R. and Parkash, B., 1992. Historical geomorphology and pedology of the Gandak megafan, Middle Gangetic Plains, India. *Earth Surface Processes and Landforms*, 17: 643-662.

Mughal, M.R., 1982.. Recent Archeological research in Cholistan desert. In: *Harappan Civilization: a contemporary perspective*, Gregory L. Possphl (Ed.), Oxford and IBH Publ. Co, New Delhi: 85-95.

Mukerji, A.B. (1975). Geomorphic patterns and processes in the Terminal Triangular Tract of Inland streams in Sutlej-Yamuna Plain. *J. Geol. Soc. India*, 16: 450-459

Mukerji, A.B. (1976). Terminal fans of Inland streams in Sutlej-Yamuna Plain India. *Z. Geomorph. N.F.*, 20: 190-204.

Nakata, T., 1982. A photo-interpretation study of active faults in the Nepal Himalayas. *J. Nepal Geol. Soc.*, 2: 67-80.

Narula, P.L., Acharyya, S.K., Banerjee, J. (Eds.), 2000. Eastern Nepal Himalaya and Indo-Gangetic Plains of Bihar. In: *Seismotectonics Atlas of India and Its Environs*.

Neal, A., 2004., Ground-penetrating radar and its use in Sedimentology: principles, problems and progress. *Earth Sci. Rev.*, 66: 261-330.

North, C.P., Wariswick, G.L., Fluvial fans: myths, misconceptions, and the end of the terminal-fan model, *J. Sediment. Res.*, 2007, 77: 693–701.

Oldham, C.F., 1874. Notes on the lost rivers of the Indian desert, *Calcutta Rev.*, 59: 1-27.

Oldham, C.F., 1893. The Sarasvati and the lost river of Indian desert. *J. Roy. Asiatic Soc.*, 25: 49-76.

Oldham, R.D., 1886. On probable changes in the Geography of the Panjab and its rivers: a Historic Geographical study, *J Asiatic Soc. Bengal*. 55: 322-343.

Olhoeft, G. R. 1984. Applications and limitations of ground penetrating radar. 54th annual international meeting and expositions of the Society of Exploration geophysicists, Dec 2-6, Atlanta, Georgia. Expanded abstracts with Biographies: 147-148.

Olsen, H., Andreasen, F. 1995. Sedimentology and ground-penetrating radar characteristics of a Pleistocene sandur deposit. *Sediment. Geol.* 99, 1–15.

Onorati, G., Poscolieri, Ventura, R., Chiarini, V. and Crucila, U., 1992. The digital elevation model for Italy for geomorphology and structural geology. *Catena*, 19:147-178.

Pal, Y., Sahai, B., Sood, R.K and Agarwal, D.P., 1980. Remote sensing of the 'lost' Sarasvati river. *Indian Acad. Sci.* , 89(3): 317-331.

Packard, F.A., 1974. The Hydraulic Geometry of a Discontinuous Ephemeral Stream on a Bajada near Tucson, Arizona. Univ.Arizona, Ph.D. Thesis (Unpubl.), 127 p.

Pandya, A.V., 1967. The lost Sarasvati. Vallabh Vidyanagar Press. Vallabh Vidhyanagar (Anand Gujarat). 167p

Pareek, H.S., 1984.: Prequaternary geology and Mineral resources of Northwestern Rajasthan. *Mem. Geol. Soc. India*, 22: 517-527.

Parkash, B. Sharma, R.P. and Roy, A.K., 1980, The Siwalik Group (Molasse), sediments shed by the collision of continental plates. *Sediment. Geol.*, 25: 127-159.

Parkash, B., Awasthi, A.K and Gohain, K., 1983, Lithofacies of the Markanda terminal fan, Kurukshetra district, Haryana. *Spec. Publ. Intern. Assoc. Sediment.*, 6: 337-344.

Parkash, B. and Kumar, S., 1991. The Indo-Gangetic Basin, In: *Sedimentary Basins of India- Tectonic Context*, Tandon, S.K., Pant, C.C. and Casshyap, S.M. (Eds.), Gyanodaya Prakashan, Nainital, India: 147-170.

Parkash, B., Kumar, S., Rao, M.S., Giri, S.C., Kumar, C.S., Gupta, S. and Pankaj Srivastava, 2000. Holocene tectonic movements and stress field in the western Gangetic Plains. *Current Sci.*, 79: 438-449.

Parkash, B., S., Rao, S.M., Giri, S.C., Kumar, C.S., and Gupta, S. and Srivastava, P. (2001). Active tectonics of the western Gangetic Plain. In: O.P Verma (Ed.). *Research Highlights in the Earth system Sciences, DST Spec. 2: 141-158.*

Pati, P., 2008. Holocene Tectono-sedimentary evolution of parts of the Middle Gangetic Plain. (Unpubl.) Ph.D thesis, Deptt. of Earth Sciences, IIT Roorkee, India, p.

Radhakrishna and S.S. Merh. 1999 Vedic Sarasvati: Evolutionary History of a Lost River of Northwestern India *Geol. Soc. India Mem.*, 43: 47-51.

Raike, R.L., 1968, Kalibangan: Death from natural causes, *Antiquity*, 42(168): 286-291.

Rao, M.B., Ramchandra. , 1973. The sub-surface geology of Indo-Gangetic plains. *J. Geol. Soc. India*, 14: 217-242.



Rao, Y.S.N., A.A. and Rao, D.P., 1974. On the structure of the Siwalik Range between the rivers Yamuna and Ganga. *Him. Geol.*, 4: 137-150.

Raychoudhary, S.P., 1963. Saline alkali soils of India: Morphology, genesis of some selected saline and alkali soils of Bihar, U. P. and Panjab., *Indian. J. Aqri. Sci.*, 33: 28-33.

Research Highlights in the earth system Sciences, DST Spec. Vol.2 on Seismology, 141-158p.

Reynolds, J.M., 1997. *An Introduction to Applied and Environmental Geophysics*. Wiley, Chichester. p.

Riapson, F.J., 1914. Ancient India from the earliest times to the first century A.D., In: *Cambridge History of India*, Cambridge Univ. Press.

Roy, R.B., Ghosh, B and Pandey, S., 1967, Landscape-soil relationship in Chohtan block in Barmar districts in Western Rajasthan. *J. Indian Soc. Soil. Sci.*, 15: 53-59.

Sadler, S.P., and Kelly, S.B., 1993, Fluvial processes and cyclicity in terminal fan deposits: an example from the Late Devonian of southwest Ireland: *Sedimentary Geology*, v. 85, p. 375–386.

Sahu, B. K., 1982. Multigroup discrimination of sedimentary depositional environments using sphericity distribution statistics. *Mathematical Geology*, 14: 577-586.

Sangwan, B.S., 1978, Pedogenic characterisation of the soils of Southern Haryana.,Unpub;. Ph.D. Thesis., Univ. of Udaipur.

Sarma, S.C., 1974. The description of rivers in the Rigveda. *Geogr. Observer*, 10: 79-85.

Sastri, V.V., Bhandari, L.L., Raju, A.T.R. and Datta, A.K., 1971. Tectonics framework and subsurface stratigraphy of the Ganga basin. *J. Geol. Soc. Ind.*, 12(3): 222-233.

Schoeneberger, P.J., Wysocki, D.A., Benham, E.C. and Broderson, W.D., 1998. *Field book for describing and sampling soils*. National Resources Conservation Service, U.S.D.A., National Soil Survey Center, Lincoln, NE.

Sehgal, J.L and Coninck, F.D., 1971. Identification of 14 A and 7 A Clay minerals in Panjab soils. *J. Indian Soc. Soil Sci.*, 29: 572-574.

Sehgal, J.L and Stoop, G., 1972. Pedogenic calcite accumulation in arid and semi-aridic regions of the Indo-Gangetic alluvial plain of erstwhile Panjab (India)-their morphology and origin., *Geoderma*, 8: 59-72.

Sehgal, J.L., 1974.. Nature and geographic distribution of clay minerals in the soils of different moisture regimes in Punjab, Haryana and Himachal Pradesh. Proc. Ind. Nat. Science Acad., 40B: 151-159.

Sen, A., 1958. Influence of climatic factors on salinity of Indian soils. Indian J. Agri. Sci., 28: 61-64.

Shankarnarayan, H.S and Hirekerur. L.R., 1972. Characterization of some soils of north Indian plains. J. Indian. Soc. Soil. Sci., 20: 157-167.

Sharma, S., Joachimski, M., Sharma M., Tobschall, H.J., Singh, I.B., Sharma C., Chauhan, M.S. and Morgenroth, G., 2004. Late glacial and Holocene environmental changes in Ganga plain, Northern India, Quat. Sci. Rev., 23(1-2):145-159.

Sidhu, P.S., 1976. Aeolian additions to the soils of North-West India. Podologie, , 27(3): 323-336.

Sidhu, P.S and Gikes, R.J., 1977. Mineralogy of the soils developed in alluvium in Indo- gangetic plain (India). Soil. Sci. Soc. Am. J., 41; 1194-1201.

Sidhu, P.S., Hall, G.F., and Sehgal, J.L., 1976. Influence of aeolian dust, of the surface soil properties in the Central Panjab. Ann. Arid Zone, 15: 89-94.

Simenson, G.H and Boersma, L., 1972. Soil morphology and water table relations. II. Correlation between annual water table fluctuations and profile features. Soil. Sci. Soc. Am. Proc., 36: 649-653.

Singh Gurdev, 1952, Geographer, 5, 27, 12.

Singh, A.N., Misra, D.S. and Babu, P.S., 1988. Comparative evaluation of IRS-IA LISS-I and LANDSAT-4 MSS DATA for delineation of salt-affected soils in a part of Sultanpur District, Uttar Pradesh. Nat. Sem. on Ind. Remote Sensing Satellite-1A Mission and its application Potential, Hyderabad: 21-22.

Singh, G., 1971. The Indus Valley culture (seen in context of post-Glacial climate and ecological studies in north-west. India), Archaeological and Physical Anthropology in Oceania, 6(2): 177-189.

Singh, G., Joshi, R.D. and Singh, A.B., 1972. Stratigraphic and radiocarbon evidence for the age and development of three salt lake deposits in Rajasthan, India. Quat. Res., 2: 496-505.

Singh, G., Joshi, R.D., Chopra, S.K and Singh, A.B., 1974, Late Quaternary history of vegetation and climate of the Rajasthan desert, India. Philos. Transac. Royal Soc. London., 267(889): 467-501.

Singh, G., Wasson, R.J. and Agarwal, D.P., 1990. Vegetational and seasonal climatic change since the last full glacial in the Thar Desert, northwestern India. Rev. Paleobot Palynol., 64: 351-358.

Singh, I.B., 1987. Sedimentological history of Quaternary deposits in Gangetic Plain. *Ind. J. Earth Sci.*, 14(3-4): 272-282.

Singh, I.B. and Bajpai, V.N., 1989. Significance of syndepositional tectonics in facies development, Gangetic alluvium near Kanpur, Uttar Pradesh. *J. Geol. Soc. Ind.*, 34: 61-66.

Singh, I.B. and Ghosh, D.K., 1992. Interpretation of Late Quaternary geomorphic and tectonic features of Gangetic Plain using remote sensing techniques. In: *Proceed. of Nat. Symp. on Remote Sensing for Sustainable Development*, Lucknow: 278-373.

Singh, I.B., Ansari, A.A., Chandel, R.S. and Misra, A., 1996. Neotectonic control on drainage systems in Gangetic Plain, Uttar Pradesh. *Jour. Geol. Soc. Ind.*, 47: 599-609.

Singh, I.B., Pradeep Srivastava, Sharma, S., Sharma, M., Singh, D.V., Rajagopalan, G. and Shukla, U.K., 1999. Upland Interfluvial (Doab) deposition: Alternative model to muddy overbank deposits. *Facies*, 40: 197-210.

Singh, I.B., Rajagopalan, G., Agarwal, K.K., Pradeep Srivastava, Sharma, M. and Sharma, S., 1997. Evidence of Middle to Late Holocene neotectonic activity in the Ganga Plain. *Current Sci.*, 73(12): 1114-1117.

Singh, S., Parkash, B., Arora, M., Rao, M.S., Bhosle, B. 2006. Geomorphology, Pedology and Sedimentology of the Deoha/Ganga-Ghaghara Interfluvial, Upper Gangetic Plains (Himalayan Foreland Basin) - Extensional Tectonic Implications. *Catena*, 67:183-203.

Singhai, S.K., Parkash, B. and Manchanda, M.L., 1991. Geomorphological and Pedological Evolution of Haryana State. *Bull. Oil Natural Gas Comm.*, 28(2): 37-60.

Singhvi, A.K. and Krubetsck, M.R., 1995. Luminescence Dating: A review and a perspective for Arid Zone Sediments. *Ann. Arid Zone*, 35 (3): 289-279.

Smith, M. J. and Clark, D. C., 2005. Methods for the visualization of digital elevation models for landform mapping. *Earth Surf. Process. Landforms*, 30: 885-900

Srivastava, A. and Singh, R.P., 1998. Subsurface control on salt-affected regions of Indo-Gangetic basin. *J. Geol. Soc. Ind.*, 52: 473-476.

Stein, A., 1942, A survey of ancient sites along the lost Sarasvati River., *Geogr. J.*, 99: 173-182.

Thompson, C., McMechen, G. Szerbiak, R. and Gaynor, N., 1995. Three-Dimensional GPR Imaging of complex stratigraphy within the Ferron Sandstone, Castle Valley, Utah, *Proceed. Symp. on Application of*

Geophysics on Engineering and Environmental Problem (SAGEEP), Boston, Massachusetts, 27-31 March: 435-443.

Thussu, J.L. (1995). Quaternary stratigraphy and sedimentation of the Indo-Gangetic plains Haryana. *J. Geol. Soc. India*, 46: 533-544.

Tiwari, R. N. (1976) Cyclic Sedimentation of Middle Coniacian Formation in the eastern part of the Subhercynian Chalk Basin, Germany, Proc. Ind. Assoc. Sed. 1st convention, University, Aligarh.

Tooth, S., 1999. Floodouts in Central Australia. In: Miller, A.J. and Gupta, A. (Eds.), *Varieties of fluvial form*, John Wiley and Sons, Chichester: 219-247.

Tooth, S. 2000a., Downstream changes in dryland river channels: the Northern Plains of arid central Australia. *Geomorphology*, 34: 33-54.

Tooth, S., 2000b., Processes, form and changes in dryland rivers; a research work. *Earth Sci. Rev.*, 51: 67-107.

Turnbridge, I.P., 1984, Facies model for a sandy ephemeral stream and clay playa complex; the Middle Devonian Trentshoe Formation of North Devon, U.K.: *Sedimentology*, 31:697–715.

U.S.D.A., 1966., *Soil Survey Manual*, Hand book No. 18, Oxford and IBH, New Delhi, 503p.

U.S.S.L.S., 1968., *Diagnosis and Improvement of Saline and Alkaline Soils*, Hand book No. 60. Oxford and IBH, New Delhi, 160p.

Valdiya, K.S. 2002. *Sarasvati, The River that Disappeared..* Sangam Books Ltd., 128 p.

Vancraeynest. L. (1998). *Bijdrage tot de studie van de tephromluminescentie-dateringsmethode en toe passing op archeologisch keramiek en eolische sedimenten.* Doctoraats thesis, Universiteit Gent.

Vashishtha, M., 1962, The ancient geography of north-west India., *National Geogr. J. India.*, 8: 3-4, 197-214.

Voelcher, J.A., 1887, Report on the improvement of Indian agriculture., In: Manchanda. M.L., 1978., Ph. D Thesis., H.A.U., Hissar.

Wadia, D.N., 1966, *Geology of India*, McMillan and Co. Ltd., London, 536 pp.

Wilhelmy, H., 1969, Das urstromtal zur ostrand der Indusbene und das Sarasvati-problem, *Z. Geomorph Suppl Bd.*, 8: 7 6-93.

Yash Pal, Baldev Sahai, Sood, R.K and Agarwal, D.P. (1980). Remote sensing of the "Lost" Saraswati River. *Proc. Ind. Acad. Sci. (Earth and Planetary Sciences)*, v.89 (3), pp.317-33

## FIELD DESCRIPTION OF IMPORTANT/TYPICAL PEDONS

### APPENDIX-1

#### QIMS-VI

##### Oldest Piedmont

<b>Pedon</b>	:	<b>V-36</b>
Classification	:	Coarse loamy Udic Ustochrepts
Location	:	Rampur, 2 km from Sahzadpur.
Landform	:	Dissected Piedmont Plain
Landuse	:	Sugarcane, mustard, wheat
Climate	:	Semi-arid
Present material	:	Alluvium
Hydrology (a) Drainage	:	– Good
		(b) Depth of groundwater – 20 m
Moisture condition in profile	:	slightly moist
Evidence of erosion	:	Dissected topography
Presence of salt/alkali	:	Nil
Human influence	:	Nil

##### Horizon cm – (Depth Morphological description)

A 0-18	Light yellowish brown (10 YR 6/4, d), loam, hard (dry) slightly sticky, slightly plastic, few, coarse vertical and common, medium interstitial pores, many medium, few fine roots; gradual wavy boundary.
B 18-58	Brown to dark brown (10 YR 4/3, m), silt-loam, friable (moist), slightly sticky, slightly plastic, common medium vertical and common medium to fine interstitial pores, very weakly developed clay argillans, gradual wavy boundary.
Bt1 58-102	Brown to dark brown (10YR 4/3, m), silt loam, moderate subangular blocky, medium thick clay argillans, friable,moist, common to medium interstitial pores, many fine roots; few ferro-manganese concretions, gradual wavy boundary.
Bt2 102-155	Yellowish brown (10 YR 5/4, m), silty clay loam, friable (moist), strong subangular blocky, slightly sticky and slightly plastic, common medium to fine interstitial pores with random vertical pores, few fine roots, few ferro-manganese concretions, common distinct, thick clay argillans, gradual wavy boundary.
CB 155-175	Two colours, dark yellowish brown (10 YR 4/3, m) and yellowish brown (10 YR 5/4, m), silty clay, weak subangulat blocky. friable (moist), slightly sticky, slightly plastic, common fine vertical and interstitial pores, few fine to medium dark yellowish brown (10 YR 4/6) mottles and faint clear smooth boundary.
C 175-187	Two colours, yellowish brown (10 YR 5/4, m), and dark yellowish brown (10 YR 4/4), friable (moist), loam, structureless, slightly sticky, slightly plastic to non-plastic, common fine interstitial pores, very few fine roots, clear smooth boundary.

<b>Pedon</b>	:	<b>VA</b>
Classification	:	Fine loamy Typic Haplustalf
Location	:	Village Gopal Mohan, near village Mohari,
Landform	:	Dissected Piedmont Plain
Landuse	:	Sugarcane, wheat, bajra
Climate	:	Semi-arid
Present material	:	Alluvium
Hydrology (a) Drainage	:	– Well-drained
		(b) Depth of groundwater – Upland –50 m, lowland-30 m
Moisture condition in profile	:	moist after 10 cm
Evidence of erosion	:	Regional E3, particular E
Presence of salt/alkali	:	Nil
Human influence	:	Brick-klin.

##### Horizon (cm) – Depth Morphological description

A	0-10	Brown (10 YR 5/3, d), (10 YR 3/3, m), sandy loam, slightly sticky, non-plastic, fine and very fine interstitial pores, no effervescence, clear, smooth boundary, medium roots are abundant.
Bw	10-33	Dark brown (10 YR 2,5/3), loam, weakly developed subangular blocky, slightly sticky, plastic, fine and very fine interstitial pores, no effervescence, common fine roots; gradual wavy boundary.
B1t	-120	Dark brown (10 YR 3/3, m), sandy loam, moderately developed subangular blocky, slightly sticky, plastic, fine and very fine interstitial pores; no effervescence; few, fine roots; patchy clay argillans, dark brown (7, 5 YR 3/3, many coarse, faint, mottling; few, Fe/Mn concretions, gradual wavy boundary.
B2t	120-155	Dark brown (10 YR 3/3, m); sandy loam; strongly developed subangular blocky; slightly sticky, slightly plastic; fine and very fine interstitial pores, thick clay argillans; no effervescence; concretions; clear smooth boundary.
C	155-180	Dark brown (10 YR 3/3, m); sandy loam; subangular blocky, non-sticky, non-plastic; fine interstitial pores; no effervescence; dark brown (7, 5 YR 3/3), many, fine, Fe/Mn concretions; clear smooth boundary.

<b>Pedon</b>	:	<b>VC-36</b>
Classification	:	Fine loamy Typic Ustochrepts.
Location	:	Near Bilaspur village, district Ambala
Landform	:	Non-Dissected Piedmont Plain
Landuse	:	Sugarcane, bajra, wheat,
Climate	:	Ustic
Present material	:	Alluvium
Hydrology Drainage – Well-drained		
(b) Depth of groundwater – 25 m		
Moisture condition in profile	:	Slightly moist
Evidence of erosion	:	Nil
Presence of salt/alkali	:	Nil
Human influence	:	Nil.

Horizon (cm) – Depth Morphological description

Ap	0-18	Dark brown (10 YR 4/4), sandy loam, sticky, slightly plastic; fine and very fine interstitial pores; common, fine; common, medium roots; no effervescence; clear smooth boundary.
Bw	18-46	Yellowish brown (10 YR 5/4); weak subangular blocky; slightly sticky, slightly plastic; fine and very fine interstitial pores; few, fine Fe/Mn concretions; no effervescence; gradual smooth boundary.
B2t	46-89	Dark brown (10 YR 5/4); loam; strongly developed subangular blocky; slightly sticky, slightly plastic; fine and very fine interstitial pores; patchy clay argillans, common fine Fe/Mn concretions; no effervescence; gradual smooth boundary; sand pockets.
B3t	89-108	Dark brown (10 YR 4/4); sandy loam; moderately developed subangular blocky; slightly sticky plastic; fine and very interstitial pores; common fine Fe/Mn concretions; sand pockets; thick clay argillans, no effervescence; gradual smooth boundary.
C	108-150	Dark brown (10 YR 4/4); sandy loam; y; slightly sticky, slightly plastic; fine and very fine interstitial pores; common fine Fe/Mn concretions; medium sand pockets; no effervescence.

## QIMS-V

### Old Piedmont-I (OdPd-I)

<b>Pedon</b>	:	<b>V-41R</b>
Classification	:	Coarse loamy Typic Palaeorthids
Location	:	Riwasa
Landuse	:	Nil
Climate	:	Semi-arid to arid
Present material	:	Alluvium

Hydrology (a) Drainage – Well drained	
(b) Depth of groundwater – at higher depth	
Moisture condition in profile	: Dry throughout
Evidence of erosion	: Nil
Presence of salt/alkali	: Nil
Human influence	: Nil
Horizon-(cm)	Depth Morphological description
A 0-10	Light yellowish brown (10 YR 5/4, d) and brown (10 YR, 5/3, m); sandy loam; friable; structureless; friable (dry and moist); slightly-sticky, slightly-plastic; common medium roots; strong effervescence; gradual wavy boundary.
AP 10-40	Dark yellowish brown (10YR 4/3, d) and darkish brown (10YR 4/3, m); sandy loam; slightly-plastic (wet); friable (moist); few fine roots.
Bw 0-63	Light yellowish brown (10 YR 5/3, m) and light yellowish brown 10 YR 6/3, d); sandy loam; hard (dry); thin argillans, weak angular blocky; slightly-sticky, slightly-plastic (wet); friable (moist); common fine interstitial pores; few fine roots; common fine interstitial pores; few fine roots; strongly calcareous; gradual wavy boundary.
Bt1 63-121	Yellowish brown (10 YR 4, 5/4 m); and pale brown (10 YR 6/3, two colours of soil matrix; sandy loam; strongly developed subangular blocky; slightly sticky plastic; few coarse vertical and common, medium to fine interstitial pores; very few fine roots; thick argillans, Fe./Mn concretions, about 10-15% by volume; common medium dark brown (10 YR ¾) oxidation mottles; no effervescence; gradual wavy boundary.
C 121-180	Grayish white (10 YR 8/2, d); loam; massive thick deposition of lacustrine marl (mainly calcium carbonate i.e more than 65%); hard (dry), plastic (wet), medium to coarse voids, many vughs and channels; vughs are filled with calcium carbonate rich material; features related to extensive animal activity; channels are filled with loose coil-matrix material; presence of ostrocofa fossils; violent effervescence.

#### Karnal Terminal Fan

<b>Pedon</b>	:	<b>V-44</b>
Classification	:	Coarse loamy Typic Ustochrepts
Location	:	2 km north of Birohar (Karnal)
Climate	:	Semi-arid to arid
Present material	:	Alluvium
Hydrology (a) Drainage – Well drained		
(b) Depth of groundwater – 8 m		
Moisture condition in profile	:	slightly moist above kankars
Evidence of erosion	:	Nil
Presence of salt/alkali	:	Nil
Human influence	:	Nil
Horizon (cm) – Depth	Morphological description	
Akp 0-15	Light yellowish brown (10 YR 5/4, d) and brown (10 YR 5/3, m); loam; friable; friable (moist); non-sticky, slightly-plastic (wet); very fine roots; strong effervescence; gradual wavy boundary.	
B1w 15-50	Yellowish brown (10 YR 4/3, d) and darkish brown (10YR 4/3, m); loam; weakly developed subangular blocky; non-sticky, slightly-plastic (wet); slightly-friable (moist); very fine roots, strongly calcareous; violent effervescence; gradual wavy boundary.	
B2w 50-100	Dark brown (10 YR 4/3, m); loam; slightly hard (moist), weakly developed subangular blocky; non-sticky, non-plastic; few medium to fine interstitial pores; presence of coarse fragments (about 5% by volume); gradual wavy boundary.	
C 100-140	Dark whitish gray (10 YR 7/2, m); sandy loam; massive structure; hard (dry); slightly-plastic (wet); common coarse tubular and fine interstitial pores; thick deposition of lacustrine marl; channels are filled with loose soil matrix material;	

#### Old Piedmont-II

<b>Pedon</b>	:	<b>VC-39</b>
Classification	:	Coarse loamy Udic Ustochrepts

Location : Village Chandakheri  
 Landform : Piedmont  
 Landuse : Sugarcane, Mustard, wheat,  
 Climate : Udic to Ustic  
 Present material : Alluvium

Hydrology (a) Drainage – Moderately well drained

(b) Depth of groundwater – 5 m

Moisture condition in profile : Slightly moist below 10 cm depth  
 Evidence of erosion : Nil  
 Presence of salt/alkali : Nil  
 Human influence : Cultivated

Horizon (cm) – Depth Morphological description

AP 0-8 Vary pale brown (10 YR 7/4, d), Yellowish brown (10 YR 5/4, m); Sandy loam; friable (dry), loose soil; non-sticky, non-plastic; medium to fine interstitial pores; medium to fine roots; no effervescence; clear smooth boundary.

Bw 25-53 Yellowish brown (10 YR 4, 5/4, m); sandy loam; weakly developed subangular blocky; non-sticky, non-plastic; few coarse to medium and common fine interstitial pores; no effervescence; clear smooth boundary.

Bt1 25-53 Yellowish brown (10 YR 4.5/4); sandy loam; friable (moist); moderately developed subangular blocky; slightly sticky plastic; clay argillans present, few coarse vertical and common, medium to fine interstitial pores; very few fine roots; no effervescence; clear smooth boundary.

Bt 2 53-72 Yellowish brown (10 YR 4, 5/4 m); and pale brown (10 YR 6/3, two colours of soil matrix; sandy loam; well-developed sub-angular blocky; slightly sticky plastic; few coarse vertical and common, medium to fine interstitial pores; very few fine roots; Fe./Mn concretions, about 10-15% by volume; common medium dark brown (10 YR 3/4) oxidation mottles; thick argillans no effervescence; gradual wavy boundary.

Bt3 72-123 Yellowish brown (10 YR 4, 5/4, m); and pale brown (10 YR 6/3, m), two colours of soil matrix; sandy loam, moderately developed sub-angular blocky; slightly sticky, slightly plastic; few coarse vertical channels and common medium to fine interstitial pores; common medium Fe/Mn concretions, about 15% by volume, percentage is increasing downward; common medium, dark brown (10 YR 3/4) oxidation mottles, distinct; thick argillans no effervescence; gradual wavy boundary.

C 122-170 Tw3o colours of soil-matrix i.e. (Yellowish brown, (10 YR 4.5/4, m) and pale brown, 10 YR 6/3, m), percentage of yellow patches by volume is higher than above mentioned horizons; loam; sub-angular blocky; slightly sticky, slightly plastic; coarse ferro-manganese concretion, about 20% by volume; few coarse and common medium size dark brown (10 YR 3/4) oxidation mottles are distinct.

#### Fluvial Plain (FIPn)

**Pedon** : **V-19**  
 Classification : Coarse loamy Typic Ustochrepts  
 Location : Mithathal (Bhiwani)  
 Landform : Plain  
 Landuse : Nil  
 Climate : Semi-arid  
 Present material : Alluvium  
 Hydrology (a) Drainage – Moderately well drained

(b) Depth of groundwater – 10 m

Moisture condition in profile : Slightly moist  
 Evidence of erosion : Nil  
 Presence of salt/alkali : Nil  
 Human influence : An archaeological site

Horizon (cm) – Depth Morphological description

Ap 0-26 Light brownish gray (10 YR 6/2, d); loam friable (dry); non-sticky, non-plastic; few medium and common fine interstitial pores; may medium and common fine interstitial pores; many medium and fine roots; no effervescence; gradual wavy boundary.



Ak 26-58	Pale brown (10 YR 6/3, d); loam; weak; non-sticky, slightly plastic (wet); friable (moist); common fine interstitial pores; common fine roots; strongly calcareous; gradual wavy boundary.
Bwk 58-96	Brown (10 YR 5/3, m); silt loam; weak subangular blocky slightly-plastic (wet); slightly firm (moist); common coarse, few medium and common fine interstitial pores; moderate effervescence; common medium and fine roots; gradual wavy boundary.
Bw1k 96-115	Dark brown (10 YR 4/3, m), sandy loam, friable (moist), non-sticky, non-plastic; weakly developed subangular blocky to structure less; many vertical and medium interstitial pores, coarse fragments (10% by volume); gradual wavy boundary.
Ck 115-134	Grayish brown (10 YR 5/2, m), silt loam; structureless, loose grains; non-sticky and slightly-plastic (wet), friable (moist); common fine to very fine interstitial pores; strongly calcareous, gradual wavy boundary.

#### Aravalli Hills and Pediment Plain

<b>Pedon</b>	:	<b>V51</b>
Classification	:	
Location	:	Village Kishanpura near Khizabad
Landform	:	Low hills and Pediment plains
Landuse	:	Sugarcane, mustard, wheat,
Climate	:	Semi-arid
Present material	:	Alluvium
Hydrology (a) Drainage – good		
	(b) Depth of groundwater – 25 m	
Moisture condition in profile	:	Slightly moist
Evidence of erosion	:	Nil
Presence of salt/alkali	:	Nil
Human influence	:	Cultivated land
Horizon (cm) – Depth Morphological description		
Ap 0-8		Light yellowish brown (10 YR 6/2, d), loam, slightly hard (dry), slightly sticky, slightly plastic; common, medium to fine interstitial pores, common medium and many fine roots; gradual wavy boundary.
Bwk 8-33		Dark brown (10 YR 4/3, m); loam; slightly hard (moist), very weakly developed subangular blocky; non-sticky, non-plastic; few medium to fine interstitial pores; common fine roots; presence of coarse fragments (about 5% by volume); gradual wavy boundary.
B1wk 33-73		Dark brown (10 YR 4/3, m), sandy loam, friable (moist), non-sticky, non-plastic; weakly-developed subangular blocky to structureless; many vertical and medium interstitial pores, very few very fine roots; coarse fragments (10% by volume); gradual wavy boundary.
B2wk 73-140		Dark brown (7, 5 YR 3/3, m), sandy loam; friable (moist), weak subangular blocky, non-sticky and non-plastic, common medium to fine interstitial pores; very coarse sand as the pieces of rock fragments.
C 140-150		Layer with maximum percentage of boulders by volume.

#### Old Piedmont-I

<b>Pedon</b>	:	<b>V-41R</b>
Classification	:	Coarse loamy Udic Ustochrepts
Location	:	½ km from Badli Bus Stand (Jhajjar)
Landform	:	Piedmont---
Landuse	:	Peddy, sugarcane and wheat
Climate	:	Semi-arid
Present material	:	Alluvium
Hydrology (a) Drainage – Good		
	(b) Depth of groundwater – 10 m	
Moisture condition in profile	:	Moist below 20 cm
Evidence of erosion	:	Nil
Presence of salt/alkali	:	slightly-saline

Human influence : Cultivated land

#### Horizon Depth- Morphological description

- AP 0-10 Light yellowish brown (10 YR 6/3, m), and brown (10 YR 4/3, m), sandy loam; structureless, non-sticky, slightly plastic (wet); slightly friable (moist); fine interstitial pores; common very fine roots; strong effervescence; gradual wavy boundary.
- Btk 15-50 Brown (10 YR 4/3, m); sandy loam; moderately developed subangular blocky; non-sticky, slightly plastic (wet); friable (moist); moderately developed subangular blocky; common fine roots; common fine to very fine interstitial pores; strong effervescence; gradual wavy boundary.
- Btk1 50-100 Dark yellowish brown (10 YR 4.5/3.5, m); sandy loam; non-sticky, slightly-plastic (wet); friable (moist); moderately developed subangular blocky; common fine roots; common fine to very fine interstitial pores; strong effervescence; gradual wavy boundary.
- C 100-140 Whitish gray (10 YR 6/3, m), silt loam; coarse to medium calcium carbonate concretions; strong effervescence.

### QIMS-IV

#### Old Yamuna Plain-III

**Pedon** : **V-12**  
Classification : Coarse loamy Typic Ustochrepts  
Location : Village Murthal  
Landform : Plain  
Landuse : Peddy, Sugarcane, pulses  
Climate : Semi-arid  
Present material : Alluvium  
Hydrology (a) Drainage – good  
(b) Depth of groundwater – 7 to 9m  
Moisture condition in profile : slightly moist  
Evidence of erosion : Nil  
Presence of salt/alkali : Nil  
Human influence : Cultivated land

#### Horizon (cm) – Depth Morphological description

- Ap 0-15 Light yellowish brown (10 YR 6/2, d), loamy sand, non-sticky, slightly plastic (wet); slightly friable (moist); common medium interstitial pores, common medium and fine roots; weak effervescence; gradual wavy boundary.
- Bt 15-70 Brown to darkbrown (10 YR 4/3, m), sandy loam; moderately developed subangular blocky; non-sticky, thin clay argillans, slightly plastic (wet); friable (moist) few fine interstitial pores; no effervescence; gradual wavy boundary.
- B1t 70-108 Dark yellowish brown (10 YR 4/4, m), loamy sand; non-sticky, slightly-plastic (wet); patchy thick clay argillans, friable (moist); moderately developed subangular blocky; common fine to very fine interstitial pores; no effervescence; gradual wavy boundary.
- C 108-180 Dark brown to brown (10 YR 4/3, m), sandy loam; friable (moist), structureless, non-sticky and slightly-plastic (wet), common fine interstitial pores; no effervescence; gradual wavy boundary.

#### Old Yamuna Plain-II

**Pedon** : **V-64**  
Classification : Coarse loamy Udic Ustochrepts  
Location : ½ km from Jameswar temple, Narayangarh (Ambala)  
Landform : Plain

Landuse : Sugarcane, wheat and mustard  
 Climate : Semi-arid  
 Present material : Alluvium  
 Hydrology (a) Drainage – well drained  
                   (b) Depth of groundwater – 13 m  
 Moisture condition in profile : Moist below 10 cm  
 Evidence of erosion : Nil  
 Presence of salt/alkali : Nil  
 Human influence : Cultivated land

Horizon (cm) – Depth Morphological description

AP 0-8 Brownish yellow (10 YR 6/6, d); sandy loam, hard (dry); granular; non-sticky, non-plastic; few coarse and many medium vertical and interstitial pores; common medium roots; no effervescence; gradual wavy boundary.

Bwk 8-33 Dark yellowish brown (10 YR 4/4, m); loam; weak subangular blocky; slightly – sticky, slightly plastic (wet); friable (moist); few coarse and common medium interstitial pores; common fine roots; no effervescence; gradual wavy boundary.

Bt1 33-73 Dark yellowish brown (10 YR 4/4, m); loam; slightly-sticky, slightly-plastic (wet); slightly friable (moist); thick argillans, strongly-developed subangular blocky; common medium to fine interstitial pores; no effervescence; common fine roots; clear smooth boundary.

Bw1 73-140 Dark yellowish brown (10 YR 4/4, m), loam; weakly developed subangular blocky; non-sticky and slightly-plastic (wet), slightly friable (moist); common medium to fine interstitial pores; common very fine roots; coarse to fine dark brown (10 YR 3/3) oxidation mottles and Fe/Mn concretions; no effervescence; clear smooth boundary.

C 141-150 Light yellowish brown (10 YR 6/4, m) and dark yellowish brown (10 YR 4/4, m); loam; structureless; non-sticky and slightly plastic (wet); slightly friable (moist), common medium to fine interstitial pores; common medium dark brown (10 YR 3/3) oxidation mottles, 10% by volume and Fe/Mn concretions no effervescence.

**Old Yamuna Plain-I**

**Pedon** : **VA-41**  
 Classification : Coarse loamy Ustic Ustochrepts  
 Location : Near Urlana  
 Landform : Plain  
 Landuse : Sugarcane, wheat and mustard  
 Climate : Semi-arid  
 Present material : Alluvium  
 Hydrology (a) Drainage – well drained  
                   (b) Depth of groundwater – 19-21 m  
 Moisture condition in profile : Moist  
 Evidence of erosion : Nil  
 Presence of salt/alkali : Non-saline  
 Human influence : Cultivated land

Horizon (cm) – Depth Morphological description

AP 0-10 Yellowish brown (10 YR 5/4, m); loam; structureless; non-slightly-sticky, slightly-plastic; few medium and common fine interstitial pores; many medium roots; moderate effervescence; clear smooth boundary.

A 10-20 Dark yellowish brown (10 YR 4/4, m); loam; slightly-sticky, slightly plastic (wet); friable (moist); few medium and common fine interstitial pores; common fine roots; moderate effervescence, 5% by volume soft calcium carbonate concretions; gradual smooth boundary.

Bw 20-90 Dark yellowish brown (10 YR 4/4, m); silt loam; slightly-sticky, slightly-plastic (wet); slightly friable (moist); weakly developed subangular blocky; few medium and common fine interstitial pores; moderate effervescence; few fine roots; clear smooth boundary.

Bw190-152 Brown (10 YR 5/3, m); silt loam; weakly developed subangular blocky; slightly sticky and slightly plastic (wet); friable (moist), few medium and common fine to very fine interstitial pores; strong effervescence; gradual wavy boundary.

C 152-180 Yellowish brown (10 YR 5/4, m); silt loam; slightly-sticky and slightly-plastic (wet), slightly friable (moist); few medium and common fine interstitial pores; 30-35% coarse, hard calcium carbonate concretions; violent effervescence.

#### Old Yamuna Plain-I

Pedon : V-61  
 Classification : Fine loamy Natric Ustochrepts  
 Location : 3 km from Kaithal, right side of Thanesar  
 Landform : Plain  
 Landuse : Peddy, Sugarcane, and wheat  
 Climate : Semi-arid  
 Present material : Alluvium  
 Hydrology (a) Drainage – Good  
 (b) Depth of groundwater – 3-4 m  
 Moisture condition in profile : Slightly Moist  
 Evidence of erosion : Nil  
 Presence of salt/alkali : Strongly salt-affected  
 Human influence : Nil

Horizon (cm) – Depth Morphological description

AP 0-30 Pale brown (10 YR 6/3, d) and brown (10 YR 4/3, m); loam; platy structure; slightly-sticky, slightly-plastic (wet); few medium and common fine interstitial pores, common fine roots; strong effervescence; gradual wavy boundary.

Bw1 30-50 Brown (10 YR 4/3, m); silt loam; platy structure; slightly-sticky, slightly plastic (wet); friable (moist); few coarse, few medium and fine interstitial pores; few fine and many medium roots; moderate effervescence; gradual wavy boundary.

Bw2 50-90 Dark brown (10 YR 3/3, m); silt loam; slightly-sticky, slightly-plastic (wet); slightly friable (moist); weakly developed subangular blocky; few fine roots; common fine interstitial pores; moderate effervescence; clear smooth boundary.

Bt2 90-145 Brown (10 YR 4/3, m), silt loam; strongly developed subangular blocky; slightly-sticky and plastic (wet), friable (moist); thick clay argillans, common fine interstitial pores; few coarse and fine roots; strong effervescence; gradual wavy boundary.

C 145-170 Yellowish brown (10 YR 5/4, m); silt loam; massive; few fine interstitial pores; slightly-sticky and slightly plastic (wet); violent effervescence.

#### Fluvial Alluvial Plain

Pedon : V-36  
 Classification : Fine loamy Natric Ustochrepts  
 Location : ½ km from Badi-Ghaso, near Narwana  
 Landform : Plain  
 Landuse : Gram, bajra, mustard and wheat  
 Climate : Semi-arid  
 Present material : Alluvium  
 Hydrology (a) Drainage – Moderately well drained  
 (b) Depth of groundwater – 15-20 m  
 Moisture condition in profile : Slightly Moist  
 Evidence of erosion : Nil  
 Presence of salt/alkali : Non-saline  
 Human influence : Cultivated land

Horizon (cm) – Depth Morphological description

A 0-10 Brown (10 YR 5/3, m) silt loam; platy structure; slightly sticky, slightly –plastic (wet), friable (moist); few medium and common fine interstitial pores, common fine roots; moderate effervescence; gradual wavy boundary.

Bw 10-38 Brown (10 YR 4/3, m); silt loam; moderately developed platy structure; slightly-sticky, slightly plastic (wet); friable (moist); common fine interstitial pores; common fine roots; moderate effervescence; gradual wavy boundary.

B1t 38-78 Dark yellowish brown (10 YR 3/4, m) loam; slightly-sticky, slightly-plastic (wet); slightly friable (moist), moderately developed platy structure; few fine roots; common fine interstitial pores; strong effervescence; gradual wavy boundary.

B2t 78-115	Brown (10 YR 3.5/3, m), clay loam; moderately developed platy structure; non-sticky and slightly-plastic (wet), friable (moist); common fine interstitial pores; few coarse and fine roots; strong effervescence; 20 % by volume calcium carbonate concretions; gradual wavy boundary.
Bw 115-130	Pale brown (10 YR 6/3, m); sandy loam; non-sticky, non-plastic; strongly calcareous, about 20% by volume calcium carbonate concretions; few fine to very fine interstitial pores; gradual wavy boundary.
C 130-180	Yellowish brown (7.5 YR 4/3, m); loam; slightly sticky and slightly plastic (wet); few fine interstitial pores; violent effervescence.

### **QIMS-III**

#### **Old Katha Plain**

<b>Pedon</b>	:	<b>V-38</b>
Classification	:	Coarse loamy Typic Ustochrepts
Location	:	Siswal village
Landform	:	Plain
Landuse	:	Nil
Climate	:	Semi-arid
Present material	:	Alluvium
Hydrology (a) Drainage	–	Moderately well drained
	(b)	Depth of groundwater –13 m
Moisture condition in profile	:	Slightly Moist
Evidence of erosion	:	Nil
Presence of salt/alkali	:	Non-saline
Human influence	:	An archaeological site

#### Horizon (cm) – Depth Morphological description

Ap 0-11	Light gray (10 YR 7/2, d); and brown (10 YR, 5/3, m); sandy loam; friable; typical thick platy structure; friable (dry and moist); slightly-sticky; slightly-plastic; common medium interstitial pores; strong effervescence; gradual wavy boundary.
Bw 11-45	Very pale brown (10 YR 7/3, d) and darkish brown (10 YR 4/3, m); sandy loam; weak angular blocky; slightly-sticky, slightly-plastic (wet); friable (moist); few common fine interstitial pores; strong effervescence; gradual wavy boundary.
Bw1 45-85	Brown (10 YR 5/3, m) and light yellowish brown (10 YR 6/3, d); silt loam; hard (dry); weak angular blocky; slightly-sticky, slightly-plastic (wet); friable (moist); common fine interstitial pores; strongly calcareous; clear smooth boundary.
Bw2 85-99	Very pale brown (10 YR 7.5/4, m); sandy loam; structureless, indurated grains; non-sticky and non-plastic (wet); slightly friable (moist), common fine interstitial pores; clear smooth boundary.
C1 42-150	Dark yellowish brown (10 YR 4/4, m); sandy loam; non-sticky, slightly-plastic (wet); friable (moist); structureless; fine interstitial pores; some sandy pockets; strong effervescence; gradual wavy boundary.
C 116-138	Yellowish brown (10 YR 5/4, m); sandy loam; structureless; non-sticky and non-plastic (wet); slightly friable (moist), common fine interstitial pores; clear smooth boundary.

#### **Young Katha Plain**

<b>Pedon</b>	:	<b>V-73</b>
Classification	:	Coarse loamy Typic Ustochrepts
Location	:	½ km from Kachhwa bus stand
Landform	:	Upland Plain
Landuse	:	Peddy, Sugarcane, wheat and berseem
Climate	:	Semi-arid
Present material	:	Alluvium
Hydrology (a) Drainage	–	Good
	(b)	Depth of groundwater – 7 – 8 m
Moisture condition in profile	:	Dry to slightly moist

Evidence of erosion	:	Nil
Presence of salt/alkali	:	alkaline, presently non alkaline after gypsum treatment
Human influence	:	Cultivated land
Horizon (cm) – Depth Morphological description		
AP 0-10		Light yellowish brown (10 YR 6/3, m); clay; slightly hard (dry); slightly sticky, slightly plastic (wet); slightly friable (moist); common fine to very fine interstitial pores; few fine roots; weak effervescence; smooth wavy boundary.
Bwk1 10-30		Light yellowish brown (10 YR 6/3, m); silt-loam; weak subangular blocky; slightly-sticky, slightly plastic (wet); few fine interstitial pores; few fine roots; weak effervescence; gradual wavy boundary.
Bwk2 30-65		Dark yellowish brown (10 YR 4/3, m); loam; weak subangular blocky/structureless; non-sticky, slightly plastic (wet); few fine interstitial pores; strong effervescence; gradual wavy boundary.
CB 65-100		Light yellowish brown (10 YR 6/3, m); loam; slightly-sticky, slightly-plastic (wet); friable (moist); weak subangular blocky; fine interstitial pores; weak effervescence; gradual wavy boundary.
C 100-135		Yellowish brown (10 YR 6/4, m), sandy loam; structureless; slightly-sticky and slightly-plastic (wet), common fine interstitial pores; weak effervescence; gradual wavy boundary.

#### Old Yamuna Terminal Fan

Pedon	:	V-43
Classification	:	Fine loamy Typic Natrustalfs
Location	:	village Gudah
Landform	:	Upland Plain
Landuse	:	Nil
Climate	:	Semi-arid
Present material	:	Alluvium
Hydrology (a) Drainage – Imperfectly drained		
(b) Depth of groundwater – 5 – 6 m		
Moisture condition in profile	:	Moist
Evidence of erosion	:	Nil
Presence of salt/alkali	:	Strongly salt-affected
Human influence	:	

#### Horizon (cm) – Depth Morphological description

AP 0-7		Very pale yellowish brown (2.5 YR 7/4, d) and brown to dark brown (10 YR 4/3, m); silt-loam; slightly hard (dry); slightly sticky, slightly plastic (wet); slightly friable (moist); strongly calcareous; many very fine vertical and oblique discontinuous pores; few fine roots; strong effervescence; smooth wavy boundary.
Bw 7-29		Brown to dark brown (10 YR 4/3, m), silt – loam; moderate medium subangular blocky; sticky and plastic (wet); firm (moist) strongly calcareous; many very fine interstitial pores; few fine roots; strong effervescence; smooth clear boundary.
Bt1 29-43		Dark yellowish brown (10 YR 3/4, m); silt loam; very –sticky and plastic (wet); firm (moist); clay argillans in patches, strong medium to coarse subangular blocky strongly calcareous; very few very fine roots; patchy thin argillans; many very fine vertical and oblique discontinuous pores; clear and smooth boundary.
Bt2 43-60		Dark brown (10 YR 3/3, 5, m), silt loam; strongly developed medium to coarse subangular blocky; sticky and plastic (wet), thick clay argillans, strongly calcareous; many very fine vertical and oblique discontinuous pores; clear smooth boundary.
C 60-102		Pale brown (10 YR 6/3, 5, m); silty clay loam; structureless, very firm (moist); sticky and plastic (wet); strongly calcareous; many very fine vertical and oblique discontinuous inped pores.

#### Sonipat Terminal Fan

Pedon	:	V-58
-------	---	------

Classification	:	Coarse loamy Typic Natrustalfs
Location	:	Nioauli village
Landform	:	Upland Plain
Landuse	:	Peddy, Sugarcane, pulses
Climate	:	Semi-arid
Present material	:	Alluvium
Hydrology (a) Drainage		– Good
		(b) Depth of groundwater – 15 – 20 m
Moisture condition in profile	:	Slightly moist
Evidence of erosion	:	Nil
Presence of salt/alkali	:	Non-saline
Human influence	:	Cultivated land

#### Horizon (cm) - Depth Morphological description

AP 0-10	Light yellowish brown (10 YR 6/3, m); sandy loam; non-sticky, plastic (wet); slightly friable (moist); common medium to fine interstitial pores; common fine roots; moderate effervescence; gradual wavy boundary.
AB 10-38	Light yellowish brown (10 YR 6/3, m); sandy-loam; weak subangular blocky; non-sticky, slightly plastic (wet); few fine interstitial pores; few very fine roots; moderate effervescence; gradual wavy boundary.
Bw1 38-78	Light yellowish brown (10 YR 6/3, m); sandy loam; non-sticky, slightly-plastic (wet); slightly friable (moist); weak subangular blocky; fine interstitial pores; sand pockets after 80 cm depth; few very fine roots; medium calcareous carbonate concretions; gradual wavy boundary.
Bt 78-115	Dark yellowish brown (10 YR 4/3, m); loam; strong moderate subangular blocky structure less; non-sticky, slightly plastic (wet); few fine interstitial pores; strong effervescence; gradual wavy boundary.
Bw2 115-180	Dark yellowish brown (10 YR 4/4, m); sandy loam; non-sticky, slightly-plastic (wet); friable (moist); weak subangular blocky; fine interstitial pores; some sandy pockets; strong effervescence; gradual wavy boundary.
C 180-250	Light yellowish brown (10 YR 6/3, m), sandy loam; structureless; non-sticky and slightly-plastic (wet), common fine to very fine interstitial pores; strong effervescence; gradual wavy boundary.

### QIMS-II

#### Young Chautang Terminal fan-II

Pedon	:	V-71
Classification	:	Coarse loamy Udic Ustochrepts
Location	:	Rasouli 8.3 km from Panipat
Landform	:	Plain
Landuse	:	Sugarcane and mustard
Climate	:	Semi-arid
Present material	:	Alluvium
Hydrology (a) Drainage		– Well drained
		(b) Depth of groundwater – 20 m
Moisture condition in profile	:	Moist
Evidence of erosion	:	Nil
Presence of salt/alkali	:	Nil
Human influence	:	Brick-kiln

#### Horizon (cm) – Depth Morphological description

Apk 0-20	Dark brownish (10 YR 4/3, m); sandy loam; hard (dry); sticky, slightly-plastic; few medium and common fine interstitial pores; common fine roots; no effervescence; gradual wavy boundary.
AB 20-27	Dark brown (10 YR 4/3, m); sandy load; medium weak subangular blocky; sticky, slightly plastic (wet); slightly firm (moist); few fine interstitial pores; moderate effervescence; gradual wavy boundary.

Bw1 27-68	Dark brown (10 YR 4/3, m); silt loam; sticky, slightly-plastic (wet); slightly firm (moist); weak subangular blocky; few fine interstitial pores; oderate effervescence; gradual wavy boundary.
Bw2 68-105	Dark brown (10 YR 4/4, m); silt loam; weak subangular blocky; slightly-sticky and slightly-plastic (wet), slightly friable (moist); common fine to very fine interstitial pores; strongly calcareous, about 20% by volume calcium carbonate concretions; gradual wavy boundary.
C 105-150	Yellowish brown (10 YR 5/4, m); loam; non-sticky and slightly plastic (wet); slightly friable (moist), few fine interstitial pores; few medium brown (10 YR 5/4) oxidation mottles; strongly calcareous.

#### Young Chautang Terminal fan-IV

<b>Pedon</b>	:	<b>V-39</b>
Classification	:	Coarse loamy calcareous Natric Ustochrepts
Location	:	8 km from Narnound towards 35 °E
Landform	:	Plain
Landuse	:	Sugarcane, maize and wheat
Climate	:	Semi-arid
Present material	:	Alluvium
Hydrology (a) Drainage – Poorly drained		
(b) Depth of groundwater – 2 m		
Moisture condition in profile	:	Moist
Evidence of erosion	:	Nil
Presence of salt/alkali	:	Non-saline
Human influence	:	Cultivated land
Horizon (cm) – Depth Morphological description		
AP 0-2		Light yellowish brown (10 YR 6/3, m), sandy loam; slightly friable (moist); non-sticky, non-plastic (wet); common fine and very fine interstitial pores, common fine roots; week effervescence; gradual wavy boundary.
Bw 2-19		Dark yellowish brown (10 YR 4/3, m); silt loam; weak subangular blocky with some part of platy structure; slightly-sticky, slightly plastic (wet); slightly friable (moist); common fine to very fine interstitial pores; few fine roots; moderate effervescence; gradual wavy boundary.
B1w 19-50		Yellowish brown (7.5 YR 4/3, m); silt loam; slightly-sticky, slightly-plastic ((wet); slightly friable (moist); weak platy structure; few medium roots; common fine interstitial pores; strong effervescence; clear smooth boundary.
B2w 50-95		Brown (7.5 YR 4/2, m), sandy loam; moderate platy structure; slightly-sticky and slightly-plastic (wet), slightly friable (moist); common fine to very fine interstitial pores; very few fine roots; about 10% by volume calcium carbonate concretions; strong effervescence; gradual wavy boundary.
C 95-115		Yellowish brown (7.5 YR 4/3, m); sandy loam; structureless; slightly-sticky and slightly plastic (wet); friable (moist), common fine to very fine interstitial pores; strong effervescence; clear smooth boundary.

#### Young Chautang Terminal fan-III

<b>Pedon</b>	:	<b>V-54</b>
Classification	:	Coarse loamy calcareous Natric Ustochrepts
Location	:	2.5 km from Nilokheri towards west
Landform	:	Plain
Landuse	:	Nil
Climate	:	Semi-arid
Present material	:	Alluvium
Hydrology (a) Drainage – Poorly drained		
(b) Depth of groundwater – 2 m		
Moisture condition in profile	:	Moist throughout (2-115 cm)
Evidence of erosion	:	Nil
Presence of salt/alkali	:	Saline
Human influence	:	Barren land



Horizon – Depth Morphological description

AkP 0-10	Light whitish gray (2.5 YR 7/1, m), loam; weak platy structure; friable (moist); non-sticky, non-plastic; common fine and very fine interstitial pores, violent effervescence; smooth boundary.
Bw 10-39	Light yellowish brown (10 YR 5/4, m); sandy loam; slightly-sticky, slightly-plastic (wet); slightly friable (moist); weak subangular blocky; medium fine and very fine interstitial pores; violent effervescence; many moderately hard calcium carbonate concretions; gradual wavy boundary.
Bt 39-69	Dark yellowish brown (10 YR 5/3.5, m), loam; moderate subangular blocky; non-sticky and slightly-plastic (wet), clay cutons, common fine to very fine interstitial pores; weak effervescence; gradual wavy boundary.
Bwk1 80-103	Brown to dark brown (10 YR 4/3, m); sandy loam; weak subangular blocky; non-sticky and slightly plastic (wet); firm (moist), common fine to very fine discontinuous, random and vertical pores; very few fine fibrous roots; strong effervescence; clear smooth boundary.
Bwk2 1103-123	Dark yellowish brown (10 YR 5/3, m); silt loam; weak subangular blocky; non-sticky and slightly plastic (wet); slightly friable (moist), common fine to very fine interstitial pores; very few coarse roots; strong effervescence; gradual wavy boundary.
C 123-180	Darkish reddish brown (2.5 YR 5/3, m); loam; massive; non-sticky and slightly plastic (wet), common fine to very fine interstitial pores; wetness in soil; strong effervescence.

**Old Sutlej Pain-II**

<b>Pedon</b>	:	<b>G-5</b>
Classification	:	Coarse loamy Udic Ustochrepts
Location	:	2.5 km before Chanut on Hansi-Barwala road
Landform	:	Plain
Landuse	:	Wheat, mustard and Bajra
Climate	:	Semi-arid
Present material	:	Alluvium
Hydrology (a) Drainage – Moderately well drained		
(b) Depth of groundwater – 7 m		
Moisture condition in profile	:	Slightly moist below 10 cm
Evidence of erosion	:	Nil
Presence of salt/alkali	:	Non-saline
Human influence	:	Cultivated land

Horizon (cm) – Depth Morphological description

AP 0-12	Light yellowish brown (10 YR 6/4, d) and dark brown (10 YR 4/3, m); loam; slightly hard (dry; structureless, slightly-sticky, slightly-plastic (wet); few medium and common fine and very fine interstitial pores, many fine roots; weak effervescence; gradual wavy boundary.
AB 12-31	Yellowish brown (10 YR 5.5/4, m); sandy loam; weak subangular blocky; slightly-sticky, slightly plastic (wet); slightly hard (moist); few medium and common fine to very fine interstitial pores; few fine roots; weak effervescence; gradual wavy boundary.
Bw 31-70	Dark brown (10 YR 4/3, m) sandy loam; weak subangular blocky; slightly-sticky and slightly-plastic (wet), slightly friable (moist); common fine to very fine interstitial pores; few fine roots; gradual wavy boundary.
B1w 70-160	Dark brown (10 YR 4/3, m); sandy loam; weak subangular blocky; sticky and plastic (wet); common medium and fine interstitial pores; few very fine roots; slightly calcareous.
C 160-180	Yellowish brown (7.5 YR 4/3, m); loam; slightly sticky and slightly plastic (wet); few fine interstitial pores; violent effervescence

**Young Chautang Terminal fan - II**

<b>Pedon</b>	:	<b>V-71</b>
--------------	---	-------------

Classification : Coarse loamy Typic Ustochrepts  
 Location : 300 m (45° W from village bhiwani-Rohila)  
 Landform : Aeolian – plain  
 Landuse : Bajra, gram and mustard  
 Climate : Semi-arid  
 Present material : Alluvium  
 Hydrology Drainage – Well drained  
 Moisture condition in profile : Slightly moist  
 Evidence of erosion : Nil  
 Presence of salt/alkali : Non-saline  
 Human influence : Cultivated land

Horizon (cm) – Depth Morphological description

AP 0-20 Light yellowish brown (10 YR 6/3, d) sandy loam; structureless; non-sticky, non-plastic (wet), slightly friable (moist), medium interstitial pores; very few fine roots; violent effervescence; abrupt boundary.

Bw 20-27 Dark yellowish brown (10 YR 5/3, m); sandy loam; weak subangular blocky; non-sticky, non-plastic (wet), slightly friable (moist); medium interstitial pores; common fine roots; violent effervescence; gradual wavy boundary.

Bw1 27-68 Brown to dark brown (10 YR 4/3, m); sandy loam; slightly-sticky, slightly-plastic (wet); slightly friable (moist); weak subangular blocky; many fine and very fine discontinuous and random pores; common very fine fibrous roots; slight effervescence; clear smooth boundary.

BC 68-105 Brown to dark brown (10 YR 4/3, m); sandy loam; weak subangular blocky; non-sticky and slightly plastic (wet); firm (moist), common fine to very fine discontinuous, random and vertical pores; very few fine fibrous roots; strong effervescence; clear smooth boundary.

C 105-150 Dark yellowish brown (7.5 YR 4/4, m); sandy loam; granular ; non-sticky, non-plastic (wet), slightly friable (moist); common medium interstitial pores; more than 50% by volume, calcium carbonate concretions.

**PARTICLE SIZE DISTRIBUTION IN SOIL PROFILES OF DIFFERENT MEMBERS OF MORPHO-STRATIGRAPHIC SEQUENCES**

**APPENDIX-2**

QIMS-PEDONS	HORIZON	DEPTH (CM)	SAN D	SILT	CLAY	TEXTURAL CLASS	Ec (mmhos /cm) / pH	
QIMS-II								
V-39 (YgCgTFn-IV)	Ap	0-02	43.76	49.26	06.98	Loam	2.083/7.83	Md.S/Moderately alkaline
	Bw	02-19	41.20	51.00	07.80	Loam	2.087/7.60	Md.S/Mildly alkaline
	B1w	19-50	50.53	31.63	17.84	Sandy loam	1.140/7.63	M.S/Mildly alkaline
	B2w	50-95	31.50	61.32	07.18	Loam	2.119/7.87	Md.S/Moderately alkaline
	C	95-115	31.27	62.09	06.64	Silt loam	1.562/7.56	M.S/Mildly alkaline
V-54 (YgCgTFn-III)	Akp	0-10	31.76	55.80	12.44	Silt loam	1.186/7.83	M.S/Moderately alkaline
	AB	10-39	28.00	52.88	19.12	Loam	1.157/7.60	M.S/Mildly alkaline
	Bw	39-61	23.52	64.96	11.52	Silt loam	2.149/8.13	Md.S/Moderately alkaline
	Bwk	61-102	48.80	35.92	15.28	Sandy clay loam	2.160/8.87	Md.S/Strongly alkaline
	Bw1k	102-123	35.12	50.56	14.32	Loam	3.160/8.01	Md.S/Moderately acidic
C	123-180	21.37	68.18	10.45	Silt loam	2.280/7.56	Md.S/Mildly alkaline	
G5 (OdSjPn-II)	Ap	0-12	51.49	46.96	01.55	Sandy loam	0.283/6.83	N.S/Neutral
	AB	12-31	46.67	50.68	02.65	Loam	0.251/7.00	N.S/Neutral
	Bw	31-70	47.86	48.88	03.26	Loam	0.144/7.03	N.S/Neutral
	Bw1	70-105	55.17	40.36	04.47	Sandy loam	0.868/7.87	N.S/Moderately alkaline
	C	105-150	64.72	31.56	03.72	Sandy loam	0.156/7.53	N.S/Mildly alkaline
V-71 (YgCgTFn-II)	Akp	0-20	53.28	40.16	06.56	Loam	3.280/8.23	Md.S/Moderately alkaline
	AB	20-27	61.76	30.24	08.00	Sandy loam	3.253/8.21	Md.S/Moderately alkaline
	Bw1	27-68	63.84	23.04	13.12	Sandy loam	2.346/8.03	Md.S/Moderately alkaline
	Bw2	68-95	60.48	30.72	08.80	Sandy loam	1.162/8.07	M.S/Moderately alkaline
	C	95-130	64.00	27.04	08.96	loam	2.263/7.73	Md.S/Mildly alkaline
QIMS-III								
V-38 (OdKaPn)	Ap	0-11	69.88	24.60	05.52	Sandy loam	0.280/6.23	N.S/Slightly acidic
	Bw	11-45	52.64	36.02	11.34	Sandy loam	0.543/6.01	N.S/Slightly acidic
	Bw1	45-85	58.64	36.16	05.20	Loam	0.066/6.03	N.S/Medium acidic
	Bw2	85-99	52.96	35.52	11.52	Sandy loam	0.602/6.47	N.S/Slightly acidic
	C1	99-126	72.80	23.04	04.16	Sandy loam	0.630/6.19	N.S/Slightly acidic
	C2	126-150	68.32	25.60	06.08	Sandy loam	0.730/6.19	N.S Slightly acidic
V-73 (YgKaPn)	Ap	0-10	76.00	17.22	06.78	Sandy loam	0.540/8.23	N.S/Moderately alkaline
	Bw1k	10-30	62.88	27.52	09.60	Sandy loam	0.823/7.01	N.S/ Neutral
	Bw2	30-65	68.28	15.68	16.08	Sandy loam	0.666/8.03	N.S/Moderately alkaline
	CB	65-100	60.53	25.53	13.84	Sandy loam	0.862/8.47	N.S/Moderately alkaline

	C	100-135	79.60	11.84	08.56	Sandy loam	0.510/8.21	N.S/Moderately alkaline
V-43 (OdYTFn)	Ap	0-7	43.68	47.84	08.48	Loam	0.242/8.03	N.S/Moderately alkaline
	Bw	7-29	38.32	52.40	09.28	Silt loam	0.233/7.91	N.S/Moderately alkaline
	Btk	29-43	31.84	56.00	12.16	Silt loam	0.676/7.10	N.S/Neutral
	Btk1	43-60	31.52	54.72	13.76	Silt loam	0.512/7.17	N.S/Neutral
	C	60-102	39.68	51.04	09.28	Silt loam	1.110/6.11	N.S/Slightly alkaline
V-58 (StTFn)	Ap	0-10	38.70	54.44	08.86	Silt loam	0.340/7.11	N.S/Neutral
	AB	10-18	49.36	41.60	09.04	Loam	0.423/7.81	N.S/Mildly alkaline
	Bw1	18-58	43.30	45.09	11.61	Loam	0.666/7.60	N.S/ Mildly alkaline
	Bt	58-75	44.34	27.83	27.83	Clay loam	0.162/7.41	N.S/ Mildly alkaline
	C	75-130	55.12	36.16	08.72	Clay loam	0.510/7.68	N.S/ Mildly alkaline
					QIMS-IV			
V-12 (OdYPn-III)	AP	0-15	81.37	15.73	02.90	Loamy sand	0.383/6.25	N.S/Slightly acidic
	AB	15-30	66.73	29.10	04.17	Sandy loam	0.514/6.70	N.S/Neutral
	Bwk	30-60	75.17	21.15	03.68	Loamy sand	0.363/6.73	N.S/Neutral
	Bt	60-89	74.14	20.54	05.32	Loamy sand	0.547/6.43	N.S/Neutral
	C	89-120	63.10	35.90	01.00	Sandy loam	0.337/6.50	N.S/Slightly acidic
V-64 (OdYPn-II)	AP	0-8	53.04	40.16	06.80	Loam	0.481/6.15	N.S/Slightly acidic
	Bwk	8-33	46.16	38.50	15.34	Loam	0.212/6.79	N.S/Neutral
	Bt1	33-73	60.00	29.08	10.92	Sandy loam	1.243/6.70	N.S/Neutral
	Bw1	73-140	76.64	16.16	07.20	Sandy loam	0.931/6.19	N.S/Slightly acidic
	C	140-150	74.72	20.00	05.28	Sandy loam	0.891/7.19	N.S Neutral
VA-41 (OdYPn-I)	A	0-10	65.76	28.28	05.96	Sandy loam	0.883/6.25	N.S/Slightly acidic
	Ap	10-20	69.71	25.62	04.67	Sandy loam	0.814/6.70	N.S/Neutral
	Bw	20-90	33.64	54.34	12.02	Silt loam	0.863/6.73	N.S/Neutral
	Bw1	90-152	23.54	69.12	07.34	Silt loam	0.937/6.59	N.S/Slightly acidic
	C	152-180	83.94	14.38	01.68	Loamy sand	0.631/7.08	N.S Neutral
V-61 (OdYPn-II)	AP	0-30	59.68	32.98	07.34	Sandy loam	0.143/7.55	N.S/Mildly alkaline
	Bw	30-50	52.00	41.28	06.72	Sandy loam	0.461/7.11	N.S/Neutral
	Bw1	50-80	39.68	52.00	08.32	Silt loam	0.733/7.69	N.S/Mildly alkaline
	Bt	80-105	28.80	48.16	23.04	Loam	0.242/7.42	N.S/Mildly alkaline
	C	105-140	39.84	54.56	05.60	Silt loam	0.431/6.69	N.S/Neutral
					QIMS-V			
V-41R	A	0-10	54.08	37.18	08.74	Sandy loam	0.818/8.23	N.S/Moderately alkaline
	Ap	10-40	41.76	48.20	10.04	Loam	0.943/8.01	N.S/Moderately alkaline

(OdPt-I)	Bt	40-63	38.72	49.28	12.00	Loam	0.546/8.03	N.S/Moderately alkaline	
	Bt1	63-121	35.52	49.12	15.36	Loam	0.806/8.47	N.S/Strongly alkaline	
	C	121-180	47.68	43.36	08.96	Loam	0.630/8.19	N.S/Moderately alkaline	
VC-39 (OdPt-II)	Ap	0-8	52.16	47.84	11.20	Sandy loam	1.318/8.11	M.S /Moderately alkaline	
	Bw	8-25	58.88	30.88	10.24	Sandy loam	1.643/7.51	M.S/Mildly alkaline	
	Btk	25-48	50.40	35.16	14.44	Sandy loam	1.546/7.73	M.S /Mildly alkaline	
	Bt1k	48-76	50.88	35.36	13.76	Sandy loam	1.106/7.87	M.S /Moderately alkaline	
	Bt2k	76-103	50.56	39.36	10.08	Sandy loam	1.130/8.19	M.S/Moderately alkaline	
V-44 (KrTFn)	C	103-140	45.28	46.56	08.16	Loam	1.331/7.59	M.S/Mildly alkaline	
	A	0-15	62.53	34.65	02.82	Sandy loam	2.218/7.50	Md.S /Mildly alkaline	
	Bw	15-40	68.06	15.49	16.45	Sandy loam	2.123/7.70	Md.S/Mildly alkaline	
	Bt1	40-90	66.15	22.85	11.00	Sandy loam	1.416/8.03	Md.S/Moderately alkaline	
	Bt2	90-140	37.89	57.55	04.56	Silt loam	3.100/8.23	Md.S/Moderately alkaline	
V-19 (FIPn)	C	140-187	45.38	46.56	08.16	Loam	1.130/8.19	M.S/Moderately alkaline	
	A	0-26	42.72	42.56	14.72	Loam	0.243/7.25	N.S/Neutral	
	AkP	26-58	36.13	49.12	14.72	Loam	0.561/7.71	N.S/Mildly alkaline	
	Bwk	58-96	32.26	51.00	16.74	Silt loam	0.533/7.37	N.S/Neutral	
	Bw1K	96-115	31.99	56.54	11.47	Silt loam	0.442/7.02	N.S/Neutral	
V-S1 (OdPt)	Ck	115-134	42.71	50.51	06.78	Loam	0.331/7.59	N.S/Mildly alkaline	
	QIMS-VI								
	A	0-18	49.92	37.44	12.64	Loam	0.583/6.55	N.S/Slightly acidic	
	Bw	18-58	16.20	70.52	13.28	Silt loam	0.564/6.78	N.S/Neutral	
	Bt	58-102	14.00	67.52	18.48	Silt loam	0.563/6.77	N.S/Neutral	
VC-36 (OdPt)	Bt1	102-155	11.20	70.72	18.08	Silty clay loam	0.537/6.29	N.S/Slightly acidic	
	CB	155-175	13.60	68.16	18.24	Silty clay loam	0.527/6.98	N.S/Neutral	
	C	175-187	46.56	43.20	10.24	Loam	0.549/6.45	N.S/Slightly acidic.	
	A	0-19	61.49	31.72	6.79	Silty loam	0.606/6.25	N.S/Slightly acidic	
	Bw	19-33	33.12	45.44	21.44	Loam	0.658/6.64	N.S/Neutral	
VC-36 (OdPt)	Bt2	33-70	29.92	49.28	20.80	Sandy loam	0.644/6.57	N.S/Neutral	
	Bt3	70-105	59.36	28.50	11.84	Sandy loam	0.640/6.68	N.S/Neutral	
	C	105-130	67.52	17.92	14.56	Sandy loam	0.623/6.12	N.S/Slightly acidic	

Note- N.S- Non Saline, M.S- Mildly Saline, Md.S- Moderately Saline

---

**QIMS-II****Sample No. V-53 Microstructures**

Weakly developed subangular blocky structures. Peds were separated by channels and voids. Ped faces were unaccommodated to each other. Voids were irregular. Microstructures were intergrain channel, compact grain and vughy type. Channel width varying from 50 to 300  $\mu\text{m}$ . Void and channel walls serrated coated with ferric oxide residue. Estimated porosity was 10-20%.

**Basic Mineral Components**

c/f ratio at 20  $\mu\text{m}$ ; ratio was 20:80.

**(a) Coarse Fraction**

Coarse fraction consists of anhedral quartz (12%); feldspars weathered broken, weathered muscovite and biotite (4%) were present. Quartz grains varying in size from 50-500  $\mu\text{m}$ , fractured surrounded by ferric oxide residues.

**(b) Fine Fraction**

Fine fraction constitutes fractured quartz, weathered feldspars, mica, biotite flakes sparitic calcite and other unidentifiable clay minerals.

**Groundmass**

The c/f related distribution was open to double spaced porphyric, crystallitic, stippled speckled, poro-striated b-fabric. Micromass was brownish in colour uniform throughout the section.

**Pedofeatures**

Ferriargillan, argillan hypocoating along the void and channel surfaces. Fe-Mn nodules with distinct boundaries varying in size from 200-300  $\mu\text{m}$ . Rootlets were also observed in the section.

**Sample No. V-3****Microstructures**

Weakly developed subangular blocky structures. Peds separated by channels and voids. Ped faces were unaccommodated to each other. Voids were irregular to subcircular in shape. Microstructures were intergrain channel, channel type. Channel width varying from 125 to 250  $\mu\text{m}$ . Void and channel walls serrated coated with fine ferric oxide residue. Estimated porosity was 15-20%.

**Basic Mineral Components**

c/f ratio at 20  $\mu\text{m}$ ; ratio was 40:60.

**(a) Coarse Fraction**

Coarse fraction consists of anhedral quartz (10%); weathered feldspars, highly weathered muscovite and biotite (4%) were present. Quartz grains were 625-875  $\mu\text{m}$ , fractured surrounded by ferric oxide residues.

**(b) Fine Fraction**

Fine fraction constitutes fractured quartz, weathered feldspars, mica, biotite flakes calcite and other unidentifiable clay minerals.

#### **Groundmass**

The c/f related distribution was open to double spaced porphyric, crystallitic, stippled speckled, poro-striated b-fabric. Micromass was brownish colour uniform throughout the section.

#### **Pedofeatures**

Ferriargillan argillan hypocoating along the void and channel surfaces. Fabric pedofeatures were observed. Channels were partially filled with nodules. Fe-Mn nodules with distinct boundaries varying in size 125-750  $\mu\text{m}$ .

#### **Sample No. V-71 Microstructures**

Weakly developed subangular blocky structures. Peds were separated by channels and voids. Ped faces were partially accommodated to each other. Voids were irregular to subcircular in shape. Microstructures were spongy, vughy type. Channel width varying from 10 to 50  $\mu\text{m}$ . Void and channel walls rough, serrated. Estimated porosity was 5-8%.

#### **Basic Mineral Components**

c/f ratio at 30  $\mu\text{m}$ ; ratio was 50:50.

##### **(a) Coarse Fraction**

Coarse fraction consists of anhedral quartz (8%); feldspars absent, muscovite and biotite grains subhedral elongated (10%) were seen. Quartz grains were 25-125  $\mu\text{m}$ . fractured surrounded by ferric oxide residues.

##### **(b) Fine Fraction**

Fine fraction constitutes fractured quartz, micaceous and other unidentifiable clay minerals.

#### **Groundmass**

The c/f related distribution was open to double spaced porphyric, crystallitic, stippled speckled, parallel striated b-fabric. Micromass was dark brownish.

#### **Pedofeatures**

Ferriargillan hypocoating along the void and channel surfaces. Channels were filled with secondary argillan coating. Fe-Mn nodules with distinct boundaries varying in size from 25-50  $\mu\text{m}$ . Excrement pedofeatures common. Rootlets replaced by secondary minerals. Animal activities in the form of burrows were common in the section.

#### **Sample No. G-5**

##### **Microstructures**

Moderately to weakly developed subangular blocky structures. Peds were separated by channels and voids. Ped faces were partially accommodated to each other. Voids were irregular to subcircular. Microstructures were intergrain channel and spongy type. Channel width varying from 25 to 500  $\mu\text{m}$ . Void and channel walls were rough. Estimated porosity was 10-15%.

##### **Basic Mineral Components**

c/f ratio at 30  $\mu\text{m}$ ; ratio was 40:60.

##### **(a) Coarse Fraction**

Coarse fraction consists of anhedral quartz (10-15%); weathered feldspars, laths of muscovite (5-10%) were present. Quartz grains were 25-625  $\mu\text{m}$ , fractured surrounded by ferric oxide rings.

**(b) Fine Fraction**

Fine fraction constitutes quartz, weathered feldspars, mica flakes and other unidentifiable clay minerals.

**Groundmass**

The c/f related distribution was open to double spaced porphyric, crystallitic, stippled speckled, parallel unstriated b-fabric. Micromass was brownish to light brownish in colour. Ferric oxide fillings along the channel walls.

**Pedofeatures**

Ferriargillan and argillan hypocoating along the void and vesicle surfaces. Excrement pedofeatures present in scattered forms. Fe-Mn nodules with distinct boundaries varying in size from 25-750  $\mu\text{m}$ .

**QIMS-III**

**Sample No. V-43**

**Microstructures**

Weakly developed crumb structures. Peds separated by channels and voids. Ped faces were unaccommodated to each other. Voids were irregular to subcircular. Microstructure was intergrain channel type. Channel width varying from 50 to 150  $\mu\text{m}$ . Void and channel walls were rough. Estimated porosity was 5-10%.

**Basic Mineral Components**

c/f ratio at 30  $\mu\text{m}$ ; ratio was 40:60.

**(a) Coarse Fraction**

Coarse fraction consists of anhedral quartz (8%); weathered feldspars, laths of muscovite (4%) were observed. Quartz grains varying in size from 25-625  $\mu\text{m}$ , fractured surrounded by ferric oxide rings.

**(b) Fine Fraction**

Fine fraction constitutes quartz, mica flakes and other unidentifiable clay minerals.

**Groundmass**

The c/f related distribution was open to double spaced porphyric, crystallitic, stippled speckled, porostriated b-fabric. Micromass was brownish to yellowish brown in colour, distributed randomly throughout the section.

**Pedofeatures**

Ferriargillan and argillan hypocoating along the aggregate surfaces. Fabric pedofeatures common. Excrement pedofeatures present in scattered forms. Fe-Mn nodules were absent.

**Sample No. V-43**



### **Microstructures**

Peds were absent. Voids were irregular to subcircular in shape. Microstructures were intergrain channel, vughy type. Void and channel walls serrated coated with fine ferric oxide residue. Estimated porosity was 10-15%.

### **Basic Mineral Components**

c/f ratio at 20  $\mu\text{m}$ ; ratio was 60:40.

#### **(a) Coarse Fraction**

Coarse fraction consists of anhedral quartz (10%); weathered feldspars, weathered muscovite and biotite (6%) were present. Quartz grains varying in size from 650-850  $\mu\text{m}$ , fractured surrounded by ferric oxide residues.

#### **(b) Fine Fraction**

Fine fraction constitutes fractured quartz, weathered feldspars, biotite and other unidentifiable clay minerals.

### **Groundmass**

The c/f related distribution was open to double spaced porphyric, crystallitic, stippled speckled, parallel striated b-fabric. Micromass was light brownish to grayish in colour varying throughout the section.

### **Pedofeatures**

Ferriargillan and argillan typic hypocoating along the void and channel surfaces. Fabric pedofeatures were observed. Channels were filled by nodules. Fe-Mn nodules with distinct boundaries, corroded and recrystallized material embedded within the nodules forming a sieve like structure.

### **Sample No. V-58**

#### **Microstructures**

Moderately developed subangular blocky structures. Peds were separated by channels and voids. Ped faces were partially accommodated to each other. Voids were elongated to irregular in shape. Microstructures were intergrain channel, vughy type. Channel width varying from 125 to 250  $\mu\text{m}$ . Void and channel walls serrated coated with fine ferric oxide residue. Estimated porosity was 5-10%.

#### **Basic Mineral Components**

c/f ratio at 20  $\mu\text{m}$ ; ratio was 40:60.

#### **(a) Coarse Fraction**

Coarse fraction consists of anhedral quartz (4%); weathered feldspars, highly weathered muscovite and biotite (6%) were present. Quartz grains were 125-1375  $\mu\text{m}$ , fractured surrounded by ferric oxide residues.

#### **(b) Fine Fraction**

Fine fraction constitutes fractured quartz, weathered feldspars, mica, biotite flakes, calcite and other unidentifiable clay minerals.

### **Groundmass**

The c/f related distribution was open to double spaced porphyric, crystallitic, mosaic

speckled, porostriated and parallel striated b-fabric. Micromass was brownish in colour, uniform throughout the section.

#### **Pedofeatures**

Ferriargillan argillan hypocoating along the void and aggregate surfaces. Fabric pedofeatures were seen. Fe-Mn nodules with distinct boundaries, rounded to elongate varying in size 625  $\mu\text{m}$  to 0.375 mm. Rootlets were replaced by calcitic material.

#### **Sample No. V-73 Microstructures**

Moderately developed subangular blocky structures. Peds were separated by channels. Ped faces were unaccommodated to each other. Voids were irregular to subcircular in shape. Microstructures were intergrain channel and vughy type. Channel width varying from 20 to 90  $\mu\text{m}$ . Void and channel walls rough. Estimated porosity was 5-8%.

#### **Basic Mineral Components**

c/f ratio at 30  $\mu\text{m}$ ; ratio was 50:50.

##### **(a) Coarse Fraction**

Coarse fraction consists of anhedral quartz (6%) with diffused boundaries; weathered feldspars with rims of alterations, muscovite and biotite grains subhedral elongated (9%) were seen. Quartz grains were 30-60  $\mu\text{m}$ , fractured surrounded by ferric oxide residues.

##### **(b) Fine Fraction**

Fine fraction constitutes fractured quartz, mica minerals, calcite, weathered feldspars and other unidentifiable clay minerals.

#### **Groundmass**

The c/f related distribution was open to double spaced porphyric, crystallitic, mosaic speckled striated b-fabric. Micromass was dark brownish.

#### **Pedofeatures**

Ferriargillan and argillan hypocoating along the void and channel surfaces. Some channels were filled with secondary argillan coating. Fe-Mn nodules with diffused boundaries varying in size from 10-50  $\mu\text{m}$ . Fine strands of rootlets were also seen.

#### **Sample No. V-38**

##### **Microstructures**

Moderately to weakly developed subangular blocky structures. Peds were separated by channels and voids. Ped faces were partially accommodated to each other. Voids were irregular to subcircular. Microstructure was intergrain channel and spongy type. Channel width varying from 25 to 400  $\mu\text{m}$ . Void and channel walls were rough, serrated. Estimated porosity was 5-7%.

##### **Basic Mineral Components**

c/f ratio at 30  $\mu\text{m}$ ; ratio was 40:60.

**(a) Coarse Fraction**

Coarse fraction consists of anhedral quartz (5%); feldspars were absent, highly weathered laths of muscovite and biotite (5%) were present. Quartz grains were 20-625  $\mu\text{m}$ , fractured surrounded by ferric oxide residues.

**(b) Fine Fraction**

Fine fraction constitutes quartz, weathered mica and biotite flakes and other unidentifiable clay minerals.

**Groundmass**

The c/f related distribution was open to double spaced porphyric, crystallitic, stippled speckled, random striated b-fabric. Micromass was brownish in colour. Thin ferric oxide fillings along the channel walls.

**Pedofeatures**

Ferriargillan and argillan hypocoating along the void and channel surfaces. Excrement pedofeatures present in scattered forms. Bow like organic structures coated with sesquioxides were observed. Fe-Mn nodules absent.

**Sample No. V-96**

**Microstructures**

Moderately developed subangular blocky structures. Peds were separated by channels and voids. Ped faces were partially accommodated to each other. Voids were irregular to subcircular microstructures were intergrain channel and spongy type. Channel width varying from 25 to 400  $\mu\text{m}$  Void and channel walls were rough. Estimated porosity was 10-15%.

**Basic Mineral Components**

c/f ratio at 30  $\mu\text{m}$ ; ratio was 40:60.

**(a) Coarse Fraction**

Coarse fraction consists of anhedral quartz (5%); feldspars were absent, highly weathered laths of muscovite and biotite (5%) were present. Quartz grains were 20-625  $\mu\text{m}$ . fractured surrounded by ferric oxide residues.

**(b) Fine Fraction**

Fine fraction constitutes quartz, weathered mica and biotite flakes and other unidentifiable clay minerals.

**Groundmass**

The c/f related distribution was open to double spaced porphyric, crystallitic, stippled speckled, reticulate striated b-fabric. Micromass was brownish in colour. Thin ferric oxide fillings along the channel walls.

**Pedofeatures**

Ferriargillan hypocoating along the void and channel surfaces. Excrement pedofeatures present in scattered forms. Bow like organic structures coated with sesquioxides were observed. Fe-Mn nodules with distinct boundaries varying in size from 250-1250  $\mu\text{m}$ .

**QIMS-IV**

**Sample No. V-12**

**Microstructures**

Moderately developed sub-angular blocky structures. Peds were separated by channels and voids. Ped faces were partially accommodated to each other. Voids were irregular to oval. Microstructure was intergrown channel type. Channel width varying from 125 to 625  $\mu\text{m}$ . Void and channel walls were rough. Estimated porosity was 10-15%.

**Basic Mineral Components**

c/f ratio at 30  $\mu\text{m}$ ; ratio was 40:60.

**(a) Coarse Fraction**

Coarse fraction consists of anhedral quartz (18%); feldspars were absent, laths of muscovite (12%) were present. Quartz grains were 30-250  $\mu\text{m}$ , fractured surrounded by ferric oxide rings.

**(b) Fine Fraction**

Fine fraction constitutes quartz, mica flakes and other unidentifiable clay minerals.

**Groundmass**

The c/f related distribution was open to double spaced porphyric, crystallitic, stippled speckled, parallel striated b-fabric. Groundmass was dark brownish in colour.

**Pedofeatures**

Ferriargillan and argillan hypocoating along the aggregate surfaces. Fabric pedofeatures common. Excrement pedofeatures present in scattered forms. Fe-Mn nodules with distinct boundaries varying in size from 50-750  $\mu\text{m}$ .

**Sample No. V-61**

**Microstructures**

Moderately to well developed subangular blocky structures. Peds were separated by channels. Ped faces were partially accommodated to each other. Voids were irregular to subcircular in shape. Microstructures were intergrain channel and channel type. Channel width varying from 25 to 250  $\mu\text{m}$ . Void and channel walls rough. Estimated porosity was 15-20%.

**Basic Mineral Components**

c/f ratio at 30  $\mu\text{m}$ ; ratio was 40:60.

**(a) Coarse Fraction**

Coarse fraction consists of anhedral quartz (12%) with diffused boundaries; feldspars absent, muscovite and biotite grains subhedral elongated (15%) were seen. Quartz grains were 25-50  $\mu\text{m}$ , fractured surrounded by ferric oxide rims.

**(b) Fine Fraction**

Fine fraction constitutes fractured quartz, mica minerals, sparitic calcite, and other unidentifiable clay minerals.

**Groundmass**

The c/f related distribution was open to double spaced porphyric, crystallitic, stippled speckled, granostriated, b-fabric. Micromass was grayish and brownish.

**Pedofeatures**

Ferriargillan and argillan hypocoating along the void and channel surfaces. Excrement pedofeatures were seen scattered in the thin section. Fe-Mn nodules with diffused boundaries varying in size from 25-150  $\mu\text{m}$ .

**Sample No. V-36**

### **Microstructures**

Weakly developed sub-angular blocky structures. Peds were separated by channels and voids. Ped faces were completely accommodated to each other. Voids were irregular to subcircular. Microstructure was intergrain channel type. Channel width varying from 50 to 250  $\mu\text{m}$ . Void and channel voids were rough. Estimated porosity was 8-10%.

### **Basic Mineral Components**

c/f ratio at 30  $\mu\text{m}$ ; ratio was 45:55.

#### **(a) Coarse Fraction**

Coarse fraction consists of anhedral to subhedral quartz (15%); feldspars were absent. laths of muscovite (10%) were present. Quartz grains were 30-250  $\mu\text{m}$ , partially fractured surrounded by ferric oxide rings.

#### **(b) Fine Fraction**

Fine fraction constitutes quartz, mica flakes and other unidentifiable clay minerals.

### **Groundmass**

The c/f related distribution was open to double spaced porphyric, crystallitic, stippled speckled striated b-fabric. Ferric oxide gel was filled in the pores and channels. Groundmass was light brownish in colour.

### **Pedofeatures**

Ferriargillan argillan hypocoating along the void surfaces, minerals, aggregates and along the channels. Fabric pedofeatures commonly seen. Fe-Mn nodules were absent.

### **Sample No. VB1**

#### **Microstructures**

Moderate to weakly developed sub-angular blocky structures. Peds were separated by channels and voids. Ped faces were partially accommodated to each other. Voids were irregular to subcircular. Microstructure was spongy type. Channel width varying from 25 to 250  $\mu\text{m}$ . Void and channel voids were smooth. Estimated porosity was 10-15%.

#### **Basic Mineral Components**

c/f ratio at 30  $\mu\text{m}$ ; ratio was 40:60.

#### **(a) Coarse Fraction**

Coarse fraction consists of anhedral to subhedral quartz (12%); feldspars were absent, biotite and muscovite laths (10%) were present. Quartz grains were 50-100  $\mu\text{m}$ , partially fractured surrounded by ferric oxide ring.

#### **(b) Fine Fraction**

Fine fraction constitutes quartz, mica flakes and other unidentifiable clay minerals.

### **Groundmass**

The c/f related distribution was open to double spaced porphyric, crystallitic, unistrial, parallel striated b-fabric. Ferric oxide gel was filled in the pores and channels. The micromass was brownish in colour.

### **Pedofeatures**

Ferriargillan hypocoating along the void surfaces and along the channels. Fabric pedofeatures commonly seen. Depletion pedofeatures were also visible. Ferriargillan coating 25-75  $\mu\text{m}$ . Fe-Mn. Concretions with smooth distinct boundaries varying in size between 125-750  $\mu\text{m}$ .

### **Sample No. V-55**

### **Microstructures**

Moderately developed subangular blocky structures. Peds were separated by channels and voids. Ped faces were partially accommodated to each other. Voids were irregular to subcircular in shape. Microstructures were intergrain channel, vughy type. Channel width varying from 125 to 250  $\mu\text{m}$ . Void and channel walls serrated coated with fine ferric oxide residue. Estimated porosity was 5-10%.

### **Basic Mineral Components**

c/f ratio at 30  $\mu\text{m}$ ; ratio was 30:70.

#### **(a) Coarse Fraction**

Coarse fraction consists of anhedral quartz (5%); feldspars absent, muscovite and biotite grains subhedral oriented in a particular direction (5%) were present. Quartz grains were 25-250  $\mu\text{m}$ , fractured surrounded by ferric oxide residues.

#### **(b) Fine Fraction**

Fine fraction constitutes fractured quartz, micaceous flakes, calcite and other unidentifiable clay minerals.

### **Groundmass**

The c/f related distribution was open to double spaced porphyric, crystallitic, mosaic speckled, parallel striated b-fabric. Micromass was brownish in colour varying throughout the section.

### **Pedofeatures**

Ferriargillan hypocoating along the void and aggregate surfaces as well as individual grains. Fe-Mn nodules (25-75  $\mu\text{m}$ ) with diffused boundaries. Rootlets (25  $\mu\text{m}$ ) were replaced by calcitic material. Organic activity clearly seen

### **QIMS-V**

### **Sample No. G**

#### **Microstructures**

Moderately to weakly developed sub-angular blocky structures. Peds were separated by channels and voids. Ped faces were partially accommodated to each other. Voids were irregular subcircular. Microstructure was intergrain channel and micro-aggregates type. Channel width varying from 25 to 625  $\mu\text{m}$ . Void and channel walls were rough. Estimated porosity was 15-20%.

#### **Basic Mineral Components**

c/f ratio at 30  $\mu\text{m}$ ; ratio was 40:60.

#### **(a) Coarse Fraction**

Coarse fraction consists of anhedral quartz (15%); feldspars were absent, laths of muscovite (5%) were present. Quartz grains were 30-150  $\mu\text{m}$ , partially fractured surrounded by ferric oxide rings.

#### **(b) Fine Fraction**

Fine fraction constitutes quartz, mica flakes and other unidentifiable clay minerals.

### **Groundmass**

The c/f related distribution was open to double spaced porphyric, crystallitic, stippled speckled, mosaic speckled, circular striated b-fabric. Ferric oxide gel was filled in the voids and channels. Groundmass was brownish in colour.

### **Pedofeatures**

Ferriargillan hypocoating along the void and aggregate surfaces, and along the channels.

Thickness of coating was 50-250  $\mu\text{m}$ . Excrement pedofeatures were seen at places. Fe-Mn nodules with distinct boundaries varying in size from 75-500  $\mu\text{m}$ .

#### **Sample No. V-25**

##### **Microstructures**

Weakly developed subangular blocky structures. Peds were separated by channels and voids. Ped faces were partially accommodated to each other. Voids were irregular to subcircular in shape. Microstructures were intergrain channel, channel and vughy type. Channel width varying from 10 to 75  $\mu\text{m}$ . Void and channel walls rough. Estimated porosity was 5-10%.

##### **Basic Mineral Components**

c/f ratio at 30  $\mu\text{m}$ ; ratio was 60:40.

###### **(a) Coarse Fraction**

Coarse fraction consists of anhedral quartz (8%); weathered feldspars with alterations on the rim were present, muscovite and biotite grains subhedral elongated (5%) were seen. Quartz grains were 10-50  $\mu\text{m}$ , fractured surrounded by ferric oxide residues.

###### **(b) Fine Fraction**

Fine fraction constitutes fractured quartz, micaceous minerals, calcite, weathered feldspars and other unidentifiable clay minerals.

##### **Groundmass**

The c/f related distribution was open to double spaced porphyric, crystallitic, granostriated, reticulate striated b-fabric. Micromass was light brownish.

##### **Pedofeatures**

Ferriargillan and argillan hypocoating along the void and channel surfaces. Channels were filled with secondary argillan coating. Excrement pedofeatures common. Fe-Mn nodules with diffused boundaries varying in size from 25-75  $\mu\text{m}$ . Fine strands of rootlets replaced by secondary minerals were also seen.

#### **Sample No. V-44**

##### **Microstructures**

Moderately to well developed subangular blocky structures. Peds were separated by channels. Ped faces were partially accommodated to each other. Voids were subcircular in shape. Microstructures were intergrain channel, channel and vughy type. Channel width varying from 10-75  $\mu\text{m}$ . Void and channel walls smooth. Estimated porosity was 10-15%.

##### **Basic Mineral Components**

c/f ratio at 30  $\mu\text{m}$ ; ratio was 50:50.

###### **(a) Coarse Fraction**

Coarse fraction consists of anhedral quartz (18%) with diffused boundaries; feldspars highly weathered, muscovite grains subhedral elongated and calcite (8%) were seen. Quartz grains were 25-50  $\mu\text{m}$ , fractured surrounded by ferric oxide rims.

###### **(b) Fine Fraction**

Fine fraction constitutes fractured quartz, mica minerals, calcite, and other unidentifiable clay minerals.

##### **Groundmass**

The c/f related distribution was open to double spaced porphyric, crystallitic, mosaic speckled, reticulated striated, b-fabric. Micromass was grayish and brownish.

#### **Pedofeatures**

Ferriargillan and argillan and calcetan hypo- and quasi-coating along the void, grain and channel surfaces. Excrement pedofeatures were also seen in the section. Fe-Mn nodules with diffused boundaries varying in size from 25-150  $\mu\text{m}$ . Strands of rootlets partially filled with secondary minerals were also seen.

#### **Sample No. V-47**

##### **Microstructures**

Moderately to well developed subangular blocky structures. Peds were separated by channels. Ped faces were partially accommodated to each other. Voids were rounded and oval in shape varying from 50-250  $\mu\text{m}$ . Microstructures were intergrain channel, channel and vughy type. Channel width varying from 25-250  $\mu\text{m}$ . Void and channel walls smooth. Estimated porosity was 10-15%.

##### **Basic Mineral Components**

c/f ratio at 30  $\mu\text{m}$ ; ratio was 40:60.

###### **(a) Coarse Fraction**

Coarse fraction consists of anhedral quartz (10%); feldspars not found, weathered muscovite grains subhedral elongated and calcite (10%) were seen. Quartz grains were 25-50  $\mu\text{m}$ , fractured surrounded by ferric oxide rims.

###### **(b) Fine Fraction**

Fine fraction constitutes fractured quartz, calcite, muscovite and other unidentifiable clay minerals.

#### **Groundmass**

The c/f related distribution was open to double spaced porphyric, crystallitic, mosaic speckled, prostriated b-fabric. Micromass was dark brownish.

#### **Pedofeatures**

Ferriargillan and hypocoating along the void, grain and channel surfaces. Ferriargillan coating varying in size from 20-30  $\mu\text{m}$ . Fe-Mn nodules with diffused boundaries varying in size from 20-500  $\mu\text{m}$ . Mineral aggregates in clusters were also occurring in the section.

#### **A-IV.4.8 Sample No. S42/5**

##### **Microstructures**

Weakly developed subangular blocky structures. Peds were separated by channels and voids. Ped faces were partially unaccommodated to each other. Voids were irregular to subcircular in shape. Microstructures were intergrain channel, vughy type. Channel width varying from 25 to 250  $\mu\text{m}$ . Void and channel walls rough. Estimated porosity was 5-8%.

##### **Basic Mineral Components**

c/f ratio at 30  $\mu\text{m}$ ; ratio was 50:50.

###### **(a) Coarse Fraction**

Coarse fraction consists of anhedral quartz (16%); feldspars absent, muscovite and biotite grains subhedral oriented in a particular direction (10%) were present. Quartz grains were 25-125  $\mu\text{m}$ , fractured surrounded by ferric oxide residues.



**(b) Fine Fraction**

Fine fraction constitutes fractured quartz, micaceous flakes and other unidentifiable clay minerals.

**Groundmass**

The c/f related distribution was open to double spaced porphyric, crystallitic, mosaic speckled, reticulate striated b-fabric. Micromass was brownish in colour.

**Pedofeatures**

Ferriargillan hypocoating along the void and channel surfaces. Fe-Mn nodules with diffused boundaries with recrystallised material embedded within the nodules. Excrement pedofeatures common.

**QIMS-VI**

**Sample No. VS1**

**Microstructures**

Moderately to well developed sub-angular blocky structures. Peds were separated by channels and voids. Ped faces were partially accommodated to each other. Voids were irregular, oval to subcircular. Microstructures were intergrain channel and channel type. Channel width varying from 25 to 250  $\mu\text{m}$ . Void and channel walls were rough. Estimated porosity was 10-15%.

**Basic Mineral Components**

c/f ratio at 30  $\mu\text{m}$ ; ratio was 30:70.

**(a) Coarse Fraction**

Coarse fraction consists of anhedral to subhedral quartz (8%); feldspars were absent, laths of muscovite (1-2%) were present. Quartz grains were 30-250  $\mu\text{m}$ , partially fractured surrounded by ferric oxide rings.

**(b) Fine Fraction**

Fine fraction constitutes quartz, mica flakes and other unidentifiable clay minerals.

**Groundmass**

The c/f related distribution was open to double spaced porphyric, crystallitic, stippled speckled reticulate striated b-fabric. Ferric oxide gel was partially filled in the pores and channels. Groundmass was brownish in colour.

**Pedofeatures**

Ferriargillan argillan hypocoating along the void and aggregate surfaces, minerals, aggregates and along the channels. Thickness of coating was 50-500  $\mu\text{m}$ . Excrement pedofeatures commonly seen. Corroded Fe-Mn nodules (50-100  $\mu\text{m}$ ) with recrystallised materials embedded in it. Rootlets of 500  $\mu\text{m}$  size were also seen.

**Sample No. VA**

**Microstructures**

Moderately to well developed subangular blocky structures. Peds were separated by channels and voids. Ped faces were unaccommodated to each other. Voids were irregular to subcircular. Microstructures were intergrain channel, channel and vughy type. Channel width varying from 50 to 3750  $\mu\text{m}$ . Void and channel walls were smooth and coated with ferric oxide residue. Estimated porosity was 15-20%.

**Basic Mineral Components**

c/f ratio at 20  $\mu\text{m}$ ; ratio was 10:90.

**(a) Coarse Fraction**

Coarse fraction consists of anhedral quartz (1%); feldspars were absent, weathered muscovite and biotite (2%) was present. Quartz grains were 125-500  $\mu\text{m}$ , fractured surrounded by ferric oxide residues.

**(b) Fine Fraction**

Fine fraction constitutes quartz, mica and biotite flakes and other unidentifiable clay minerals.

**Groundmass**

The *c/f* related distribution was open to double spaced porphyric, crystallitic, stippled speckled, parallel striated, porostriated b-fabric. Voids depletion features. Micromass was dark brownish in colour.

**Pedofeatures**

Thin ferriargillan typic hypocoating along the void and channel surfaces. Excrement pedofeatures present in scattered forms. Fabric and depletion pedofeatures were commonly seen. Fe-Mn nodules absent.

**Sample No. V-36**

**Microstructures**

Moderately to well developed sub-angular blocky structures. Peds were separated by channels and voids. Ped faces were partially accommodated to each other. Voids were irregular subcircular. Microstructures were spongy and channel type. Channel width varying from 25 to 500  $\mu\text{m}$ . Void and channel walls were smooth. Estimated porosity was 10-15%.

**Basic Mineral Components**

*c/f* ratio at 30  $\mu\text{m}$ ; ratio was 35:75.

**(c) Coarse Fraction**

Coarse fraction consists of anhedral quartz (10%); feldspars were absent, laths of muscovite (2%) were present. Quartz grains were 30-250  $\mu\text{m}$ , highly fractured surrounded by ferric oxide rings.

**(d) Fine Fraction**

Fine fraction constitutes quartz, mica flakes and other unidentifiable clay minerals.

**Groundmass**

The *c/f* related distribution was open to double spaced porphyric, crystallitic, stippled speckled and cross striated b-fabric. Ferric oxide gel was filled in the voids and channels. Groundmass was brownish in colour.

**Pedofeatures**

Ferriargillan typic and hypocoating along the aggregate surfaces. Fabric pedofeatures common. Thickness of coating was 50-250  $\mu\text{m}$ . Corroded Fe-Mn nodules with diffused boundaries. Elongated Fe-Mn nodules were also commonly seen varying in size from 75-625  $\mu\text{m}$  width & 125-150  $\mu\text{m}$ .